TECHNISCHE UNIVERSITÄT MÜNCHEN

Lehrstuhl für Entwicklungsgenetik

Function of Pitx3 and miRNAs in midbrain dopaminergic neurons

Changgeng Peng

Vollständiger Abdruck der von der Fakultät Wissenschaftszentrum Weihenstephan für Ernährung, Landnutzung und Umwelt der Technischen Universität München zur Erlangung des akademischen Grades eines

Doktors der Naturwissenschaften

genehmigten Dissertation.

Vorsitzender: Univ.-Prof. Dr. S. Scherer

Prüfer der Dissertation:

1. Univ.-Prof. Dr. W. Wurst
2. Univ.-Prof. A. Schnieke, Ph.D.

Die Dissertation wurde am 05.03.2012 bei der Technischen Universität München eingereicht und durch die Fakultät Wissenschaftszentrum Weihenstephan für Ernährung, Landnutzung und Umwelt am 12.07.2012 angenommen.

Index

Zusammenfassung

Pitx3 ist ein wichtiger Homeodomänen-Transkriptionsfaktor für die Entwicklung und das Überleben von dopaminergen Neuronen im Di- und Mesencephalon (mdDA Neurone) der Säugetiere. Polymorphismen in diesem Gen werden mit der Parkinsonschen Erkrankung (Morbus Parkinson) in Verbindung gebracht. In Mäusen bewirkt der Verlust der Pitx3-Expression ein Absterben der mdDA Neurone insbesondere in der Substantia nigra pars compacta (SNc), der Region, die auch bei Parkinson-Patienten am meisten betroffen ist. Derzeit ist immer noch unklar, wie Pitx3 das Überleben von mdDA Neuronen in der SNc fördert und welche durch Pitx3 regulierte Faktoren (Zielgene) daran beteiligt sind. In dieser Arbeit zeige ich, dass eine transiente Expression des Glia-Wachstumsfaktors „Glial cell line-derived neurotrophic factor" (GDNF) im ventralen Mittelhirn (VM) des Mausembryos die Transkription von Pitx3 über den NF-kB Signalweg induziert, und dass Pitx3 wiederum für die Expression des Hirn-spezifischen Wachstumsfaktors „brain-derived neurotrophic factor„ (BDNF) in einer Subpopulation rostrolateraler (SNc) mdDA Neurone notwendig ist. Der Verlust der BDNF-Expression in $Pitx3^{-/-}$ Mäusen korreliert mit einem erhöhten Absterben der SNc mdDA Zellen, während in Zellkulturversuchen die Behandlung von primären VM Zellen mit BDNF das Überleben der $Pitx3^{-/-}$-mdDA Neurone begünstigt. Von besonderer Bedeutung ist jedoch, dass in Abwesenheit von Pitx3 lediglich BDNF aber nicht GDNF mdDA Neuronen vor 6-Hydroxydopamin (6-OHDA)-induziertem Zelltod schützt. Da die Vorwärts-Regulierung der GDNF-, Pitx3- und BDNF-Expression auch im adulten Nagergehirn fortbesteht, deuten diese Daten darauf hin, dass eine Störung der regulatorischen Interaktion zwischen diesen drei Faktoren auch zu dem Verlust von SNc mdDA Neuronen im Gehirn der Parkinson-Patienten beitragen könnte.

MicroRNAs (miRNAs) sind eine Klasse von nicht-kodierenden kleinen RNAs (~21 Nukleotide), die posttranskriptionell die Genexpression entweder durch den direkten Abbau von Boten-RNAs (mRNAs) und/oder durch die Hemmung ihrer Translation regulieren. In einer Studie wurde gezeigt, dass miRNAs für das Überleben von mdDA Neuronen notwendig sind. Die Identität dieser miRNAs ist jedoch noch nicht bekannt. Anhand einer konditionalen Knock-out Maus ($En1^{+/Cre}$; $Dicer1^{flox/flox}$ Mäuse), der alle durch das Dicer1-Enzym prozessierte RNAs (reife miRNAs und andere nicht-kodierende RNAs) in der Mittel-/Hinterhirnregion (MHR) fehlen, konnte ich zeigen, dass miRNAs für den Zellzyklus-Austritt und neuronale Differenzierung der mdDA und anderer neuraler Vorläufer im VM notwendig sind. Außerdem konnte ich zeigen, dass die in $En1^{+/Cre}$; $Dicer1^{flox/flox}$ Mäusen gestörte

neuronale Differenzierung hauptsächlich durch den Verlust der *miR-200*-Familie verursacht wird, deren Zielgene die Transkriptionsfaktoren Sox2 und E2F3 sind. Sox2 spielt eine wichtige Rolle bei der Aufrechterhaltung der proliferativen und multipotenten Eigenschaften neuraler Vorläuferzellen, indem es ihre Differenzierung hemmt und die Expression von Zellzyklus- und anderen Stammzell-charakeristischen Genen in diesen Zellen aufrecht erhält. E2F3 ist ein wichtiger Zellzyklus-Faktor, der den Übergang von der G1- zur S-Phase und von der G2- zur M-Phase im Zellzyklus reguliert. Ohne die negative Regulierung durch die *miR-200*-Familie sind die Sox2-positiven und E2F3-positiven Zellzahlen und Areale neuraler Vorläuferzellen in den *En1$^{+/Cre}$; Dicer1$^{flox/flox}$* Mäusen auf Kosten der postmitotischen Neuronen vergrößert. Eine Überexpression von *miR-200* in primären ventralen Mittelhinterhirn-Kulturen fördert die neuronale Differenzierung, während die Hemmung („Knockdown") von *miR-200* die Expression von Sox2 und E2F3 aufrecht erhält und dadurch die neuronale Differenzierung in diesen Kulturen hemmt. Ferner konnte ich zeigen, dass die Expression von *miR-200* direkt durch die Sox2 und E2F3 Transkriptionsfaktoren gesteuert wird. Dadurch besteht eine unilaterale negative Rückkopplung zwischen der Expression von *miR-200*, Sox2 und E2F3, welche die Proliferation und neuronale Differenzierung neuraler Vorläuferzellen steuert. Diese Ergebnisse zeigen eine neue Funktion von *miR-200* im zentralen Nervensystem der Säuger auf, und geben einen ersten Hinweis darauf, wie *miR-200* in einem breiteren Kontext den Übergang von einer proliferierenden pluri-/multipotenten Stamm- oder Vorläuferzelle zu einer postmitotischen und ausdifferenzierenden Zelle bewirken kann.

Da sich der Phänotyp der *En1$^{+/Cre}$; Dicer1$^{flox/flox}$* Mäuse nicht allein auf die mdDA Neurone beschränkt sondern die gesamte MHR betrifft, ist dieses Mausmodell nicht für weitere Studien zur Funktion von miRNAs in mdDA Neuronen geeignet. Deshalb habe ich, zusammen mit meinen Kollegen, zwei weitere Cre-exprimierende Mauslinien hergestellt, die eine gezielte Inaktivierung des Dicer1 Enzyms in den mdDA Vorläufern oder in den ausdifferenzierenden bzw. adulten mdDA Neuronen ermöglichen sollen. Es handelt sich dabei um eine *Shh-Cre-SBE1* transgene Mauslinie und eine induzierbare *Aldh1a1$^{+/Cre-ERT2}$* knock-in Mauslinie, die jedoch zeitlich bedingt noch nicht vollständig etabliert sind.

1 Abstract

Pitx3 is a critical homeodomain transcription factor for the proper development and survival of meso-diencephalic dopaminergic (mdDA) neurons in mammals. Several variants of this gene have been associated with human Parkinson's disease (PD), and lack of *Pitx3* in mice causes the preferential loss of substantia nigra pars compacta (SNc) mdDA neurons that are most affected in PD. It is currently unclear how Pitx3 activity promotes the survival of SNc mdDA neurons, and which factors act up- and downstream of Pitx3 in this context. Here I show that a transient expression of Glial cell line-derived neurotrophic factor (*GDNF*) in the murine ventral midbrain (VM) induces transcription of *Pitx3* via NF-κB-mediated signaling, and that Pitx3 is in turn required for activating the expression of brain-derived neurotrophic factor (*BDNF*) in a rostrolateral (SNc) mdDA neuron subpopulation during embryogenesis. The loss of *BDNF* expression correlates with the increased apoptotic cell death of this mdDA neuronal subpopulation in $Pitx3^{-/-}$ mice, whereas treatment of VM cell cultures with BDNF augments the survival of the $Pitx3^{-/-}$ mdDA neurons. Most importantly, only BDNF but not GDNF protects mdDA neurons against 6-hydroxydopamine (6-OHDA) induced cell death in the absence of *Pitx3*. As the feed-forward regulation of GDNF, Pitx3 and BDNF expression also persists in the adult rodent brain, these data suggest that the disruption of the regulatory interaction between these three factors contributes to the loss of mdDA neurons in $Pitx3^{-/-}$ mutant mice and perhaps also in human PD.

MicroRNAs (miRNAs) are a class of non-protein coding small RNAs (~21 nucleotides) which posttranscriptionally regulate gene expression by degradation of mRNA and/or inhibition of translation. One report has shown that miRNAs are required for the survival of mdDA neurons, but it is still not known which specific miRNAs participate in this process. By using $En1^{+/Cre}$; $Dicer1^{flox/flox}$ conditional knock-out mice, which lack all mature miRNAs and other non-coding RNAs in the mid-/hindbrain region (MHR), I found that miRNAs are required for the cell cycle exit and neuronal differentiation of mdDA and other neural progenitors in the murine VM. I also found that the general neuronal differentiation defect in the $En1^{+/Cre}$; $Dicer1^{flox/flox}$ mice can be mostly attributed to the loss of the *miR-200* family in these mice, which directly targets the transcription factors Sox2 and E2F3. Sox2 plays a vital role in maintaining neural progenitor identity by inhibiting their differentiation and activating the expression of cell cycle genes. E2F3 is a critical cell cycle factor that promotes the transition from G1 to S phase and from G2 to M phase of the cell cycle. Without the negative regulation by the *miR-200* family, $Sox2^{+}$ and $E2F3^{+}$ neural progenitors are increased and

expanded in *En1*$^{+/Cre}$; *Dicer1*$^{flox/flox}$ mice at the expense of postmitotic neurons. Overexpression of *miR-200* in primary ventral mid-/hindbrain cultures promotes neuronal differentiation, whereas functional knockdown of *miR-200* maintains the expression of Sox2 and E2F3 and thereby inhibits neuronal differentiation in these cultures. Furthermore, I could show that the expression of *miR-200* is in turn controlled by Sox2 and E2F3, thereby establishing a unilateral negative feedback loop between *miR-200*, Sox2 and E2F3 expression controlling the proliferation and differentiation of neural progenitors. These results establish a novel function of *miR-200* in the mammalian central nervous system, and provide first insights on how the *miR-200* family might promote in a broader context the transition from a proliferating, pluri-/multipotent stem/progenitor cell to a postmitotic and differentiating cell.

As *En1*$^{+/Cre}$; *Dicer1*$^{flox/flox}$ mice have a general defect of neuronal differentiation in the MHR, which is not restricted to mdDA neural progenitors, this mouse model is unsuitable for further studies regarding the role of miRNAs in mdDA neuron development and survival. I have therefore generated, together with my colleagues, two new Cre-expressing mouse lines that will enable the selective inactivation of the Dicer1 enzyme in mdDA neural progenitors or in differentiating/adult mdDA neurons. These are a *Shh-Cre-SBE1* transgenic mouse line and an inducible *Aldh1a1*$^{+/Cre-ERT2}$ knock-in mouse line. Due to time limitations, these mouse lines have not been fully established yet.

2 Part 1: Function of Pitx3 in midbrain dopaminergic neurons

2.1 Introduction

The majority of the brain's dopamine (DA) is synthesized by neurons located in two nuclei of the mammalian ventral midbrain (VM): the substantia nigra pars compacta (SNc) innervating predominantly the dorsolateral striatum; and the ventral tegmental area (VTA) projecting mainly to limbic and cortical areas of the brain (Bjorklund and Dunnett, 2007). The SNc neurons control the execution of voluntary movements, and their selective degeneration in PD is responsible for the characteristic motor symptoms of this disease (Dauer and Przedborski, 2003).

During development, mesodiencephalic DA (mdDA) precursors arise from progenitors located in the midbrain floor plate (FP) (Smidt and Burbach, 2007). It is assumed that SNc neurons derive from a rostrolateral and VTA neurons from a caudomedial mdDA precursor subpopulation (Smits et al., 2006). Several secreted and transcription factors are involved in the specification of the mdDA fate in neuroepithelial progenitors and in their differentiation into mature mdDA neurons, as well as their survival throughout development and adulthood (Prakash and Wurst, 2006; Smidt and Burbach, 2007). The homeodomain transcription factor Pitx3 has gained particular interest as Pitx3 expression in the brain is restricted to mdDA neurons, and *Pitx3* mutant mice display a progressive and preferential loss of the SNc mdDA neurons during embryonic and postnatal development (Smidt et al., 2004; van den Munckhof et al., 2003).

2.1.1 *Pitx3* is required for the development of subgroup mdDA neurons

Pitx3 gene was discovered in 1997 by two independent laboratories: one screened an adult forbrain cDNA library by using a probe cloned from homeobox-containing genes, and found *Pitx3* is exclusively expressed in mdDA neurons in the brain (Smidt et al., 1997); the other laboratory screened an embryonic carcinoma cDNA library by using a probe containing the homeobox region of *Pitx2,* another member of the Pitx family, and found *Pitx3* is highly expressed in the lens during eye development (Semina et al., 1997). The finding that two deletions in the *Pitx3* promoter led to a lack of *Pitx3* expression in the lens of aphakia mice facilitated scientists to investigate the function of Pitx3 in mdDA neurons by using aphakia mice carrying these spontaneous mutations (Rieger et al., 2001; Semina et al., 2000). In 2003, three groups reported that the loss of Pitx3 expression in aphakia mice caused a severe loss of SNc DA neurons, but had a lesser effect on VTA DA neurons (Hwang et al., 2003; Nunes et

al., 2003; van den Munckhof et al., 2003). This phenotype is quite similar to the characteristic phenotype of PD, namely the preferential degeneration of SNc DA neurons in PD patients, suggesting that Pitx3 may be related to human PD. Indeed, several groups found that some SNPs within this gene are associated with human PD (Bergman et al., 2010; Fuchs et al., 2009; Haubenberger et al., 2009; Le et al., 2009). Intriguingly, Pitx3 is expressed in both SNc and VTA DA neurons (Smidt et al., 2004), although only SNc DA neurons are severely affected in *Pitx3* mutant mice. This suggests that the differential requirement of Pitx3 for SNc and VTA DA neurons could be due to activation of different downstream genes by Pitx3 in these two groups of DA neurons. Thus, many efforts have been put on discovering downstream genes of *Pitx3*.

In 2005, Chung et al found that overexpression of Pitx3 in mESC increases *aldehyde dehydrogenase 2* (*AHD2*, also called *Aldh1a1*) and *G-protein-regulated inwardly rectifying K+ channel* (*Girk2*) -positive DA neurons after differentiation of these mESCs, and the expression levels of these two genes are enriched in SNc DA neurons relative to VTA DA neurons from later embryonic developmental stages on (Chung et al., 2005). This in vitro data is supported by the in vivo data which showed loss of Aldh1a1 expression in the subpopulation of mdDA neurons of Pitx3-deficient mouse from E13.5 onwards (Jacobs et al., 2007), but lack of Aldh1a1 expression was also found in the midbrain of Nurr1-deficient mice (Wallen et al., 1999). Thus, these data suggest that the expression of Aldh1a1 is not only controlled by Pitx3 also by Nurr1. At early embryonic development, *Aldh1a1* is expressed in mdDA progenitors, but from E14.5 the expression of *Aldh1a1* is restricted to SNc DA neurons (Chung et al., 2005; Jacobs et al., 2007; Wallen et al., 1999). Since Aldh1a1 is an enzyme for retinoic acid (RA) synthesis, which plays an important role in brain development (Maden et al., 2007). Jacobs et al tried to use RA to rescue the phenotype of Aphakia mice. Indeed, maternal RA complementation partially rescues SNc neurodegeneration in *Pitx3* mutant mice (Jacobs et al., 2007). Therefore it was deduced that Pitx3 might activate additional target genes to promote the survival of SNc mdDA neurons. Many other downstream genes of *Pitx3* were meanwhile found, such as the genes encoding DA biosynthetic enzymes (*TH*), transporters (*DAT*) and receptors (*D2*) (Jacobs et al., 2009; Lebel et al., 2001). Using gain-of-function, I previously found that overexpression of Pitx3 can upregulate the expression of neurotrophic factors BDNF and GDNF in SH-SY5Y cells and primary ventral midbrain cultures (Peng et al., 2007), but it needed to be validated whether these two genes are downstream genes of *Pitx3* in vivo.

In contrast to the many downstream genes of *Pitx3* discovered up to now, little is known about the genes upstream of *Pitx3*. One presumed activator of Pitx3 is *Lmx1b*, because the *Lmx1b*$^{-/-}$ mutant mouse embryos lack Pitx3 expression but have the expression of other DA markers *Th* and *Nurr1* in the midbrain (Smidt et al., 2000). However, so far no evidence has been provided to show that Lmx1b can directly regulate the expression of *Pitx3*. Another activator might be *Lmx1a*, because Chung et al observed that overexpression of Lmx1a can upregulate the expression of *Pitx3* in vitro and Lmx1a is able to bind directly to the *Pitx3* promoter (Chung et al., 2009). Surprisingly, *Lmx1a*$^{-/-}$ mutant mice still have Pitx3 expression in the midbrain (Deng et al., 2011; Yan et al. , 2011), which suggests that Lmx1a is not the only one TF for activation of Pitx3, even if Lmx1a is indeed able to activate its expression in vivo. Recently Konstantoulas et al reported that Foxp1 can directly regulate Pitx3 expression in neurons-derived from embryonic stem cells (Konstantoulas et al., 2010), but whether Foxp1 can activate the expression of Pitx3 in vivo has not yet been shown.

2.1.2 Neurotrophic factors are required for the survival of mdDA neurons

Many neurotrophic factors are able to promote the differentiation and/or survival of mdDA neurons. Transforming growth factors (TGF) have been shown to be neurotrophic factors for DA neurons. *TGF-a*$^{-/-}$ knock-out mice have a nearly 50% reduction in SNc DA neurons, but have no change in the number of VTA DA neurons at birth (Blum, 1998). *TGF-β,* another transforming growth factor, is also required for the induction of chicken mdDA neurons and for the survival of mouse mdDA neurons (Farkas et al., 2003; Poulsen et al., 1994). Loss of the two isoforms of TGF-*β* in TGF-*β2* and TGF-*β3* double knock-out mice caused a significant reduction in the number of mdDA neurons (Roussa et al., 2006). The lack of *TGF-β2* contributes more to this phenotype than of *TGF-β3* due to the fact that TH reduction in *TGF-β2*$^{-/-}$*/TGF-β3*$^{+/-}$ mice was higher than in *TGF-β2*$^{+/-}$*/ TGF-β3*$^{-/-}$ mice and that *TGF-β2* is expressed at higher levels in the ventral midbrain than *TGF-β3* (Poulsen et al., 1994; Roussa et al., 2006).

Glial cell line-derived neurotrophic factor (GDNF), a distant member of the TGF-β superfamily, was originally discovered as a neurotrophic factor for mdDA neurons (Lin et al., 1993). In cells co-expressing GDNF family receptor a 1 (GFRα1) and Ret, GDNF signal transduction is via the Ret/GFRα1 receptor complex. GDNF first forms a homodimer and binds to the GFRα1, which is linked to the plasma membrane by a Glycosyl Phosphatidylinositol (GPI) anchor, and then this complex binds to the Ret receptor tyrosine kinase to activate either the mitogen activated protein kinase (MAPK) pathway or the

phosphoinositide 3-kinase (PI3K) pathway regulating cell proliferation, differentiation, migration and survival (Airaksinen and Saarma, 2002; Jing et al., 1996; Treanor et al., 1996). In cells lacking Ret expression, the GDNF signal can also be transducted by GFRα1 in a Ret-independent manner, through activation of Src family kinase and phosphorylation of ERK/MAPK, PLC- γ and the transcription factor CREB, and induction of Fos (Poteryaev et al., 1999; Trupp et al., 1999). These results can explain why the expression of GFRα1 is not always accompanied with the expression of Ret in the brain (Kokaia et al., 1999; Trupp et al., 1997). It has been also shown that the neural cell adhesion molecule (NCAM) is an alternative signaling receptor for GDNF (Paratcha et al., 2003). GDNF binds to NCAM/GFRα1 complex and thereby activates the Src-like kinase Fyn and focal adhesion kinase FAK in the cytoplasm. Enven in the absence of GFRα1, GDNF can bind NCAM with low affinity (Paratcha et al., 2003).

Not only in vitro data, but also in vivo data support the idea that GDNF signaling can enhance the survival of mdDA neuons. It is well known that GDNF is highly transcribed in the striatum when nigrostriatal innervation takes place, and that the Ret tyrosine kinase receptor and its GDNF family co-receptors (*GFR*) α1 and 2 are expressed strongly in the VM throughout the mdDA neurogenic period (Golden et al., 1999), suggesting that GDNF is a target-derived trophic factor for mdDA neurons (Golden et al., 1999; Oo et al., 2005). Indeed, intrastriatal or intranigral injections of GDNF protein during early postnatal stages, or the constitutive activation of the Ret receptor, results in increased numbers of TH^{+} SNc neurons and an enhanced DA metabolism (Beck et al., 1996; Mijatovic et al., 2007). Moreover, conditional knock-out *GDNF* in adult stage causes 60-70% reduction of mdDA neurons at 7 months after ablation of *GDNF* (Pascual et al., 2008), and conditional *Ret* knock-out leads to a progressive loss of SNc DA neurons in postnatal stages (Kramer et al., 2007). These data suggest that the unaffected mdDA neurons in prenatal stages of the *GDNF*, *Ret* or *GFRa1* knock-out mice could be due to developmental compensations (Airaksinen and Saarma, 2002; Kramer et al., 2007; Paratcha and Ledda, 2008). As the GDNF receptors, *Ret*, *GFRa1 and GFRa2* are expressed in the ventral midbrain as early as E10.5 in mice (Golden et al., 1999), which is a couple of days before the axons of the mdDA neurons reach the striatum and receive the GDNF signal from there, it raised the possibility that GDNF signaling may also play a role in early development of the mdDA neurons, and *GDNF* could be present in the ventral midbrain when its receptors are expressed there. However it is still a debate whether *GDNF* is expressed in the midgestational VM. Several reports showed that GDNF is not expressed in the VM of mouse embryos (Hellmich et al., 1996; Golden et al., 1999), but Choi-

Lundberg and Bohn showed that *GDNF* is expressed in the embryonic rat VM by using a more sensitive RT-PCR-based detection method (Choi-Lundberg and Bohn, 1995).

Another important survival factor for mdDA neurons is the brain-derived neurotrophic factor (BDNF) (Knusel et al., 1991; Zuccato and Cattaneo, 2009). It is well known that BDNF and its receptor, TrkB, are coexpresssed in mdDA neurons (Kramer et al., 2007; Seroogy et al., 1994), but it is unknown when BDNF expression starts and how it is regulated in mdDA neurons. Binding of BDNF to TrkB receptor can activate the downstream MAPK, PI3K and PKC signalling pathways. In addition to in vitro data, the in vivo data that conditional deletion of the *BDNF* gene during midbrain development results in a selective reduction of these neurons at birth (Baquet et al., 2005) also supports the notion that BDNF is required for the survival of mdDA neurons during development.

I have previously shown that Pitx3 activates BDNF expression in primary VM cultures (Peng et al., 2007). In the present study, I demonstrate that GDNF, Pitx3 and BDNF are engaged in a feed forward regulatory pathway in the rodent VM during development and in adulthood. This feed forward interaction promotes the survival of a rostrolateral mdDA neuronal subset during embryogenesis and possibly also of adult and aging SNc neurons, and protects mdDA neurons against neurotoxic insults in vitro, suggesting that it might also be relevant for the pathogenesis of PD.

2.2 Results

2.2.1 Induction of *Pitx3* expression by NF-κB-mediated GDNF/Ret signaling

To determine whether GDNF-mediated signaling is involved in the transcriptional activation of the *Pitx3* gene during embryogenesis, I first compared the spatiotemporal expression pattern of *GDNF* and *Pitx3* in the embryonic mouse VM. *GDNF* is expressed in the mantle zone (MZ) of the midbrain basal plate (BP) (ventrolateral midbrain) at E10.5, one day prior to the onset of *Pitx3* transcription in this brain region (Fig. 1a,c,e). *Pitx3* expression is detected at E11.5 in the MZ of the adjacent floor plate (FP). At this stage, *GDNF* expression is restricted to a smaller domain in the midbrain BP (Fig. 1b,d,f), and becomes undetectable in the mouse VM at E12.5 (Supplymentary Figure S1).

Given the spatiotemporal correlation of *GDNF* expression and the initiation of *Pitx3* transcription in the embryonic VM, I next asked if GDNF can promote the expression of Pitx3 in primary VM cells in vitro. Treatment of E14 rat primary VM cell cultures (grown in the absence of neurotrophins for 7 DIV) with 10 ng/ml GDNF for 24 hrs significantly increased the number of Pitx3$^+$ cells and of Pitx3$^+$/TH$^+$ cells within the VM cell population by 1.7- and

1.3-fold, respectively (Fig. 1g-m). Under these experimental conditions, GDNF treatment did not significantly increase the number of TH$^+$ neurons (Fig. 1m).

To explore if GDNF signaling is required for induction of Pitx3 expression in vivo, I counted the number of Pitx3$^+$ cells in GDNF receptor *Ret* knockout embryos. I found that the number of Pitx3$^+$ cells in *Ret*$^{-/-}$ embryos was reduced by 17.7% at E12.5 and by 10.4% at E14.5 compared to their heterozygous or wild-type littermates (Fig. 1o-v). Pitx3 expression was particularly lost in ventromedial (insets in Fig. 1o'',r'') and lateral (not shown) TH$^+$ cells in the *Ret*$^{-/-}$ embryos, suggesting that GDNF signaling might specifically induce Pitx3 expression in a TH$^+$ mdDA neuron subpopulation. The partial recovery of Pitx3$^+$ cell numbers in the E14.5 *Ret*$^{-/-}$ embryos might be due to compensation by other GDNF receptors, such as GFRα1 and NCAM, and could explain the lack of an mdDA phenotype in postnatal *DAT-Ret*$^{flx/flx}$ mice (Kramer et al., 2007; Paratcha and Ledda, 2008).
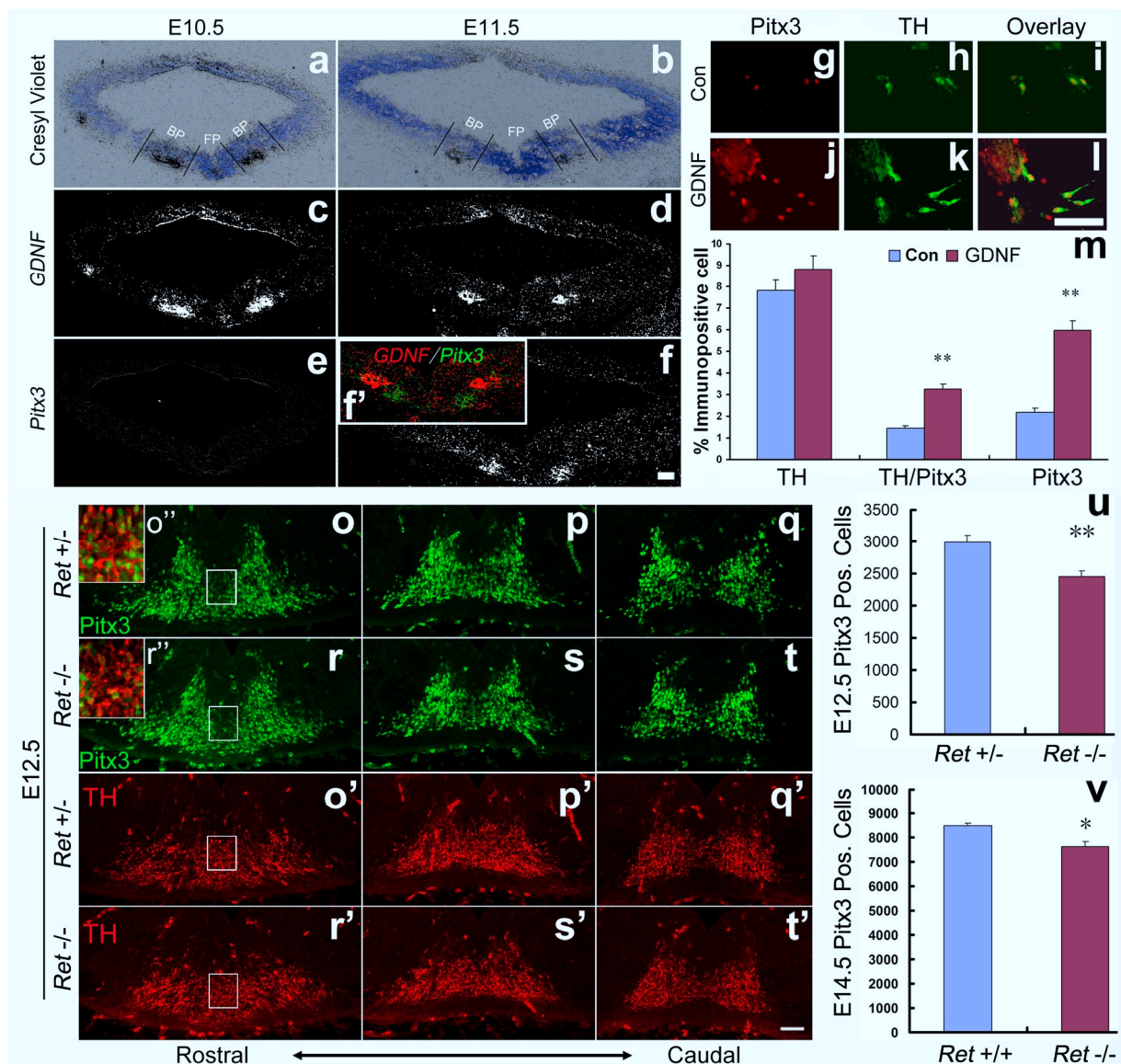
Figure 1. *GDNF/Ret* **signaling is required for activation of Pitx3 expression in an mdDA neuronal subset.** (**a-f**) Representative midbrain coronal sections of *wild-type* (C57BL/6) mouse embryos at E10.5 (**a**, **c**, **e**) and E11.5 (**b**, **d**, **f**), hybridized with riboprobes for *GDNF* (**c**, **d**) and *Pitx3* (**e**, **f**). (**a**, **b**) are Nissl-stained bright-field views of the dark-field pictures shown in (**c**, **d**). Inset (**f'**) is a pseudo-colored overlay and magnification of the VM from the consecutive sections shown in (**d**) and (**f**) (*GDNF*, red; *Pitx3*, green). *GDNF* is expressed in the midbrain basal plate (BP) at E10.5 and E11.5 adjacent to the midbrain floor plate (FP), where *Pitx3* starts to be transcribed at E11.5. (**g-l**) Immunostaining of untreated (control (Con), **g-i**) and GDNF-treated (GDNF, **j-l**) E14 rat primary VM cultures with antibodies for Pitx3 (**g**, **j**) and TH (**h**, **k**) (merged images in **i**, **l**). (**m**) Quantification of TH^+, $TH^+/Pitx3^+$ and $Pitx3^+$ cells relative to the total number of cells in untreated (Con, blue bars) and GDNF-treated (GDNF, red bars) primary rat VM cultures revealed a significant increase of $Pitx3^+$ and $Pitx3^+/TH^+$ but not of TH^+ cells in the GDNF-treated cultures as compared to untreated controls. (TH^+ cells: control, 7.82±0.47 %; GDNF-treated, 8.83±0.61 % mean±SEM; ns, not significant, $P=0.26$; $TH^+/Pitx3^+$ cells: control, 1.43±0.13 %; GDNF-treated, 3.25±0.23 % mean±SEM; double asterisks, $P<0.01$ in the independent t-test; $Pitx3^+$ cells: control, 2.19±0.19 %; GDNF-treated, 5.95±0.46 % mean±SEM; double asterisks, $P<0.01$ in the independent t-test). Data were derived from three independent experiments. (**o-t'**) Representative VM close-up views on coronal sections of $Ret^{+/-}$ (**o-q**, **o'-q'**) and $Ret^{-/-}$ (**r-t**, **r'-t'**) mouse embryos at E12.5, immunostained for Pitx3 (**o-t**) and TH (**o'-t'**). Insets (o'', r'') are merged images and higher magnifications of the boxed areas in (**o**, **o'**, **r**, **r'**). (**u**, **v**) Quantification on coronal or sagittal midbrain sections revealed a significant decrease of $Pitx3^+$ cells by 17.7% in E12.5 $Ret^{-/-}$ embryos (**u**) and by 10.4% in E14.5 $Ret^{-/-}$ embryos (**v**) as compared to their wild-type ($Ret^{+/-}$ and $Ret^{+/+}$) littermates ($Pitx3^+$ cells: E12.5 $Ret^{+/-}$, 2981±125, n=3; E12.5 $Ret^{-/-}$, 2455±85, n=3; E14.5 $Ret^{+/+}$, 8491±105, n=4; E14.5 $Ret^{-/-}$, 7609±224, n=3 mean±SEM; double asterisks, $P<0.01$ in the paired t-test; single asterisk, $P<0.05$ in the independent t-test). Scale bar: 50 μm.
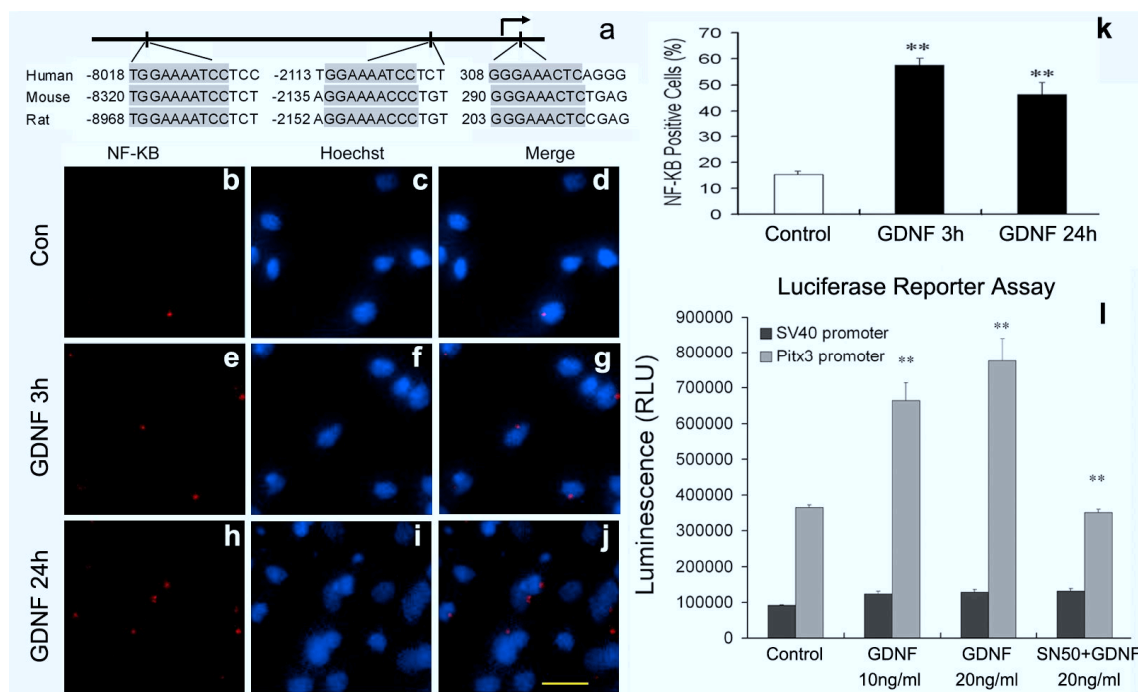
Figure 2. NF-κB mediated GDNF-signaling activates murine *Pitx3* transcription. (**a**) The human, mouse and rat *Pitx3* promoter region contains three highly conserved NF-κB BS (consensus sequence: 5'-GGGRNTYYCC-3' (R = A or G, Y = C or T, N = any nucleotide)). Position of the first nucleotide of each BS relative to the transcription start site (arrow). (**b-j**) Immunostaining for NF-κB (**b**, **e**, **h**) and nuclear staining (Hoechst; **c**, **f**, **i**) (merged images in **d**, **g**, **j**) of untreated (**b-d**) E14 rat primary VM cultures or after

treatment with GDNF for 3 hrs (**e-g**) or 24 hrs (**h-j**). (**k**) Quantification of NF-κB$^+$ cells relative to the total number of cells in these cell cultures with or without GDNF-treatment (control: 15.3±1.3 %; 3 hrs GDNF: 57.6±2.5 %; 24 hrs GDNF: 46.1±4.8 % mean±SEM; double asterisks, *P*<0.005 in the independent t-test; n=3). (**l**) Transfection of SH-SY5Y cells with *pGL3-Pitx3* promoter vector (light grey bars) and subsequent treatment of these cells with 10 or 20 ng/ml GDNF resulted in a dose-dependent activation of the *Pitx3* promoter as compared to untreated controls. Dark grey bars represent values from *pRL-SV40* vector (internal control). GDNF-mediated activation of the *Pitx3* promoter was blocked by the simultaneous application of SN50, an inhibitor of NF-κB nuclear translocation. (Control: *SV40* promoter, 96954±2863; *Pitx3* promoter, 365722±7460; GDNF 10ng/ml: *SV40* promoter, 123900±6980; *Pitx3* promoter, 663831±51615; GDNF 20ng/ml: *SV40* promoter, 128212±7174; *Pitx3* promoter, 776831±62941; SN50 + GDNF 20ng/ml: *SV40* promoter, 131242±7724; *Pitx3* promoter, 350674±9528 mean±SEM; double asterisks, *P*<0.005 in one-way ANOVA for repeated measurements). Data were derived from three independent experiments. Scale bar: 20 μm.

I next tested whether GDNF signaling directly activates the *Pitx3* promoter in rodent VM cells. GDNF-mediated signaling enhances the nuclear translocation of NF-κB protein complexes and subsequent activation of NF-κB target genes in mdDA neurons (Cao et al., 2008; Wang et al., 2008a). Analysis of the human, mouse and rat *Pitx3* promoter regions using bioinformatics prediction tools revealed the existence of conserved NF-κB binding sites (BS) in these regions (Fig. 2a), and treatment of E14 rat primary VM cultures after 7 DIV with GDNF for 3 or 24 hrs increased the nuclear translocation of NF-κB, as expected (Fig. 2b-k). To determine whether this treatment resulted in increased activation of the *Pitx3* promoter, I made use of a *Pitx3* promoter/reporter construct containing a conserved NF-κB BS. GDNF treatment of SH-SY5Y cells transfected with this *Pitx3* reporter construct resulted in a dose-dependent activation (80-110% increase) of the *Pitx3* promoter (Fig. 2l). This activation was prevented when I treated the cells with SN50, an inhibitor of NF-κB nuclear translocation (Lin et al., 1995). I thus concluded that GDNF/Ret signaling is necessary and sufficient for the activation of the *Pitx3* promoter in the embryonic rodent VM, and I identified NF-κB as a mediator of this process.

2.2.2 GDNF-mediated activation of Pitx3 expression induces *BDNF* transcription in vitro

I have previously shown that overexpression of Pitx3 up-regulates the transcription and secretion of BDNF protein from neuroblastoma cells and primary VM as well as astrocyte cultures (Peng et al., 2007; Yang et al., 2008). I therefore hypothesized that GDNF-mediated

activation of Pitx3 expression might subsequently induce the transcription of *BDNF* in these cells. To test this hypothesis, I treated E14 rat primary VM cultures after 7 DIV with GDNF and evaluated the transcription of *Pitx3* and *BDNF* under these conditions. As expected, GDNF treatment increased the transcription of *Pitx3* and *BDNF* in these cultures by 1.3- and 1.4-fold, respectively, and this effect of GDNF on *Pitx3* and *BDNF* transcription was blocked by the application of the NF-κB inhibitor SN50 (Fig. 3a,c). These results were also confirmed at protein levels (Fig. 3b). To further establish whether the GDNF-induced activation of *BDNF* transcription was mediated by Pitx3 and not by other Pitx3-independent pathways, I depleted Pitx3 in these cultures by siRNA-mediated knock-down. Quantitative RT-PCR indicated that transfection of a *Pitx3* siRNA after 1 hr of GDNF-treatment reduced *Pitx3* mRNA levels by 56%, concomitant with a 32% reduction of *BDNF* mRNA levels in these cultures (Fig. 3d,f). A slight but not significant decrease in *Pitx3* and *BDNF* mRNA levels was also observed after transfection of a control (non-silencing) siRNA oligonucleotide (Fig. 3d,f). This reduction was most likely unspecific and due to the lipofection of the oligonucleotides, as a similar decrease in mRNA levels was observed in sham-lipofected GDNF-treated cultures as compared to untransfected controls (data not shown). I also used Western blotting to confirm that *Pitx3* knock-down leads to a reduction of Pitx3 and BDNF protein levels in GDNF-treated primary VM cultures (Fig. 3e). These results therefore suggest that Pitx3 mediates the transcriptional activation of the *BDNF* gene following treatment of primary VM cells with GDNF.
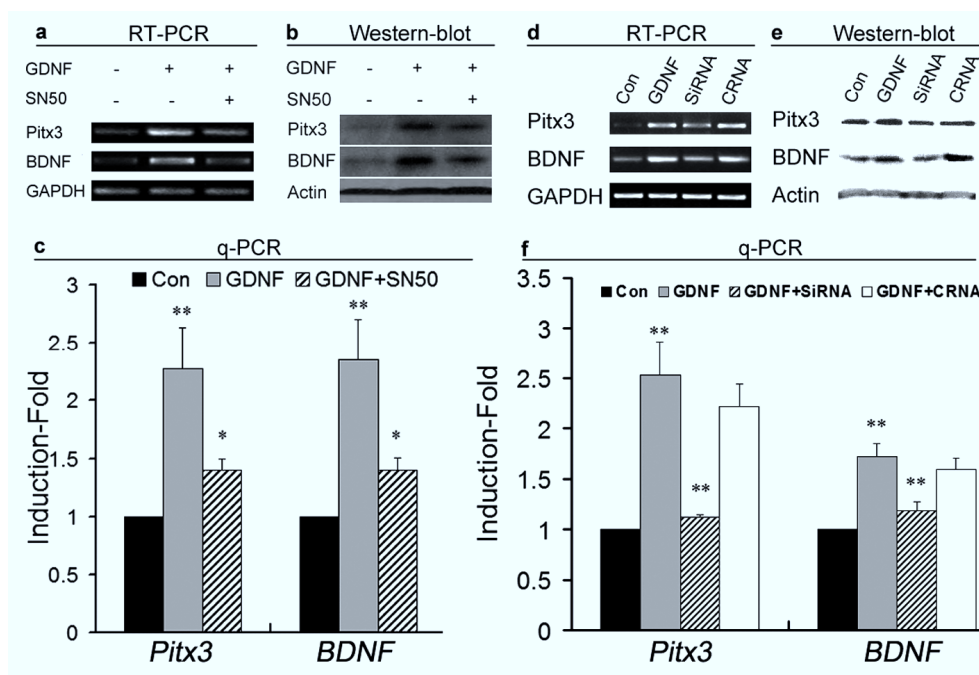
Figure 3. GDNF-mediated induction of Pitx3 expression activates *BDNF* transcription. (a) RT-PCR and **(b)** Western blot analyses of untreated (1st lane), GDNF-treated (2nd lane), and SN50 + GDNF-treated (3rd lane) E14 rat primary VM cultures showed increased Pitx3 and BDNF expression after GDNF-treatment, which was blocked by simultaneous treatment with NF-κB inhibitor SN50. **(c)** qPCR analysis indicated an 1.3-fold increase of *Pitx3* and 1.4-fold increase of *BDNF* mRNA levels after GDNF-treatment, and 70% reduction in both cases after SN50 application (Pitx3: GDNF, 2.27±0.36; GDNF + SN50, 1.40±0.09 mean±SEM.; BDNF: GDNF, 2.35±0.35; GDNF + SN50, 1.40±0.11 mean±SEM; single asterisk, $P<0.05$; double asterisks, $P<0.005$ in the one-way ANOVA for repeated measurements; n=4). **(d)** RT-PCR and **(e)** Western blot analyses of untreated (1st lane), GDNF-treated (2nd lane), *Pitx3* siRNA + GDNF-treated (3rd lane), and *control* siRNA + GDNF-treated (4th lane) E14 rat primary VM cultures revealed that siRNA-mediated knockdown of *Pitx3* (SiRNA), but not a *control* siRNA (CRNA), abolished the increased expression of BDNF in these cultures after GDNF-treatment. **(f)** qPCR analysis indicated that *Pitx3* siRNA + GDNF treatment resulted in a 56% and 32% reduction of *Pitx3* and *BDNF* mRNA levels, respectively, as compared to GDNF only-treated cultures and a control siRNA (CRNA) (Pitx3: GDNF, 2.53±0.33; GDNF + *Pitx3* siRNA, 1.12±0.02; GDNF + *control* siRNA, 2.21±0.22; mean±SEM; BDNF: GDNF, 1.73±0.12; GDNF + *Pitx3* siRNA, 1.18±0.09; GDNF + *control* siRNA, 1.59±0.11; mean±SEM; double asterisks, $P<0.005$ in the one-way ANOVA for repeated measurements). Data were derived from at least three independent experiments in each case.

2.2.3 Pitx3 is required for *BDNF* transcription in an mdDA neuronal subset in vivo

My results raised the possibility that Pitx3 is an essential regulator of *BDNF* gene expression in the rodent VM. To address this possibility, I analyzed the time-course of *BDNF* expression in wild-type (*Pitx3*$^{+/+}$ and *Pitx3*$^{+/GFP}$ mice) and *Pitx3* null mutant (*Pitx3*$^{GFG/GFP}$) mice, which allow the fate-mapping of Pitx3-expressing (GFP^{+}) cells (Maxwell et al., 2005). In wild-type mouse embryos, *Pitx3* expression in the VM was first detected around E11.0-E11.5 (Fig. 1e,f) (Smidt et al., 1997); at this or earlier stages, *BDNF* expression was not detected in the VM (Fig. 4a-c and data not shown). I found that *BDNF* was widely transcribed in the wild-type and *Pitx3*$^{+/GFP}$ VM at E12.5, and exhibited a particularly prominent expression domain in the rostrolateral and medial VM overlapping with GFP^{+} (Pitx3^{+}) mdDA neurons (Fig. 4e-g'' and Supplementary Fig. S2). Remarkably, *BDNF* expression in this rostrolateral and medial domain was entirely lost in the *Pitx3*$^{GFP/GFP}$ embryos at E12.5, although the corresponding GFP^{+} neurons were still present in this domain and despite the persistent expression of *BDNF* in the adjacent Pitx3-negative (GFP^{-}) VM tissue of the null mutants (Fig. 4h-j'').
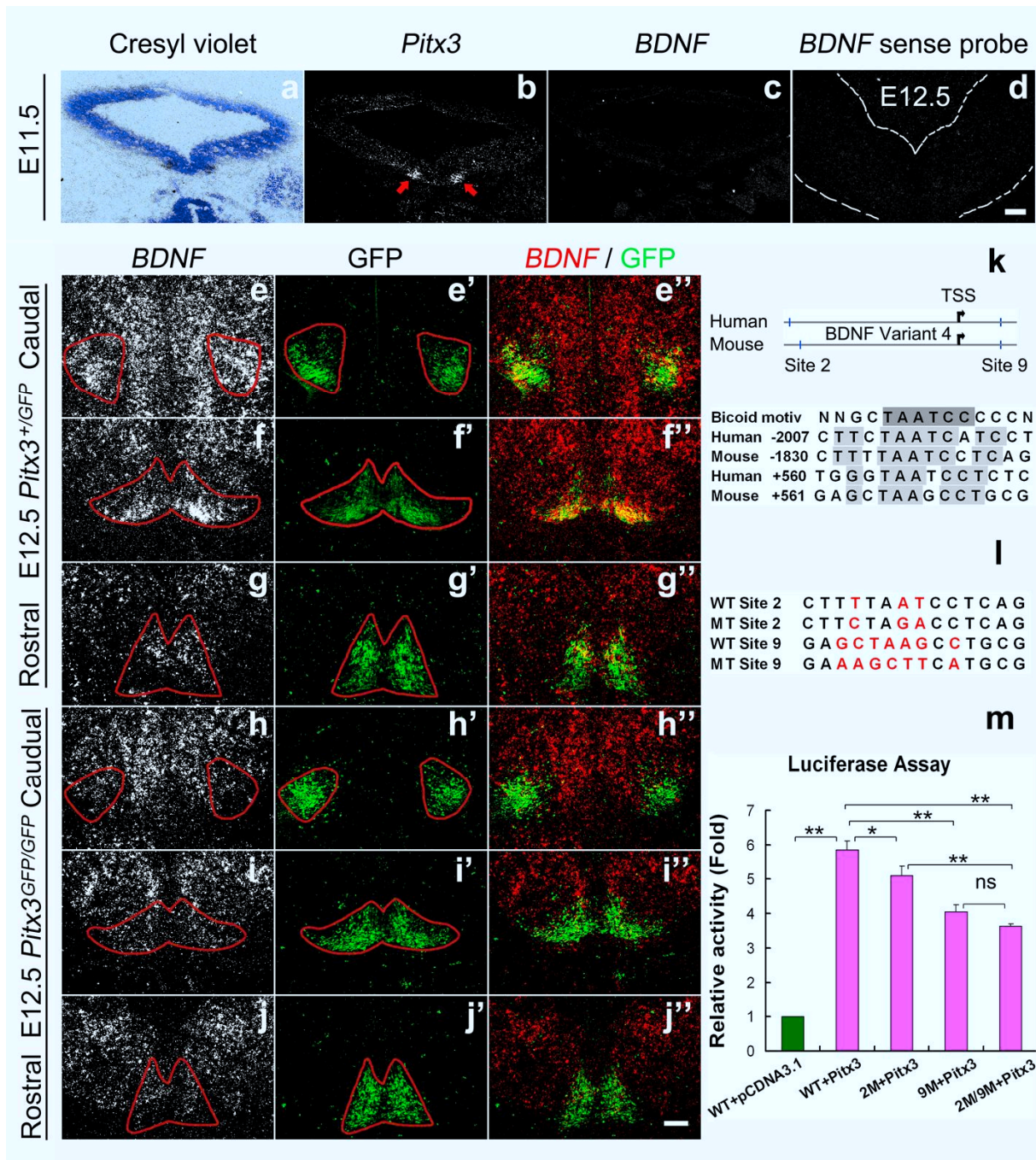
Figure 4. Pitx3 is required for the onset of *BDNF* transcription in an mdDA neuronal subpopulation at E12.5. **(a-d)** Representative midbrain coronal sections of wild-type mouse embryos at E11.5 (a-c, consecutive sections) and E12.5 (d), hybridized with *Pitx3* (**b**), *BDNF* anti-sense (**c**) and *BDNF* sense (**d**) riboprobes. (**a**) Nissl-stained bright-field view of the dark-field picture shown in (**b**). *BDNF* is not expressed in the murine VM at E11.5, although *Pitx3* starts to be expressed in a bilateral VM domain at this stage (red arrows in **b**). **(e-j'')** Representative coronal sections at different rostro-caudal levels of the midbrain from E12.5 *Pitx3*[+/GFP] (**e-g''**) and *Pitx3*[GFP/GFP] (**h-j''**) mice, hybridized with *BDNF* anti-sense riboprobe (**e-j**), or immunostained for GFP (**e'-j'**). Merged images are shown in (**e''-j''**). *BDNF* expression is not induced in a rostrolateral and medial GFP[+] mdDA domain of the *Pitx3*[GFP/GFP] embryos at E12.5 (**h-j''**). Note that the *BDNF* sense probe does not give a signal at this stage in wild-type embryos (section shown in **d**), demonstrating the specificity of the *BDNF* anti-sense riboprobe. **(k-m)** Two highly conserved *Pitx3/Bicoid-like* TF BS in the human and mouse *BDNF* promoter regions (Site 2 and Site 9, positions relative to the transcription start site (TSS, arrow)) were tested for *BDNF* promoter activation by Pitx3 (**k**).

Co-transfection of *pGL3-BDNF* promoter vector containing these two conserved *Pitx3* BS (WT) and *pcDNA3.1-Pitx3* vector (red bars) into HEK293 cells resulted in a 4.9-fold activation of the *BDNF* promoter relative to the control (*pcDNA3.1* only, green bar) (Pitx3: 5.86 ± 0.24 mean±SEM; double asterisks, $P < 0.005$ in the one-way ANOVA for repeated measurements) (**m**). Site-directed mutagenesis of *Pitx3* BS 2 (MT Site 2) and/or 9 (MT Site 9) (**l**) attenuated significantly *BDNF* promoter activation by Pitx3 (*BDNF WT* promoter: 5.86 ± 0.24; *BDNF* promoter with MT Site 2 (2M): 5.11 ± 0.27; *BDNF* promoter with MT Site 9 (9M): 4.04 ± 0.22; *BDNF* promoter with MT Site 2 and MT Site 9 (2M/9M): 3.6 ± 0.08; mean±SEM; single asterisk, $p < 0.05$; double asterisks, $P < 0.005$ in the one-way ANOVA for repeated measurements) (**m**). Data were derived from three independent experiments. Scale bar: 100 µm.

To determine whether Pitx3 can directly activate the transcription of the *BDNF* gene, I searched for conserved *Pitx3*/*Bicoid-like* BS within the mouse and human *BDNF* promoters. I found two highly conserved *Pitx3*/*Bicoid-like* BSs in these two species, one located approximately 1.8-2.0 kb upstream (referred to as BS2) and the other one located approximately 560 bp downstream (referred to as BS9) of the putative transcription start site (TSS) for the mouse *BDNF* variant 4 (Fig. 4k). Co-transfection of a luciferase reporter construct containing 2.6 kb of mouse *BDNF* promoter sequences (including these two highly conserved *Pitx3* BS and 7 other putative *Pitx3* BS) and a Pitx3 expression vector resulted in a 4.9-fold increase in luciferase (promoter) activity relative to the control (Fig. 4m). Moreover, site-directed mutagenesis of either one of these two conserved *Pitx3* BS decreased the Pitx3-induced activation of the *BDNF* promoter by 15% (BS 2) and 37% (BS 9) (Fig. 4l,m), whereas mutation of both BS 2 and 9 resulted in a 47% decrease of *BDNF* promoter activity after Pitx3 co-transfection (Fig. 4m).

To establish if the loss of *BDNF* expression in the rostrolateral and medial VM of the *Pitx3*$^{GFP/GFP}$ embryos is rapidly followed by the death of GFP^{+} (Pitx3^{+}) mdDA neurons in these embryos, I assessed the proportion of apoptotic (cCasp3^{+}) and GFP^{+} cells relative to the total number of GFP^{+} mdDA neurons in wild-type (*Pitx3*$^{+/GFP}$) and mutant (*Pitx3*$^{GFP/GFP}$) embryos at E12.5 (Fig. 5a-e). This proportion was significantly increased by approximately 3-fold in the rostral but not caudal VM of the *Pitx3*$^{GFP/GFP}$ embryos as compared to their wild-type littermates (Fig. 5e), indicating that the lack of *BDNF* expression indeed correlates with a reduced survival of mdDA neurons in the rostral VM of the *Pitx3*$^{GFP/GFP}$ embryos.
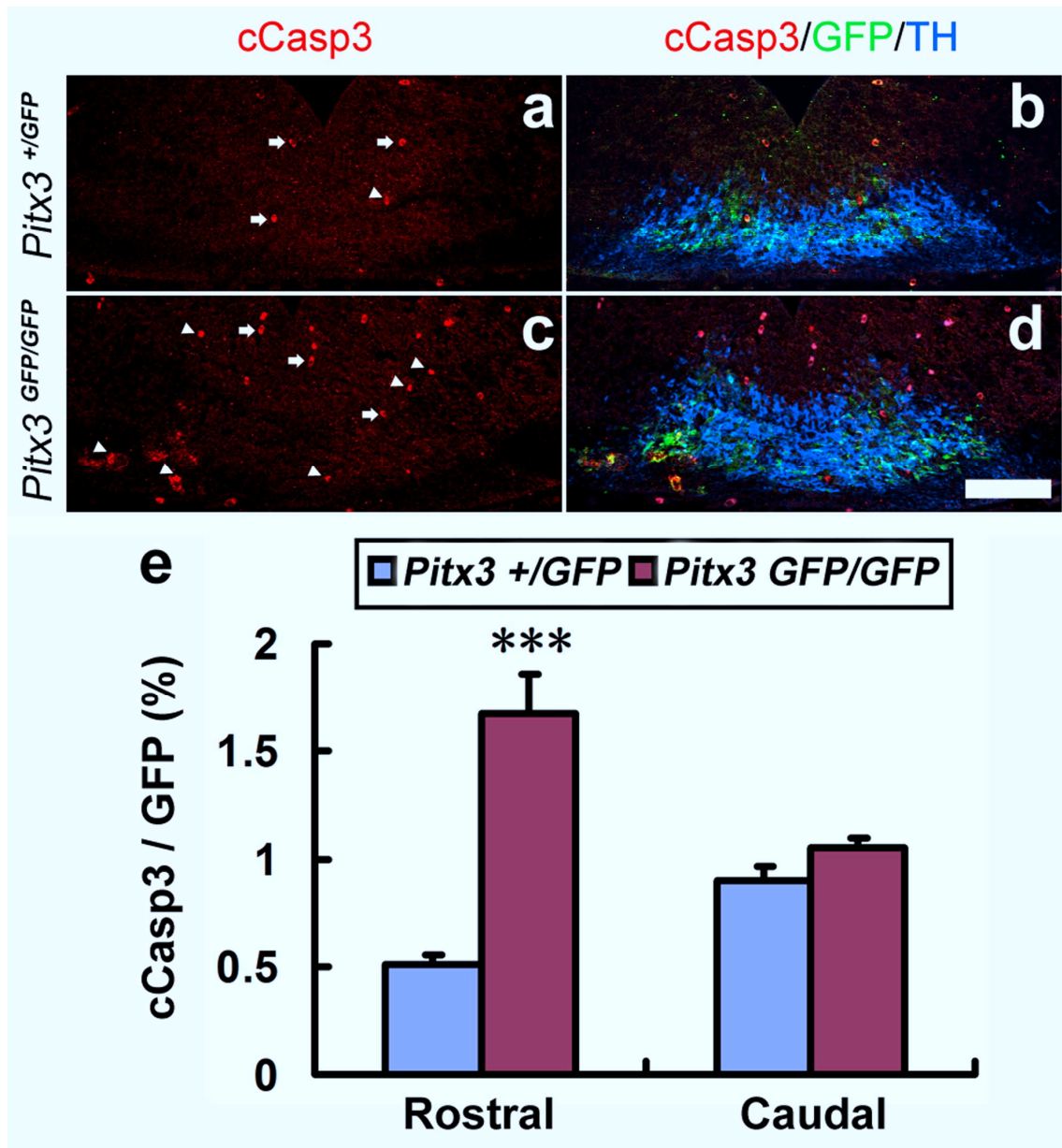
Figure 5. The loss of *BDNF* expression correlates with an increased apoptotic cell death of mdDA neurons in the E12.5 *Pitx3*$^{GFP/GFP}$ rostral VM. (**a-d**) Triple immunostaining for cleaved Caspase 3 (cCasp3), GFP and TH on representative midbrain coronal sections of *Pitx3*$^{+/GFP}$ (**a**, **b**) and *Pitx3*$^{GFP/GFP}$ (**c**, **d**) embryos at E12.5 revealed an increase of apoptotic Pitx3$^+$ mdDA neurons (cCasp3$^+$ (red) and GFP$^+$ (green) double-labelled cells, white arrowheads) in the mutant VM. White arrows point at erythrocytes that were stained unspecifically for cCasp3. (**e**) Quantification of cCasp3$^+$/GFP$^+$ double-labelled cells relative to the total amount of GFP$^+$ (Pitx3$^+$) cells in these sections showed a significant increase of apoptotic mdDA neurons in the rostral (cCasp3$^+$/GFP$^+$ cells: E12.5 *Pitx3*$^{+/GFP}$, 0.506±0.047 %; E12.5 *Pitx3*$^{GFP/GFP}$, 1.676±0.185 %; n=3 mean±SEM; triple asterisks, $P<0.001$ in the independent samples t-test), but not caudal (cCasp3$^+$/GFP$^+$ cells: E12.5 *Pitx3*$^{+/GFP}$, 0.902±0.068 %; *Pitx3*$^{GFP/GFP}$, 1.056±0.042 %; n=3 mean±SEM) VM of the *Pitx3*$^{GFP/GFP}$ embryos. Scale bar: 100 μm.

I next investigated the effect of *Pitx3* inactivation on BDNF expression in late gestational and postnatal mdDA neurons. *BDNF* expression was still not detected in the rostrolateral and

medial VM domain of *Pitx3*$^{GFP/GFP}$ embryos at E14.5 (Fig. 6a-f'') and E16.5 (data not shown). Loss of *Pitx3* resulted in a notable decrease of TH$^+$ SNc mdDA neurons in the null mutant VM at postnatal day 30 (P30), concomitant with a strong reduction of BDNF-expressing cells in the same region (Fig. 6g-l''). Notably, *BDNF* transcription appeared to be very low or almost undetectable in the caudomedial mdDA domain throughout embryonic development (Fig. 4e-g'', Fig. 6a-c''), and this mdDA neuronal subset was less affected in the *Pitx3*$^{GFP/GFP}$ null mutants at embryonic and postnatal stages (Fig. 4h-j'', Fig. 5e, Fig. 6d-f'' and j-l''; (Maxwell et al., 2005)). Collectively, these results indicate that Pitx3 directly activates the *BDNF* promoter in an mdDA neuron subpopulation located in the rostrolateral and medial VM of the mouse embryo, and suggest that the Pitx3-mediated activation of BDNF expression is necessary for the survival of this mdDA neuronal subset at embryonic and postnatal stages.
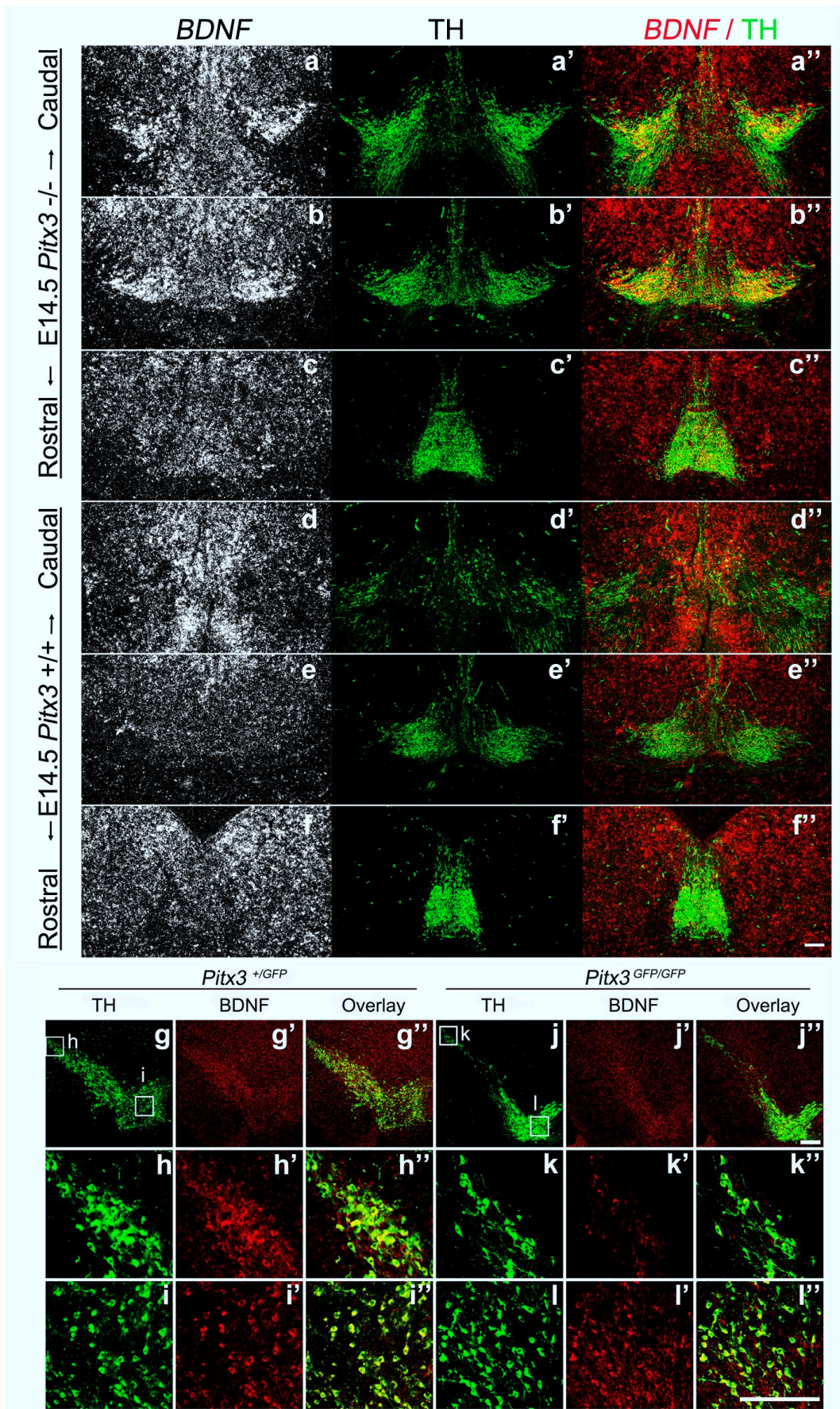
Figure 6. Lack of *BDNF* expression in an mdDA neuronal subpopulation that disappears at later embryonic/postnatal stages in the absence of *Pitx3*. (a-l'') Representative coronal midbrain sections

from E14.5 (**a-f''**, different rostro-caudal levels) and P30 (**g-l''**) Pitx3$^{+/GFP}$ (**a-c''**; **g-i''**) and Pitx3$^{GFP/GFP}$ (**d-f''**; **j-l''**) mice, hybridized with a *BDNF* riboprobe (**a-f**), or immunostained for TH (**a'-f'**, **g-l**) and BDNF (**g'-l'**). Merged images are shown in (**a''-f''**) and (**g''-l''**). *BDNF* is expressed strongly in a rostrolateral TH$^+$ mdDA domain in the wild-type (*Pitx3$^{+/GFP}$*) embryos (**a-c''**; **g-i''**), but this *BDNF$^+$* domain was completely lost in the VM of *Pitx3$^{GFP/GFP}$* embryos at E14.5 (**d,d'',e,e'',f,f''**), concomitant with a strong reduction at E14.5 (**d'-f'**) and followed by the almost complete loss at P30 (**j-l''**) of the rostrolateral (SNc) TH$^+$ mdDA neurons in these mutants. Scale bar: 100 μm.

2.2.4 BDNF augments the survival of mdDA neurons in *Pitx3* null mutant primary VM cultures

To further investigate if the lack of *BDNF* expression contributes to the loss of mdDA neurons in *Pitx3$^{GFP/GFP}$* mice (Fig. 5 and Maxwell et al., 2005), I tested whether BDNF treatment is sufficient to rescue the numbers of mdDA neurons in primary VM cultures derived from E11.5 *Pitx3$^{GFP/GFP}$* embryos. I found a reduction of GFP$^+$ cell numbers (cells that would express Pitx3 in the wild-type) by 13% , of TH$^+$ cells by 37.5%, and of GFP/TH double-positive cells by 40% in the untreated *Pitx3$^{GFP/GFP}$* cultures as compared to untreated wild-type (*Pitx3$^{+/GFP}$*) cultures (Fig. 7a-f,m). This result is consistent with in vivo data from E12.5 *Pitx3$^{GFP/GFP}$* mice, showing a reduction of GFP$^+$ cells by 21%, of TH$^+$ cells by 54% and of GFP/TH double-positive cells by 48% relative to the *Pitx3$^{+/GFP}$* controls (Maxwell et al., 2005), and confirms a selective loss of GFP$^+$ and TH$^+$ cells in the absence of *Pitx3* also in primary VM cultures. Notably, BDNF treatment of *Pitx3$^{GFP/GFP}$* VM cultures increased the numbers of GFP$^+$ cells by 29.6%, of TH$^+$ cells by 84.7% and of TH/GFP double-positive cells by 66.7% relative to the untreated *Pitx3$^{GFP/GFP}$* cultures, thereby reaching similar numbers as in the BDNF-treated wild-type (*Pitx3$^{+/GFP}$*) cultures (Fig. 7g-m). To determine if this was due to a survival-promoting effect of the BDNF treatment on the cultured mdDA neurons, I assessed the proportion of apoptotic (cCasp3$^+$) mdDA (GFP$^+$) neurons in the untreated and BDNF-treated VM cultures from wild-type (*Pitx3$^{+/GFP}$*) and mutant (*Pitx3$^{GFP/GFP}$*) embryos. As expected, this proportion was significantly increased in the untreated *Pitx3$^{GFP/GFP}$* VM cultures as compared to the untreated controls (Fig. 7n-s,w). Notably, the increased death of GFP$^+$ cells in the *Pitx3$^{GFP/GFP}$* VM cultures was rescued back to control levels by the addition of BDNF to these cultures (Fig. 7t-w), indicating that in the absence of *Pitx3*, exogenous BDNF application prevents the cell death of cultured *Pitx3*-null (*Pitx3$^{GFP/GFP}$*) mdDA neurons.
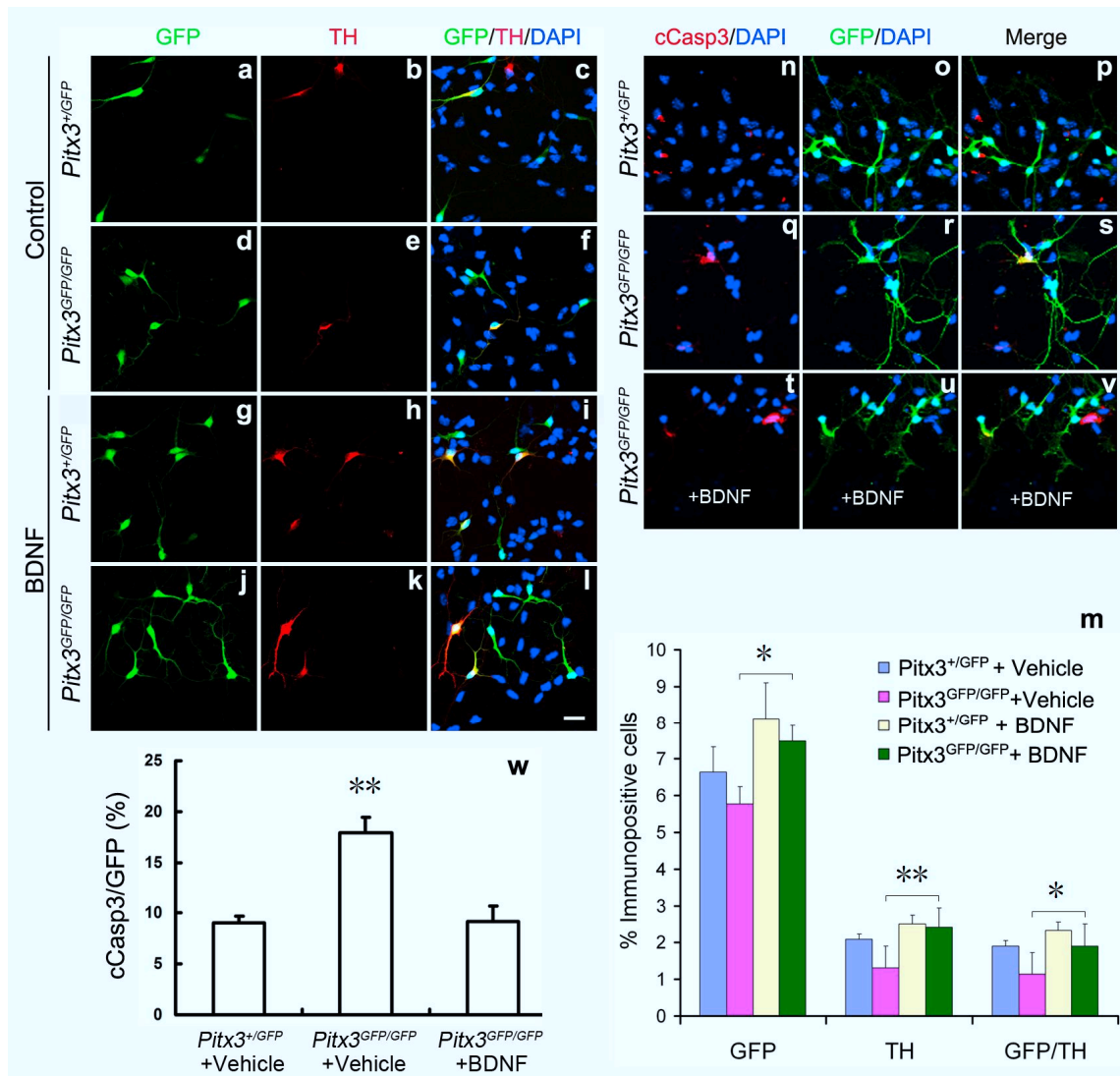
Figure 7. BDNF augments the survival of mdDA neurons in _Pitx3GFP/GFP_ primary VM cultures. (a-v) Primary VM cultures derived from E11.5 _Pitx3+/GFP_ (**a-c**, **g-i**, **n-p**) and _Pitx3GFP/GFP_ (**d-f**, **j-l**, **q-v**) embryos were treated with vehicle (0.1% BSA) (**a-f**, **n-s**) or 20 ng/ml BDNF (**g-l**, **t-v**) for 4 d and immunostained for GFP (green in **a**, **d**, **g**, **j**, **o**, **r**, **u**), TH (red in **b**, **e**, **h**, **k**) and cCasp3 (red in **n**, **q**, **t**); merged images with DAPI stain in (**c**, **f**, **i**, **l**, **p**, **s**, **v**). (**m**) Quantification of GFP and TH immunopositive cells in these 4 experimental groups revealed an increased number of GFP$^+$ and TH$^+$ mdDA neurons in the BDNF-treated relative to the untreated _Pitx3GFP/GFP_ VM cultures (GFP$^+$ cells: _Pitx3+/GFP_ untreated, 6.64±0.69 %; _Pitx3GFP/GFP_ untreated, 5.78±0.46 %; _Pitx3+/GFP_ BDNF-treated, 8.11±0.99 %; _Pitx3GFP/GFP_ BDNF-treated, 7.49±0.44 %; TH$^+$ cells: _Pitx3+/GFP_ untreated, 2.09±0.14 %; _Pitx3GFP/GFP_ untreated, 1.31±0.60 %; _Pitx3+/GFP_ BDNF-treated, 2.51±0.24 %; _Pitx3GFP/GFP_ BDNF-treated, 2.42±0.53 %; TH$^+$/GFP$^+$ cells: _Pitx3+/GFP_ untreated, 1.91±0.15 %; _Pitx3GFP/GFP_ untreated, 1.14±0.59%; _Pitx3+/GFP_ BDNF-treated, 2.34±0.22 %; _Pitx3GFP/GFP_ BDNF-treated, 1.90±0.60 %; mean±SEM). (**w**) Quantification of the relative amount of apoptotic (cCasp3$^+$) mdDA neurons (GFP$^+$) in these cultures showed an increase of apoptotic cells in the untreated _Pitx3GFP/GFP_ VM cultures as compared to the untreated controls, that was rescued by the addition of BDNF protein to the mutant cultures (cCasp3$^+$/GFP$^+$ cells: _Pitx3+/GFP_ untreated, 9.11±0.55 %; _Pitx3GFP/GFP_ untreated, 17.92±1.46 %; _Pitx3GFP/GFP_ BDNF-treated, 9.12±1.63 %). Paired t-test was used for statistical analysis of treatment effects within the same genotype, and one way ANOVA was used for statistical analysis of genotype differences for the same treatment. Single asterisk, _P_<0.05; double asterisks,

P<0.005. Data were derived from three independent experiments. Scale bar: 20 μm.

2.2.5 Intrastriatal injection of GDNF up-regulates Pitx3 and BDNF expression in the adult SNc

My previous results strongly suggested the existence of a feed-forward mechanism for the initiation and/or maintenance of GDNF, Pitx3 and BDNF expression in the murine VM during embryonic development. I therefore hypothesized that this feed-forward mechanism might also persist in the adult brain, as it is known that GDNF released from striatal target cells is taken up and retrogradely transported to the soma of mdDA neurons, where it promotes their survival in the early postnatal and adult rodent brain (Kholodilov et al., 2004; Oo et al., 2003; Tomac et al., 1995). To test this hypothesis, I injected GDNF protein unilaterally into the striatum of adult rats, and 48 hrs later I analyzed the endogenous expression levels of Pitx3 and BDNF proteins in the ipsilateral (GDNF-treated) SNc relative to the contralateral (vehicle-treated) control side. I found that Pitx3 and BDNF protein levels were increased by 2.8- and 6.1-fold, respectively, in the ipsilateral (GDNF-treated) SNc, as determined by immunohistochemistry (Fig. 8a-l) and on Western blots (Fig. 8n-p). These data provide direct evidence that retrograde GDNF signaling stimulates Pitx3 and BDNF expression in mature SNc mdDA neurons.
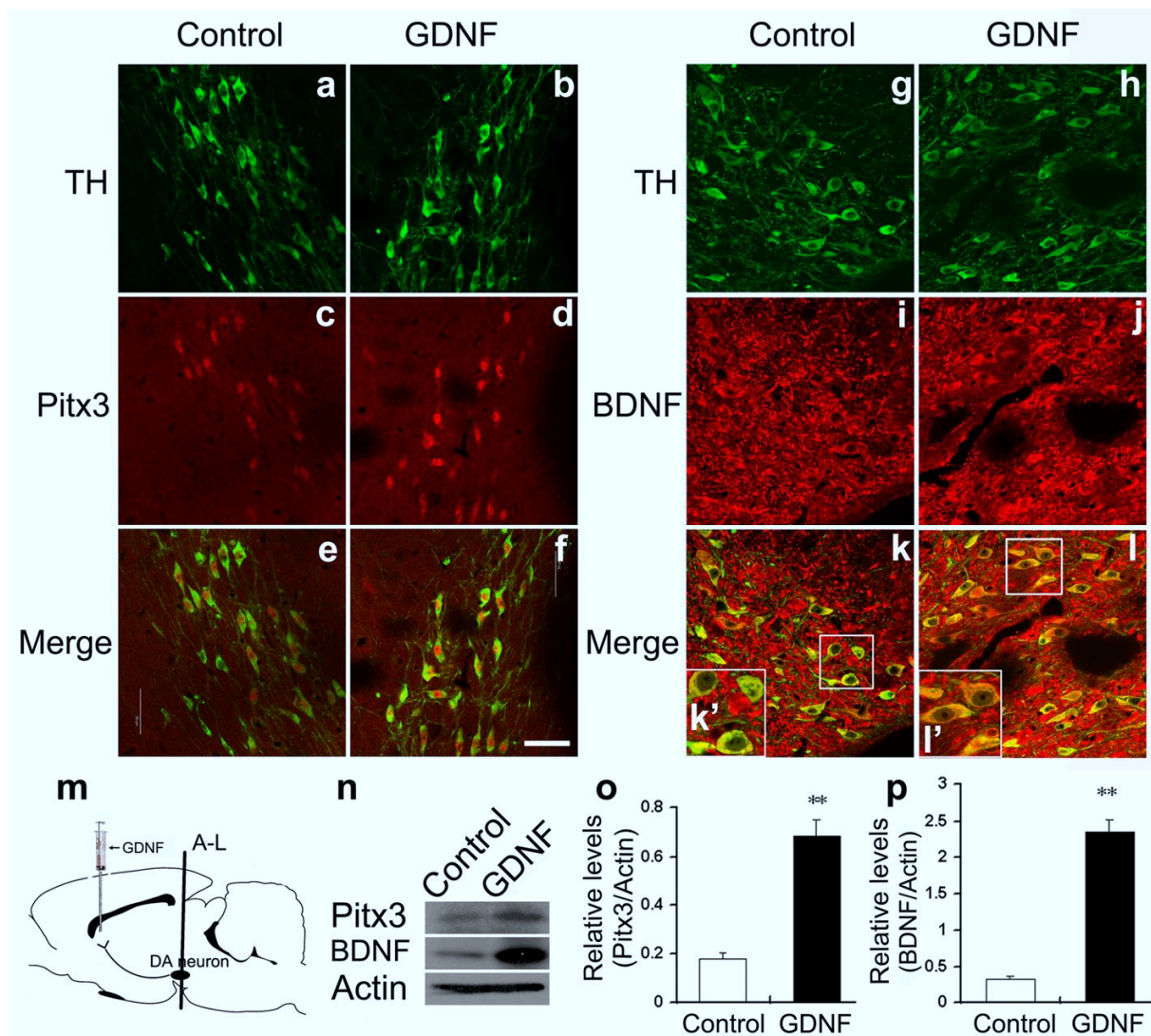
Figure 8. Intrastriatal Injection of GDNF up-regulates Pitx3 and BDNF expression in the adult SNc.
(a-l) Representative coronal sections from the SNc of adult male rats who had received an unilateral injection of 0.9% saline (control, **a**, **c**, **e**, **g**, **i**, **k**) and of 15 ng/μl GDNF into the contralateral side of the striatum (**b**, **d**, **f**, **h**, **j**, **l**) 48 hrs before, immunostained for TH (**a**, **b**, **g**, **h**), Pitx3 (**c**, **d**) and BDNF (**i**, **j**). Merged images are shown in (**e**, **f**, **k**, **l**). Insets in (**k'**, **l'**) are higher magnifications of the boxed areas in (**k**, **l**), respectively. **(m)** Schematic drawing of the striatal injection site and position of the VM sections shown in (**a-l**). **(n)** Western blots using protein extracts from vehicle-treated control and GDNF-treated contralateral side of the VM showed that unilateral intrastriatal injection of GDNF leads to a 2.8-fold increase of Pitx3 expression (quantification in (**o**)) and 6.1-fold increase of BDNF expression (quantification in (**p**)) in the ipsilateral mdDA neurons (control: Pitx3, 0.18±0.02; BDNF, 0.33±0.04 mean±SEM; GDNF-treated (GDNF): Pitx3, 0.68± 0.07; BDNF, 2.35±0.18; double asterisks, $P<0.01$ in the independent samples t-test for repeated measurements; n=3). Scale bar: 50 μm.

2.2.6 BDNF, but not GDNF, protects *Pitx3*^{-/-} mdDA neurons against 6-OHDA neurotoxicity

Given the previous result, I wanted to know if the neuroprotective effect of GDNF against 6-OHDA toxicity on mdDA neurons might be due to Pitx3-mediated activation of BDNF

expression in these neurons. Therefore, I treated wild-type ($Pitx3^{+/GFP}$) and $Pitx3$ null mutant ($Pitx3^{GFP/GFP}$) VM cultures after 3 DIV with 6-OHDA, and assessed the effect of a previous 2 hr incubation with GDNF or BDNF on these 6-OHDA-treated cultures. Treatment with 6-OHDA significantly reduced the numbers of TH$^+$ cells in both wild-type and mutant cultures (Fig. 9a-f,m-r,y), as expected. Prior incubation with GDNF or BDNF significantly rescued the numbers of TH$^+$ mdDA neurons in the wild-type ($Pitx3^{+/GFP}$) VM cultures, reaching a similar level as under normal (untreated) conditions (Fig. 9g-l,y). Remarkably, the numbers of TH$^+$ mdDA neurons in the 6-OHDA-treated $Pitx3^{GFP/GFP}$ VM cultures were only rescued back to normal (untreated) levels after a previous incubation of these cells with BDNF, but not with GDNF (Fig. 9s-y), indicating that GDNF cannot protect TH$^+$ mdDA neurons against 6-OHDA-induced neurotoxicity in the absence of $Pitx3$.
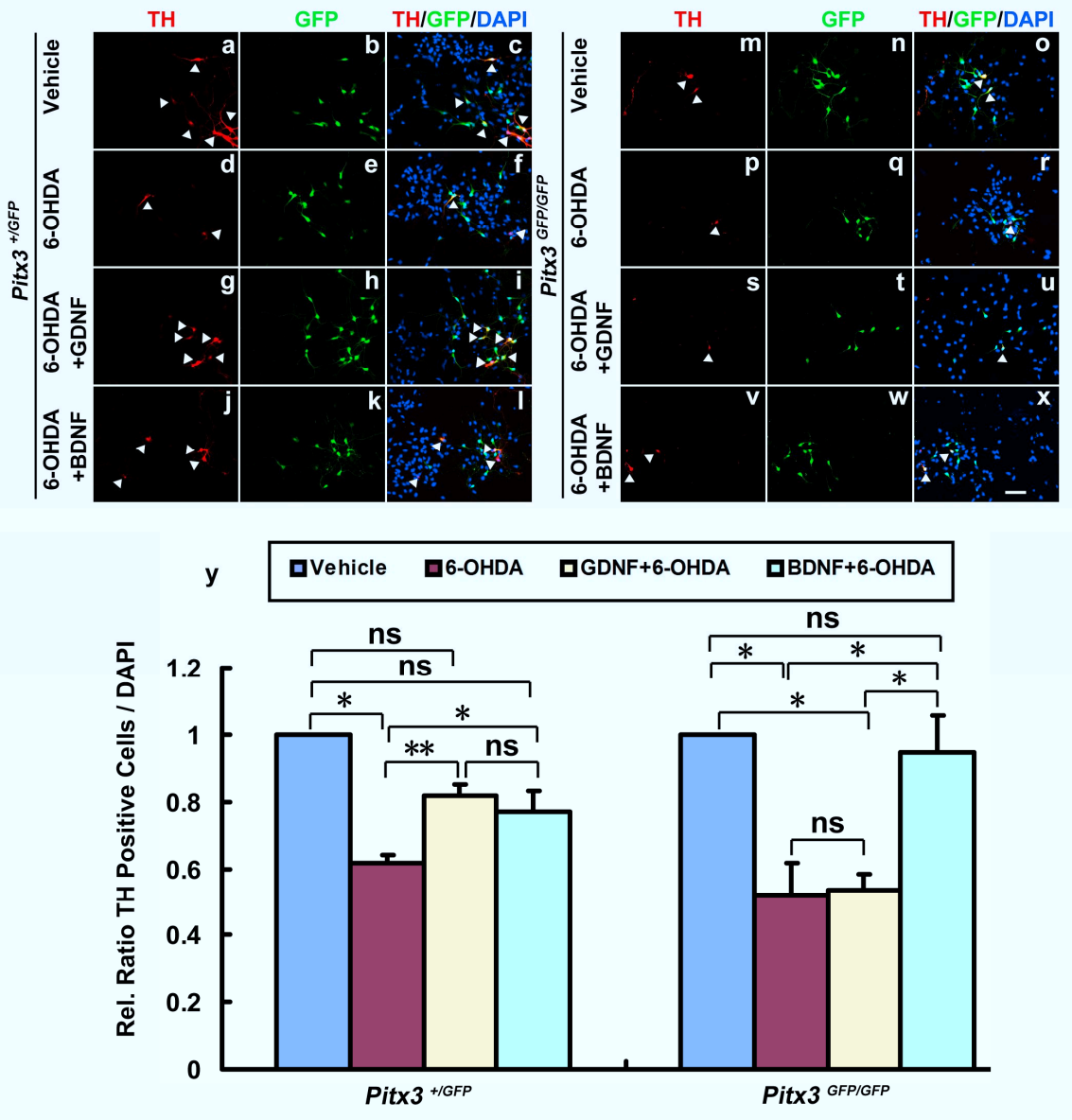
Figure 9. BDNF, but not GDNF, protects *Pitx3* null mutant mdDA neurons against 6-OHDA neurotoxicity. (**a-x**) Primary VM cultures derived from E11.5 $Pitx3^{+/GFP}$ (**a-l**) and $Pitx3^{GFP/GFP}$ (**m-x**)

embryos were treated after 3 DIV with vehicle (0.1% BSA) (**a-f, m-r**), 20 ng/ml GDNF (**g-i, s-u**) or 20 ng/ml BDNF (**j-l, v-x**); after 2 hrs, cells were incubated with 10 µM 6-OHDA (**d-l, p-x**) or vehicle (PBS; **a-c, m-o**) for 24 hrs, and immunostained for TH (red in **a, d, g, j, m, p, s, v**) and GFP (green in **b, e, h, k, n, q, t, w**); merged images with DAPI stain in (**c, f, i, l, o, r, u, x**). (**y**) Quantification of TH immunopositive cells in these 8 experimental groups revealed that in $Pitx3^{+/GFP}$ VM cultures, both GDNF and BDNF protect TH$^+$ mdDA neurons against 6-OHDA toxicity, but in $Pitx3^{GFP/GFP}$ VM cultures, only BDNF (and not GDNF) protects these neurons against 6-OHDA toxicity (TH$^+$/DAPI$^+$ cells (white arrowheads): $Pitx3^{+/GFP}$ vehicle-treated, normalized to 1; $Pitx3^{+/GFP}$ 6-OHDA-treated, 0.615±0.025; $Pitx3^{+/GFP}$ 6-OHDA + GDNF-treated, 0.816±0.037; $Pitx3^{+/GFP}$ 6-OHDA + BDNF-treated, 0.768±0.066; mean±SEM, n=3; $Pitx3^{GFP/GFP}$ vehicle-treated, normalized to 1; $Pitx3^{GFP/GFP}$ 6-OHDA-treated, 0.521±0.096; $Pitx3^{GFP/GFP}$ 6-OHDA + GDNF-treated, 0.533±0.051; $Pitx3^{GFP/GFP}$ 6-OHDA + BDNF-treated, 0.946±0.111; mean±SEM; n=4). Paired t-test was used for statistical analysis of treatment effects. Single asterisk, P<0.05; double asterisks, P<0.01; ns, not significant. Data were derived from at least 3 independent experiments. Scale bar: 50 µm.

To determine if these two neurotrophic factors exerted their protective effect on the 6-OHDA-treated wild-type ($Pitx3^{+/GFP}$) and mutant ($Pitx3^{GFP/GFP}$) VM cultures by a reduction of neurotoxin-induced apoptotic cell death, I assessed the relative proportion of apoptotic (cCasp3$^+$) and GFP$^+$ mdDA neurons in the 6-OHDA treated VM cultures alone and after previous incubation with GDNF or BDNF. As expected, treatment with 6-OHDA alone significantly increased the numbers of apoptotic mdDA neurons in these cultures, irrespective of their genotype (Fig. 10a-f,m-r,y). In line with my previous findings, BDNF significantly decreased the numbers of apoptotic mdDA neurons down to normal (untreated) levels in 6-OHDA-treated both $Pitx3^{+/GFP}$ and $Pitx3^{GFP/GFP}$ cultures (Fig. 10j-l,v-x,y), whereas GDNF only decreased these numbers significantly in $Pitx3^{+/GFP}$ but not in $Pitx3^{GFP/GFP}$ 6-OHDA-treated cultures (Fig. 10g-i,s-u,y). Altogether, these results strongly suggest that GDNF exerts its neuroprotective and survival-promoting effect on at least a subpopulation of mdDA neurons through the activation of Pitx3-mediated BDNF expression in these cells. In the absence of $Pitx3$, GDNF cannot protect the mutant mdDA neurons against 6-OHDA-induced neurotoxicity and apoptotic cell death, and these cells are only rescued by the exogenous application of BDNF acting downstream of GDNF and Pitx3, as suggested by my previous results.
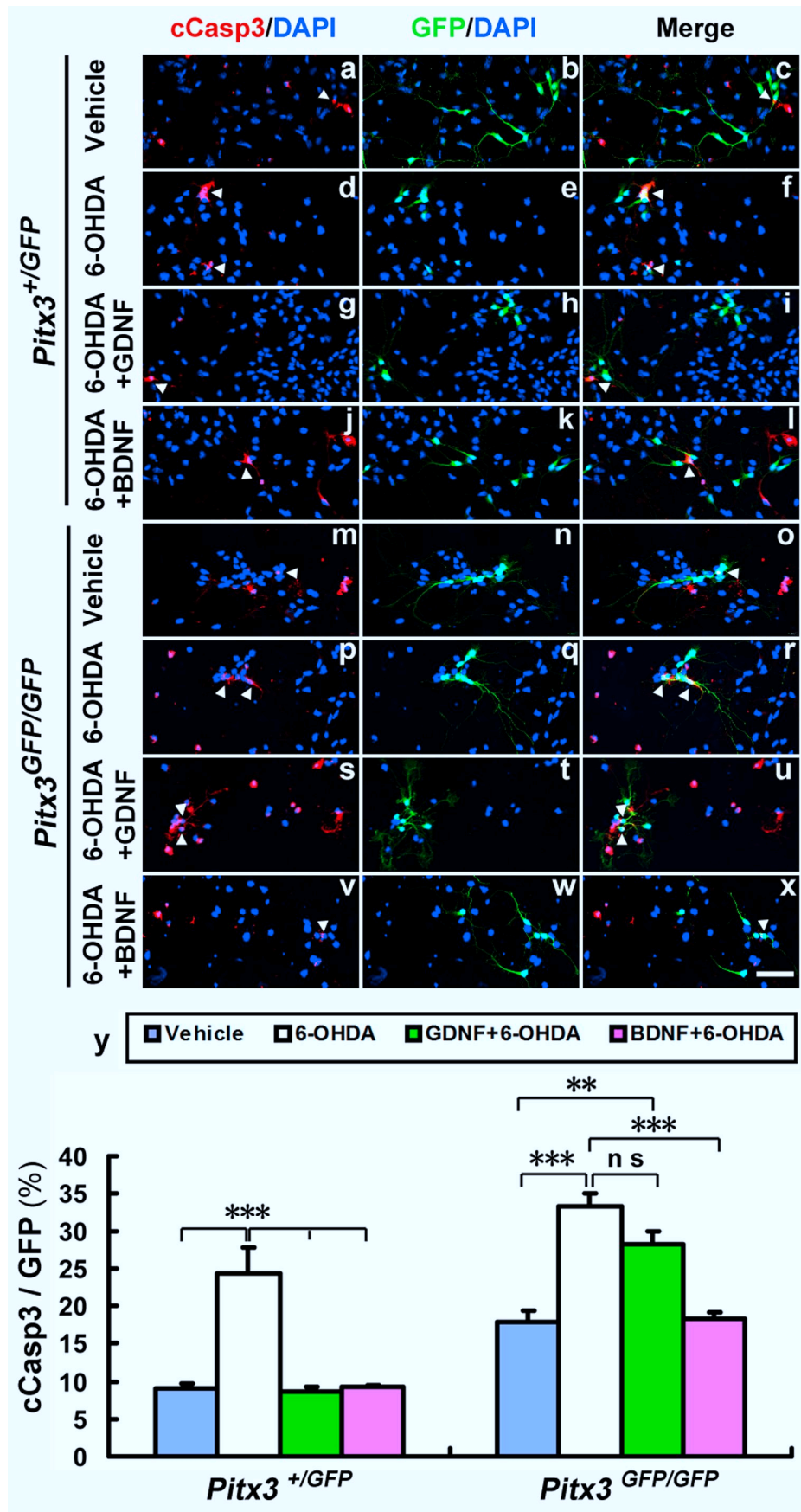
Figure 10. GDNF does not protect against 6-OHDA-induced apoptotic cell death of *Pitx3* null mutant mdDA neurons. (**a-x**) Primary VM cultures derived from E11.5 *Pitx3*[+/GFP] (**a-l**) and *Pitx3*[GFP/GFP] (**m-x**)

embryos were treated after 3 DIV with vehicle (0.1% BSA) (**a-f, m-r**), 20 ng/ml GDNF (**g-i, s-u**) or 20 ng/ml BDNF (**j-l, v-x**); after 2 hrs, cells were incubated with 10 µM 6-OHDA (**d-l, p-x**) or vehicle (PBS; **a-c, m-o**) for 24 hrs, and immunostained for cCasp3 (red in **a, d, g, j, m, p, s, v**) and GFP (green in **b, e, h, k, n, q, t, w**); blue, DAPI stain; merged images in (**c, f, i, l, o, r, u, x**). (**y**) Quantification of the relative amount of apoptotic ($cCasp3^+$) mdDA neurons (GFP^+) in these 8 experimental groups revealed that both GDNF and BDNF prevent the 6-OHDA-induced cell death of $Pitx3^{+/GFP}$ mdDA neurons, but only BDNF (and not GDNF) prevents the 6-OHDA-induced cell death of $Pitx3^{GFP/GFP}$ mdDA neurons ($cCasp3^+/GFP^+$ cells (white arrowheads): $Pitx3^{+/GFP}$ vehicle-treated, 9.11±0.55 %; $Pitx3^{+/GFP}$ 6-OHDA-treated, 24.29±3.49 %; $Pitx3^{+/GFP}$ 6-OHDA + GDNF-treated, 8.70±0.55 %; $Pitx3^{+/GFP}$ 6-OHDA + BDNF-treated, 9.25±0.11 %; mean±SEM, n=3; $Pitx3^{GFP/GFP}$ vehicle-treated, 17.92±1.46 %; $Pitx3^{GFP/GFP}$ 6-OHDA-treated, 33.36±1.74 %; $Pitx3^{GFP/GFP}$ 6-OHDA + GDNF-treated, 28.11±1.86 %; $Pitx3^{GFP/GFP}$ 6-OHDA + BDNF-treated, 18.35±0.78 %; mean±SEM; n=3). One way ANOVA was used for statistical analysis of treatment effects. Double asterisks, $P<0.005$; triple asterisks, $P<0.001$. Data were derived from 3 independent experiments. Scale bar: 50 µm.
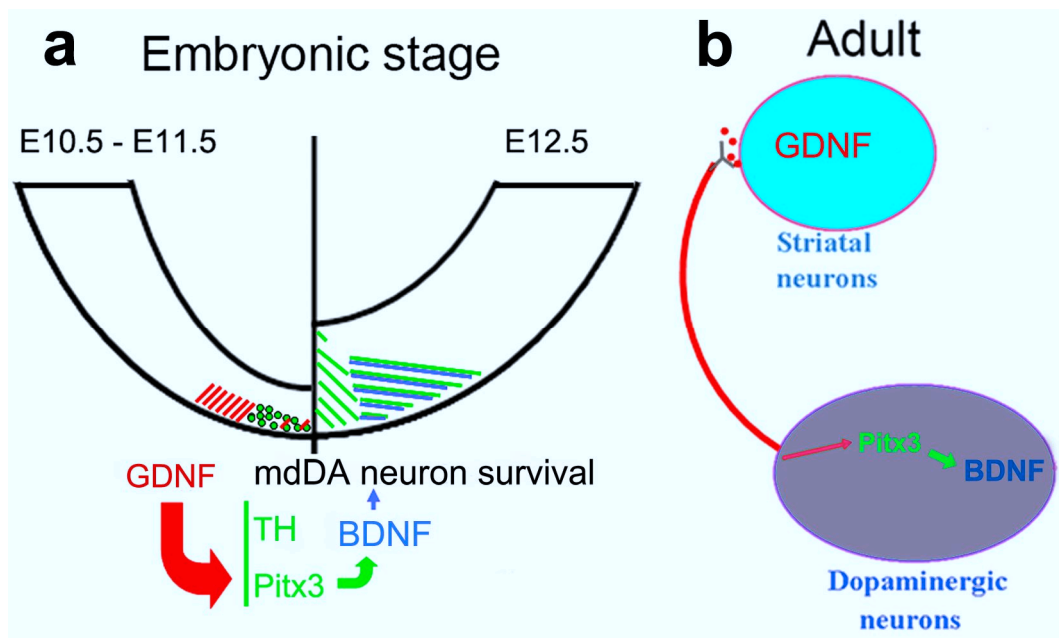
Figure 11. Feed forward regulation of GDNF, Pitx3 and BDNF expression in the embryonic and adult rodent brain. (**a**) During development, *GDNF* (red) is transiently expressed in the midbrain BP of the E10.5/E11.5 mouse embryo, where it is required for the NF-κB-mediated induction of *Pitx3* expression in an mdDA neuronal subset within the adjacent midbrain FP. Pitx3 (green) is in turn necessary for the activation of *BDNF* expression in a rostrolateral/medial mdDA neuronal subpopulation at E12.5. Neurotrophic support of this mdDA neuronal subset by BDNF (blue) might be required for their survival throughout development and their protection against neurotoxic insults. (**b**) In the adult brain, striatal uptake and retrograde axonal transport of GDNF (red) to the cell soma maintains the proper levels of Pitx3 (green) and BDNF (blue) expression in SNc mdDA neurons, and might thereby contribute to the sustained survival and neuroprotection of these neurons throughout adulthood.

2.3 Discussion

The secreted factors GDNF and BDNF, and the transcription factor Pitx3, are individually required for the proper development of mdDA neurons or for their survival during postnatal and adult stages (Baquet et al., 2005; Oo et al., 2009; Pascual et al., 2008; Smidt and Burbach, 2007), but it remained unclear whether a regulatory interaction exists between these three factors during embryonic development or in the adult brain. Here I show that NF-κB-mediated GDNF/Ret signaling is, at least in part, sufficient for the activation of Pitx3 expression, which is in turn required for the transcription of *BDNF* in a rostrolateral and medial mdDA neuronal subpopulation, thereby promoting the survival of these neurons during mouse embryonic development (Fig. 11). I also show that this feed-forward regulation of GDNF, Pitx3 and BDNF expression is still active in the adult rodent brain, and that, in the absence of *Pitx3*, BDNF but not GDNF protects mdDA neurons against 6-OHDA toxicity in vitro. Altogether, my data indicate that the regulatory interaction between GDNF, Pitx3 and BDNF is necessary for the survival and protection of mdDA neurons against neurotoxic insults during embryogenesis, and that this regulatory interaction might also be relevant for the survival and neuroprotection of adult mdDA neurons (Fig. 11).

2.3.1 GDNF/Ret signaling activates Pitx3 expression in an mdDA neuronal subpopulation

The relevance of GDNF signaling for the normal development of mdDA neurons in vivo has remained controversial until now. Inactivation of the murine *GDNF*, *Ret* and *GFRa1* genes apparently does not interfere with prenatal mdDA neuron differentiation or survival (Airaksinen and Saarma, 2002; Kramer et al., 2007; Paratcha and Ledda, 2008). Moreover, persistent overexpression of GDNF driven by the *TH* promoter leads to a reduction of SNc DA neurons (Chun et al., 2002), whereas intrastriatal or intranigral injections of GDNF protein during early postnatal stages, or the constitutive activation of the Ret receptor, results in increased numbers of TH^+ SNc neurons and an enhanced DA metabolism (Beck et al., 1996; Mijatovic et al., 2007). The transient but detectable expression of *GDNF* in the midgestational VM that I have shown in my work might have been missed by previous in situ hybridization studies due to lower sensitivity or slight differences in the staging of the embryos (Hellmich et al., 1996); Golden et al., 1999), but *GDNF* expression in the embryonic rat VM was also shown by (Choi-Lundberg and Bohn, 1995) using a more sensitive RT-PCR-based detection method. My and previous findings therefore suggest that the transient expression of GDNF in

the rodent VM might have two different functions during development: on the one hand, GDNF signaling might activate *Pitx3* transcription in an mdDA precursor subpopulation; on the other hand, GDNF might provide transient trophic support to developing progenitors and postmitotic neurons in this region of the brain. The requirement of GDNF signaling for these two processes, however, might be compensated by other factors during embryonic development, leading to the absence of an mdDA phenotype in the *GDNF*, *Ret* and *GFRa1* null mutants at birth (Airaksinen and Saarma, 2002; Paratcha and Ledda, 2008). My and previous results also suggest that the tight regulation of GDNF protein levels is critical for proper mdDA neuron development. The notion that a transient (rather than persistent) expression of GDNF during embryonic development might have an important permissive role is supported by the observation that sustained GDNF expression in differentiating TH$^+$ SNc neurons results in a marked reduction of these neurons shortly after birth (Chun et al., 2002).

2.3.2 Pitx3 is necessary for the activation of *BDNF* transcription in an mdDA neuronal subset

Pitx3 is required for the initiation of *TH* expression in an mdDA neuronal subset during development, and for the survival of these neurons during subsequent pre- and postnatal stages (Maxwell et al., 2005; Smidt and Burbach, 2007). *Aldh1a1* was identified as a target gene that could mediate the pro-survival activity of Pitx3, as maternal RA complementation partially rescues the loss of mdDA neurons in *Pitx3* mutants (Jacobs et al., 2007). Here I identify *BDNF* as another target gene of Pitx3 in the rostrolateral and medial mdDA neuronal subpopulation that is most affected in *Pitx3*$^{-/-}$ mice (Smidt et al., 2004; Maxwell et al., 2005). Because BDNF treatment augmented the survival of mdDA neurons in primary VM cultures prepared from E11.5 *Pitx3*$^{GFP/GFP}$ null mutant embryos, I suggest that the failure to induce *BDNF* expression in rostrolateral and medial (SNc) mdDA precursors during development contributes to the preferential degeneration of these neurons in the *Pitx3*$^{GFP/GFP}$ mice. Interestingly, retinoid signaling via retinoic acid receptors (RARs) was recently shown to induce *BDNF* transcription and to prevent the inflammatory degeneration of mdDA neurons in vitro and in vivo (Katsuki et al., 2009). While my data strongly suggest a direct activation of the *BDNF* gene by Pitx3, I cannot exclude that Pitx3 might indirectly maintain BDNF expression through the induction of *Aldh1a1* and subsequent local production of RA in an mdDA neuronal subset.

29

2.3.3 GDNF protects mdDA neurons against 6-OHDA toxicity only in the presence of Pitx3

Treatment of *Pitx3*^{GFP/GFP} null mutant VM cultures with 6-OHDA resulted in an increased survival of mdDA neurons in these cultures only after pre-incubation with BDNF, but not with GDNF, suggesting that GDNF acts upstream of Pitx3 and BDNF to protect mdDA neurons against cytotoxic insults and to increase their survival under these conditions. BDNF is in fact more potent than GDNF to promote the survival of mdDA neurons after unilateral 6-OHDA lesion of the SNc in organotypic cultures of the rat VM (Stahl et al., 2011). Moreover, GDNF appears to promote primarily the survival of calbindin-expressing VTA neurons under basal conditions (Meyer et al., 1999) and of VTA and rostromedial SNc neurons after 6-OHDA lesion (Barroso-Chinea et al., 2005), which are the cell groups that are not affected by the loss of *BDNF* expression in our *Pitx3*^{GFP/GFP} mice. Together, my and previous findings therefore suggest that GDNF acts as a potent survival factor for those medial mdDA neuronal subpopulations projecting to the GDNF-rich ventral striatum (Barroso-Chinea et al., 2005). However, the rostrolateral mdDA neurons projecting to the dorsolateral striatum (where lower levels of *GDNF* are expressed, (Barroso-Chinea et al., 2005)), depend on Pitx3-mediated local BDNF synthesis for their survival and neuroprotection.

2.3.4 The feed-forward regulation of GDNF, Pitx3 and BDNF expression in the adult SNc might be relevant for the pathogenesis of PD

I also found that the intrastriatal delivery of GDNF protein in the adult rat brain increased the expression of Pitx3 and BDNF in the ipsilateral SNc. This finding raises the possibility that retrograde transport of GDNF or local signaling at axon terminals in the striatum controls the levels of Pitx3 and BDNF proteins in adult mdDA neurons (Fig. 11), and might have implications for the pathogenesis and treatment of PD. Among all neurotrophic factors, GDNF exhibits the most severe decrease in the SNc of PD patients (Chauhan et al., 2001). Reduced intranigral GDNF levels might lead to reduced Pitx3 expression and thus to decreased expression of BDNF in SNc mdDA neurons. This might render these neurons more susceptible to death in the diseased brain. A reduction of *BDNF* mRNA and protein levels in the SNc of PD patients has been consistently reported by several groups (Chauhan et al., 2001; Howells et al., 2000; Mogi et al., 1999; Parain et al., 1999). Interestingly, some of these studies also noted in the patients the preferential loss of a subset of SNc neurons that normally express high levels of BDNF (Parain et al., 1999; Howells et al., 2000). Moreover, several

polymorphisms in non-coding regions of the *PITX3* gene (which might alter PITX3 expression) are associated with idiopathic or early onset PD (Bergman et al., 2010; Fuchs et al., 2009; Haubenberger et al., 2009; Le et al., 2009), and one polymorphism in the promoter region of the human *BDNF* gene was associated with familial PD (Parsian et al., 2004). These findings, together with my results and the observation that conditional ablation of the *BDNF* gene during mouse development leads to the selective loss of a subset of TH$^+$ neurons in the SNc but not VTA (Baquet et al., 2005), raise the intriguing possibility that the rostrolateral (SNc) mdDA neuron subpopulation expressing high levels of BDNF is most affected by the loss of *PITX3* in human PD patients, and cannot be protected by the exogenous application of GDNF. I suggest that a developmental failure to induce normal expression of Pitx3 coupled to age-related decreases in GDNF levels (Miyazaki et al., 2003) might lead to a depletion of BDNF in SNc neurons and predispose them to neurodegeneration (Porritt et al., 2005). According to this model, alterations in this neurotrophic factor reinforcement loop might lead to reduced neurotrophic support of SNc mdDA neurons, thus contributing to PD. Further dissection of the molecular underpinnings of this regulatory network might therefore facilitate the development of novel therapeutic approaches for the treatment of PD.

3 Part 2: MicroRNA function in the development of mdDA neurons

3.1 Introduction

3.1.1 Biogenesis of miRNA and its function in neurogenesis

MicroRNAs (miRNAs) are a class of non-protein coding small RNAs (~21 nucleotides) which posttranscriptionally regulate gene expression by degradation of mRNA and/or inhibition of translation (Ambros, 2004; Bartel, 2004). MiRNA genes diversely exist in animal and plant genomes and are transcribed mostly by RNA polymerase II, but few miRNAs in mammals are transcribed by RNA polymerase III (Borchert et al., 2006). For many miRNAs, the primary transcript (pri-miRNA) is processed in the nucleus into precursor miRNA (pre-miRNA) by an enzyme complex that contains RNaseIII enzyme Drosha and the double-stranded RNA binding protein DGCR8 (Zeng et al., 2005). Some miRNAs encoded in introns of other genes (these intronic miRNAs are named as mirtrons) can bypass Drosha processing prior to export (Berezikov et al., 2007; Ruby et al., 2007). Pre-miRNA (~70 nucleotides) and mirtron are exported into the cytoplasm by exportin 5 (Lund et al., 2004; Yi et al., 2003), and are further cleaved by the Dicer1 RNase III enzyme complex into a (~21/22 nt) miRNA duplex (Saito et al., 2005). Normally, only one strand of the duplex, termed the mature miRNA, is then preferentially incorporated into the miRNA-induced silencing complex (miRISC) to base-pair with the target mRNA (Bartel, 2004). In some cases, the other strand of the duplex, termed the miRNA* species, can also be loaded into the miRISC complex to regulate another set of target genes although its concentration is usually much lower than the miRNA strand (Fig. 12, Liu et al., 2008). MiRNAs regulate gene expression through base-pairing of 7 nucleotides (termed seed sequence, position 2-8 from the 5' end of the miRNA) with the complementary sequence in the 3' UTR of the target genes, but also in the 5' UTR or coding sequence (CDS) (Lytle et al., 2007; Tay et al., 2008). The repression caused by miRNAs can be either by degrading the target mRNA directly or by inhibiting the translation of target mRNA, which depends on the degree of sequence complementarity between the miRNA and its target mRNA (Brennecke et al., 2005; Brodersen and Voinnet, 2009). Previously, miRNAs were considered to only marginally regulate the expression of target genes as a fine-tuner. But recently, this notion has been challenged by Mukherji et al. (2011), who nicely showed that miRNAs can act both as a switch, when the target expression is below the threshold level, and as a fine-tuner when it is above the threshold level. The threshold level and the repression strength are co-related with the number and the affinity of

the binding sites (BSs) on the target gene, as well as the abundance of the miRNA (Mukherji et al., 2011).
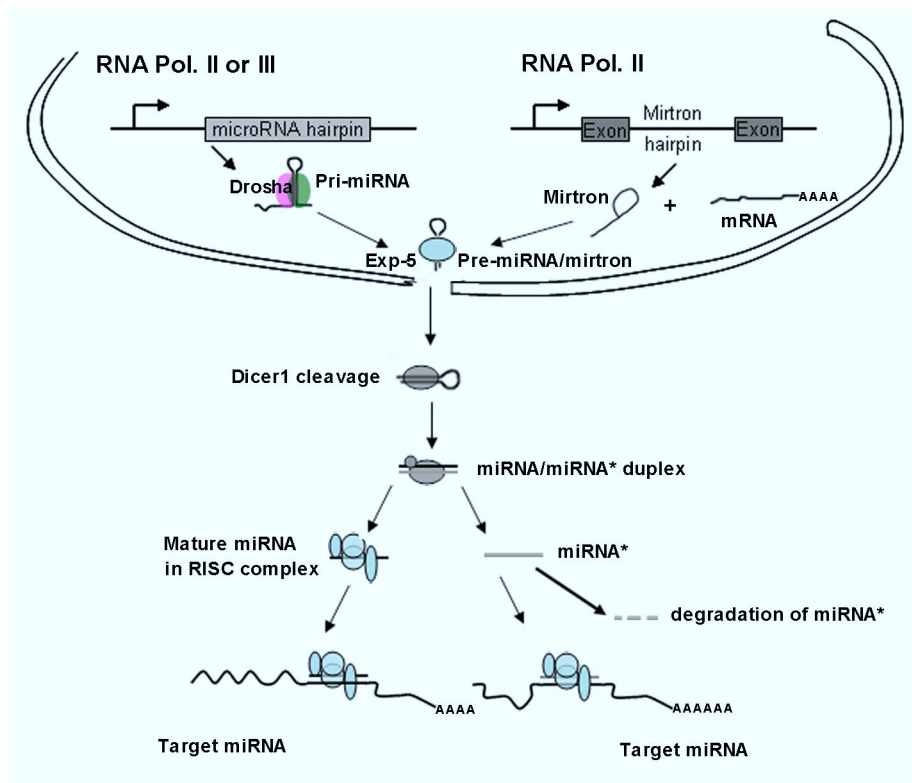
Figure 12. Biogenesis of canonical miRNAs or mirtrons.

More and more evidences support the idea that miRNAs play crucial roles during embryonic and adult neurogenesis in the brain, which needs to generate the proper number of functional neurons throughout life. The process of neurogenesis includes the self-renewal and fate specification of neural stem cells (NSCs), as well as their differentiation into neurons. Depletion of miRNAs by tissue specific ablation of *Dicer1*, an essential enzyme for miRNA biogenesis (described above), showed that miRNAs are required for neurogenesis, oligodendrogenisis and astrogenesis, as well as later for the survival of neurons and the myelination of Schwann cells (Bremer et al., 2010; Choi et al., 2008; Davis et al., 2008; De Pietri Tonelli et al., 2008; Li et al., 2011; Pereira et al., 2010). *DAT-Cre* and *Wnt1-Cre* mediated conditional knockout of *Dicer1* in mice showed that some miRNAs are necessary for the development and survival of mdDA neurons (Huang et al., 2010; Kim et al., 2007). One example is *miR-133b*, which was shown to target the transcription factor *Pitx3* and thereby presumably affects the survival mdDA neurons, although in vivo *miR-133b* knock-down, knock-out or overexpression experiments were not performed in this study (Kim et al., 2007). Detailed investigation of individual or sets of miRNA(s) demonstrated that, for example, *miR-9*, *miR-124* and *let-7* are brain-specific or –enriched miRNAs whose expression

33

levels sharply increase during the transition from a neuronal precursor to a neuron. These miRNAs promote neural differentiation by targeting the transcriptional repressors of neuronal genes or cell cycle exit/neuronal differentiation like TLX, Sox9 and REST (RE1 silencing transcription factor), that are expressed in neural progenitors but not in postmitotic neurons (Conaco et al., 2006; Krichevsky et al., 2006; Lim et al., 2005; Packer et al., 2008; Zhao et al., 2010; Zhao et al., 2009). The conserved *miR-200* family was reported to be enriched in neural progenitors of the olfactory bulbs and to be important for olfactory neurogenesis by targeting the Notch and TGFβ signaling pathway and Foxg1 in these cells (Choi et al., 2008). Collectively, these data show that miRNAs may play crucial roles in the regulation of neural development by modulating the expression of key multipotency or pro-neural transcription factors.

3.1.2 Stratagies and techniques for studying miRNA functions

3.1.2.1 Manipulation of miRNA expression

Several strategies have been used to investigate the functions of miRNAs in intact organisms. One strategy is the conditional knock-out of *Dicer1* or *Drosha* to deplete miRNAs that are processed by these two enzymes or at least one of them in a specific region/tissue and/or at a specific time point. This usually resulted in severe phenotypes that were explained at least in part by a search for specific candidate miRNAs (see paragraph above), but it is difficulty to know the exact contribution of each candidate miRNA to the phenotype. A second strategy is the manipulation of the expression of an individual candidate miRNA (or of a cluster of candidate miRNAs) by knock-out of the corresponding miRNA gene, knock-down of this/these miRNA(s) by chemical antagonists (antagomirs, morpholinos, etc) and/or by transgenic overexpression of a miRNA (Lu et al., 2007; Thai et al., 2007). Another strategy is transferring a sponge vector (described in the following paragraph) into the genome to competitively inhibit the function of the miRNA of interest by sequestering this miRNA (Ebert et al., 2007; Loya et al., 2009; Zhu et al., 2011). Sponge vector can be designed to functionally knock-down all members of one miRNA family, so it is better than the knock-out strategy if the members of a miRNA family locate in different loci.

3.1.2.2 MiRNA identification

In order to find candidate miRNAs which may play roles in certain biological events, such like proliferation, differentiation, cell cycle exit and survival, three major approaches have been used to profile the miRNA expression in tissues/samples. The first technology is miRNA

microarray analysis, in which the total RNA is extracted from the tissue(s) of interest and hybridized to miRNA microarrays, and then the intensity of the hybridization signal is read out as an indication of miRNA expression levels. By comparing the expression profile of two matched samples, a list of miRNAs with changed expression levels will come out quickly. However, this method has some limitations in both sensitivity (due to the relative low expression levels of many miRNAs in the tissue(s)), and resolution (due to the small size of mature miRNAs (~21/22 nt) and to the fact that members of a miRNA families often differ in only one single or several nucleotides) (Liu and Zhao, 2009; Millar and Waterhouse, 2005). The data obtained from miRNA microarray analysis usually need to be confirmed by other means such as quantitative RT-PCR, which is another technology used for measuring changes in the expression levels of miRNAs. Customer-designed or common miRNA qPCR arrays are available from many vendors. This method is more sensitive than the microarray-based method, and can well distinguish the members in one miRNA family, so it has been widely used (Chen et al., 2005). Although the above approaches are easy to perform, they have a bias towards the known miRNAs. To discover new miRNAs, next generation sequencing technologies, such as the Illumina, SOLid and Roche 454 platforms, provide improved options. Many reviews have summarized the principles and applications of these technologies (Metzker, 2010; Morozova and Marra, 2008). Here I briefly introduce the workflow of sequencing miRNA using Illumina technology which I used to profile miRNAs in mouse mid-/hindbrain tissues (Fig. 13). Small RNAs (10–40 nt in size) are isolated from the total RNA population and ligated with adaptors by T4 RNA ligase, and then amplified by RT-PCR. The PCR products are purified and hybridized to the nucleotides which are complementary to the sequence of the adaptors, and that have been immobilized on a flowcell surface. DNA clusters are subsequently generated on the flowcell surface by isothermal bridge amplification based on PCR using anchored DNA as templates and high-fidelity DNA polymerase. Finally, the DNA clusters are sequenced in a base-by-base manner through synthesis with the reversible fluorescently-labeled terminators-based technology.

Workflow
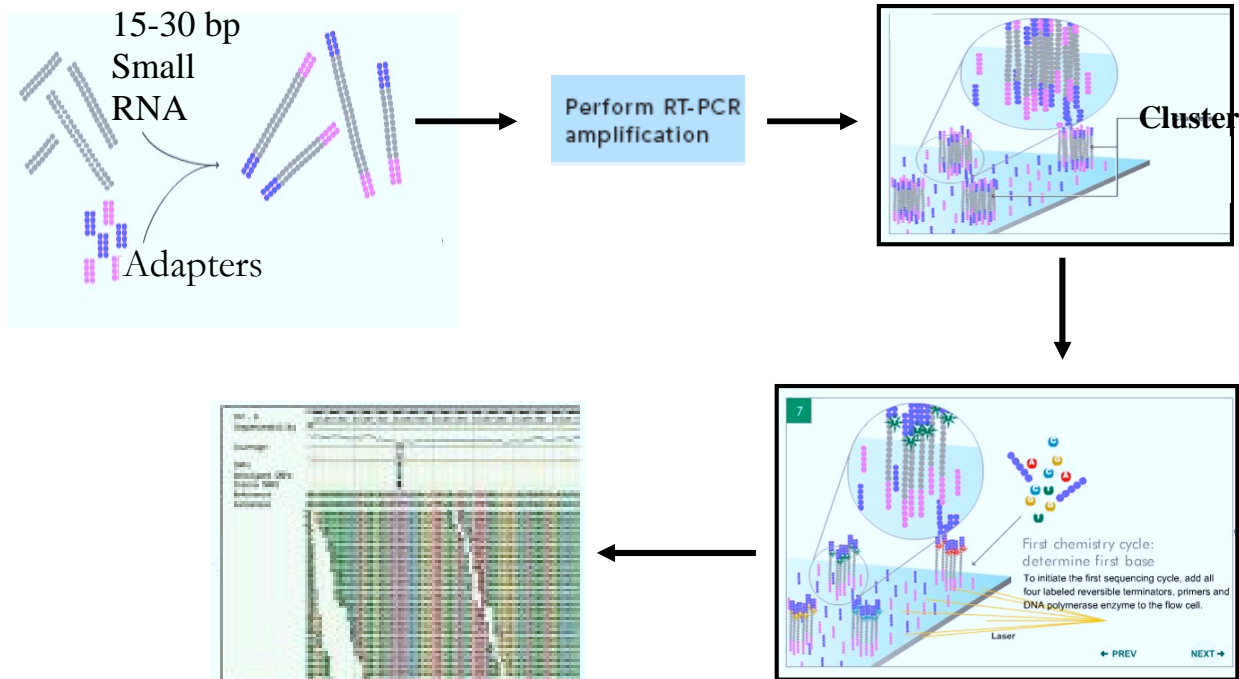
Figure 13. The workflow of profiling miRNAs by Illumina's next generation sequencing technology. Adapted from Illumina website (http://www.illumina.com/).

3.1.2.3 Identification and validation of miRNA targets

To indentify and validate the targets of a miRNA of interest, several methods have been developed to either overexpress or down-regulate miRNAs in vivo and/or in vitro. First, synthesized oligos are widely used in gain- and loss-of miRNA function assays (Leucht et al., 2008). Synthesized RNA duplexes (also called miRNA mimics) and miRNA precursors are often employed to augment the function of endogenous miRNAs. Conversely, the antisense oligos to mature miRNAs (antagomirs or morpholinos) can block the activity of the miRNA of interest by complementary binding to this miRNA. Morpholino oligos can also be designed to block the Drosha or Dicer1 nucleolytic processing sites of pri-miRNAs or pre-miRNAs, or to block the binding site (BS) of the miRNA of interest in its target mRNA, thereby inhibiting or interfering with the activity of the particular miRNA.

In addition, vector-based methods to overexpress or down-regulate miRNAs are also broadly used. Both RNA polymerase III promoters (like U6 and H1 promoters) and RNA polymerase II promoters (like CMV and CAG promoters) can be used for driving miRNA expression (Grimm et al., 2006; Sun et al., 2006). In addition to using the sequence of the miRNA gene, scientists also use small hairpin RNA expression cassettes (pre-miRNA mimics)

to overexpress miRNAs (Shan et al., 2009; Sun et al., 2006). The RNA transcribed from the hairpin RNA expression cassette can make a stem-loop structure that is subsequently processed by Dicer1 into the mature miRNA. The advantage of using this hairpin RNA expression cassette is to avoid the expression of miRNA* (if the pre-miRNA generates a functional miRNA*), which usually targets a different group of genes, thereby enabling the identification of effects that are specifically caused by the miRNA of interest (Lau et al., 2008).

For down-regulation of miRNAs, scientists have more recently used the so-called "sponge vectors" for the overexpression of miRNA target sequences within the 3' UTR of a reporter gene, thereby "soaking up" endogenous miRNA to inhibit its function (Ebert et al., 2007). In the original design, the miRNA target sequence of a sponge vector contains several repetitive sequences complementary to the miRNA of interest with mismatches at positions 9-12. More recently, Ameres et al. (2010) showed that a fully complementary sequence to a miRNA can also block the function of that miRNA by degradation of the miRNA (Ameres et al., 2010). The expression of miRNA target sequences in the sponge vector can be driven by RNA polymerase III and RNA polymerase II promoters, and the effects are equal (Ebert et al., 2007). The advantage of using RNA polymerase II promoters is that the miRNA target sequence can be cloned downstream of a reporter gene (usually GFP), thereby enabling the tracing of cells overexpressing this vector. As mentioned above, sponge vectors have also been used to generate transgenic animals for the in vivo knock-down of miRNAs (Loya et al., 2009; Zhu et al., 2011). A sponge mouse might in fact be a good substitute for a miRNA knockout mouse, as it is difficult to make a miRNA knockout mouse in many instances due to the small size of miRNA genes and the intronic location of some miRNAs (mirtrons), as well as different loci of multi-copy miRNAs.

3.1.3 Sox family and the function of Sox2 in neural stem cells

Neural stem cells (NSCs) are a subset of undifferentiated progenitors that retain the capacity to self-renew and the potential to give rise to all major neural lineages (neuron, glia and astrocyte) in the nervous system (Gage, 2000). One of the factors that are important to maintain the identity of NSCs, but also of embryonic stem cells (ESCs), is the transcription factor Sox2 (Graham et al., 2003; Masui et al., 2007; Suh et al., 2007). Sox2 belongs to the Sox (Sry-related high-mobility-group (HMG) box) family of transcription factors, which in mouse and human comprise 20 proteins sharing at least 50% similarity in the HMG box domain (Schepers et al., 2002). The HMG domain proteins were discovered due to their high

mobility during sorting of non-histone chromosomal proteins using SDS-PAGE (Goodwin and Johns, 1973; Goodwin et al., 1973). They have two or more copies of a so-called canonical HMG domain which has a twisted L-shape containing three alpha helices and an N-terminal beta strand. This structure enables the HMG domain to bind the DNA in the minor groove, thereby inducing a significant bend of the DNA conformation (review in (Weiss, 2001)). This feature makes HMG domain proteins unique because most other transcription factors bind DNA in the major groove. HMG box proteins carrying only one non-canonical HMG domain that shares ~20% identity with the canonical HMG domain and conserves the ability to alter the DNA conformation were later identified. The HMG box proteins fall into two families: the T-cell factor (TCF) lymphoid enhancer binding factor (LEF-1) family, and the Sox family.

Sox proteins are divided into eight groups (from A to H, with two B subgroups, B1 and B2) based on their homology within and outside the HMG box domain and on their functional properties (Schepers et al., 2002). Within one group, the Sox proteins share more than 70% identity. Due to the high conservation of the HMG box domain among the entire family, all Sox proteins bind to a similar hexameric core sequence $^A/_T{}^A/_T CAA^A/_T$ (Harley et al., 1994; Mertin et al., 1999; van de Wetering et al., 1993). The preferences for the nucleotides-flanking this consensus sequence vary among the Sox proteins, which is one reason why each Sox protein has specific target genes (Mertin et al., 1999). As mentioned above, the Sox B group includes two subgroups: B1 (Sox1-3) and B2 (Sox14 and Sox21), which function in an opposite manner with Sox B1 members acting as transactivators and Sox B2 proteins acting as repressors. Moreover, Sox B2 proteins can antagonize the activity of Sox B1 proteins (Sandberg et al., 2005).

Sox B1 proteins, including Sox1, Sox2 and Sox3, share more than 90% amino acid residue identity within the HMG box domain. Sox2 is initially expressed in the inner cell mass and extraembryonic ectoderm of early mouse embryos, and later expressed in NSCs/neural progenitor cells of the developing and adult central nervous system (CNS) (Avilion et al., 2003; Cai et al., 2002; Graham et al., 2003; Suh et al., 2007). The loss of Sox2 function in mouse embryos results in a loss of the pluripotent inner cell mass and in the early lethality of these embryos, and ablation of Sox2 in ESCs failed to maintain their stemness and induced their differentiation into trophectodem-like cells (Avilion et al., 2003; Masui et al., 2007). Similar to its function in ESCs, Sox2 marks neural progenitors (including NSCs) in the developing CNS and maintains their identity by regulating their proliferation and inhibiting their differentiation into neurons (Graham et al., 2003). Most of the fetal Sox2^{+} NSCs

differentiate into mature cells to build up the CNS during development, but a part of them retains the multipotency and capacity to self-renew into adulthood, and continuously gives rise to neural cells throughout life (Arnold et al., 2011; Suh et al., 2007). The possible molecular mechanisms by which Sox2 maintains the capacity of stem cells as a stemness master gene were elucidated by identifying its target genes in ESCs, neural progenitors and other types of cells. Many cell cycle genes, including *FoxM1*, *Ccna2* (*Cyclin A2*), *Ccnb2* (*Cyclin B2*), and *Ccnd1* (*Cyclin D1*), were found to be target genes of Sox2, indicating that Sox2 promotes the proliferation and inhibits the cell cycle exit of stem cells mainly by activating the expression of these genes (Chen et al., 2008; Tompkins et al., 2010). To maintain the pluripotency of stem cells, Sox2 was shown to form a heterdimer with POU domain protein Oct3/4 to coactivate the expression of critical transcription factors, such as UTF1 (undifferentiated embryonic cell transcription factor 1), Nanog, and Sox2 itself, as well as the expression of extrinsic signaling factors and receptors such as Fgf4 and Notch that are essential for ESCs (Feldman et al., 1995; Liu et al., ; Luo et al., 2005; Nishimoto et al., 1999; Tanaka et al., 2004; Taranova et al., 2006; Tomioka et al., 2002; Yu et al., 2008; Yuan et al., 1995). More recently, it was shown that SOX2, together with NANOG, OCT4 and LIN28, is able to induce pluripotent stem cells from human somatic cells (Yu et al., 2007). In NSCs, it has been shown that Sox2 cooperates with the POU protein Brn2 to regulate the expression of Nestin, which is a marker for NSCs (Tanaka et al., 2004). Taken together, most data show that Sox2 maintains the stemness of pluri-/multipotent cells by regulating the expression of vital transcription factors and extrinsic signaling genes, and promotes their proliferation through the regulation of cell cycle genes. However, little is known about the down-regulation of Sox2 expression during the transition from neural progenitors to postmitotic neurons.

3.1.4 Function of E2F3 in cell cycle regulation

E2Fs play important roles in cell proliferation and differentiation by regulating the expression of cell cycle genes. The E2F transcription factor was originally identified by its ability to bind to and activate the adenoviral E2 promoter (Kovesdi et al., 1986). The E2F family has 8 members which contain one or two conserved DNA binding domains (DBDs) and are divided into two groups, activators (E2F1-E2F3) and repressors (E2F4-E2F8), based on sequence homology and functional properties (Fig. 14A, Chen et al., 2009). E2Fs (except E2F7 and E2F8) have a dimerization domain through which they form a heterodimer with dimerization partner (DP) proteins. Although formation of the E2F/DP complex is required for E2F activity, the functional specificity of the E2F/DP complex is determined by the E2F protein. The

activity of the E2F/DP complex is tightly regulated by the retinoblastoma (RB) tumour suppressor and the RB-related pocket proteins p107 and p130, that directly associate with E2F1- E2F5 proteins via their RB binding domain within the transactivation domain. Binding of RB to E2F masks the transactivation domain, and thereby inhibits the activity of the E2F/DP complex. Moreover, RB association with E2F can form an active transcriptional repressor complex by recruiting histone deacetylase to the target gene promoter. During progression from G1 to S-phase of the cell cycle, RB is phosphorylated by cyclin dependent kinases, and phosphorylated RB releases the E2F/DP complex which can then activate the expression of its target genes (Fig. 14B, Reviewed by Chen et al., 2009; DeGregori, 2002; Dyson, 1998).

Overexpression of the activator E2Fs (E2F1-E2F3) can induce quiescent cells to enter the S-phase of the cell cycle, but the accumulation of regulated E2F activity in G1 phase is not observed for E2F2 (Leone et al., 1998). Both E2F1 and E2F3 are important for initial cell cycle entry (after quiescence), whereas only E2F3 is required for subsequent cell cycle re-entry (Leone et al., 1998). *E2F3* knock-out mice have the most severe phenotype among all activating E2Fs (*E2F1*, *E2F2* and *E2F3*) mutant mice. *E2F3*^{-/-} mice with pure FVB or 129Sv genetic background die during embryonic development, and only few *E2F3*^{-/-} mice with a mixed (C57/BL6 x 129Sv) genetic background survive (Cloud et al., 2002). Although all E2Fs can bind to the E2F consensus sequence $TTT^C/_G{}^C/_GCGC$, each E2F regulates a specific set of target genes, suggesting that the specifity of E2F function is not only determined by its DNA binding domain, but also by its dimerization domain which mediates the interaction between E2F and other transcription factor partners (Black et al., 2005). Humbert et al has also shown that the loss of *E2F3* in mouse embryonic fibroblasts causes a dramatic down-regulation of *cyclin A2*, *cdc2*, *cdc6*, *PCNA* and *PRM2*, but the loss of *E2F1* had no effect on the expression of these genes (Humbert, 2000).An isoform of *E2F3*, named *E2F3b*, lacks the Cyclin A binding domain and has been assigned to the repressor group (Adams et al., 2000; Leone et al., 2000). The expression of *E2F3a* (former E2F3) and *E2F3b* is controlled by different promoters and their expression patterns are distinct, with *E2F3* being expressed only in cycling cells and *E2F3b* being expressed in both quiescent and cycling cells (Adams et al., 2000; Leone et al., 2000). It has been shown that the E2F3 protein levels and activities are regulated during the cell cycle (Leone et al., 1998). More recently it has been shown that E2F3 also regulates the genes involved in G2/M transition of the cell cycle (He et al., 2008; Ishida et al., 2001; Polager et al., 2002). In G0 and the early phase of G1, the expression of E2F3 is repressed by RB in an E2F element-dependent manner and the activity of the residual

E2F3 is inhibited by RB. During later G1 phase, RB is phosphorylated by cyclin-dependent kinases and E2F3 is thus released from RB-mediated repression, thereby activating its own expression (Adams et al., 2000; Dyson, 1998; Lees et al., 1993; Leone et al., 1998; Muller et al., 2001). Like many other E2Fs, E2F3 can autoregulate its own expression via E2F elements within its promoter (Adams et al., 2000). This feed-forward amplification loop facilitates the accumulation of E2F3 protein in a fast manner and within a short time. Accumulating free E2F3/DP complexes (phosphorylated RB detaches from the complex) then activate the expression of cell cycle-dependent genes, such as *cyclin A2*, *cdc2*, *cdc6* and *PCNA* which promote the transition from G1 to S-phase. During late S phase, these S phase-specific genes have to be downregulated again to enable the progression of the cell cycle. The activity of E2F3 thus also has to be shut down during late S phase. Indeed, the activity and the protein levels of E2F3 are dramatically downregulated in late S phase (Humbert et al., 2000; Leone et al., 1998). The fast inactivation of E2F3 during S phase is very likely achieved in three ways: firstly, cyclin A/cdk2 and cyclin E/cdk2 phosphorylate E2F3/DP to inhibit the DNA binding ability of the complex; secondly, dephosphorylated RB binds to the E2F3/DP complex to inhibit its transactivating capacity and to induce their ubiquitin-mediated degradation; thirdly, repressor E2Fs (E2F3b-E2F8) bind to the E2F3 promoter and repress transcription from this promoter (Dyson, 1998). However, the precise regulation of E2F3 activity and activation during cell cycle progression is still unclear, and there may be additional mechanisms involved in the cyclic inactivation of E2F3, since this regulatory step is very important for the appropriate proliferation of cells. Inactivation of one allele of *E2F3* in an *RB^-/-* background completely suppresses the inappropriate proliferation and p53-dependent apoptosis of cells observed in the *Rb^-/-* mutant embryos, suggesting that *E2F3* makes a major contribution to the apoptosis resulting from RB loss and that a precise regulation of E2F3 is required for normal cell proliferation (Ziebold et al., 2001). In G2 phase, the expression levels of *E2F3* are upregulated again to activate the expression of genes involved in G2/M transition, such as Aurora-A (He et al., 2008). E2F3 protein levels are downregulated again during M-phase. The fluctuation of E2F3 protein levels during the cell cycle occurs in two waves with a high peak in G1 and a low peak in G2 phase, followed by a fast decline in S and M phase. This cyclic fluctuation of E2F3 protein levels is necessary because otherwise the cell cycle might be arrested and the cells will die (Ebelt et al., 2005).
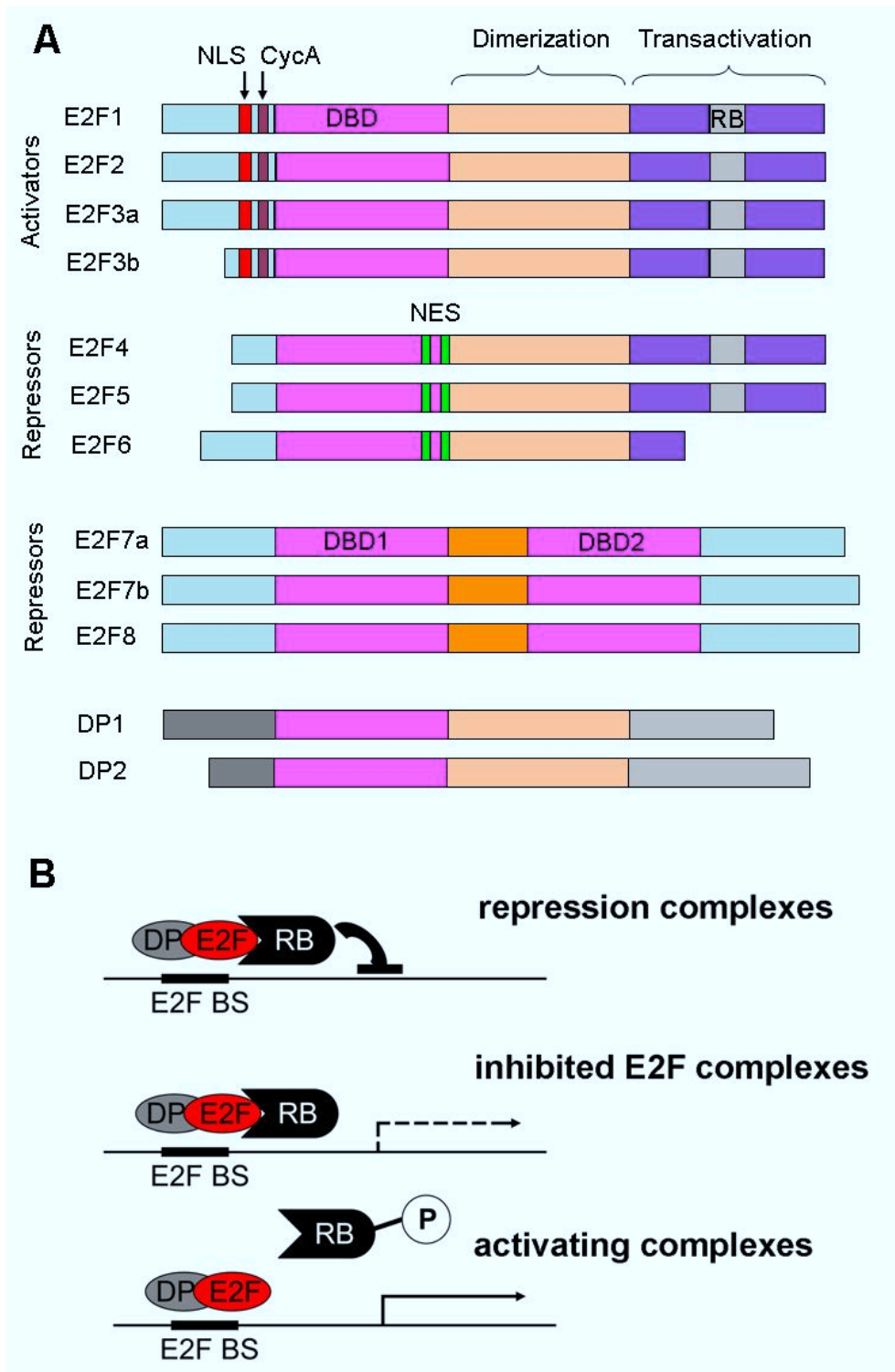
Figure 14. Schematic structutre of E2Fs and DPs and regulation of E2F/DP activity by RB. (A) E2Fs and DPs share a winged-helix DNA binding domain (DBD) which facilates the interaction between E2Fs and DPs. Based on sequence homology and functional properties, the E2F family has been traditionally divided into activator (E2F1–E2F3) and repressor (E2F4–E2F8) subgroups. E2F1–E2F6 bind DNA as heterodimers with DP proteins through the heterodimerization domain. RB binds within the transactivation domain of E2F1–E2F3. Two isoforms are transcribed from E2F3 locus by different promoters, and the more recently discovered isoforn is named E2F3b. E2F1-E2F3 have a nuclear localization signal (NLS) sequence and a cyclin A-binding site (CycA). E2F4 and E2F5 have bipartite nuclear export signals (NES) that mediate their export to the cytoplasm. Repressors E2F6–E2F8 do not possess the carboxy-terminal

features of E2F4 and E2F5 and so are assumed to repress E2F-responsive genes independently of RB and related pocket proteins (reviewed by Chen et al., 2009). **(B)** Binding of RB to E2F repressor/DP complex can recruit histone deacetylases to silence the target gene promoter, while RB binding to E2F activator/DP complex can inhibit the activity of this complex, and this inhibition is reversible by dephosphorylation of RB.

Here I show that the number of mdDA and of other ventral mid-/hindbrain neurons is reduced and their terminal differentiation is affected in $En1^{+/Cre}$; $Dicer1^{flox/flox}$ ($Dicer1$ cKO mice) mice, suggesting that miRNAs are required for the proper differentiation of these neurons. I also found that the loss of the miR-200 family makes a major contribution to the cell cycle exit and neuronal differentiation defects of the $Dicer1$ cKO mice. I could show that miR-200 targets the transcription factors Sox2 and E2F3 to exert these effects. Moreover, the expression of miR-200 is in turn regulated by Sox2 and E2F3. This unilateral negative feedback loop involving miR-200, Sox2 and E2F3 controls the proliferation and differentiation of neural stem/progenitor cells in the murine mid-/hindbrain region.

3.2 Results

3.2.1 Morphological changes and increased apoptosis in $En1^{+/Cre}$; $Dicer1^{flox/flox}$ mice

To explore the function of $Dicer1/miRNAs$ in the formation of the mid-/hindbrain boundary (MHB) and in the development of the mid-/hindbrain region (MHR) and of associated neuronal populations including the mdDA neurons, I crossed $En1^{+/Cre}$ mice (Kimmel et al., 2000) with $Dicer1^{flox/flox}$ mice (Fig. 15, Cobb et al. 2005) to obtain $En1^{+/Cre}$; $Dicer1^{flox/flox}$ mice ((hereafter referred to as $Dicer1$ cKO). PCR genotyping of these mice is shown in Fig. 16).
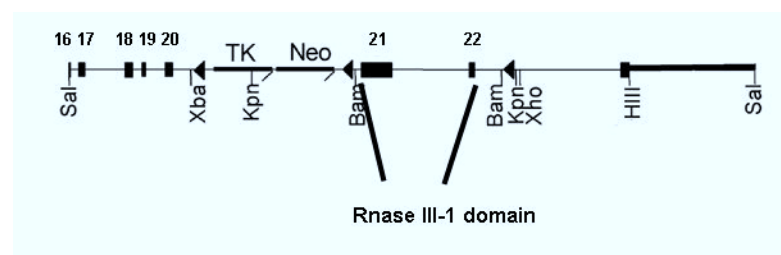

Figure 15. Floxed *Dicer1* allele. In the $Dicer1^{+/flox}$ mice two *loxP* sites are flanking exons 21 and 22 of the *Dicer1* gene which correspond to the Rnase III-1 domain, essential for Dicer1 activity.
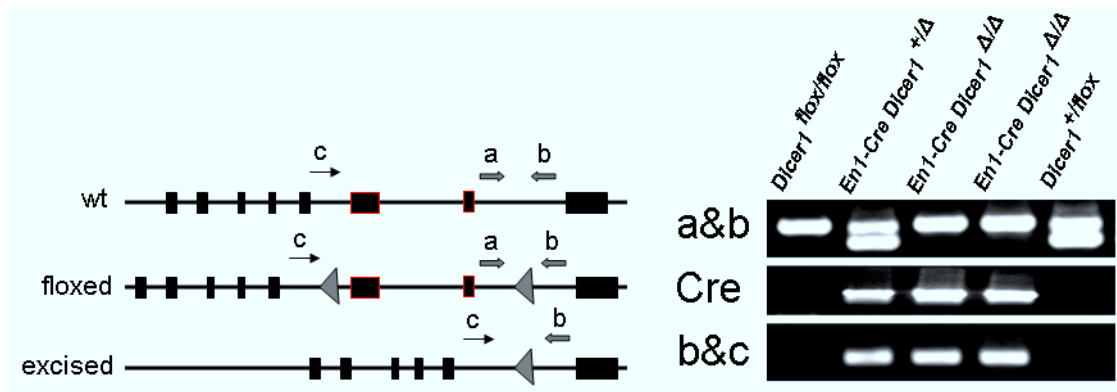
Figure 16. Genotyping PCR of *Dicer1 cKO* mice. Genomic DNA extracted from limb tissue (containing both En1$^+$ and En1$^-$ cells) of mouse embryos were used as DNA template for PCR. Primer pair a&b can distinguish *Dicer1^{lox}* allele (upper band) and *Dicer1$^+$* allele (lower band); Primer pair c&b only detects excised *Dicer1* allele which is the result of Cre-mediated recombination.

The *Dicer1 cKO* mice died shortly after birth, probably due to feeding problems (Fig. 17). After *En1$^{+/Cre}$*-mediated recombination of the floxed *Dicer1* alleles at around embryonic day E9.0 (Puelles et al., 2003), *Dicer1* mRNA was lost from E9.5 onwards within the *En1$^+$* domain across the MHB (Fig. 18A). Detection of *miR-124*, one of the most abundant miRNAs in the brain (Lagos-Quintana et al., 2002), was used to establish the time-point at which the loss of Dicer1-mediated processing of pre-miRNAs affects the expression of mature miRNAs in the MHR of *Dicer1 cKO* mice. A reduction of mature *miR-124* following the loss of *Dicer1* expression in the MHR of *Dicer1 cKO* mice was detected by ISH with LNA probes (Exiqon, Denmark) at E11.5, and mature *miR-124* was completely lost within the *En1$^+$* domain (MHR) at E12.5 (Fig. 18B), which indicates that the deletion of Dicer1 enzyme at E9.5 results in a complete loss of mature miRNAs latest after 2–3 days within the MHR. In line with this finding, the first morphological changes in the MHR of *Dicer1 cKO* mice became visible at E12.5. A progressive thinning of the MHR neuroepithelium was evident at E12.5 and a progressive loss of dorsal and ventral MH tissues became visible at E14.5 in the *Dicer1 cKO* embryos, resulting in the complete absence of dorsal MH structures, such as the superior/inferior colliculi and the cerebellum, in the P0 *Dicer1 cKO* pups (Fig. 18C). To fate map the En1$^+$ and *Dicer1$^{+/-}$* or *Dicer1$^{-/-}$* cells, I crossed the transgenic gene *CAG-CAT-EGFP* (Nakamura et al., 2006) into the *Dicer1 cKO* mice, and found that almost all En1$^+$ (GFP$^+$) cells were lost in the dorsal MHR of *Dicer1 cKO* mice at P0 (Fig. 18C). The progressive tissue loss could be caused by an increased cell death. To test this hypothesis I examined the expression of cleaved caspase3, a marker for apoptotic cells, in the *Dicer1 cKO* mice by immunostaining of different embryonic stages. As expected, an increased apoptotic cell death was detected in the dorsal and ventral MHR of the *Dicer1 cKO* embryos from E11.5 onwards,

but not at E10.5 (Fig. 18D, 19, and Fig. S3). Apoptotic cells were massively increased especially in the dorsal MHR of the *Dicer1 cKO* mice. Altogether, these data indicate that the absence of Dicer1-processed mature miRNAs in the MHR results in a progressive loss of MH tissues, that is in part due to the increased apoptotic cell death of the corresponding cells.

Figure 17. Newborn *Dicer1 cKO* pups (right pup) did not have milk in their stomach (white arrows; left pup is a wild-type littermate) and died shortly later.
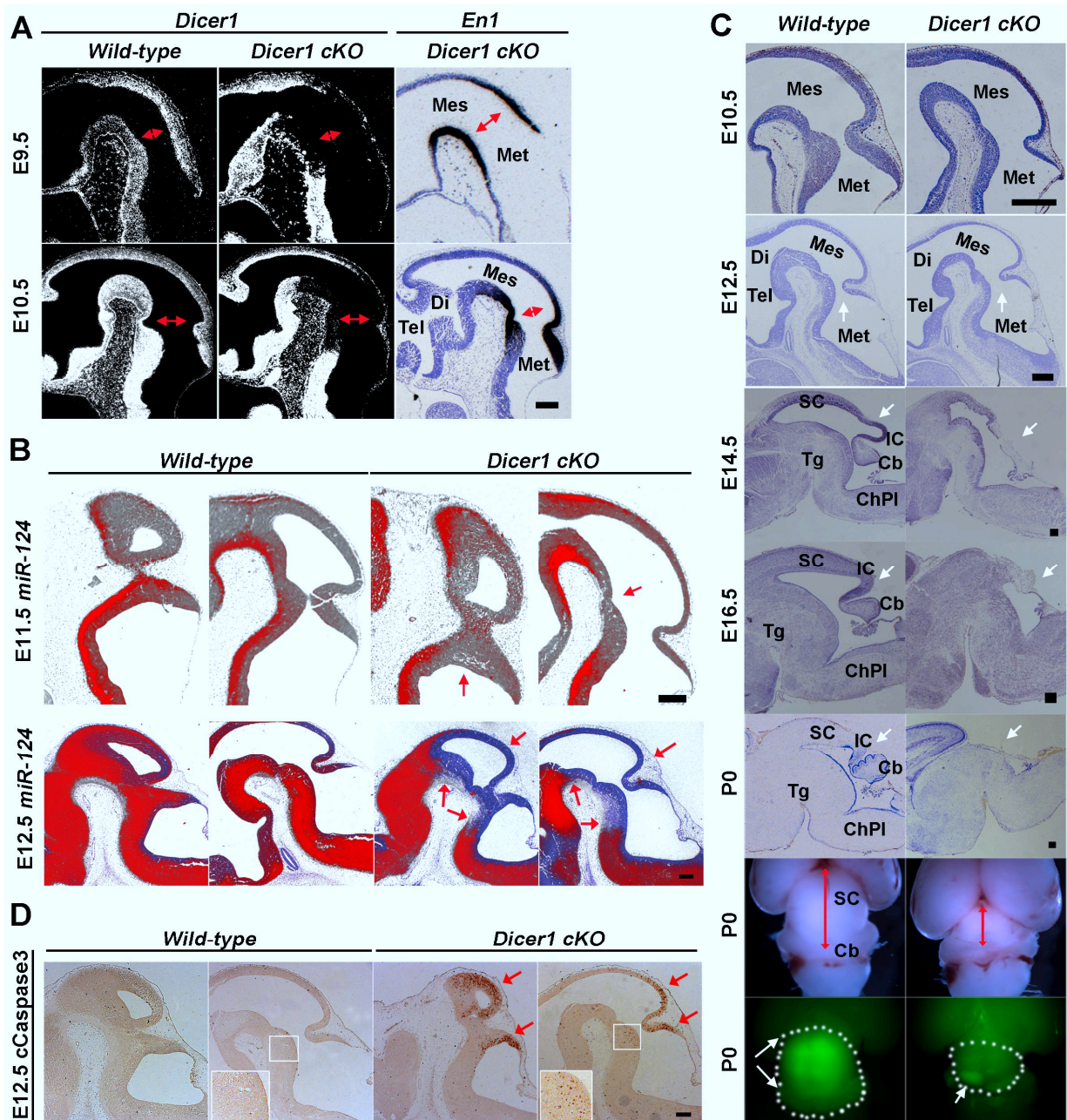
Figure 18. Loss of *Dicer1* function in the MHR leads to progressive loss of MH tissues and increased cell death.

(A) *Dicer1* expression was abolished within the *En1*$^+$ domain of *Dicer1 cKO* mice from E9.5 onwards. Red double arrows mark the approximate position of the MHB. Scale bar: 100 μm.

(B) Decreased expression at E11.5 and complete loss at E12.5 of mature *miR-124* in the MHR of *Dicer1 cKO* embryos. Red arrows point to *miR-124*-loss region. Scale bar: 100 μm.

(C) A thinner MH neuroepithelium was apparent in the *Dicer1 cKO* embryos at E12.5, and a progressive loss of dorsal and ventral MH tissues became visible in these embryos at E14.5, resulting in the complete absence of the caudal midbrain and rostral hindbrain in the P0 *Dicer1 cKO* pups (white arrows). Bottom panels: dorsal view of the MHR in *En1*$^{+/Cre}$; *Dicer1*$^{+/flox}$; *CAG-CAT-EGFP* and *En1*$^{+/Cre}$; *Dicer1*$^{flox/flox}$; *CAG-CAT-EGFP* (*Dicer1 cKO*) pups at P0, showing the almost complete loss of En1$^+$ (GFP$^+$) cells (white arrows) concomitant with a strong reduction of the dorsal MHR in the *Dicer1 cKO* mice (white circle). Scale bar: 200 μm. Abbreviations: Cb, cerebellum; ChPl, choroid plexus; Di, diencephalon; IC, inferior colliculus; Mes, mesencephalon; Met, metencephalon; SC, superior colliculus; Tel, telencephalon; Tg, tegmentum.

(D) Massive increase of apoptotic (cCaspase3$^+$) cells in the dorsal MHR of *Dicer1 cKO* embryos at E12.5, whereas ventral MHR tissues were less affected (insets) in the mutants. Scale bar: 100 μm.

Figure 19. Increased spoptosis in the MHR of *Dicer1 cKO* embryos from E11.5 onwards.
(A) Immunostaining for cleaved caspase3 (cCaspase3) showed that apoptosis was not increased in the MHR of E10.5 *Dicer1 cKO* embryos.
(B) Apoptotic cell death was dramatically increased in the dorsal and to a lesser extent in the ventral MHR of *Dicer1 cKO* embryos. Scale bar = 50 μm.

3.2.2 Establishment of the MHB and patterning of the MHR are not affected in the *Dicer1 cKO* embryos

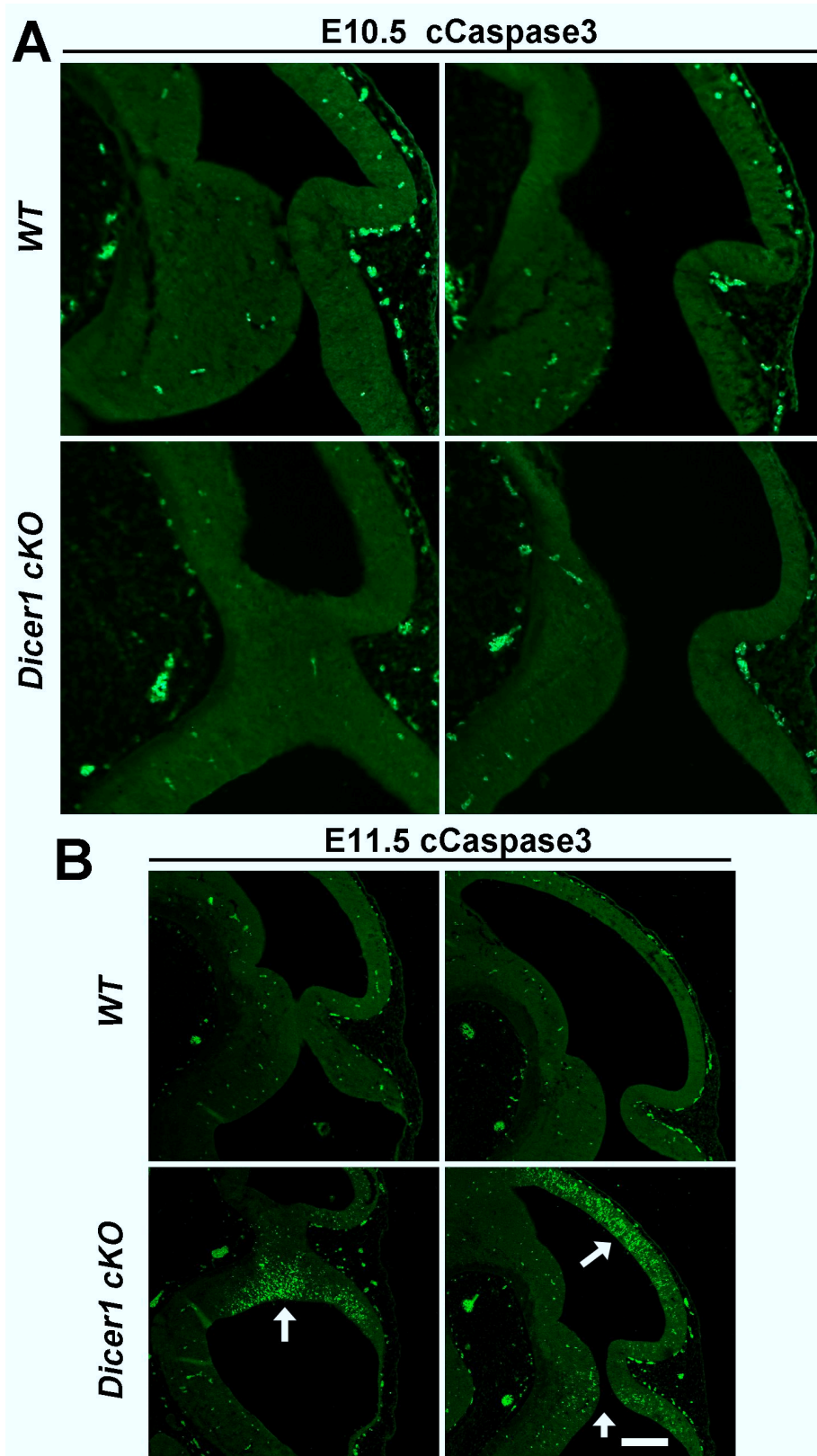Although its appearance was temporally delayed, the MHR phenotype of the P0 *Dicer1 cKO* pups strongly resembled the MHR phenotype of mouse mutants for the IsO (isthmic organizer) genes *Wnt1* (McMahon and Bradley, 1990), *Fibroblast growth factor 8* (*Fgf8*) (Chi et al., 2003), *Engrailed* (*En*) *1/2* (Simon et al., 2001; Wurst et al., 1994), *Lmx1b* (Guo et al., 2007), and *Pax2* (Schwarz et al., 1997). I therefore assessed the expression of these IsO and of other A/P and D/V patterning genes in the *Dicer1 cKO* embryos by ISH, but the expression of *Wnt1*, *Fgf8*, *En1*, *Lmx1b*, *Pax2*, *Otx2*, *Gbx2* and *Sonic hedgehog* (*Shh*) was not altered in the MHR of these embryos at E9.5, E10.5 and E12.5 (Fig. 20 and data not shown). Nevertheless, the protein but not the mRNA expression levels of these genes might be affected in the *Dicer1 cKO* embryos. Due to the lack of good working antibodies for some of the crucial IsO factors such as Wnt1 and Fgf8, I used an indirect approach by detecting known target genes of the Fgf8 signaling pathway in the MHR of the *Dicer1 cKO* embryos. However, the expression of the direct targets and negative modulators of the Fgf8 signaling pathway, *Sef* (*Il17rd*), *Sprouty* (*Spry*) *1* and *2*, and *Dusp6* (*Mkp3*) (Guillemot and Zimmer), was also not altered in the mutant embryos at E10.5 and E12.5 (Fig. 21). Finally, a loss of MHR tissues might also result from a precocious differentiation and failure to maintain the MHB due to the lack of the neurogenic basic-helix-loop-helix (bHLH) *Hes* TF genes (Hirata et al., 2001). I therefore assessed the expression of *Hes1*, *Hes3* and *Hes5* in the MHR of the *Dicer1 cKO* embryos, but again, the expression of these genes was not affected in the mutants at E10.5 and E12.5 (Fig. 22). Altogether, my data indicate that the A/P and D/V patterning of the MHR and the maintenance of the MHB are not affected by the loss of Dicer1-processed mature miRNAs in this region of the brain.
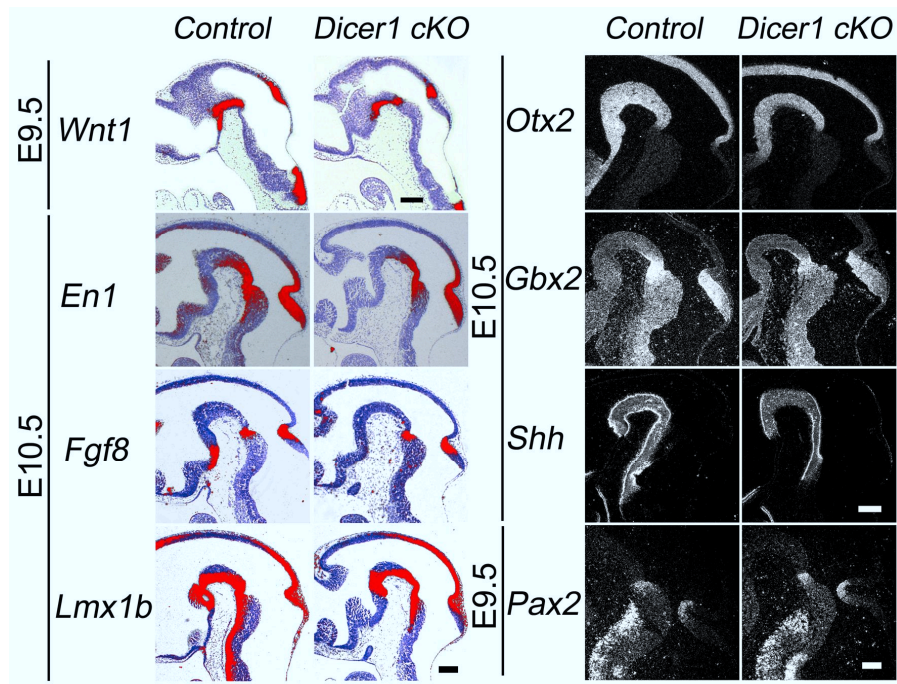
Figure 20. The expression of the isthmic organizer and floor plate genes *Wnt1*, *En1*, *Fgf8*, *Lmx1b*, *Otx2*, *Gbx2*, *Shh* and *Pax2* was not altered in the *Dicer1 cKO* mice. The expression of above genes was analyzed in three stages between E9.5 and E12.5, and in each stage at least 3 control (wild type or heterozygous) mice and 3 *Dicer1 cKO* mice were subjected to ISH. Scale bar = 200 μm.
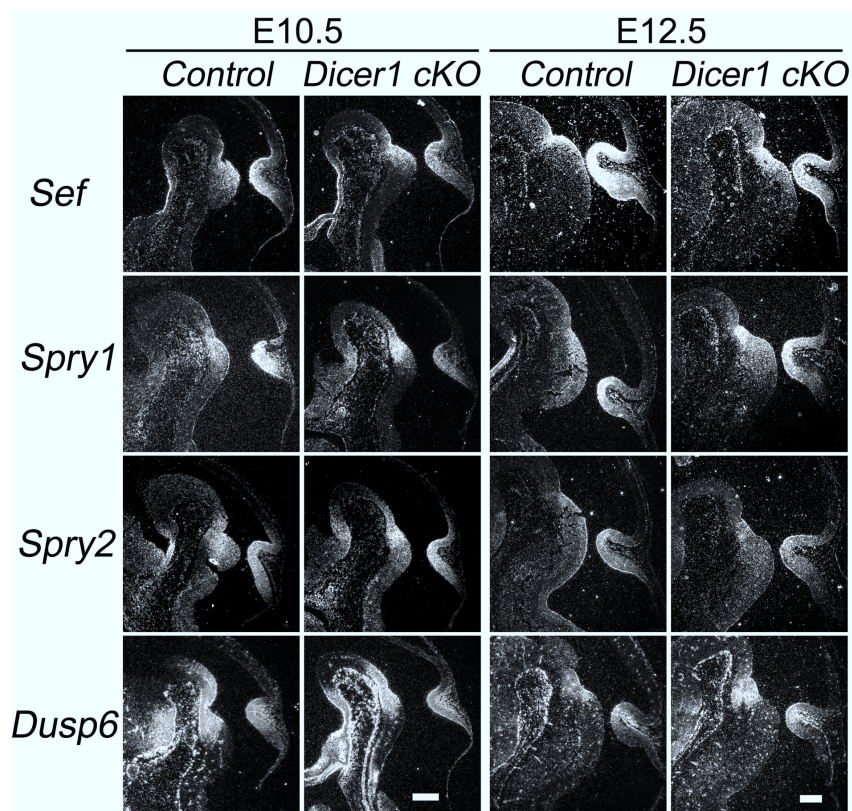
Figure 21. Fgf8 signaling pathway was not altered in the *Dicer1 cKO* embryos. Expression of the direct target genes of the Fgf8 signaling pathway, *Sef1*, *Spry1/2* and *Dusp6*, was not affected in the *Dicer1 cKO* embryos at E10.5 or E12.5, indicating that Fgf8 protein level was not altered in the MHR of the mutant embryos. Scale bar = 200 μm.
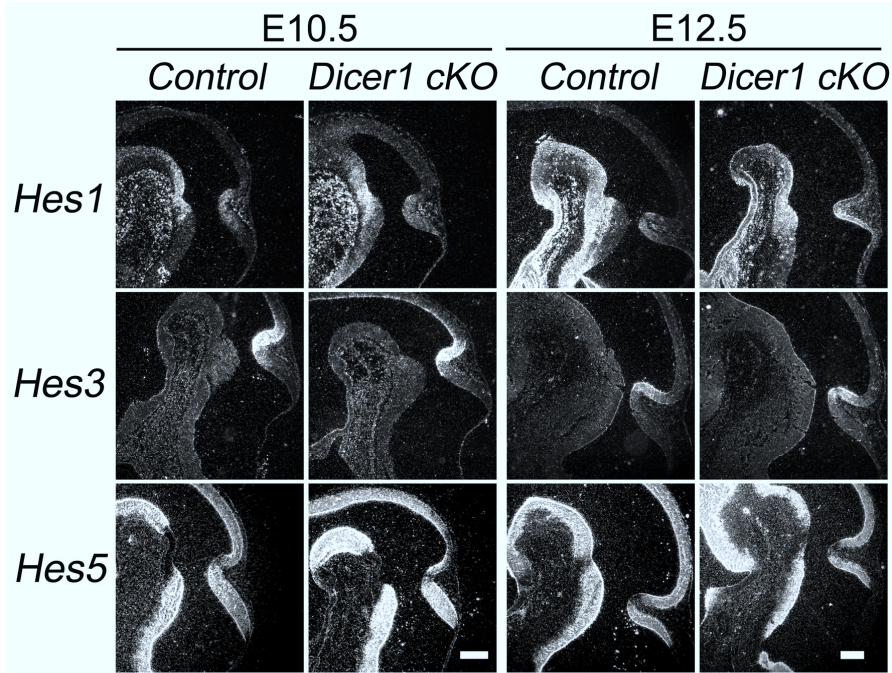
Figure 22. Expression of the neurogenic bHLH TFs *Hes1*, *Hes3* and *Hes5* was not altered in the *Dicer1 cKO* embryos at E10.5 or E12.5, indicating that the maintenance of the MHB was not affected in the mutant embryos. Scale bar: 200 μm.

3.2.3 The size of neuronal populations is reduced in the MHR of *Dicer1 cKO* mice

Apoptosis was strongly increased in the dorsal MHR of the *Dicer1 cKO* mice, but ventral neural tissues appeared less affected by apoptotic cell death in the mutant embryos (Fig. 18, 19). To determine the extent of ventral MH (vMH) tissue loss and to establish whether the neuronal populations residing in the ventral MHR (GFP$^+$ (En1$^+$) domain in the *Dicer1 cKO; CAG-CAT-EGFP* embryos) develop normally in the *Dicer1 cKO* embryos, I assessed the identity and numbers of midbrain dopaminergic (mDA), red nucleus (RN) and oculomotor (OM) neurons (all residing in the ventral midbrain), and of rostral hindbrain serotonergic (5HT) neurons. Notably, the Pitx3$^+$ mDA and Pou4f1$^+$ RN neuron numbers were strongly reduced by ~76–90%, and the Isl1$^+$ OM and 5HT$^+$ serotonergic neuron numbers were decreased by ~33–47% in the E12.5 *Dicer1 cKO* embryos as compared to their heterozygote littermates (Fig. 23), thus indicating that although these neuronal populations were correctly specified, their progenitors did not generate the appropriate amount of neuronal offspring in the *Dicer1 cKO* embryos. It should also be noted that a more severe reduction was found in neuronal populations that are generated at later time-points (mDA and RN neurons are born at E10.5 to E11.5, 2-3 days after Cre-mediated ablation of *Dicer1*) than in neuronal populations that are generated at earlier time-points (OM neurons are born at E9.5, only 1 days after Cre-mediated ablation of *Dicer1*). At this early time-point it is very likely that some Dicer1

50

protein and/or miRNAs were still present in OM neural progenitors and their progeny, as the lifespan of Dicer1 protein and some miRNAs is quite long (Davis et al., 2008). There are many TH+ cells that do not express Pitx3 in the E12.5 *Dicer1 cKO* mice (Fig. S5), suggesting that some miRNAs target the repressor(s) of Pitx3 and that the terminal differentiation of mdDA neurons requires Dicer1 and miRNAs.
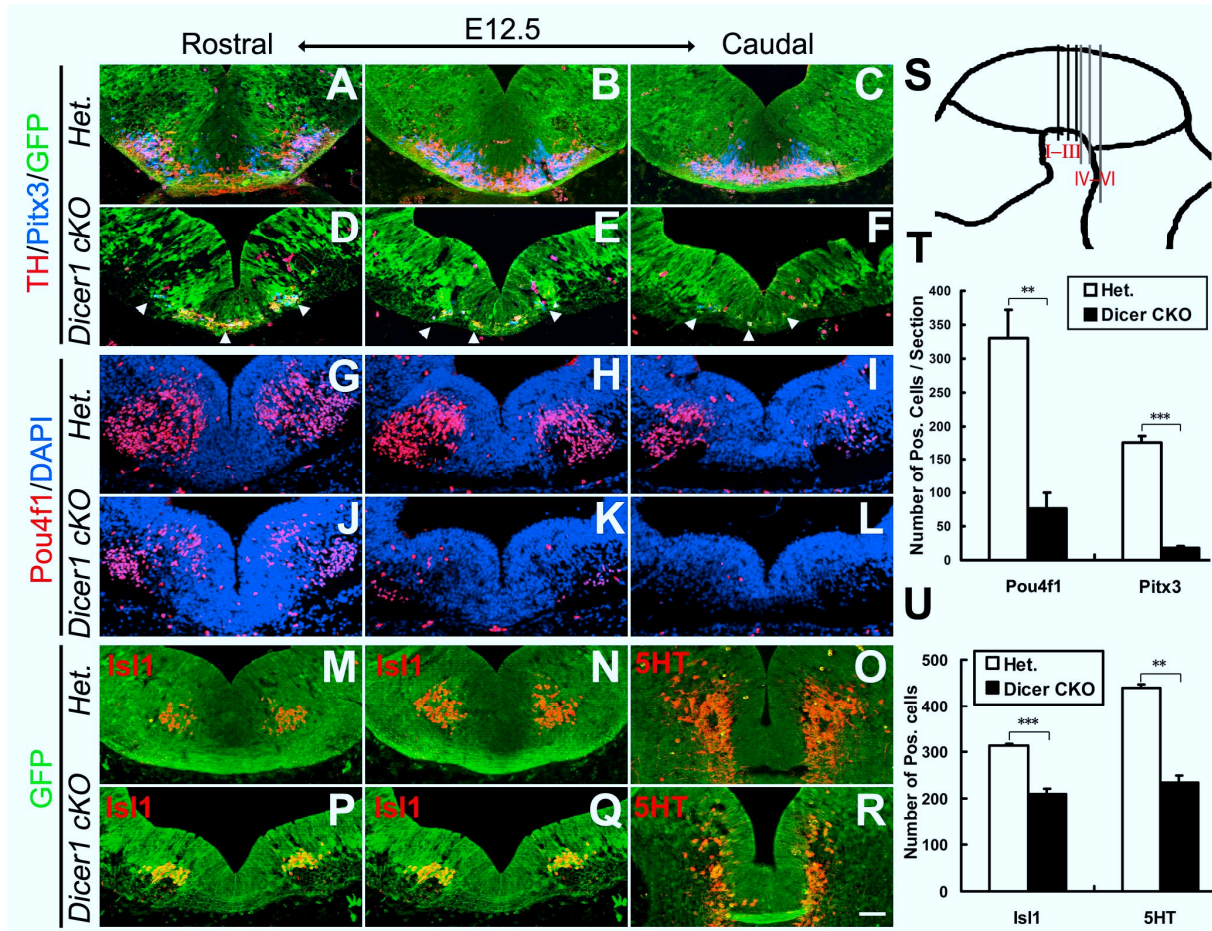
Figure 23. Correct specification but reduced size of vMH neuronal populations in the E12.5 *Dicer1 cKO* embryos.

(A-L, T) The numbers of Pitx3$^+$ and TH$^+$ mdDA and of Pou4f1$^+$ red nucleus neurons were drastically reduced in the ventral midbrain of E12.5 *Dicer1 cKO; CAG-CAT-EGFP* embryos as compared to their heterozygote littermates (Pitx3$^+$ cells: *Het.*, 175.89±9.34; *Dicer1 cKO*, 17.89±3.42; Pou4f1$^+$ cells: *Het.*, 330.67±41.79; *Dicer1 cKO*, 76.89±22.87; mean ± SEM, N=3; triple asterisks, P<0.001; double asterisks, P<0.005 in independent-samples *t* test). The rostrocaudal position of the sections is depicted in (S) by I to III. White arrowheads in (D-F) point at Pitx3$^+$ cells.

(M-R, U) The numbers of Isl1$^+$ oculomotor nucleus neurons in the ventral midbrain and of 5HT$^+$ serotonergic neurons in the ventral rostral hindbrain were diminished in E12.5 *Dicer1 cKO; CAG-CAT-EGFP* embryos as compared to their heterozygote littermates (Isl1$^+$ cells: *Het.*, 314.33±4.1; *Dicer1 cKO*, 210±10.8; 5HT$^+$ cells: *Het.*, 439±7.22; *Dicer1 cKO*, 233±16.74; mean ± SEM, N=3; triple asterisks, P=0.001; double asterisks, P<0.005 in independent-samples *t* test). The rostrocaudal position of the sections is depicted in (S) by IV to VI. Scale bar: 50 μm.

3.2.4 Cell cycle exit defects in the *Dicer1 cKO* mice

As the amount of apoptosis in the ventral MH (vMH) of E11.5 and E12.5 *Dicer1 cKO* mice (Figure 1D and S1) does not correspond to the severe tissue loss already evident at these stages (Fig. 23), I hypothesized that a failure of vMH neural progenitors to exit the cell cycle and to generate the correct number of neuronal progeny might contribute to the loss of vMH neural tissues in the mutant embryos. To test this hypothesis, I performed a cell cycle exit assay by injecting EdU into the pregnant dams at E11.5, 24 hrs before sacrificing the mice. Co-labelling for EdU and Ki67 (a marker for proliferating cells in all phases of the cell cycle) showed that the ratio of EdU/Ki67 double-positive cells per total number of EdU$^+$ cells (cells that remain in the cell cycle) was remarkably increased in the *Dicer1 cKO* embryos (Fig. 24). I concluded that vMH neural progenitors fail to exit the cell cycle and thus to generate the proper amount of postmitotic progeny that can differentiate into mDA, OM, RN and 5HT neurons in the *Dicer1 cKO* embryos, thereby contributing to the vMH tissue loss in the absence of a strongly increased apoptosis in this region of the mutant brain.
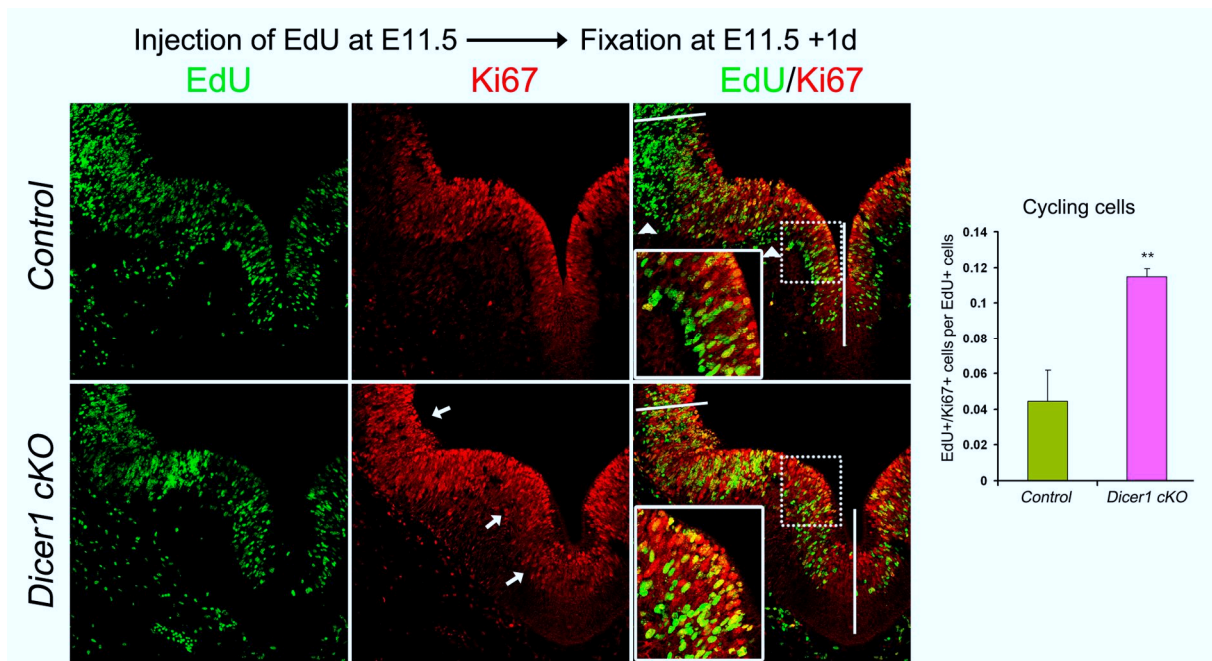
Figure 24. Cell cycle exit was defect in the *Dicer1 cKO* mice. Double-labelling for EdU (injected at E11.5, 24 hrs before dissection of the embryos) and Ki67 revealed that the fraction of cell cycle re-entry after 24 hrs (EdU$^+$/Ki67$^+$ double-positive cells per total EdU$^+$ cells) was significantly increased in the vMH of the *Dicer1 cKO* embryos (*Control* (*Het.* and *WT*): 0.0444±0.0175; *Dicer1 cKO*: *0.1147±0.0046*; mean ± SEM, N=3; P<0.005 in independent-samples *t*-test). White lines delimit the vMH area that was used for quantification of EdU/Ki67 single- and double-positive cells.

3.2.5 *MiR-200* family members are severely downregulated in the MHR of *Dicer1 cKO* mice

Neural tissue was progressively lost in the MHR of the *Dicer1 cKO* embryos mainly due to an increased apoptosis in the dorsal MHR and to a cell cycle exit defect in the ventral MHR of the mutants, but these defects are not due to the misexpression of crucial patterning and neurogenic factors in this region of the *Dicer1 cKO* embryos. MiRNAs have been implicated in the regulation of cell proliferation, cell death, and neuronal differentiation in the CNS (Coolen and Bally-Cuif, 2009), but their role in the control of cell cycle exit of neural progenitors is less well established. To find candidate miRNAs that might target known regulators of cell cycle progression and neural progenitor maintenance, I first determined the miRNA expression profile in the MHR (also including some En1^{+}-domain-beyond *wild-type* tissue) of E12.5 *Dicer1 cKO* embryos as compared to their *En1$^{+/Cre}$*; *Dicer1$^{+/flox}$* heterozygous littermates, using next generation sequencing (NGS) technology. The most strongly downregulated miRNAs in the mutant MHR were the five members of the *miR-200* family (*miR-200a/b/c*, *141* and *429*, Fig. 25 B), which were also expressed at lower levels in the MHR of *En1$^{+/Cre}$*; *Dicer1$^{+/flox}$* heterozygous mice at E12.5 as compared to E10.5 (Fig. 25 C). By contrast, *let-7b* and *miR-125a*, two members of the *let-7* and *miR-125* families promoting neuronal differentiation (Coolen and Bally-Cuif, 2009), were strongly upregulated in the MHR of the E12.5 as compared to the E10.5 heterozygous embryos (Fig. 25 C), suggesting that the expression of the *miR-200* family declines with increasing neuronal differentiation in the MHR.

The *miR-200* family consists of five members located within two clusters on separate chromosomes (chromosome 6 (*miR-200c/141* cluster) and chromosome 4 (*miR-200b/a/429* cluster) in the mouse) (Fig. 25D, (Peter, 2009). They can be further divided into two subgroups according to their seed sequences, which differ by just one nucleotide: subgroup I comprises *miR-200a* and *miR-141*, and subgroup II comprises *miR-200b/c* and *miR-429* (Fig. 25D, (Peter, 2009). As *miR-200c* showed the highest expression level relative to the other *miR-200* family members in the MHR based on my NGS data (Fig. 25B and Table 3.1), I detected this miRNA in wild-type and *Dicer1 cKO* MH tissues using LNA-based ISH. *MiR-200c* is strongly expressed in the ventricular (VZ), subventricular (SVZ) and intermediate zone (IZ), but not in the mantle zone (MZ) of the E12.5 wild-type MHR (Fig. 25E). The expression of *miR-200c* was complementary to the transcription of *miR-124* (a miRNA promoting neuronal differentiation, (Coolen and Bally-Cuif, 2009)) in the IZ and MZ of the E12.5 wild-type embryo (Fig. 25E). Notably, *miR-200c* was undetectable and *miR-124* was

barely detectable in the MHR of the *Dicer1 cKO* embryos at E12.5 (Fig. 25E), thus validating my NGS approach and confirming the near-complete ablation of mature miRNAs in the MHR of the *Dicer1 cKO* embryos.
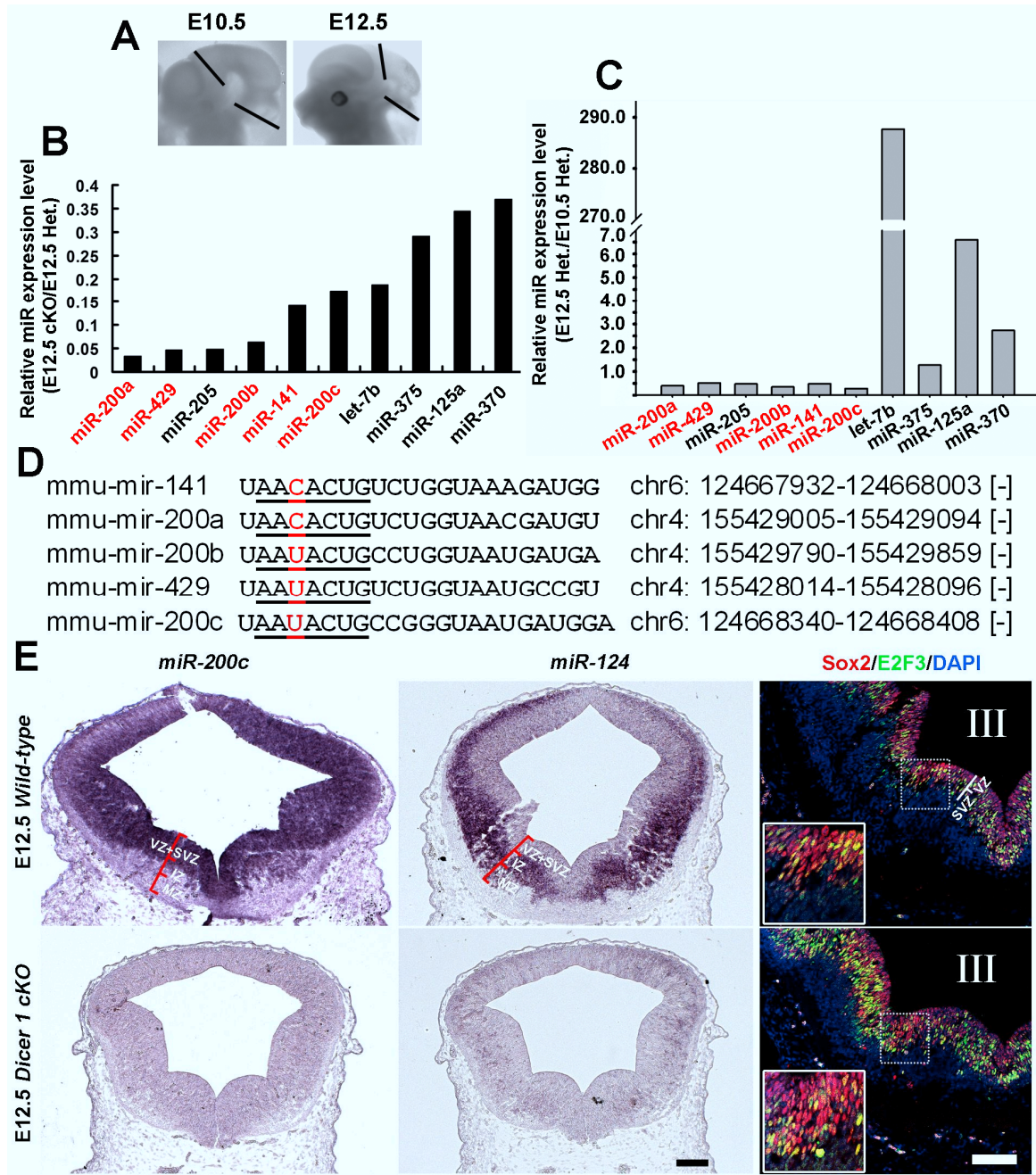
Figure 25. Severe loss of *miR-200* family members in the MHR of *Dicer1 cKO* embryos.

(A) Pictures depicting the MHR (delimited by black lines) that was dissected from E10.5 and E12.5 embryos and used for miRNA expression profiling.

(B) The five miR-200 family members (*miR-200a*, *miR-200b*, *miR-200c*, *miR-141* and *miR-429*) were among the top 10 most downregulated miRNAs in the MHR of E12.5 *Dicer1 cKO* embryos as compared to E12.5 $En1^{+/Cre}$; $Dicer^{+/flox}$ heterozygous embryos.

(C) The expression levels of the *miR-200* family members were strongly down-regulated in the MHR of $En1^{+/Cre}$; $Dicer^{+/flox}$ heterozygous embryos at E12.5 as compared to E10.5.

(D) Sequence and chromosomal location of the five murine miR-200 family members.

(E) *MiR-200c* is strongly expressed in the ventricular (VZ) and subventricular zone (SVZ) and in a complementary pattern to *miR-124*, which is strongly expressed in the intermediate (IZ) and mantle (MZ) zones of the MH neuroepithelium. A similar expression pattern of *miR-200c* was also observed in the forebrain and hindbrain as in the midbrain. Expression of both miRNAs was completely abolished in the *Dicer1 cKO* embryos at E12.5. Expression of the predicted *miR-200c* targets Sox2 and E2F3 is also confined to the VZ/SVZ and IZ of the MH neuroepithelium, similar to *miR-200c*, although E2F3 is expressed in a salt-and-pepper pattern in single cells sparing the layer immediately adjacent to the third ventricle (III). Scale bars: 100 μm.

Table 3.1 Expression level of high decreased miRNAs (reads number)

miRNA	E10.5 Heter.	E12.5 Heter.	E12.5 Dicer1 cKO	E12.5Dicer1 cKO / E12.5 Heter.	E12.5 Heter./ E10.5 Heter.
mmu-miR-463	1	1	0	0	1
mmu-miR-470	3	2	0	0	0.666667
mmu-miR-200a	724	290	4	0.033545	0.400552
mmu-miR-429	402	207	4	0.046995	0.514925
mmu-miR-205	1150	548	11	0.048817	0.476522
mmu-miR-200b	864	305	8	0.06379	0.353009
mmu-miR-141	280	136	8	0.143058	0.485714
mmu-miR-200c	1699	474	34	0.174447	0.278988
mmu-let-7b	54	15535	1198	0.187546	287.6852
mmu-miR-375	1462	1854	222	0.29121	1.268126
mmu-miR-125a	8682	57266	8128	0.345183	6.595946
mmu-miR-370	10723	29359	4472	0.370444	2.737946

The *miR-200* family members might generally regulate the proliferation, cell cycle exit and differentiation of pluri- or multipotent stem cells, including neural stem cells (NSC). To establish whether this is the case, I used an in vitro paradigm to differentiate mouse embryonic stem cells (mESC) into Tubb3^{+} neurons (Fig. 26A) (Bibel et al., 2007b), and determined the miRNA profile in these cells at three different stages of the differentiation protocol: mESC representing the initial pluripotent state, embryoid bodies (EB) representing neuroectoderm commitment, and differentiated neurons as the end state. Known miRNAs were enriched at the expected stages of the differentiation procedure (Fig. 26B), such as *miR-295* in the undifferentiated ESC stage (Martinez and Gregory, 2010; Wang et al., 2008b), *miR-9* in the committed neuroectoderm and differentiated neuron stage, and *let-7c* in the differentiated neuron stage (Coolen and Bally-Cuif, 2009; Krichevsky et al., 2006), thus validating my approach. As expected, the *miR-200* family members were highly expressed in the undifferentiated mESC; their expression levels decreased to an intermediate level in committed neuroectodermal cells and dropped to their lowest levels in the differentiated neurons (~30–100-fold lower levels than in the mESC) (Fig. 26C). Notably, *miR-200c* still showed the highest expression levels in differentiated neurons among all *miR-200* family members Fig. 26C). I concluded that the *miR-200* family members are highly expressed in

undifferentiated pluri-/multipotent stem cells (mESC and NSC) and their expression levels decline along the commitment and differentiation of these cells into neurons both in vivo and in vitro. Their loss in the MHR of the *Dicer1 cKO* embryos might thus contribute to the cell cycle exit defects of ventral neural progenitors observed in these mutants.
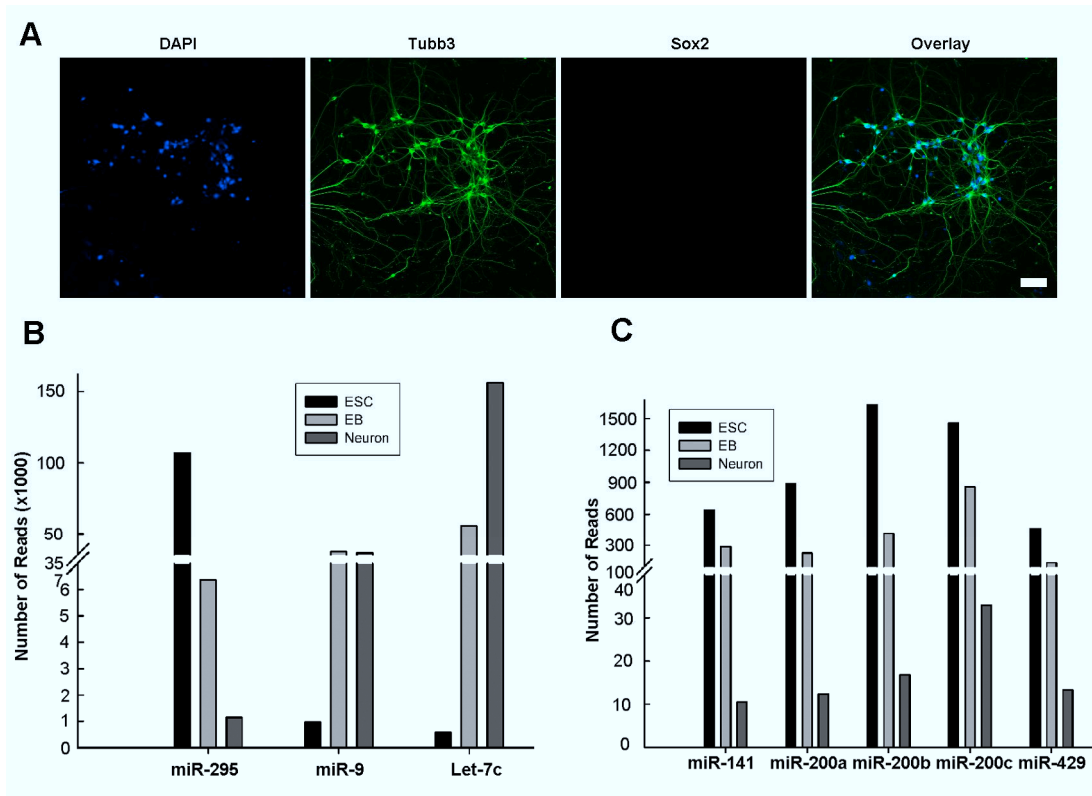
Figure 26. Differentioation of ES cells into neurons.

(A) mES cells were differentitated into (glutamatergic) neurons using the protocol of (Bibel et al., 2007), a fraction of the cells were grown on poly-D-lysine-coated coverslips until the end of the differentiation procedure, fixed and immunostained for Sox2 (red, a marker for undifferentiated ESC and neural progenitors) and Tubb3 (green, a marker for differentiating neurons). More than 90% of the cells were Tubb3^{+}/Sox2^{-} at the end of the differentiation procedure, which means the differentiation procedure was successful and that the samples can be used for RNA isolation and miRNA profiling. Scale bar: 50 μm.

(B) MiRNAs expression in the three stages of ES differentiation procedure was profiled using next generation technology. Validity of this approach was shown by the selective enrichment of known ESC-expressed miRNA (*miR-295*) or neuron-related miRNAs (*miR-9* and *let-7c*) at the corresponding steps of the differentiation procedure (ESC: undifferentiated ESC; EB: embryoid bodies; Neuron: differentiated neurons).

(C) The expression of all five miR-200 family members was highest in the undifferentiated (ESC) stage, and decreased along the differentiation procedure to lowest levels in the differentiated (neuron) stage.

3.2.6 Sox2^{+} and E2F3^{+} neural progenitor cells accumulate in the MHR of *Dicer1 cKO* embryos

I next searched for possible targets of the *miR-200* family members whose de-regulation in MH tissues might cause the cell cycle defects observed in the *Dicer1* cKO embryos. Two of the predicted targets of the *miR-200* family using bioinformatics tools (Targetscan,

http://www.targetscan.org) are the Sox2 and E2F3 TFs. Sox2 is required for the maintenance of self-renewing NSC (Graham et al., 2003; Pevny and Nicolis, 2010), and E2F3 plays a pivotal role in cell cycle progression, particularly in promoting the S-phase entry of proliferating cells (DeGregori, 2002; Leone et al., 1998). Both TFs were co-expressed with miR-200c in the MHR of E12.5 wild-type mice (Fig. 25E); whereas Sox2 expression was mostly confined to the neural progenitors in the VZ/SVZ, E3F3 was expressed in a salt-and-pepper pattern in single cells that extended from the VZ/SVZ into the IZ of the vMHR and spared the cell layer immediately adjacent to the third ventricle (Fig. 25E). I therefore hypothesized that these two TFs might be direct targets of the miR-200 family, and in fact, the numbers of cells expressing Sox2 or E2F3 were apparently increased in the ventral MHR of the *Dicer1 cKO* embryos (Fig. 25E). To establish this in more detail, I determined the changes in Sox2 and E2F3 expression as well as in proliferating S-phase (EdU$^+$) cells within the MHR of the mutant embryos as compared to their wild-type littermates from E10.5 to E12.5. I focussed my analyses on the vMHR as this was the region where I had previously detected the cell cycle exit defects in the mutant embryos, and as the dorsal MHR of mutants has a massive apoptosis from E11.5 onwards. At E10.5, the Sox2$^+$ domain was not obviously increased, but the Tubb3$^+$ (a marker for postmitotic neurons) domain was clearly reduced in the vMHR of the *Dicer1 cKO* embryos, indicating that the differentiation of neural progenitors into postmitotic neurons was affected in the mutant embryos at or even before E10.5 (Fig. 27A). At E11.5, the Sox2$^+$ domain was visibly expanded at the expense of the Tubb3$^+$ domain, and the numbers of Sox2$^+$, E2F3$^+$ (G1/S-phase) and EdU$^+$ (S-phase) neural progenitors in the vMHR of the *Dicer1 cKO* embryos was increased by 25% (Sox2$^+$ and E2F3$^+$ cells), and 18% (EdU$^+$ cells) (Fig. 27B-F). The increase of Sox2$^+$ cells in the mutant embryos was due to the enlargement of the Sox2$^+$ domain and not due to an increase in Sox2$^+$ cell density (Fig. 27D, E). At E12.5, the numbers of Sox2$^+$, E2F3$^+$ and EdU$^+$ neural progenitor cells were further increased by nearly 2-fold, and the thinning of the Tubb3$^+$ domain in the MZ became even more evident in the vMHR of the *Dicer1 cKO* embryos (Fig. 27G-J). Remarkably, the proportion of EdU$^+$ (S-phase) cells that co-expressed E2F3 (EdU/E2F3 double-positive cells per total amount of EdU$^+$ cells) and the number of EdU/E2F3 double-positive cells were increased by 80% and 2-fold, respectively, in the vMHR of the *Dicer1 cKO* embryos as compared to their wild-type littermates (Fig Fig. 27K). Furthermore, the expansion of the Sox2$^+$ and E2F3$^+$ proliferating neural progenitor domain in the vMHR of the *Dicer1 cKO* embryos was accompanied by an apparent change of vMH morphology and medio-lateral expansion of the cavity of the third ventricle in the mutant

embryos (Fig. 27A, B, G). Altogether, my results indicated that proliferating (EdU$^+$/Sox2$^+$/E2F3$^+$) neural progenitors accumulate over time in the vMHR of the *Dicer1 cKO* embryos, and that their failure to exit the cell cycle and to generate the proper amout of Tubb3$^+$ neuronal progeny might be due to the over-expression of Sox2 and in particular of E2F3 in these cells. The increase in the number of Sox2$^+$ and E2F3$^+$ positive cells supports the prediction that they could be direct targets of *miR-200*. The expression of E2F3 increases during G1 phase, is highest at the transition between G1 and S-phase, and shut down again during S phase. E2F3 expression increases again during G2 phase, and is definitely shut down in M phase, leading to an oscillating expression pattern during the cell cycle (He et al., 2008). During a normal cell cycle, cells have downregulated E2F3 expression in late S phase, and this was the case in wild-type embryos. However, in the *Dicer1 cKO* mice, approx. 3-fold more EdU$^+$ cells (S phase cells) still expressed high levels of E2F3 (Fig Fig. 27K), indicating that E2F3 expression is not shut down promptly during the S phase due to the loss of miRNAs in these embryos, thus leading to the cell cycle defects in the *Dicer1 cKO* mice (Fig. 27G, K).
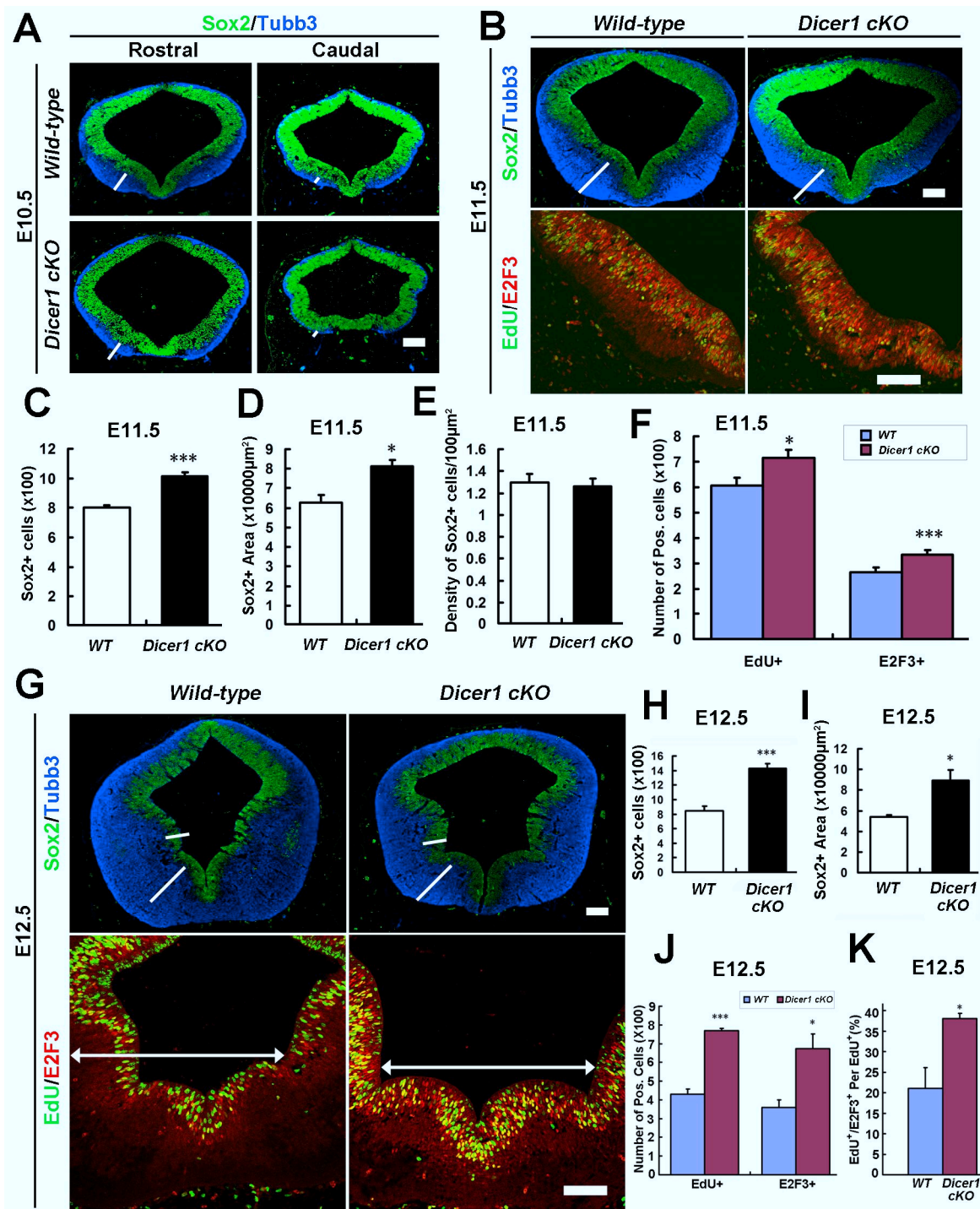
Figure 27. Accumulation of proliferating Sox2$^+$/E2F3$^+$ neural progenitors and reduced neuronal differentiation in the vMHR of the *Dicer1 cKO* embryos.

(A) The thickness (white lines) of the Tubb3$^+$ (differentiating postmitotic neurons) layer was reduced and of the Sox2$^+$ (proliferating neural progenitors) layer was increased in the vMHR of the E10.5 *Dicer1 cKO* embryos.

(B-F) E11.5 *Dicer1 cKO* embryos exhibit a thinner neuroepithelium, a reduced Tubb3$^+$ layer (white lines) and increased numbers of Sox2$^+$, E2F3$^+$ and proliferating (EdU$^+$) neural progenitor cells in the vMHR, but the density of Sox2$^+$ cells was not changed (Sox2$^+$ cells (C): *WT*, 804±11.37; *Dicer1 cKO*, 1012.5±29.17; triple asterisks, P=0.001; Sox2$^+$ area (D): *WT*, 62669±3950; *Dicer1 cKO*, 81115±3223; single asterisk, P<0.05; Sox2$^+$ cell density/100 m^2 (E): *WT*, 1.297±0.075; *Dicer1 cKO*, 1.257±0.075; P=0.72; mean ± SEM, statistical significance was estimated by independent-samples *t* test, N=3; EdU$^+$ cells (F): *WT*,

605.25±31.91; *Dicer1 cKO*, 716.25±32.09; single asterisk, P<0.05; E2F3$^+$ cells (F): *WT*, 266.5±18.32; *Dicer1 cKO*, 333.5±19.64; triple asterisks, P<0.001; mean ± SEM, statistical significance was estimated by paired-samples *t* test, N=4).

(G-J) E12.5 *Dicer1 cKO* embryos show an expanded Sox2$^+$ and reduced Tubb3$^+$ domain (white lines depict the thickness of the corresponding layer in *WT* or *Dicer cKO* embryos), and strongly increased numbers of Sox2$^+$, E2F3$^+$ and EdU$^+$ neural progenitor cells in the vMHR (Sox2$^+$ cells (H): *WT*, 845.75±67.45; *Dicer1 cKO*, 1433±59.16; triple asterisks, P=0.001; Sox2$^+$ area (I): *WT*, 53941.75±1945; *Dicer1 cKO*, 89127.75±10292; single asterisk, P<0.05; N=4; EdU$^+$ cells (J): *WT*, 430±27.4; *Dicer1 cKO*, 770±10.6; triple asterisks, P<0.001; E2F3$^+$ cells (J): *WT*, 360±39.3; *Dicer1 cKO*, 673±78.5; single asterisk, P<0.05; N=3; mean ± SEM, statistical significance was estimated by independent-samples *t* test). Note also the medio-lateral broadening of the ventricular cavity in the vMHR of the *Dicer1 cKO* embryos (white arrows in G).

(K) The proportion of EdU/E2F3 double-labelled cells per total amount of EdU$^+$ (S-phase) cells and the number of EdU$^+$/E2F3$^+$ cells were strongly increased in the E12.5 *Dicer1 cKO* embryos (the ratio of EdU$^+$/E2F3$^+$ per EdU$^+$ (%): *WT*, 21±5.1; *Dicer1 cKO*, 38.1±1.2; the number of EdU$^+$/E2F3$^+$ cells: *WT*, 96±23.4; *Dicer1 cKO*, 293.7±13.3; single asterisk, P<0.05; N=3; mean ± SEM, statistical significance was estimated by independent-samples *t* test).

3.2.7 Overexpression of *miR-200* promotes neuronal differentiation of neural progenitors

The data from my in vivo experiments indicate that *miR-200c* is expressed in the VZ/SVZ of the vMHR, and suggest that the *miR-200* family members might regulate cell cycle exit and neuronal differentiation of vMH neural progenitors by targeting the expression of Sox2 and E2F3 in these cells. To establish this more conclusively, I generated different *miR-200* OE vectors for the overexpression of *miR-200* family members in primary cultures derived from the vMHR of E11.5 wild-type mice. I cloned the *miR-200c/141* cluster into my *miR-200* OE vectors (pcDNA6.2-EmGFP vector (Lau et al., 2008)), because this cluster represents both seed sequence subgroups of the *miR-200* family with potentially different target mRNAs. Careful testing of these *miR-200* OE vectors indicated that overexpression of the *miR-200c/141* cluster under the control of the *CAG* promoter (*pcDNA6.2-EmGFP-miR-200c-141* OE vector) resulted in intermediate *miR-200c* and very high *miR-141* levels in the transfected cells, and caused an extensive cell loss in the primary vMHR cultures (Fig. S5). Overexpression of the *miR-200c* gene alone under the control of the *CAG* promoter (*pcDNA6.2-EmGFP-miR-200c* OE vector) resulted in high levels of *miR-200c* and very low levels of *miR-141* in the transfected cells, whereas overexpression of the *miR-200c/141* cluster under the control of the *U6* promoter (*pU6-miR-200c-141-CAG-EGFP* OE vector) resulted in moderate levels of *miR-200c* and *miR-141* in the transfected cells (Fig. S5). Co-transfection of these three *miR-200* OE vectors with a *Sox2 3'UTR* sensor vector harbouring one *miR-200c* BS and no *miR-141* BS, showed that all three vectors were able to repress

luciferase expression from the sensor vector in a dose-dependent manner (Fig. S5). Based on these results, I transfected the *pU6-miR-200c-141-CAG-EGFP* OE vector (Fig. 28A) in primary vMHR cultures using Lipofectamine LTX and Plus (invitrogen, USA), which results in a transfection efficiency of 5-10% in my cultures (Fig. S5). Overexpression of *miR-200c/141* in these cultures led to a significant reduction of Sox2$^+$ and E2F3$^+$ progenitor cells, and to a significant increase of Tubb3$^+$ postmitotic neurons after 3 days post-transfection (3dpt) (Fig. 28B-E). To establish whether the overexpression of *miR-200c* also results in a reduction of Sox2 and E2F3 protein levels in these cultures, I transfected a *mmu-miR-200c* precursor miRNA into the primary vMHR cultures. After 3dpt, Sox2 and E2F3 protein levels were strongly downregulated in the *mmu-miR-200c*-treated as compared to the control-treated primary cells (Fig. 28F). These data show that overexpression of *miR-200* family members indeed promotes the neuronal differentiation of vMHR progenitor cells by downregulating the expression of Sox2 and E2F3 in these cells.

3.2.8 Knockdown of *miR-200* maintains the multipotency of neural progenitors

To see whether the knockdown of *miR-200* family in primary vMHR cultures leads to the opposite effect, i.e. reduced neuronal differentiation of vMHR progenitor cells, thereby mimicking the phenotype observed in the vMHR of the *Dicer1 cKO* embryos, I generated a *miR-200* sponge vector containing eight repeats of a fully complementary sequence to all five miR-200 family members inserted downstream of an EGFP CDS and driven by the *CAG* promoter (Fig. 28A). The functionality of this sponge vector was tested by co-transfecting this vector together with each of the three previously mentioned *miR-200* OE vectors and a *Sox2 3'UTR* sensor vector. The reduction of luciferase expression from the sensor vector after co-transfection of a *miR-200* OE vector was in fact abolished (rescued) by the co-transfected *miR-200* sponge vector in all three cases, indicating that the sponge vector is able to knock-down even high levels of *miR-200c/141* (Fig. S5). As primary vMHR cells express rather low levels of *miR-200c* as compared to the ubiquitously expressed *U6B* RNA (Fig. S5), I expected that transfection of the *miR-200* sponge vector would fully knock-down the *miR-200* family in these cells. Indeed, the numbers of Sox2$^+$ and E2F3$^+$ neural progenitor cells were increased, and the numbers of Tubb3$^+$ postmitotic neurons were decreased after transfection of the *miR-200* sponge vector as compared to the control-transfected primary vMHR cells (Fig. 28G-J), thus recapitulating my findings in the vMHR of the *Dicer1 cKO* embryos (see Fig. 27). Altogether, my data strongly support the idea that the *miR-200* family is required to promote

the cell cycle exit and neuronal differentiation of Sox2$^+$ and E2F3$^+$ (cycling) neural progenitors in the ventral MHR of the mouse, and that the vMHR phenotype in the *Dicer1*
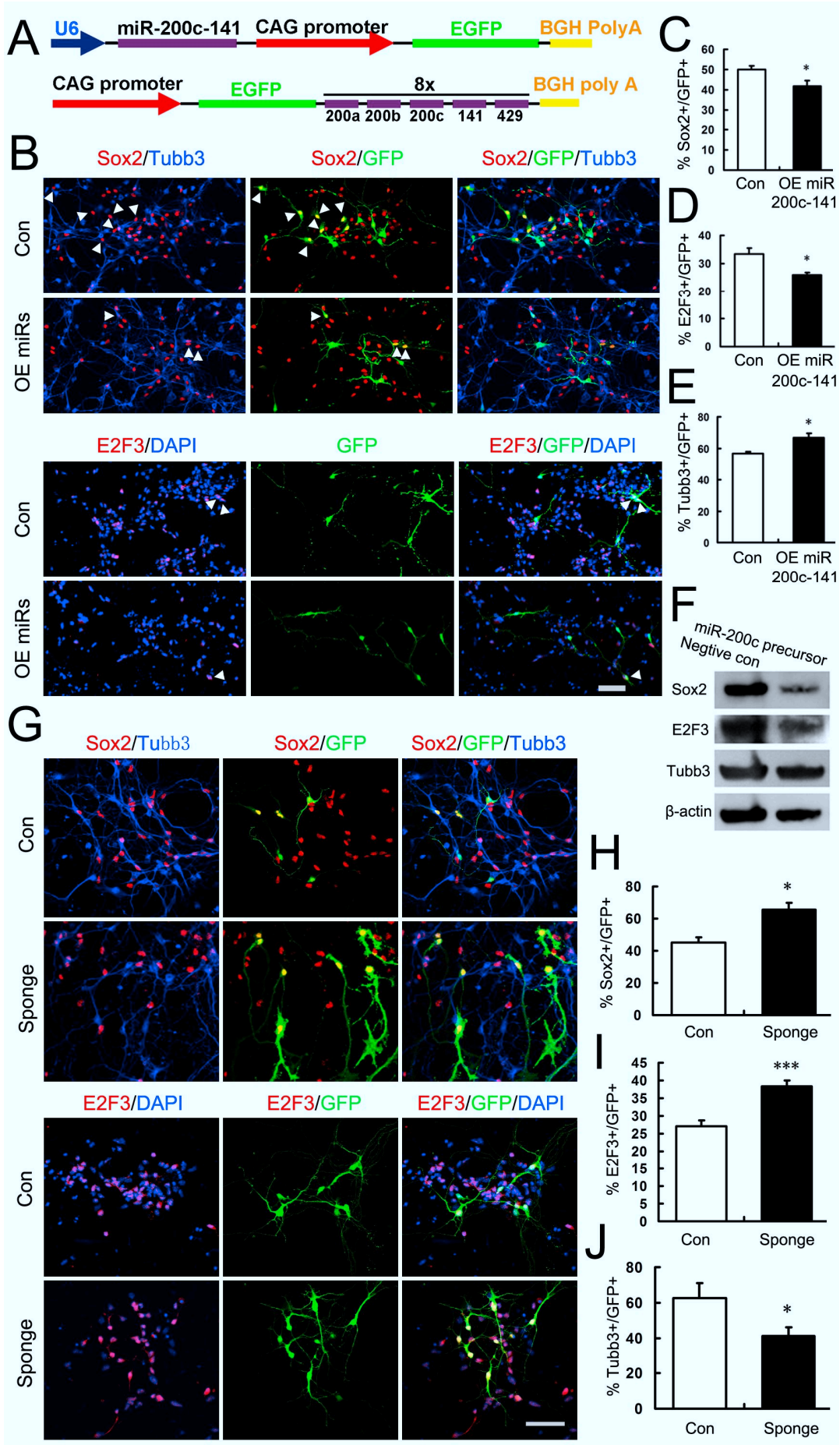
Figure 28. Overexpression of *miR-200c-141* promotes, and knockdown of the *miR-200* family suppresses neuronal differentiation of vMHR neural progenitors in vitro.

(A) Schematic drawings of the *miR-200* OE and sponge vectors used in these experiments. Top: Expression of the *mmu-miR-200c-141* gene in the *pU6-miR-200c-141-CAG-EGFP* OE vector was under control of an *U6* promoter and was monitored by the *CAG* promoter-driven EGFP expression. Transfection of this vector resulted in moderate *miR-200c* and *miR-141* expression levels (see Fig. S4). Bottom: For the *miR-200* sponge vector, eight repeats of fully complementary sequences to all five members of the *mmu-miR-200* family were inserted downstream of the *EGFP* CDS driven by a *CAG* promoter.

(B-E) Overexpression of *miR-200c-141* in E11.5 primary vMH cultures caused a decrease in Sox2$^+$ and E2F3$^+$ neural progenitor cell numbers, and an increase in Tubb3$^+$ postmitotic neurons numbers in these cultures (Control vector: Sox2$^+$ cells, 49.997±1.89; E2F3$^+$ cells, 33.453±2.07; Tubb3$^+$ cells, 56.504±1.12. miR-200 OE vector: Sox2$^+$ cells, 41.837±2.59; E2F3$^+$ cells, 25.888±0.83; Tubb3$^+$ cells, 66.639±2.67. All data are mean ± SEM; single asterisks, P<0.05 in the independent-samples *t* test, N=4).

(F) Transfection of *mmu-miR-200c* precursor miRNA strongly downregulates Sox2 and E2F3 protein levels in primary vMH cells, as compared to the control precursor-transfected cells.

(G-J) Knockdown of the *miR-200* family members in E11.5 primary vMH cultures using a miR-200 sponge vector increased the numbers of Sox2$^+$ and E2F3$^+$ neural progenitor cells, and decreased the numbers of Tubb3$^+$ postmitotic neurons in these cultures (Control vector: Sox2$^+$ cells, 44.928±3.25; E2F3$^+$ cells, 27.183 ±1.67; Tubb3$^+$ cells, 62.63±8.6. miR-200 sponge vector: Sox2$^+$ cells, 65.511±4.16; E2F3$^+$ cells, 38.255±1.82;, Tubb3$^+$ cells, 41.13±4.93. All data are mean ± SEM; single asterisks, P<0.05; triple asterisks, P=0.001 in the paired-samples *t* test, N=3).

cKO embryos is mainly caused by the loss of mature *miR-200* family miRNAs in these mutants.

3.2.9 *Sox2* and *E2F3* mRNAs are direct targets of *miR-200c*

Given the strong correlation between the overexpression or downregulation of *miR-200* family members and the decrease or increase of Sox2$^+$ and E2F3$^+$ cells, respectively, in vitro and in vivo, I wanted to confirm whether Sox2 and E2F3 are indeed direct targets of the *miR-200* family. Using bioinformatics prediction tools (Targetscan, http://www.targetscan.org), I found that there is one conserved (among vertebrates) binding site (BS) for the *miR-200b/c/429* seed sequence subgroup (II) within the mouse *Sox2* 3'UTR, and 4 conserved (in mammals) BSs for the *miR-200* family (2 BSs for each subgroup) within the mouse *E2F3* 3'UTR (Fig. 29A, B). I therefore cloned the *Sox2* 3'UTR (containing the miR-200c BS) and *E2F3* 3'UTR (containing 2 miR-200c BSs) into a luciferase reporter (sensor) vector (pGL3-basic vector, Promega), and co-transfected this vector together with *mmu-miR-200c* precursor miRNA into COS-7 cells. The *miR-200c* precursor miRNA repressed the luciferase expression from the *Sox2* 3'UTR sensor vector by ~50% and from the E2F3 3'UTR sensor vector by ~30% (Fig. 29C, D). To confirm this result, I used my *pcDNA6.2-EmGFP-miR-200c* OE vector and co-transfected it with the sensor vectors in COS-7 cells. Luciferase

expression was downregulated by ~26% (*Sox2* 3'UTR) and ~33% (*E2F3* 3'UTR) after *miR-200c* overexpression, and this repression was rescued after site-directed mutagenesis of the conserved *miR-200c* BSs in the sensor vectors (Fig. 29A, B, E, F). Notably, the luciferase expression levels after site-directed mutagenesis of the conserved *miR-200c* BSs were even higher than in the control (empty *pcDNA6.2-EmGFP* vector)–transfected cells (Figure 6E, F), which is most likely due to the repression of the sensor vectors by the endogenous expression of *miR-200c* in COS-7 cells (data not shown). These data show that *miR-200c* directly regulates *Sox2* and *E2F3* mRNA expression by binding to conserved BS(s) within their 3'UTRs.
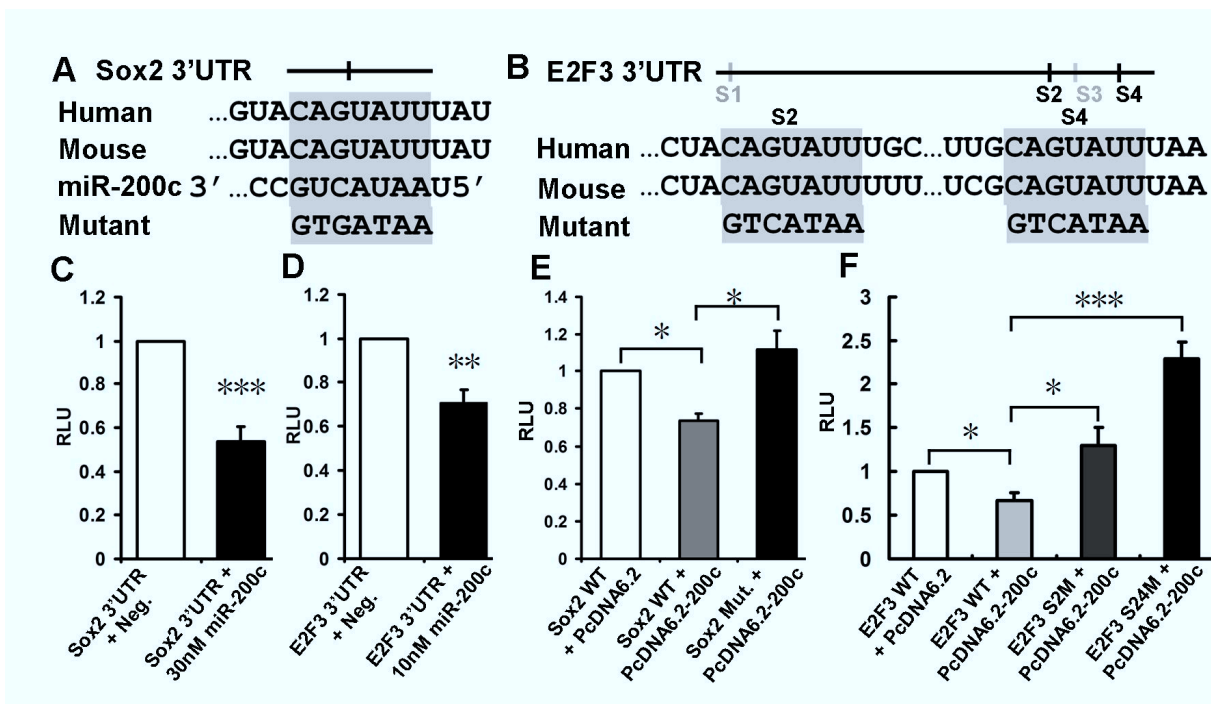
Figure 29. Sox2 and E2F3 are direct targets of *miR-200c*.
(A) Schematic drawing and relative position of one conserved binding site (BS) for *miR-200c/b/429* within the *Sox2* 3'UTR. Sequence alignments of the *miR-200c/b/429* BS in human and mouse *Sox2* 3'UTR, of the *miR-200c* seed sequence, and of the mutated *miR-200c/b/429* BS within the mouse *Sox2* 3'UTR are shown below. Seed sequences are highlighted in grey.
(B) Schematic drawing and relative positions of four conserved (in mammals) BSs for the *miR-200* family within the *E2F3* 3'UTR. BS 1 and 3 (S1 and S3) are complementary to the seed sequences of *miR-200a/141*, and BS 2 and 4 (S2 and S4) are complementary to the seed sequences of *miR-200c/b/429*. The *E2F3* 3'UTR region containing S2 to S4 was used for the sensor assays. Sequence alignments of the *miR-200c/b/429* BSs in human and mouse *E2F3* 3'UTR, and of the mutated *miR-200c/b/429* BSs (S2 and S4) within the mouse *E2F3* 3'UTR are shown below. Seed sequences are highlighted in grey.
(C, D) *MiR-200c* sensor assays with wild-type and mutant *Sox2* 3'UTR and *E2F3* 3'UTR in COS-7 cells. Transfection of 30 nM (*Sox2*) or 10 nM (*E2F3*) *mmu-miR-200c* precursor miRNA repressed luciferase expression from the *pGL3-Sox2-3'UTR* and *pGL3-E2F3-3'UTR* sensor vectors as compared to the control precursor-transfected cells (negative control was set as 1; *mmu-miR-200c* precursor + *Sox2* 3'UTR:

0.538±0.068; *mmu-miR-200c* precursor + *E2F3* 3'UTR: 0.705±0.061; mean ± SEM; triple asterisks, P<0.005; double asterisks, P<0.01 in the independent-samples *t* test, N=3).

(E) Overexpression of *miR-200c* in COS-7 cells using the *pcDNA6.2-EmGFP-miR-200c* OE vector downregulated luciferase expression from the *pGL3-Sox2-3'UTR* sensor vector, and this was rescued after site-directed mutagenesis (*Mut.*) of the *miR-200c* seed sequence within the *Sox2* 3'UTR, demonstrating the specificity of the miR-200c/*Sox2* 3'UTR interaction (*Sox2* 3'UTR *WT* + control vector was set as 1; *Sox2* 3'UTR *WT* + *miR-200* OE vector: 0.737 ± 0.037; *Sox2* 3'UTR *Mut.* + *miR-200* OE vector: 1.12 ± 0.1; mean ± SEM; single asterisks, P<0.05 in the independent-samples *t* test, N=3).

(F) Overexpression of *miR-200c* in COS-7 cells using the *pcDNA6.2-EmGFP-miR-200c* OE vector downregulated luciferase expression from the *pGL3-E2F3-3'UTR* sensor vector, and this was rescued after site-directed mutagenesis of the two *miR-200c* seed sequences (S2M and S24M) within the *E2F3* 3'UTR, demonstrating the specificity of the *miR-200c/E2F3* 3'UTR interaction (*E2F3* 3'UTR *WT* + control vector was set as 1; *E2F3* 3'UTR *WT* + *miR-200* OE vector: 0.667 ± 0.09; *E2F3* 3'UTR S2M + *miR-200* OE vector: 1.3 ± 0.2; *E2F3* 3'UTR S24M + *miR-200* OE vector: 2.29 ± 0.19; mean ± SEM; single asterisks, P<0.05; triple asterisks, P<0.005 in the independent-samples *t* test, N=3). RLU, relative luciferase units.

3.2.10 The expression of *miR-200* is regulated by Sox2 and E2F3 TFs

Although I previously showed that Sox2 and E2F3 are direct targets of *miR-200c*, both TFs and *miR-200c* were co-expressed in the VZ/SVZ of the MHR neuroepithelium (see Fig. 25). I therefore hypothesized that Sox2 and E2F3 might in turn regulate the expression of the *miR-200* family in neural progenitor cells. To test this hypothesis, I analyzed the mouse promoters of *miR-200c/141* cluster and *miR-429/a/b* cluster using Gene2promoter (Genomatix) software, and found several conserved BSs for the Sox2 and E2F TFs within the promoter region of both gene clusters. Given that the expression pattern of *miR-200* from these two clusters is similar, I only focussed on the promoter of the *miR-200c/141* cluster. I cloned the distal (Prom. 1) and proximal (Prom. 2) promoter region of the *mmu-miR-200c/141* cluster harbouring several conserved Sox2 and/or E2F3 BSs into a luciferase reporter vector (Fig. 30A). Co-transfection of this *pGL3-mmu-miR-200c/141* reporter vector and vectors encoding the Sox2 or E2F3 CDS into HEK-293 cells led to a 3–3.4-fold activation of the *mmu-miR-200c/141* distal promoter region (containing conserved Sox2 and E2F3 BSs) by E2F3 and Sox2, respectively, and to a 5-fold activation of the *mmu-miR-200c/141* proximal promoter region (containing only conserved E2F3 BSs) by E2F3 (Fig. 30B). These data strongly suggested that the Sox2 and maybe to an even greater extent the E2F3 TF might also activate the transcription of the *mmu-miR-200c/141* gene cluster in neural progenitor cells of the murine vMHR.
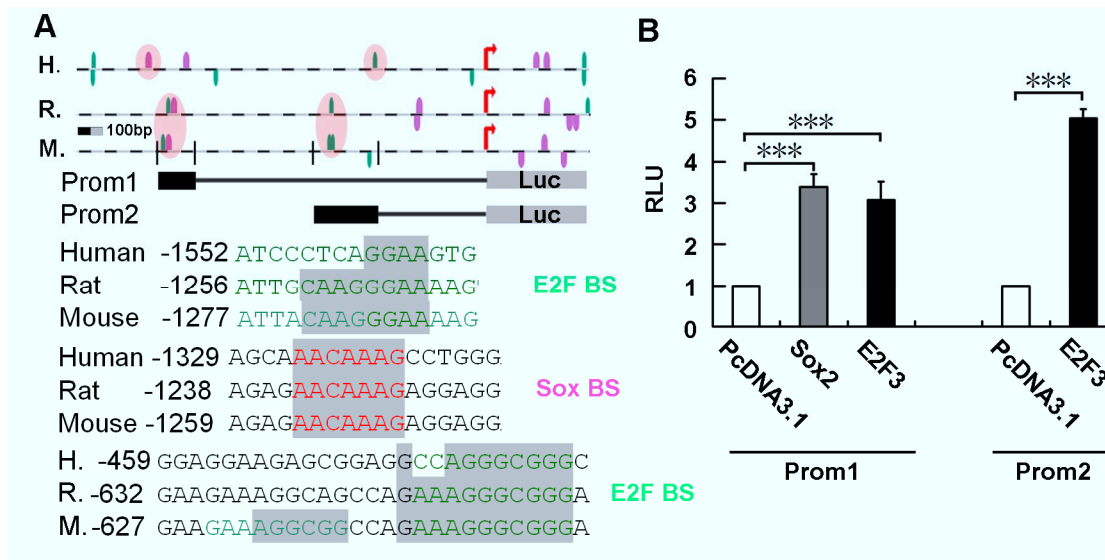
Figure 30. Sox2 and E2F3 activate the *mmu-miR-200c/141* promoter.
(A) Position and sequence of conserved BS (Pink circle) for Sox2 (magenta) and E2F3 (green) within the distal (Prom 1) and proximal (Prom 2) *mmu-miR-200c/141* promoter region.
(B) Strong (3-3.4-fold) activation of the distal *mmu-miR-200c/141* promoter (Prom 1) was seen after Sox2 and E2F3 OE in HEK-293 cells; OE of E2F3 caused an even stronger (5-fold) activation of the proximal *mmu-miR-200c/141* promoter (Prom 2). Empty vector (*pcDNA3.1*) control was set as "1". (Relative luciferase units (RLU): *pGL3-mmu-miR-200c(1)* + Sox2: 3.38 ± 0.31; *pGL3-mmu-miR-200c(1)* + E2F3: 3.08 ± 0.44; *pGL3-mmu-miR-200c(2)* + E2F3: 5.03 ± 0.23; mean ± SEM; triple asterisks, P<0.001 in the independent-samples *t* test, N=4).

3.2.11 A unilateral negative feedback loop involving *miR-200*, Sox2 and E2F3 regulates NSC proliferation and differentiation

Collectively, my data showed that Sox2 and E2F3 can activate the expression of the *miR-200* family which in turn downregulates the expression of Sox2 and E2F3 in NSCs/progenitor cells, thereby facilitating their cell cycle exit and differentiation into postmitotic neurons (Fig. 31). It is known that the ability of Sox2 to maintain the self-renewal competence and multipotency of neural progenitor is dose-dependent (Taranova et al., 2006). Sox2 autoregulation and negative regulation of Sox2 protein levels in neural progenitors by the *miR-200* family should lead to a gradual downregulation and finally complete repression of Sox2, one of the stemness master genes, in NSCs/neural progenitor cells. During the cell cycle, negative regulation of *miR-200* on E2F3, combining with autoregulation of E2F3, control the fluctuant protein level of E2F3 (He et al., 2008) to facilitate the progression of cell cycle. When cells exit the final mitosis, negative regulation of *miR-200* help to shut down the expression of E2F3, thereby pushing the cells exit the cell cycle.

67
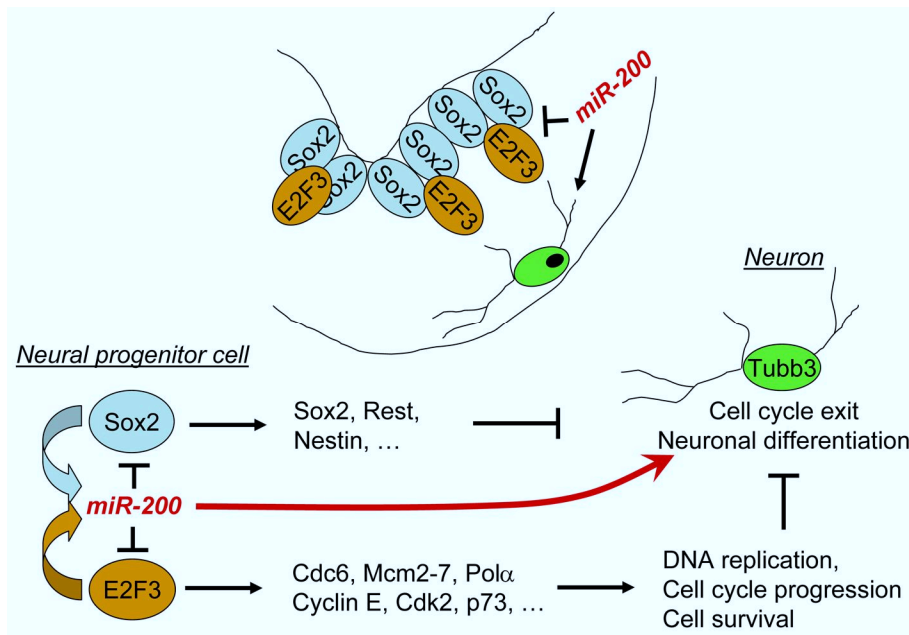
Figure 31. Proposed negative feedback loop between Sox2/E2F3 and *miR-200* in the VZ/SVZ of the MHR neuroepithelium to promote cell cycle exit and neuronal differentiation of neural progenitor cells. Transcription factors Sox2 and E2F3 autoregulate their own transcription and activate the expression of cell cycle genes, but also of *miR-200*. These miRNAs in turn downregulate the expression of Sox2 and E2F3 at the onset of NSC differentiation, thereby facilitating their cell cycle exit and differentiation into postmitotic neurons.

3.2.12 Generating two Cre-expressing mouse lines for investigating the function of miRNAs in mdDA neurons

As the *Dicer1 cKO* mice have a general defect of neuronal differentiation in the MHR, which is not restricted to mdDA neural progenitors, this mouse model is unsuitable for further studies regarding the role of miRNAs in mdDA neuron development and survival. To investigate the specific function of miRNAs in the development of mdDA neurons, a cell-specific ablation of the Dicer1 enzyme/miRNAs will be required to avoid any secondary/unspecific effects of a more wide-spread Dicer1/miRNA deletion as is the case in the *Dicer1 cKO* mice. We therefore have/want to generate two new Cre-expressing mouse lines in which Cre expression is restricted to either the floor and/or basal plate of the rostral midbrain/caudal diencephalon, where a mdDA subpopulation arises (*Shh-Cre-SBE1* mice), or to the early progenitors of these neurons and later postmitotic mdDA neurons, particularly of the SNc (*Aldh1a1$^{+/Cre-ERT2}$* mice). These Cre-expressing mouse lines can be crossed with *Dicer1$^{flox/flox}$* to obtain either region-, stage-, progenitor- or mdDA subpopulation-specific *Dicer1* mutant mice.

3.2.12.1 Generation and screening of *Shh-Cre-SBE1* transgenic mice

It was reported that a 1 kb minimal *Shh* promoter together with the *Shh Brain Enhancer 1* (*SBE1*) element directs expression of a *LacZ* reporter gene to the rostral midbrain and caudal diencephalon (Epstein et al., 1999) (Fig. 32). Using the same strategy, my colleague Dr. Jordi Guimera Vilaro constructed a transgenic vector (*Shh-Cre-SBE1* vector, Fig. 33A). Injections of the linearized vector into the male pronucleus of fertilized oocytes (zygotes) were performed at the Transgenic Facility of the Max Planck Institute of Molecular Cell Biology and Genetics in Dresden/Germany. We obtained a total of 25 transgenic founders from these pronuclei injections. These animals were further genotyped using two primer pairs as depicted in Fig. 33BC). Twenty out of the original 25 transgenic mice were confirmed to carry the full transgene. Thereafter, breeding pairs with these 20 transgenic mice were set up, and their offspring was mated with Rosa26 reporter mice which carry an insertion of a *loxp-stop-loxp-LacZ sequence* into the *Rosa26* locus (R26R mice, Soriano et al., 1999). Screening of the transgenic offspring for the correct/expected expression (Epstein et al., 1999) of the R26R transgene after *Shh-Cre-SBE1*-mediated recombination of the floxed Stop sequence was performed by LacZ staining of E10.5 embryos derived from mating pairs of *Shh-Cre-SBE1* mice and Rosa26 reporter mice. Several *Shh-Cre-SBE1* transgenic embryos were found to have Cre-mediated lacZ/beta-Gal expression in the rostral midbrain and caudal diencephalon (Fig. 34), which is similar to the *LacZ*/beta-Gal expression pattern in *Shh-LacZ-SBE1* mice (Epstein et al., 1999). However, transgenic embryos showing ectopic or ubiquitous beta-Gal expression were also observed in all transgenic mouse lines, which is probably due to positional effects on the transgene and probably also due to copy number variations. This requires further outcrossing of these mice to obtain a pure transgenic line showing the desired expression/recombination pattern of the transgene. Due to time limitations, this work and the characterization of this new *Shh-Cre-SBE1* transgenic mouse line, which needs to be done before it can be crossed with *Dicer1$^{flox/flox}$* mice, will be continued by others.
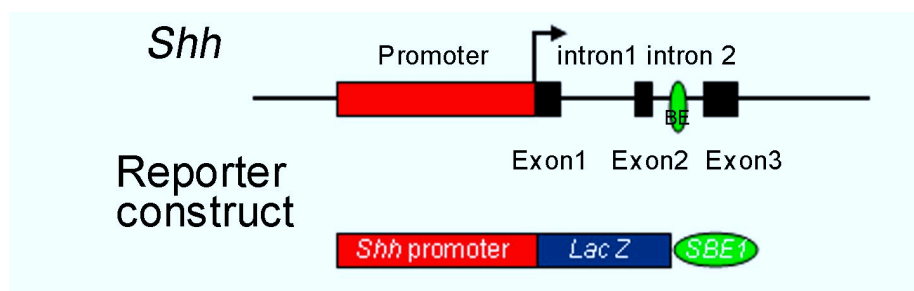
Figure 32. Location of the brain enhance element (BE) in mouse *Shh* gene and the transgenic vector construction which used by Epstein et al in 1999.
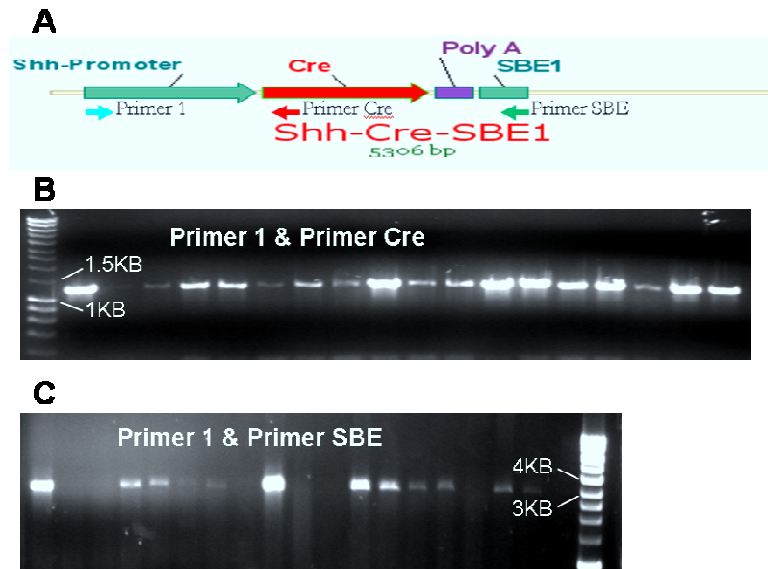
Figure 33. *Shh-Cre-SBE1* transgenic vector and the position of primer pairs used for genotyping of *Shh-Cre-SBE1* transgenic mice. 25 *Shh-Cre-SBE1* transgenic founders were genotyped by PCR using the primer pair Primer 1 & Primer Cre, which identifies the 1.2 kb minimal Shh promoter, **B**) and the primer pair Primer 1 & Primer SBE, which identifies the entire transgene (about 3.2 kb), **C**).

Figure 34. LacZ expression pattern of a *Shhp-Cre-SBE1* transgenic mouse after Cre-mediated recombination of a R26R reporter allele. Expression of beta-Gal is restricted to the rostral midbrain and caudal diencephalon floor and basal plate in this embryo, as expected from Epstein et al., 1999.

3.2.12.2 Generation of inducible *Aldh1a1$^{+/Cre\text{-}ERT2}$* knock-in mice

Expression of the retinaldehyde dehydrogenase family member 1a1 (*Aldh1a1*) starts at embryonic day 9 and is restricted to mdDA progenitors in the caudal midbrain at these early developmental stages (Fig. 35). At later developmental stages Aldh1a1 is expressed in mature mdDA neurons, and particularly in the SNc mdDA neuronal subset (Chung et al., 2005; Jacobs et al., 2007). For fate-mapping of the Aldh1a1$^+$ mdDA precursors/early postmitotic neurons, and for investigating the function of miRNAs and of other genes in these cells, we

wanted to generate an inducible Cre-expressing mouse line under the control of the *Aldh1a1* promoter region (*Aldh1a1$^{+/Cre-ERT2}$* mice). This inducible mouse line will allow the time- and space-restricted expression of Cre-recombinase in specific subsets of cells, namely either mdDA progenitors, postmitotic neurons or adult SNc DA neurons.

I therefore generated an *Aldh1a1$^{+/Cre-ERT2}$* targeting vector, again with the help of Dr. J. Guimera Vilaro (Fig 35). Using PCR, the two homology arms were amplified from C57/BL6 mouse genomic DNA, and cloned into the TOPO-TA vector. The cloned homology arms were sequenced to confirm the absence of mutations, and then subcloned with a *Cre-ERT2* sequence into the JGV targeting vector containing Neo-resistance, TK and Kanamycin-resistance genes. The size of the final *Aldh1a1$^{+/Cre-ERT2}$* targeting vector is 15706 bp (Fig. 36) and the DNA sequence of the two homology arms, *Neomycin* cassette and *Cre-ERT2* cassette was confirmed to be without any mutations after sequencing. Due to time limitations, electroporation of this targeting vector into mouse ES cells, selection of Neo-resistant clones, and genotyping of the selected clones to confirm successful homologous recombination of the transgene into the Aldh1a1 locus were performed by others. Eventually, the targeting strategy was modified due to the inability to obtain Neo-resistant mESC clones (which might be due to weak Aldh1a1 expression in mESC, Tamoxifen-independent activation of the CreERT2, and Cre-mediated self-excision of the Neo cassette) with the original targeting vector. This work will be continued by others due to time limitations.
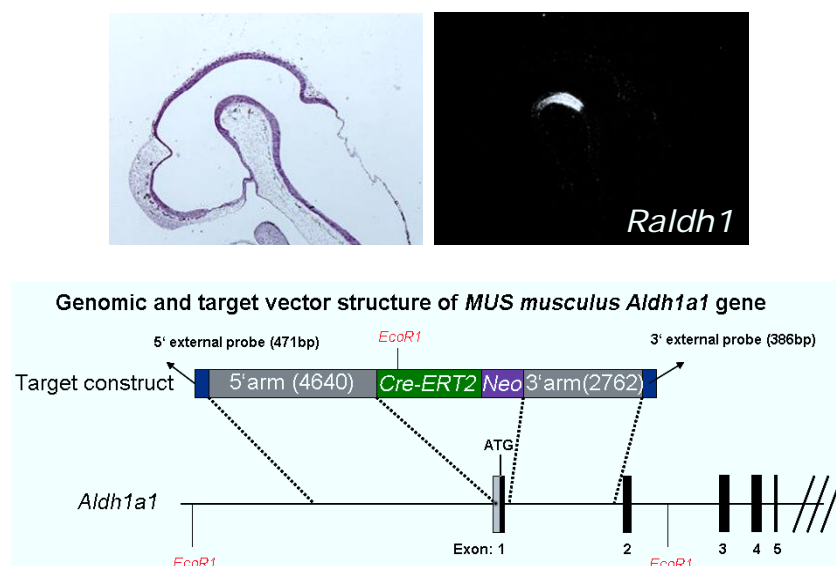
Figure 35. Expression pattern of *Aldh1a1* in an E10.5 mouse embryo (right top, courtesy from T. Fischer) and targeting strategy for the *Aldh1a1$^{+/CreERT2}$* knock-in mouse (lower, designed by J. Guimera Vilaro). 5' homologous arm overlaps with part of the exon 1, and 3' homologous arm locates in the intron 1 of *Aldh1a1* gene. After homologous recombination, *Cre-ERT2* will replace almost entire exon 1 of *Aldh1a1* gene including the start codon ATG.
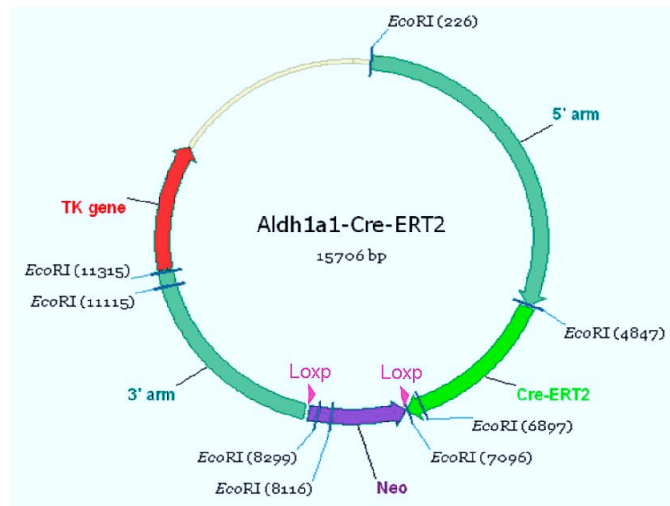
Figure 36. *Aldh1a1^{+/Cre-ERT2}* targeting vector.

3.3 Discussion

It is believed that tissue-specific miRNAs play a role in neural development. One good example is miR-9, whose expression spares the MHB where the miR-9 target gene *Fgf8* is expressed, and miR-9 is necessary for the proper establishment and maintenance of this boundary in zebrafish embryos (Leucht et al., 2008). However, no alteration of neural patterning was observed in my *Dicer1 cKO* mice, or in *Wnt1-Cre Dicer1^{flox/flox}* mice (Huang et al., 2010), suggesting that miRNAs might be not important for neural patterning of mouse mid-/hindbrain. In the *Dicer1 cKO* mice, cell death occurs one day later than the differentiation defect which was observed at E10.5, suggesting that apoptosis in the *Dicer1 cKO* mice may be not a direct consequence of loss of miRNAs rather a subsequent phenotype, although it cannot be excluded that some miRNAs expressed in En1⁺ domain may directly target apoptosis genes. The numerical reduction in numbers of neuronal populations residing within the MHR of *Dicer1 cKO* mice is caused by a general defect in neuronal differentiation. The differentiation of neural progenitors requires two conditions: cell cycle exit and silencing of repressors of neural differentiation. It is know that the expression of Sox2, a key inhibitor of neural differentiation, is shut down in neural progenitors as they exit final mitosis (Graham et al., 2003), and that the expression of E2F3, a critical transcription factor to promote the G1 to S transition during the cell cycle, is also silenced in postmitotic neurons (E2F3 is not expressed in mantle zone-resided postmitotic neurons, see Fig. 25 and 27). Interestingly, the domain of Sox2⁺ and E2F3⁺ neural progenitors (including NSCs) is expanded, and the postmitotic differentiated neuron domain is reduced in the *Dicer1 cKO* embryos. These data support the notion that the general neuronal differentiation defect in the *Dicer1 cKO* mice is

72

caused by the inability of neural progenitors to downregulate the expression of Sox2 and E2F3 at the proper time because of the loss of negatively regulatory miRNAs whose expression overlaps with the expression of Sox2 and E2F3. Using next generation sequencing technology, I found that all five members of the *miR-200* family are among the top 6 downregulated miRNAs in the *Dicer1 cKO* mice, and that *miR-200* targets Sox2 and E2F3 via conserved BS(s) within their 3' UTRs. Moreover, *miR-200* is enriched in neural progenitors and ESCs and its expression is activated by Sox2 and E2F3. I further demonstrated by gain- and loss–of-function experiments, that *miR-200* is able to repress the expression of Sox2 and E2F3 in neural progenitor cells and thereby promote their differentiation into Tubb^{+} neurons. Due to the autoactivation of Sox2 and E2F3 (that bind to and activate their own promoters (Adams et al., 2000; Johnson et al., 1994; Tomioka et al., 2002)), the reduction in Sox2 and E2F3 protein levels caused by *miR-200* will lead to a decrease of their transcription levels. *MiR-200* therefore gradually reduces the expression levels of Sox2 and E2F3 and finally shuts down their expression in neural progenitors to promote their cell cycle exit and to facilitate the induction of neuronal differentiation genes in these cells. In support of this hypothesis, Mukherji et al recently showed that miRNAs can act both as a fine-tuner at high levels of the target mRNA, and as a switch when target mRNA expression falls below a certain threshold (Mukherji et al., 2011). My in vivo and in vitro data thus suggest that the phenotype of the *Dicer1 cKO* mice is mainly caused by the loss of *miR-200* in the MHR of these mice, leading to a failure to exit the cell cycle and to downregulate the expression of Sox2 and E2F3 in neural progenitors at the correct time, and subsequently to their inability to generate the proper amount of differentiated neurons.

It is known that *miR-124*, *miR-9/9**, and *let-7b* promote the transition from a neural progenitor to a differentiated neuron (Conaco et al., 2006; Krichevsky et al., 2006; Zhao et al., 2010; Zhao et al., 2009). The expression levels of these miRNAs are strongly increased in differentiating neurons (my data and (Krichevsky et al., 2006)), and the expression of *miR-124* and *miR-9/9** is repressed by the REST complex in NSCs (Conaco et al., 2006; Packer et al., 2008), suggesting that these miRNAs function in postmitotic neurons rather than NSCs. Unlike these neuronal differentiation-promoting miRNAs, my in vivo and in vitro data from both gain- and loss-of -function experiments demonstrate that *miR-200* is expressed at high level in ESC and neural progenitors, no or only very low levels in postmitotic neurons, and promotes neuronal diffenrentiation by repressing the expression of Sox2 and E2F3. These suggest that the transition from neural progenitors to differentiated neurons is, at least partially, initiated by *miR-200* via targeting stemness factors, such like Sox2 and E2F3, and

then completed by *miR-124* and *miR-9/9** which shut down the expression of REST and of other "stemness" or non-neural genes/mRNAs to globally induce the expression of neuronal genes in postmitotic neurons. Consistent with my data, Shimono et al and Wellner et al have reported that *miR-200* family promotes differentiation of human ESC and cancer ESC into neurons or other cell types (Shimono et al., 2009; Wellner et al., 2009) by targeting Sox2, KLF4 and Bmi1. However, others had reverse conclusion that *miR-200* inhibits the differention of different types of stem cells (Gill et al., 2011; Lin et al., 2009). This discrepancy could be due to the different expression levels and different targets of *miR-200* present in various ES cell lines, as well as different differentiation protocols used in their experiments, suggesting that the function of *miR-200* family might be highly context-dependent.

It has been shown in many cases that a single miRNA or a set of coexpressed miRNAs systematically regulate(s) targets that coordinately function in one pathway and/or protein complex (Tsang et al., 2010). Thereby, miRNAs can have a substantial cumulative repression effect on a pathway and/or biological event although miRNAs regulate the expression levels of their targets only marginally when the targets are present at high levels. A recent report showed that two members of the *miR-200* family, *miR-200c* and *miR-141*, simultaneously regulate several essential components of CtBP/ZEB to repress the epithelial-mesenchymal transition (Sass et al., 2011). My data showed that *miR-200* regulates two "stemness" master transcription factors, Sox2 and E2F3, also involved in cell cycle progression of NSCs and maybe also of ESCs, as ESCs express *miR-200* and both target genes. By targeting these two cell cycle promoting TFs simultaneously, *miR-200* might negatively regulate the cell cycle progression of NSCs/ESCs in a more powerful way.

Within a single cell cycle, the expression of E2F3 oscillates with a high peak at the G1/S transition and a smaller peak in G2 phase, and its expression is rapidly downregulated during S and M phase, respectively (He et al., 2008). My data suggest that *miR-200* plays a crucial role for this oscillatory E2F3 expression during the cell cycle. Firstly, the E2F3 3'UTR contains 4 conserved and high affinity (fully match seed sequences) BSs for *miR-200*; this might increase the strength of *miR-200*-induced repression of this mRNA below a "switch" threshold level. It has been shown that the repression strength and the switch threshold of a miRNA are correlated with the number and the affinity of BSs within its target, as well as with the abundance of this miRNA, and that 4 BSs increase the repression several-fold as compared to just 1 BS (most mRNAs only contain one conserved BS for a given miRNA) (Mukherji et al., 2011). Secondly, expression of *miR-200* is regulated by E2F3 itself, which

means that the peak of *miR-200* expression levels might tightly follow the peak of E2F3 expression in late G1 phase. A high *miR-200* concentration in turn might rapidly downregulate and, depending on the threshold levels, even switch off the expression of E2F3 at a posttranscriptional level during S phase. Thirdly, E2F3 autoregulates its own expression by binding to E2F elements within its own promoter (Adams et al., 2000). *MiR-200*-induced downregulation of E2F3 protein levels will subsequently cause a reduction of *E2F3* transcription. It is also known that the expression of E2F3 is repressed by the retinoblastoma protein (RB) in G0 and during early G1-phase in an E2F element-dependent manner, and that phosphorylation of RB by cyclin-dependent kinases only during late G1 phase releases this repression of E2F3 transcription and E2F3 protein can accumulate (Adams et al., 2000; Dyson, 1998; Lees et al., 1993; Muller et al., 2001). Together, the oscillatory expression of E2F3 during the cell cycle might be controlled at the transcriptional level by RB-mediated repression and at the posttranscriptional level by the negative feedback loop involving *miR-200* and E2F3.

Taken together, my data show that a unilateral negative feedback loop involving *miR-200*, Sox2 and E2F3 controls the proliferation and differentiation of NSCs and might even have the same function in ESCs as well. It has been shown that the ability of Sox2 to maintain the multipotency and self-renewal competence of neural progenitors is dose-dependent (Taranova et al., 2006). By gradually repressing the "stemness master" gene Sox2 in these cells, *miR-200* attenuates and finally eliminates the capacity of NSCs to self-renew and proliferate. Thus, my data provide first evidences for the important role of *miR-200* in the control of the transition from a stem/progenitor cell to a postmitotic/differentiating cell. My data also suggest that miRNAs might be required for the terminal differentiation of mdDA neurons because the number of Pitx3$^+$ mdDA neurons was reduced more severely than that of TH$^+$ cells in the *Dicer1 cKO* mice. The *Shh-Cre-SBE1* transgenic and *Aldh1a1$^{+/Cre-ERT2}$* knock-in mice will be very useful tools to investigate this in more detail, because crossing these Cre-recombinase expressing mice with *Dicer1$^{flox/flox}$* mice will deplete miRNAs most likely only in a subpopulation of mdDA neurons (arising from the rostral ventral midbrain) in *Shh-Cre-SBE1;Dicer1$^{flox/flox}$* mice,* or in mdDA progenitors/precursors (if induced at early developmental stages such as E9.0-E10.5) and later in postmitotic mdDA neurons or even more specifically only in SNc DA neurons (if induced after E10.5 or peri-/postnatally) in *Aldh1a1$^{+/Cre-ERT2}$;Dicer1$^{flox/flox}$* mice. However, before these new mouse lines can be used, it still requires their establishment (*Aldh1a1$^{+/Cre-ERT2}$* knock-in mice) or full characterization (*Shh-Cre-SBE1* transgenic mice).

4. Materials and methods

4.1 Materials

4.1.1 Instruments

Table 4.1 Instruments:

autoclave	Aigner, type 667-1ST
balances	Sartorius, LC6201S, LC220-S
cassettes for autoradiography	Amersham, Hypercassette
centrifuges	Sorvall, Evolution RC;
	Eppendorf, 5415D, 5417R;
	Sigma，3K18
chambers for electrophoresis (DNA)	MWG Biotech; Peqlab
confocal microscope	Olympus, BX51; zeiss, LSM510
cold light microscope	Leica, KL1500
crystat	Mikrom, HM560
developing machine	Agfa, Curix 60
digital camera	Zeiss, AxioCam MRc
electric homogenizer	IKA, Ultra-Turrax T25 basic
fluorescence microscope	Zeiss, Axiovert 200M
freezer (−20 °C)	Liebherr
freezer (−80 °C)	Heraeus HFU 686 Basic
fridges (4 °C)	Liebherr
gel documentation system	Herolab, E.A.S.Y. Win32
gel-/blottingsystem "Criterion"	BioRad
glass homogenizer (tissue grinder, 2 mL)	KIMBLE / KONTES
glass pipettes	Hirschmann
glass capillary puller (PC-10)	Narishige
glass capillaries	World Precision Instruments
glassware	Schott
ice machine	Scotsman, AF 30
incubators (for bacteria)	New Brunswick Scientific, innova 4230
incubators (for cell culture)	Heraeus
Lab Standard Stereotaxic Instrument	Stoelting
light microscope	Zeiss, Axioplan2
liquid scintillation counter	Hidex, Triathler
luminometer	Berthold Technologies, Orion I
magnetic stirrer / heater	Heidolph, MR3001
microwave oven	Sharp R-937 IN
Hamilton syringe	Hamilton
Neubauer counting chamber	Brand
oven for hybridization	Memmert, UM 400;
	MWG-Biotech, Mini 10;
	ThermoElectron, Shake'n'Stack
PCR machine	Eppendorf, MasterCycler Gradient
perfusion pump	Watson-Marlow Bredel, 401U/D1
pH-meter	InoLab, pH Level 1

photometer	Eppendorf, Biophotometer 6131;
	PeqLab, NanoDrop ND-1000
pipettes	Gilson, Pipetman P10, P20, P200, P1000
power supplies for electrophoresis	Consort, E443;
	Pharmacia Biotech, EPS200;
	Thermo, EC250-90, EC3000-90
radiation monitor	Berthold, LB122
Real-Time PCR system	Applied Biosystems, 7900HT
SDS-Gel electrophoresis apparatus	Bio-Rad
shaker	Heidolph, Promax 2020
slide warmer	Adamas instrument, BV SW 85
sliding microtome	Leica, SM2000R
stereomicroscope	Leica, MZ75
UV-DNA/RNA-crosslinker	Scotlab, Crosslinker SL-8042;
	Stratagene, UV-Stratalinker 1800
vortex	Scientific Industries, Vortex Genie 2
water bath	Lauda, ecoline RE 112;
	Leica, HI1210;
	Memmert, WB7
Water purification system	Millipore, Milli-Q biocel
Thermomixer	Eppendorf, 5436

4.1.2 Reagents and Consumables

Table 4.2 Chemicals:

α-35S-UTP	Amersham
β-mercaptoethanol	Sigma
acetic acid	Merck
acetic anhydride	Sigma
ammonium acetate	Merck
ampicillin	Sigma
ultrapure water	Fresenius
BCIP (5-bromo-4-chloro-3-indolyl phosphate)	Roche
4-NBT (Nitro blue tetrazolium)	Roche
bis-tris	Sigma
boric acid	Merck
bromphenol blue	Sigma
calcium chloride	Sigma
chloral hydrate	Sigma
chloroform	Sigma
citric acid	Sigma
Complete® Mini (protease inhibitors)	Roche
cresyl violet acetate	Sigma
dimethylformamide	Sigma
dithiotreitol (DTT)	Roche
DMSO	Sigma
dNTP (100 mM dATP, dTTP, dCTP,	Fermentas

dGTP)

EDTA	Sigma
ethanol	Merck
ethidiumbromide	Fluka
ethylene glycol	Sigma
formaldehyde	Sigma
formamide	Sigma
(D-)glucose	Sigma
glycerol	Sigma
Hank's Balanced Salt Solution (HBSS)	Gibco
hydrochloric acid	Merck
hydrogen peroxide (30 %)	Sigma
6-Hydroxydopamine hydrobromide + ascorbic acid	Sigma
isopropanol	Merck
kanamycin	Sigma
magnesium chloride (MgCl2•4H2O)	Merck
maleic acid	Sigma
methanol	Merck
mineral oil	Sigma
Nonidet P40 (NP-40)	Fluka
paraformaldehyde	Sigma
PBS (for cell culture)	Gibco
phenol:chloroform:isoamyl alcohol	Fluka
potassium chloride	Merck
potassium ferricyanide (K3Fe(CN)6)	Sigma
potassium ferrocyanide (K4Fe(CN)6•3H2O)	Sigma
potassium hydroxid	Sigma
potassium phosphate (KH2PO4•H2O, K2HPO4)	Roth
RNaseZAP®	Sigma
sodium acetate (NaOAc)	Merck, Sigma
sodium chloride	Merck
sodium citrate	Sigma
sodium dodecylsulfate (SDS)	Merck
sodium hydrogen carbonate (NaHCO3)	Sigma
sodium hydroxide	Roth
sodium phosphate (NaH2PO4•H2O, Na2HPO4)	Sigma
sucrose	Sigma
Aqua-polymount	Polysciences
Tris (Trizma-Base)	Sigma
Triton-X 100	Biorad
Trizol	Invitrogen
Tween 20	Sigma
X-Gal	Fermentas
xylol	Fluka

Table 4.3 Bio-reagents:

agarose (for gel electrophoresis)	Biozym
DNA Ladder	Invitrogen
HiMark™ Pre-Stained protein standard	Invitrogen
bovine serum albumin	Sigma
bacto agar	Difco
bacto peptone	BD Biosciences
tryptone	BD Biosciences
yeast extract	Difco
B27 supplement	Invitrogen
BDNF protein	R&D systems
GDNF protein	R&D systems
DMEM	Gibco
DMEM:F12 (1:1)	Gibco
fetal calf serum (FCS)	PAN, Hybond
gelatin	Sigma
laminin	Sigma
Poly-D-lysine	Sigma
trypsin	Gibco
Hyb-mix	Ambion
RapidHyb buffer	Amersham
Sp6/T3/T7 RNA polymerase	Roche
salmon sperm DNA	Fluka
skim milk powder	BD Biosciences
Alkaline Phosphatase, Calf Intestinal (CIP)	NEB
DNA Polymerase (Phusion)	NEB
DNA Polymerase (Taq)	Qiagen
DNase I (RNase-free)	Roche
Klenow fragment of DNA Polymerase I	NEB
PCR-Mastermix 5x	5 PRIME
Polynucleotide kinase (PNK)	NEB
Proteinase K	Roche
restriction enzymes	NEB, Fermentas, Roche
RNase A	Serva
T4 DNA ligase	Roche

Table 4.4 Consumables:

tubes (15 mL, 50 mL)	BD Falcon
coverslips (24 x 50 mm, 24 x 60 mm)	Menzel Gläser
Criterion™ XT Bis-Tris-gels, 10 % (protein)	BioRad
embedding molds	Polysciences, Peel-A-Way
films for autoradiography	Kodak: Biomax MS, Biomax MR
filter paper	Whatman 3MM
filter tips 10 µL, 20 µL, 200 µL, 1 mL	Art, Starlab
gloves	Kimberley-Clark, Safeskin PFE
	Safeskin, Nitrile

Hybond N Plus (nylon membrane)	Amersham
multiwell plates (6, 12, 48, 96 wells)	Nunc
Pasteur pipettes	Brand
PCR reaction tubes (0.2 mL), lids	Biozym
pipette tips	Gilson
PVDF membrane (protein)	Pall Biosciences
reaction tubes (0.5 mL, 1.5 mL, 2 mL)	Eppendorf

4.1.3 Buffers and solutions

Table 4.5 Common buffers:

DNA loading buffer (6x)	0.25%	bromophenol blue
	0.2%	Xylene cyanol
	40%	Sucrose in H2O
paraformaldehyde solution (PFA, 4 %)	4 %	PFA w/v in PBS
PBS (1x)	171 mM	NaCl
	3.4 mM	KCl
	10 mM	Na2HPO4
	1.8 mM	KH2PO4
		pH 7.4
SSC (saline sodium citrate, 20x)	3 M	NaCl
	0.3 M	sodium citrate
		pH 7.0
sucrose solution (30 %)	30 %	sucrose w/v in PBS
TAE (10x)	0.4 M	Tris base
	0.1 M	acetate
	0.01 M	EDTA
TBS (10x)	0.25 M	Tris-HCl pH 7.6
	1.37 M	NaCl
TBS-T (1x)	1x	TBS
	0.05 %	Tween 20
TE (Tris-EDTA)	10 Mm	Tris-HCl pH 7.4
	1 Mm	EDTA
Tris-HCl	1 M	Tris base
		pH 7.5
Cryoprotect solution	250 ml	Glycerin
	250 ml	Ethylene Glycol
	500 ml	PBS
Borate buffer	6.183 g/l	Boric Acid Disolve in H_2O adjust pH 8.5 with NaOH
Citrate buffer (10 x)	0.1M	Tri-sodium Citrate pH6, adjust with 0.1 M citric acid monohydrate

Table 4.6 NBT/BCIP developing solutions:

Buffer 1 (1x)	100 ml/l	1 M Tris
	8.7 g/l	NaCl
		Add milliQ-H_2O,adjust pH to 7.5
		Treat with DEPC and autoclave.
Buffer 2 (1x)	100 ml/l	1M Tris
	8.7 g/l	NaCl
	1 ml	1M $MgCl_2$
		Add H_2O up to 1L, adjust pH to 9.5 with HCl.
1M $MgCl_2$:	60.99 g/l	$MgCl_2.6\ H_2O$
Color solution:	45 µl	75 mg/ml NBT
	35 µl	50 mg/ml BCIP-phosphate
		In 10 ml buffer 2.
		Prepare freshly, filter solution through
		a 0.22 um filter and store in darkness.

Table 4.7 Bacterial medium:

LB medium (Luria-Bertani)	10 g	Bacto peptone
	5 g	yeast extract
	5 g	NaCl
	ad 1 L	H2O
LB agar	98.5 %	LB-Medium
	1.5 %	Bacto agar
Ampicillin selection medium	LB medium with 50 µg/mL ampicillin	
Kanamycin selection medium	LB medium with 25 µg/mL kanamycin	
Ampicillin selection agar	LB agar with 100 µg/mL ampicillin	
Kanamycin selection agar	LB agar with 50 µg/mL kanamycin	

Table 4.8 Western blot solutions:

Blocking solution	4 %	skim milk powder in TBS-T
Loading buffer (5x)	313 mM	Tris-HCl pH 6.8
	50 %	glycerol
	10 %	SDS
	0.05 %	bromphenolblue
	25 %	β-mercaptoethanol
MES running buffer (10x, for NuPAGE gels)	500 mM	MES
	500 mM	Tris
	1 %	SDS
	10 mM	EDTA
		pH 7.2

MOPS running buffer (10x, for Criterion gels)	500 mM	MOPS
	500 mM	Tris
	1 %	SDS
	10 mM	EDTA
		pH 7.7
NuPAGE transfer buffer (10x, for NuPAGE gels)	250 mM	bicine
	250 mM	Bis-Tris
	10 mM	EDTA
	0.05 mM	chlorobutanol
NuPAGE transfer buffer (1x, for NuPAGE gels)	10 %	10x NuPAGE transfer buffer
	10 %	methanol
RIPA buffer	50 mM	Tris-HCl pH 7.4
	1 %	NP-40
	0.25 %	sodium desoxycholate
	150 mM	NaCl
	1 mM	EDTA

Table 4.9 LacZ staining solutions:

LacZ fix solution	47.4 ml	4% PFA in PBS (pH 7.4)
	2.5 ml	100 mM EGTA (pH 7.4)
	0.1 ml	1M MgCl2
Wash buffer	0.4 ml	1M MgCl2
	2 ml	2% NP40
	197.6 ml	PBS (pH 7.4)
X-Gal staining solution prepare fresh, protect from light	1 mg/mL	X-Gal
	5 mM	potassium ferricyanide
	5 mM	potassium ferrocyanide
	in	PBS

Table 4.10 Nissl staining solution:

cresyl violet staining solution	0.5 %	cresyl violet acetate
	2.5 mM	sodium acetate
	0.31 %	acetic acid
	ad 500 mL	H2O
		filter before use

Table 4.11 Fast lysis buffer (for genomic DNA):

50 mM KCl
10 mM Tris-HCl pH8.3
0.1mg/ml gelatine
Boiling to dissolve the gelatine and then cooling down to RT
Add: 0.45% NP-40 and 0.45% Tween-20
Store at -20°C
Before use, freshly add 0.5 to 1 mg/ml Proteinase K

4.1.4 Kits

Table 4.12 Kits:

ECL Detection Kit	Amersham
ECL Plus Detection Kit	Amersham
Pierce® BCA Protein Assay Kit	Thermo Scientific
Power SYBR® Green PCR Master Mix	Applied Biosystems
QIAGEN Plasmid Maxi Kit	Qiagen
QIAprep Spin Miniprep Kit	Qiagen
QIAquick Gel Extraction Kit	Qiagen
QIAquick PCR Purification Kit	Qiagen
Advantage® RT-for-PCR Kit	Clontech
Wizard Genomic DNA Purification Kit	Promega
TOPO TA Cloning Kit	Invitrogen
Transfection kit	Invitrogen, Lipfectamine 2000, Lipofectamine™ LTX and Plus Reagent
RNeasy-mini-Kit	Invitrogen
Dual luciferase assay kit	Promega
Terminal Transferase, recombinant	Roche
DIG Oligonucleotide 3'-End labeling kit	Roche
PCR kit	Fermentas
Tyramide Signal Smpification kit	PerkinElmer
Click-iT™ EdU Imaging Kit	Invitrogen

4.1.5 Antibodies

Table 4.13 Primary antibody:

Name	Species	Dilution	Producer
anti-DIG-AP Fab	Sheep	1:2000	Roche
βActin	Mouse	1:100,000	Abcam
BDNF	Rabbit	1:500	Santa Cruz Biotechnology
BrdU	Rat	1:100	AbD Serotec
Brn3a	Mouse	1:100	Santa Cruz Biotechnology
Cleaved Caspase-3	Rabbit	1:100	Cell Signaling
Doublecortin	Goat	1:250	Santa Cruz Biotechnology
E2F3	Mouse	1:150	Upstate
GFP	Chicken	1:2000	AVES Labs
Islet1	Mouse	1:100	DSHB
Ki67	Rabbit	1:200	Abcam

NeuN	Mouse	1:100	Hybridoma Bank
Nestin	Mouse	1:400	Millipore
NF-κB	Rabbit	1:100	Cell Signaling
Pitx3	Rabbit	1:300/1:100	Zymed-Invitrogen
Serotonin	Rabbit	1:1000	Immunostar
Sox2	Goat	1:500	Santa Cruz Biotechnology
TH	Rabbit	1:150	Chemicon
TH	Mouse	1:600-1000	Chemicon
TH	Mouse	1:6000	Sigma
Tuj1	Rabbit	1:500	Abcam

Table 4.14 Secondary antibody:

Name	Species	Dilution	Producer
Donkey-anti-rabbit	Alexa 594 (red)	1:500	Molecular Probes
Donkey-anti-rabbit	Alexa 488 (green)	1:500	Molecular Probes
Donkey-anti-mouse	Alexa 488 (green)	1:500	Molecular Probes
Donkey-anti-mouse	Alexa 594 (red)	1:500	Molecular Probes
Donkey-anti-goat	Alexa 488 (green)	1:500	Molecular Probes
Donkey-anti-goat	Alexa 594 (red)	1:500	Molecular Probes
Donkey-anti-rat	Alexa 488 (green)	1:500	Molecular Probes
Donkey-anti-mouse	Cy5	1:500	Jackson Immuno
Donkey-anti-rat	Cy3	1:500	Jackson Immuno
Donkey-anti-rabbit	Cy5	1:500	Jackson Immuno
Donkey-anti-goat	Cy5	1:500	Jackson Immuno
Goat-anti-mouse	HRP	1:1000	Jackson Immuno
Goat-anti-rabbit	HRP	1:1000	Jackson Immuno
Donkey-anti-goat	HRP	1:1000	Jackson Immuno

4.1.6 Cell culture media

DMEM + 10% FCS: for HEK293, COS-7, etc. cells

ES cell medium: knock out DMEM containing 15% FCS, LIF (1000U/ml) and 1% β-mercaptoethanol

EB medium: ES medium without LIF and only 10% FCS

N2 medium: DMEM-F12 medium containing 1% N2 supplement

B27 medium: DMEM-F12 medium containing 2% B27 supplement

4.1.7 *E. coli* strains

Table 4.15 *E. coli* strains:

DH5α	Invitrogen
TOP10	Invitrogen
SURE®	Stratagene

4.2 Methods

4.2.1 Molecular biology

4.2.1.1 Polymerase Chain Reaction (PCR)

PCR was used to genotype the transgenic mice or clone genes from either genomic DNA or cDNA. Universal PCR formula is listed in Table 4.16, and the specific conditions (i.e. primer sequences, annealing temperature, and the number of cycles) were adjusted individually for each PCR and listed in the corresponding section. PCRs were run on a thermal cycler. The initial denaturing step was performed at 94°C for 4 minutes, followed 3-step cycle including the denaturing step at 94°C for 30 seconds, the annealing step at suitable temperature for 30 seconds and the elongation step at 72°C for 1-2 minute(s) according to the length of PCR product.

Table 4.16 Formula for PCR reactions:

Components	Volume	Final Concentration
PCR buffer (10x)	2 µl	1x
dNTP mix (10 mM each)	1 µl	0.5 mM
Primer 1 (10 µM)	1 µl	0.5 mM
Primer 2 (10 µM)	1 µl	0.5 mM
DNA polymerase (Taq or Herculase)	0.5 µl	2.5 U
Template DNA (30-100ng)	1 µl	
MilliQ water	Up to 20 µl	

4.2.1.2 Genotyping of mice

Mouse tails (~0.5 cm) were cut from mice at weaning (3 weeks old) or embryos, and lysed with 300 µl fast lysis buffer at 55°C for overnight. To inactivate the proteinase K, the tails lysis solution was heated at 95°C for 10 minutes and then centrifuged at 14000 rpm for 5 minutes, after that 1 µl supernatant was used as template DNA for genotyping PCR. The primer pairs used for genotyping PCR are shown in table 4.17.

Table 4.17 Primer pairs for genotyping:

Gene	Forward primer Reverse primer	Length of product (bp)	Tm (°C)	Cycles
Pitx3 wt	5'-GGAGTTTGGGCTGCTTGGTG-3' 5'-CCACACCGCGATCTCTTCG-3'	512	60	35
Pitx3 KO (GFP)	5'-CCATGGTGAGCAAGGGCGA-3' 5'-CTCGAGCTTGTACAGCTCGTCCATG-3'	800	60	35
Ret (wt/lox)	5'-CCAACAGTAGCCTCTGTGTAACCCC-3' 5'-GCAGTCTCTCCATGGACATGGTAGCC-3'	300 wt ~350 floxed	62	35
Ret (excised)	5'-CGAGTAGAGAATGGACTGCCATCTCCC-3' 5'-ATGAGCCTATGGGGGGGTGGGCAC-3'	650	72	35
Dicer (wt/lox)	5'-CCATTTGCTGGAGTGACTCTG-3' 5'-TAAATCTGGCAAGCGAGACG-3'	350 wt ~450 floxed	58 60	35
Dicer (excised)	5'-AGTAATGTGAGCAATAGTCCCAG-3' 5'- TAAATCTGGCAAGCGAGACG -3'	~450	60	35
En1-Cre	5'-GTGCCTTCGCTGAGGCTTC-3' 5'-ACCTGATCCTGGCAATTTCGGC-3'	650	54	35
CAG-CAT-GFP	5'-CTGCTAACCATGTTCATGCC-3' 5'-GGTACATTGAGCAACTGACTG-3'	400	51	35
Rosa26-LacZ	5'-CAAAGTCGCTCTGAGTTGTTATC-3' 5'-CACACCAGGTTAGCCTTTAAGC-3' 5'-GCGAAGAGTTTGTCCTCA-3'	253 wt 300 Laz	50	35
Shh-Cre-SBE1 Primer1&Primer Cre	5'-ATGCAGCCTTGCCCACTTTC-3' 5'-TAGTACCGCGGAACCTGAGGAC-3'	~1200	60	35
Shh-Cre-SBE1 Primer1&Primer SBE1	5'-ATGCAGCCTTGCCCACTTTC-3' 5'-GCCCCTTGACTACCCGCTTTAC-3'	~3200	60	35

4.2.1.3 Agarose gel electrophoresis

To determine the size of double-stranded DNA, different concentration of agarose gels were prepared by melting agrose in 1x TAE buffer according to the size of DNA (i.e. 1% gel for separating 1-10kb DNA, 2.5% gel for 100b-1kb), and 1 µg/ml Ethidium Bromid (EtBr) which intercalates into double-stranded DNA was added. DNA samples mixed with loading buffer and one appropriate DNA marker were loaded into the wells and electrophoresis was conducted at 120 V in 1x TAE buffer for 30-90 minutes. Separated DNA was visualized under long wave UV light (366 nm) and photographed using Gel documentation system (E.A.S.Y Win32, Herolab).

4.2.1.4 Extraction of DNA fragments from agarose gel

After gel electrophoresis, a small piece of agarose gel containing the DNA fragments of interest was cut out under UV light and melted with 500 µl solubilization buffer from the gel

extraction kit (Qiagen) at 55°C. DNA was purified using DNA binding column according to the manufacturer's instruction.

4.2.1.5 Cloning procedures

The interesting genes' promoters, 3' UTR and cDNA were amplified from C57BL/6 mouse genomic DNA or brain cDNA by PCR with specific primers listed in Table 4.18 and Table 4.19. After gel electropheoresis, DNA fragments of correct size were extracted from the gel and ligated with pCR®II TOPO TA vector (TOPO TA cloning kit, Invitrogen) according to the manual of kit. Transformation was done according to the following protocol:

1. Thaw DH5α competent cells (store at -80°C) on ice

2. Add 5 µl Ligation solutions into competent cells, mix gently and incubate on ice for 30 minutes

3. Heat-shock the cells at 42°C for 45 seconds

4. Put back on ice for 2 minutes

5. Add 600 µl LB medium and incubate at 37°C with gentle shaking for 30 minutes

6. Spread 100 µl bacterial suspensions onto LB-agar plate containing 100 µg antibiotics, and incubate at 37°C overnight.

On the next day, single colony was inoculated into LB medium containing 100 µg antibiotics and cultured at 37°C with shaking for 16 hrs. The plasmid was extracted from bacteria using mini preparation kit (Qiagen) according to the manufacturer's protocol. Plasmids with correct insertion of the DNA fragment of interest were identified using restriction digestion and gel electrophoresis. Restriction digestions were performed according to the manufacturer's protocol. Recognition sites on DNA/plasmid for restriction endonucleases were searched using the online service http://tools.neb.com/NEBcutter2/.

The cloned genes were confirmed to have no mutation by sequencing service from the Sequiserve Company (Vaterstetten, Germany). The *Sox2* 3'UTR and the *E2F3* 3'UTR were cut out from pCR®II TOPO vector with restriction endonuclease *Xba* I/*Spe* I, purified using the gel extraction kit, and ligated with *Xba* I-digested pGL3.0-promoter vector (Promega, USA) using T4 DNA ligase (Roche) according to the manufacturer's protocol. The pGL3.0-promoter-3'UTR vectors were amplified in bacteria and isolated from bacteria later. In the same way, the *Pitx3* promoter, the *BDNF* promoter, the *miR-200a* promoter and the *miR-200c* promoter were subcloned from pCR®II TOPO vector into PGL3.0-basic vector (Promega,

USA); the *Sox2* cDNA and the *E2F3* cDNA were subcloned from pCR®II TOPO vector into pcDNA3.1 expression vector (Invitrogen, USA).

Table 4.18 Primer pairs for gene/probe cloning:

Gene	Forward primer Reverse primer	Length of product (bp)	Tm (°C)	Cycles
BDNF (probe)	5'-AGCGTGAATGGGCCCAGGGCA-3' 5'-TGTGACCGTCCCACCGGACA-3'	545	56	30
GDNF (probe)	5'-GGATGGGTCTCCTGGATG-3' 5'-CATTTCCTGGGAACCTTG-3'	813	52	30
Dicer1 (probe)	5'-CTCCTCGTTGGCTGAGAGTG-3' 5'-GGAGGAAGCCAATTCACAGG-3'	813	60	30
E2F3 (cDNA)	5'-AAGAGCAGGAGCGAGAGATG-3' 5'-GGACAACACTGCGATACACG-3'	1469	60	30
Sox2 (cDNA)	5'-GGCGAATTCATGTATAACATGATGGAGACGGAGC-3' 5'-TCTCGAGAGTCCAGCCCTCACATGTGCGACA-3'	970	62	30

Table 4.19 Primers for promoter/3'UTR cloning and mutagenesis:

Gene	Forward primer Reverse primer	Length of product (bp)	Tm (°C)	Cycles
Pitx3 promoter	5'-AAGCAAACCTTTTCTAAGGC-3' 5'-TGTGGCGGCGGCGTTCT-3'	2514	60	30
BDNF promoter	5'-TCTCGGATACCCATTTTTGC-3' 5'-CCCAACAGCTGTCGCTCTAT-3'	2616	54	30
BDNF promoter (Pitx3 BS2 mut.)	5'-CACCTGTCTGAGGTCTAG AAGAGAGGCTCCTTCTTC-3'	2616	55	30
BDNF promoter (Pitx3 BS9 mut.)	5'-CCAAGGGAAGAGGACGACTTGCGCCATGGG AAAGCTTCATGCGTCCCGGGGATCC-3'	2616	55	30
miRNA-200c promoter	5'-CACACACAAATTACAAGGGAAAAG-3' 5'-CTCTCGCTCTTCCTCCTTCA-3'	868	60	30
miRNA-200a promoter	5'-GATGGAGGGCCTGTCTATGA-3' 5'-AGCCTAGGCGGAGACTTAGC-3'	938	57	30
Sox2 3'UTR	5'-TTAACGCAAAAACCGTGATG-3' 5'-CAAGACCACGAAAACGGTCT-3'	516	55	30
Sox2 3'UTR mutant	5'-CGATGAAAAAAAGTTTTAATATTTGCAA GCAACTTTTGTAGTGATAATATCGAGATAAA CATGGCAATCAAATGTCCATTGTTTATAA-3'	516	55	30
E2F3 3'UTR	5'-TAAGGGGCTTAACTGGCGTA-3' 5'-ACTCCCAGTGTTGGGAGAAA-3'	736	55	30
E2F3 3'UTR mutant2	5'-GTAGTATCTGGCACACAAAGTAGA TGAGTACTAGTCATAATTTGTTACTTT AAGTCCTGAGATGCAGGTTCCC-3'	736	55	30
E2F3 3'UTR mutant4	5'-TGTCGTACATGTAGCTCTGTCTGTA AATAGAATCGGTCATAATAAAGCTTT AGCTTTCAGGAAAAACGAAGTAAGAA-3'	736	55	30
miRNA-200c-141 gene	5'-GCCTCGAGGAAGGCAGCCATTTTGTCTC-3'	708	60	30

5'-GGAGATCTGCCGCTTCTCTTG-3'			

4.2.1.6 Site-directed mutagenesis of the promoters and 3'UTRs

Site-directed mutageneses were done using the primers (Table 4.19) and the Quickchange®
Lightning Multi Site-Directed Mutagenesis Kit (Stratagene, USA) according to the
manufacturer's 3-step protocol. Briefly, step 1: mutant strand synthesis reaction. The kit's
unique *Pfu* Fusion –based DNA polymerase, which provides high fidelity DNA synthesis, can
extend the mutagenic primers using denatured circular plasmid DNA as template and ligate
the nick-ends during the PCR cycles. Step 2: digestion of the non-mutated (template) plasmid
DNA. The *Dpn* I endonuclease (target sequence: 5'-Gm^{6}ATC-3') provided by the kit is
specific for methylated and hemimethylated DNA and is used to digest the parental DNA
template. DNA plasmids isolated from most *E. Coli* strains are dam-methylated and therefore
susceptible to digestion. Step 3: transformation of competent cells. 2 µl of the *Dpn* I-treated
DNA was added into competent cells as described above (4.1.5). Mutated plasmid DNA was
isolated from single bacteria colony and was identified by either PCR or restriction digestion,
and further confirmed by sequencing reaction (Vaterstetten, Germany).

4.2.1.7 Isolation of plasmid DNA from *E. coli* (Maxi Prep)

To isolate a larger amount of plasmid DNA from *E.coli* for transfection, a Maxi Prep was
done using the Plasmid Maxi Kit (Qiagen). 1.5 ml bacteria suspension was inoculated into
150 ml LB medium with antibiotic (typically 100 µg ampicillin or 50 µg kanamycin) and
cultured at 37°C with shaking overnight. Bacteria were collected by centrifuging and further
processed according to the manufacturer's protocol.

After isolation of the DNA, the concentration was determined with a spectro-photometer.
The optical density (OD) was measured at a wavelength of 260 nm and the concentration was
calculated (OD260 = 1.0 corresponds to 50 µg/ml double stranded or 33 µg/mL single
stranded DNA).

4.2.1.8 Isolation of RNA

For all RNA work, RNase free solutions, tubes, and pipette tips were used. The working place
and plastic equipments were cleaned with RNa-seZAP® or 70 % ethanol and rinsed with
Milli-Q water before use. Samples were handled with fresh gloves and kept on ice to reduce
RNA degradation.

Total RNA from tissue samples or cells was isolated by using Trizol (Invitrogen). Briefly,
brain tissue was homogenized in 1 ml Trizol, for cells sample 1 ml Trizol was used to lyse
cells by pipetting the solution up and down several times. The lysate was then transferred to a

1.5 ml tube, mixed with 200 µl of chloroform, and put on ice for 5 minutes. Then it was centrifuged at 12,000 x g for 10 minutes at 4°C, the aqueous phase was carefully transferred to a new 1.5 ml tube and mixed with 0.4 ml of isopropanol for 5 minutes on ice. The mixture was centrifuged to get RNA precipitate at 12,000 x g for 10 minutes at 4°C. The pellet was washed once with 75% ethanol, and then air-dried for 10 minutes. Later it was dissolved in DEPC-treated water. RNA concentration was measured by photometer with an OD260 of 1.0 corresponding to a concentration of 40 µg/ml. RNA was stored at −80 °C until further processing.

4.2.1.9 cDNA synthesis

cDNA was synthesized using the Advantage® RT-for-PCR Kit (Clontech, USA) following the manufacturer's protocol:

1. Place 0.2–2 µg of total RNA in an RNase-free microcentrifuge tube and bring the volume up to 12.5 µl with DEPC-treated H_2O.

2. Add 0.5 µl of the random hexamer primer and 0.5 µl of the oligo(dT)18 primer.

3. Heat the RNA at 70°C for 2 min, then cool rapidly on ice before proceeding to the next step.

4. Add the components listed in Table 4.20 as indicated.

Table 4.20 cDNA Synthesis

Reagent	Volume
5X Reaction Buffer	4.0 µl
dNTP Mix (10 mM each)	1.0 µl
Recombinant RNase Inhibitor	0.5 µl
MMLV Reverse Transcriptase	1.0 µl
Total Volume	6.5 µl

5. Mix the contents of the tube by pipetting up and down.

6. Incubate the reaction at 42°C for 1 hr.

7. Heat at 94°C for 5 min to stop the cDNA synthesis reaction and to destroy any DNase activity; then spin down the contents of the tube.

4.2.1.10 Semi-quantitative PCR and Real-Time PCR Assay

For the semi-quantitative PCR, Hot start Taq polymerase (promega, USA) was used to amplify the genes of interest from cDNA with the specific primer pairs listed in Table 4.21. The annealing temperature and the number of cycles are also shown in table 4.21.

Table 4.21 Primer pairs for PCR:

Gene	Forward primer Reverse primer	Length of product (bp)	Tm (°C)	Cycles
Pitx3 RT-PCR	5'-GAGCACAGTGACTCGGAGAAGG-3'	413	60	28

	5'-AAGGCGAACGGGAAGGTC-3'			
BDNF RT-PCR	5'-AGCGTGAATGGGCCCAGGGCA-3' 5'-TGTGACCGTCCCACCGGACA-3'	369	60	28
GAPDH RT-PCR	5'-CCATGTTTGTGATGGGTGTGAACCA-3' 5'-GCCAGTGGATGCAGGGATGATGTTC-3'	251	58	22

For quantitative real-time PCR, the SYBR® Green system (Applied Biosystems, USA) was used with self-designed primer pairs (Table 4.22) and the PCR was performed according to the following protocol:

 2 µl cDNA template

 10 µl 2x SYBR® Green PCR Master Mix

 1 µl forward primer (10pmol/ µl)

 1 µl reverse primer (10pmol/ µl)

 6 µl H$_2$O

The reactions were run on a 7900HT Fast Real-Time PCR System with the SDS soft-ware v2.3 (Applied Biosystems, USA). The amplification conditions consisted of an initial step at 95°C for 10 min, followed by 40 cycles of 20s at 95°C and 1 min at 60°C. In every run, negative controls were included and Beta-actin was employed as an internal control. The expression of target gene was calculated relative to Beta-actin. Data are presented as target expression = $2^{-\Delta ct}$, with ΔCt = (target gene Ct − Beta-actin Ct) according to the $2^{-\Delta ct}$ method described by (Livak and Schmittgen, 2001).

Table 4.22 Primer pairs for SYBR Green qPCR assays:

Gene name	Primer pairs (forward & reverse)	Length of product (bp)	Tm (°C)	Cycles
Pitx3	5'-GAGTTTGGGCTGCTTGGTGAGGC-3' 5'-CCATGTTCTGGAAGCGGAGGGTGT-3'	92	60	35
BDNF	5'-GATGCCGCAAACATGTCTATGA-3' 5'-TAATACTGTCACACACGCTCAGCTC-3'	82	60	35
Beta-actin	5'-CCCGAGGCTCTCTTCCAGCC-3' 5'-TAGAGGTCTTTACGGATGTCAACGT-3'	110	60	35

4.2.1.11 MiRNA qRT-PCR

For quantification of miRNA expression, the NCode™ SYBR® Green miRNA qRT-PCR Kit (Invitrogen, USA) was used according to the supplied protocol. Briefly, 1µg of total RNA extracted from cells using Trizol was first polyadenylated and then converted to cDNA. For miRNA qPCR, the reverse primer was the NCode miRNA universal qPCR primer supplied in the kit, and the specific miRNA forward primers listed in Table 4.23 were used to detect each miRNA expression level. The amplification conditions consisted of an initial step at 95 °C for 10 min, followed by 50 cycles of 20 s at 95 °C and 1 min at 60 °C. Negative controls

were included in all PCRs, and all assays were performed in triplicate. The cycles passing threshold (Ct) were recorded. The expression of each target miRNA in primary neurons was calculated relative to U6B, a ubiquitously expressed small nuclear RNA that has been widely used as an internal control. Data are presented as target miRNA expression = $2^{-\Delta ct}$, with ΔCt = (target gene Ct − Beta-actin Ct) according to the $2^{-\Delta ct}$ method described by (Livak and Schmittgen, 2001).

Table 4.23 miRNA forward primers for qPCR:

Gene name	Forward Primers	Tm (°C)	Cycles
mmiR-200c For	5'-TAATACTGCCGGGTAATGATGG-3'	60	45
mmiR-200a For	5'-TAACACTGTCTGGTAACGATGT-3'	60	45
mmiR-141 For	5'-TAACACTGTCTGGTAAAGATGG-3'	60	45
U6B For	5'-CGCAAGGATGACACGCAAATTCG-3'	60	45

4.2.1.12 Construction of *miR-200* expression and *miR-200* sponge vectors

The gene cluster of *miR-200c-141* was amplified from C57BL/6 mouse genomic DNA using the primer pair listed in table 4.24, then cloned into pcDNA6.2-EmGFP vector or cloned together with U6 promoter into pCAG-EGFP vector. To get a moderate expression level of *miR-200* family, *miR-141* gene was removed from pcDNA6.2-EmGFP-miR-200c-141 plasmid using restriction enzyme Afe I (on *miR-200c-141*) and Xho I (on vector MCS). These three *miR-200* expression plasmids were separately transfected into HEK-293 cells and the expression level of *miR-200* was quantitatively measured by real time PCR using the NCode™ SYBR® Green miRNA qRT-PCR (Invitrogen).

Synthesized oligonucleotides (Table 4.24), which are fully complementary to the sequence of the 5 members of the *miR-200* family were annealed, ligated, gel purified and cloned into pCAG-EGFP vector to get pCAG-GFP-8 x *miR-200* sponge vector (hereafter named as *miR-200* Sponge).

Table 4.24 oligonucleotides for cloning *miR-200* expression/sponge vector:

Gene	Primer pairs (forward & reverse)	Product length (bp)	Tm (°C)	Cycles
miR200c-141	5'-GCCTCGAGGAAGGCAGCCATTTTGTCTC-3' 5'-GGAGATCTGCCGCTTCTCTTG-3'	708	60	30
miR200 oligos for construction of *miR-200* sponge vector	5' GGATCCACATCGTTACCAGACAGTGTTAGCGT CATCATTACCAGGCAGTATTAGCGTCCATCATTA CCCGGCAGTATTAGCGCCATCTTTACCAGACAGT GTTAGCGACGGCATTACCAGACAGTATTAAGATCT3' 5'AGATCTTAATACTGTCTGGTAATGCCGTCGCTA ACACTGTCTGGTAAAGATGGCGCTAATACTGCCG GGTAATGATGGACGCTAATACTGCCTGGTAATGAT GACGCTAACACTGTCTGGTAACGATGTGGATCC3'	These synthesized oligos were annealed and repeatly cloned into pCAG-EGFP vector.		

| mir-200 sponge vector | GGATCCACATCGTTACCAGACAGTGTTAGCGTCATCATTACCAGGCAGTATTAGCGTCC ATCATTACCCGGCAGTATTAGCGCCATCTTTACCAGACAGTGTTAGCGACGGCATTACC AGACAGTATTAAGATCCACATCGTTACCAGACAGTGTTAGCGTCATCATTACCAGGCAG TATTAGCGTCCATCATTACCCGGCAGTATTAGCGCCATCTTTACCAGACAGTGTTAGCG ACGGCATTACCAGACAGTATTAAGATCCACATCGTTACCAGACAGTGTTAGCGTCATCA TTACCAGGCAGTATTAGCGTCCATCATTACCCGGCAGTATTAGCGCCATCTTTACCAGA CAGTGTTAGCGACGGCATTACCAGACAGTATTAAGATCCACATCGTTACCAGACAGTGT TAGCGTCATCATTACCAGGCAGTATTAGCGTCCATCATTACCCGGCAGTATTAGCGCCA TCTTTACCAGACAGTGTTAGCGACGGCATTACCAGACAGTATTAAGATCCACATCGTTA CCAGACAGTGTTAGCGTCATCATTACCAGGCAGTATTAGCGTCCATCATTACCCGGCAG TATTAGCGCCATCTTTACCAGACAGTGTTAGCGACGGCATTACCAGACAGTATTAAGAT CCACATCGTTACCAGACAGTGTTAGCGTCATCATTACCAGGCAGTATTAGCGTCCATCA TTACCCGGCAGTATTAGCGCCATCTTTACCAGACAGTGTTAGCGACGGCATTACCAGAC AGTATTAAGATCCACATCGTTACCAGACAGTGTTAGCGTCATCATTACCAGGCAGTATT AGCGTCCATCATTACCCGGCAGTATTAGCGCCATCTTTACCAGACAGTGTTAGCGACGG CATTACCAGACAGTATTAAGATCCACATCGTTACCAGACAGTGTTAGCGTCATCATTAC CAGGCAGTATTAGCGTCCATCATTACCCGGCAGTATTAGCGCCATCTTTACCAGACAGT GTTAGCGACGGCATTACCAGACAGTATTAAGATCT | 1038 |

4.2.1.13 Analysis of protein samples

4.2.1.13.1 Preparation of protein samples

Brain tissue was homogenized in RIPA buffer with a glass homogenizer, and the cultured cells were directly lysed in RIPA buffer. The cell debris was pelleted by centrifugation at 13,000 rpm for 15 min at 4 °C, afterwards the supernatant containing soluble proteins was transferred to a new tube and stored at -80 °C until use. The protein concentration was measured by bicinchoninic acid (BCA) assay. Briefly, 1 µl of protein sample was diluted in 49 µl RIPA buffer and then added into 1 ml of BCA working reagent. Samples were incubated in a 37 °C incubator for 30 min, cooled down to RT and then the absorption of each sample was measured at 562 nm in a photometer. The concentration of protein in samples can be calculated according to a BSA standard curve.

4.2.1.13.2 Western blot analysis

About 20 µg proteins from each sample were mixed with 5x loading buffer, denatured at 95 °C for 5 min, chilled on ice and then loaded on a precast gel from Invitrogen (NuPAGE® Novex). A prestained protein maker was loaded to estimate the size of the protein bands. Electrophoresis was performed at 120 V for about 2 hrs until the proteins were well separated according to their size. Afterwards, the gel was blotted on a methanol-activated PVDF membrane. Blotting was performed at 50 V for 4 hrs at 4 °C with the Biorad system.

After blotting, the membrane was blocked with blocking solution (4 % skim milk in TBS-T) for 1 hr at RT, and then incubated with the primary antibody (diluted in blocking solution) at 4 °C overnight. Afterwards, the membrane was washed three times with TBS-T for 10 min each, incubated with the secondary, horseradish-peroxidase-conjugated antibody in TBS-T for 1 hr at RT, and washed again three times. The protein-blotted side of memembrane was covered and incubated with ECL detection reagent for 1-2 minutes and then exposed to a chemiluminescent film for several seconds to several minutes, depending on the intensity of the signal. Exposed films were developed using a developing machine, and optical densities

of the specific protein bands were quantified with an Image Analyzer (Quantity One-4.2.0; Bio-Rad, USA).

4.2.2 Animal breeding

C57BL/6 mice were purchased from Charles River. Adult male and pregnant female Sprague Dawley rats were purchased from the Experimental Animal Center (Shanghai, China). Generation and genotyping of *Pitx3$^{-/GFP}$* knock-in mice is described by Zhao et al. (2004). Mice carrying the floxed *Ret* allele and a transgene encoding the Cre recombinase driven by the dopamine transporter (*Dat*) promoter (Kramer et al., 2007) often undergo Cre-mediated excision in the germline; their progeny thus carries one *Ret*-null allele in all cells (*Ret$^{+/-}$* mice). *Ret$^{+/-}$* mice were intercrossed and their offspring was genotyped by PCR. Newborn *Ret$^{-/-}$* pups lacked kidneys and died shortly after birth, thus confirming that these mice were *Ret*-null mutants. *Dicer1$^{+/flox}$* mice were imported from Dr. Matthias Merkenschlager's lab (Cobb et al., 2005). *Dicer1$^{+/flox}$* mice were intercrossed to obtain *Dicer1$^{flox/flox}$* mice, and *Dicer1$^{flox/flox}$* mice were crossed with *En1$^{+/Cre}$* mice (Kimmel et al., 2000) to obtain *En1$^{+/Cre}$; Dicer1$^{+/flox}$* mice. Due to *En1*-driven Cre recombinase expression in the female germline, I used only male *En1$^{+/Cre}$; Dicer1$^{+/flox}$* mice that were crossed to female *Dicer1$^{flox/flox}$* mice to obtain *En1$^{+/Cre}$; Dicer1$^{flox/flox}$* (*Dicer1 cKO*) mice. To fate-map the *Dicer1*-ablated cells in the *Dicer1 cKO* mice, transgenic *CAG-CAT-EGFP* mice (Nakamura et al., 2006) were crossed with the *Dicer1 cKO* mice to obtain *En1$^{+/Cre}$; Dicer1$^{flox/flox}$; CAG-CAT--GFP* mice.

All mice were kept at the Helmholtz Zentrum München in accordance to German and institutional guidelines. Animal treatment was conducted in accordance with the Laboratory Animal Care Guidelines approved by Shanghai Institutes for Biological Sciences, Chinese Academy of Sciences (Shanghai, China), or under federal guidelines as approved by the HMGU Institutional Animal Care and Use Committee (Munich, Germany).

4.2.3 Collection of embryos

Collection of embryonic stages of was done from timed pregnant females. Mating pairs were set up in afternoon and the vaginal plug was checked in the morning of the following day. Noon of the day of vaginal plug detection was designated as embryonic day 0.5 (E0.5). At noon, embryos were dissected from CO_2-asphyxiated pregnant dams, and immediately put into pre-cooled 4 °C PBS. The head of E9.5, E10.5 and E12.5 embryos and the brain of old stage embryos (E14.5 to P0) was dissected and transferred to 4% paraformaldehyde (PFA) for

fixation at 4 °C overnight; and a small piece of tail of the mouse embryo was used to extract DNA for genotyping.

4.2.4 Preparation of paraffin sections

4.2.4.1 Embedding of embryos

Overnight fixed the mouse heads (E9.5-E13.5 stage) or brains (E14.5-P0 stage) were further processed according to the following protocol:

	30% Ethanol	60% Ethanol	70% Ethanol	70% Ethanol	85% Ethanol	95% Ethanol	100% Ethanol	Xylol	Paraffin
E9.5	1h	1h	1h	4°C o/n	10 min	10 min	10 min	7 min	60°C o/n
E10.5	1h	1h	1h	4°C o/n	10 min	10 min	10 min	7 min	60°C o/n
E11.5	1h	1h	1h	4°C o/n	15 min	15 min	15 min	10 min	60°C o/n
E12.5	1h	1h	1h	4°C o/n	15 min	15 min	15 min	10 min	60°C o/n
E13.5	1h	1h	1h	4°C o/n	20 min	20 min	20 min	12 min	60°C o/n
E14.5	1h	1h	1h	4°C o/n	30 min	30 min	30 min	15 min	60°C o/n
E18.5	1h	1h	1h	4°C o/n	45 min	45 min	45 min	20 min	60°C o/n

Notice: all steps in dehydration with shaking, and xylol treatment should be stopped once the whole tissue has turned transparent.

Afterwards the embryos were embedded in paraffin and stored at 4°C.

4.2.4.2 Sectioning of mouse tissues

Paraffin-embedded tissue was sectioned on a microtome (Leica Microsystems, Germany) at a thickness of 8μm. Coronal or sagittal sections were mounted on slides in series of 4-8 according to the stage of embryos. Sections were dried at 37°C overnight and then stored at 4°C.

4.2.5 Preparation of frozen sections

Adult rats and mice were sacrificed by CO_2 asphyxiation, and intracardially perfused with PBS followed by 4% PFA; brains were dissected, and post-fixed in 4% PFA for 24 hrs. After post-fixation, brains were equilibrated in 30 % sucrose solution for 48 hrs at 4 °C, and then embedded into OCT compound (Gene Research Lab, Germany) and frozen at -80°C. Frozen brains were sectioned at 12 μm or 40 μm using a cryostat (Leica Microsystems, Germany). Sections were mounted on slides (12 μm) or collected in cryoprotection solution (40 μm) in series of 8, and stored at −20 °C.

4.2.6 In situ hybrydization (ISH)

The ISH was used to detect mRNAs and miRNAs using radiolabeled probes or DIG-labeled probes on mouse embryo sections. To avoid degradation of RNA during the procedure, all solutions were autoclaved, glasswares were baked and disposable gloves were used.

4.2.6.1 Linearization of plasmid/template DNA

Twenty µg of a plasmid containing a target gene cDNA were linearized with a suitable restriction enzyme (shown in table 4.25) at 37°C for 4hrs or overnight. Linearized DNA was analyzed by gel electrophoresis, purified using the PCR-purification kit, and eluted in 40 µl DEPC-treated water. The concentration of linearized DNA was measured in a photometer.

Table 4.25

Riboprobes for detection of mRNA			
Gene	Enzyme for linearizing of plasmid	RNA polymerase	References
BDNF	Xba I	Sp6	(Peng et al., 2011)
BDNF (sense probe)	Hind III	T7	(Peng et al., 2011)
GDNF	Xba I	Sp6	(Peng et al., 2011)
GDNF (sense probe)	Hind III	T7	(Peng et al., 2011)
Pitx3	Not I	Sp6	(Brodski et al., 2003)
Dicer1	Xba I	Sp6	See 4.2.1.5
En1	Hind III	T7	(Fischer et al., 2011)
Fgf8	Pst I	T7	(Martinez et al., 1999)
Wnt1	Hind III	T7	(Fischer et al., 2011)
Lmxb1	Xho I	Sp6	(Prakash et al., 2006)
Otx2	EcoR I	Sp6	(Prakash et al., 2006)
Gbx2	Hind III	T7	(Prakash et al., 2006)
Hes1	Hind III	T3	(Takebayashi et al., 1994)
Hes3	Hind III	T3	(Fischer et al., 2011)
Hes5	Hind III	T3	(Fischer et al., 2011)
Sef1	Nco I	Sp6	(Fischer et al., 2011)
Spry1	EcoR I	T7	(Fischer et al., 2011)
Spry2	Sac II	T3	(Fischer et al., 2011)
Mkp3	Sal I	T7	(Fischer et al., 2011)
Pax2	BamH I	T3	(Nornes et al., 1990)
Shh	Hind III	T3	(Fischer et al., 2011)
Ngn1	Nhe I	T7	(Fischer et al., 2011)
LNA probes for detection of miRNA			
mmu-miR-124			Exiqon, EQ 56993
mmu-miR-200c			Exiqon, EQ 56944
scramble-miR control			Exiqon, #99004-00

4.2.6.2 Probe labelling

Riboprobes were transcribed with RNA polymerase using linearized plasmid DNA template and the following protocol:

x µl (1.5 µg DNA) linearized plasmid DNA template
x µl DEPC-H2O (total volume is 30 µl)
3 µl 10x transcription buffer
3 µl NTP-mix (rATP/rCTP/rGTP 10 mM each)
1 µl 0.5 M DTT
1 µl RNasin (RNAse-Inhibitor, Roche)
8 µl 35S-thio-rUTP from Perkin Elmer (13 µl from Hartmann;
12.5 mCi/mM; 1250 Ci/mmol)
1 µl T7, T3 or SP6 RNA polymerase (20 units/µl)

The reaction solutions were mixed gently by tapping the Eppendorf-tube and given a quick spin, then incubated at 37 °C for 3 hrs in total. After 1 hr, 0.5 µl of RNA polymerase was added. To eliminate the template DNA, 2 µl RNase-free DNase I (Roche) was used to digest DNA for 15 minutes at 37 °C. Afterwards, the riboprobes were purified using RNeasy MinElute Cleanup Kit (Qiagen) according to the supplied protocol. 1 µl of riboprobe was used to measure radioactivity with 2 ml scintillation liquid in a beta-counter. Only labelled riboprobes exhibiting values above 0.5 million cpm were used for further experiments. At -20 ° C, the riboprobes could be stored for up to one week.

4.2.6.2 Pretreatment of paraffin sections

Paraffin sections (8 µm) used for ISH were pretreated as following protocol:

Step	Time	Solution	Remarks
1. dewax	2 x 15 min	Xylol	check dewaxing, time can be prolonged
2. rinse	2 x 5 min	100 % Ethanol	
3.	5 min	70 % Ethanol	
4.	3 min	Dest.H$_2$0	
5.	3 min	PBS	
6.	20 min	4 % PFA/PBS	on ice
7.	2 x 5 min	PBS	
8.	7 min	20 µg/ml Proteinase K in Proteinase-K-buffer	add 200 µl of Proteinase K (20 mg/ml)
9.	5 min	PBS	
10.	20 min	4 % PFA/PBS	same solution from step 6
11.	5 min	PBS	
12.	10 min	200 ml of 0,1 M triethanolamine-HCl (pH8) (1x TEA)	add 600 µl acetic anhydride; (for the second rack add anothertime 600 µl acetic anhydrid); rapidly stirring
13.	2 x 5 min	2xSSC	
14.	1 min	60 % Ethanol/H$_2$O	
15.	1 min	70 % Ethanol/H$_2$O	
16.	1 min	95 % Ethanol/H$_2$O	
17.	1 min	100 % Ethanol	

18. Air dry (dust free!)

4.2.6.3 Prehybridization

Air-dried sections were prehybridized with hybridization buffer (90 µl per slide and with cover slip) for 1 hr at 58°C in a humid chamber (50% formamide, 10% 20x SSC, 10% hybrid mix in DEPC-water).

4.2.6.4 Hybridization

Hybridization mix containing riboprobe (35 000 to 70 000 cpm/µl) was prepared by mixing 35^S -labelled-riboprobe with an appropriate amount of hybridization buffer. After prehybridization, the coverslip was removed and 100 µl hybmix was added on each slide. Slides were covered with coverslip, put into a humid chamber and incubated in an oven at 58°C overnight.

4.2.6.4 Wash

On the next day, slides were taken out from incubator and coverslips were removed, and then washed in following solutions:

Step	Time	T°C	Solution	Remarks
1.	4 x 5 min	RT	4xSSC	
2.	20 min	37 °C	NTE (20µg/ml RNaseA)	add 500 µl RNaseA(10mg/ml) to 250 ml of NTE
3.	2 x 5 min	RT	2xSSC/1 mM DTT	add 50 µl of 5 M DTT/250 ml
4.	10 min	RT	1xSSC/1 mM DTT	add 50 µl of 5 M DTT/250 ml
5.	10 min	RT	0,5xSSC/1mM DTT	add 50 µl of 5 M DTT/250 ml
6.	2 x 30 min	64 °C	0,1xSSC/1 mM DTT	add 50 µl of 5 M DTT/250 ml
7.	2 x 10 min	RT	0,1xSSC	
8.	1 min	RT	30 % Ethanol in 300 mM NH$_4$OAc	
9.	1 min	RT	50 % Ethanol in 300 mM NH$_4$OAc	
10.	1 min	RT	70 % Ethanol in 300 mM NH$_4$OAc	
11.	1 min	RT	95 % Ethanol	
12.	2 x 1 min	RT	100 % Ethanol	
Air dry in dust free area				

4.2.6.5 Autoradiography of Slides

Dried sections were exposed to a special high performance X-ray film (BioMax MR from Kodak) for three days. This step is to check if the in situ hybridization worked well or not.

4.2.6.6 Dipping and Development of Slides

The photographic emulsion NTB2 (Integra Biosciences, IBO 5666, Kodak, diluted 1:1 with H$_2$O) is sensitive against light, metal and movement. Before use, the emulsion was melted in a water bath at 42 °C for at least 1 hr. The slides were put into a holder and dipped slowly into

the emulsion for 15 seconds. Afterwards, the slides within holder were put on a paper towel and dried in a dark-drawer overnight at RT. The slides were then stored into light-tight black boxes with silica gel (desiccant) at 4 °C for 4 to 6 weeks.

After exposure, the boxes with slides were equilibrated at RT for at least 1 hr. The slides were taken out from the boxes and developed in KODAK D 19 developer (Sigma P5670) for 4 minutes at RT, rinsed in tap water for 30 seconds, fixed in KODAK fixer (cat# 197 1720) for 6 minutes, and rinsed in running tap water for 20 minutes. The emulsion on the back side of the slides was scratched off with a razor blade. Finally, Nissl (cresyl violet) staining (see below 3.2.7.1) was performed on sections.

4.2.6.7 MiRNA ISH

Locked nucleic acid (LNA)-modified detection probes for *miR-124*, *miR-200c* and negative control (Exiqon, Denmark) were labeled either with digoxigenin (DIG) or with 35S-thio-ATP by using DIG Oligonucleotide 3'-End labeling kit (Roche) or Terminal transferase kit (Roche), respectively. ISH was performed on paraffin sections according to the following protocol:

Paraffin sections (8 µm) used for ISH were pretreated as follows:

Table 4.26 ISH DAY I

Step	Time	Solution	Remarks
1. dewax	2 x 15 min	Xylol	check dewaxing, time can be prolonged
2. rinse	2 x 5 min	100 % Ethanol	
3.	5 min	70 % Ethanol	
4.	5 min	30 % Ethanol	
5.	3 min	Dest.H$_2$0	
6.	2 x 5 min	PBS	
7.	20 min	4 % PFA/PBS	on ice
8.	2 x 5 min	PBS	
9.	5 min	10 µg/ml Proteinase K in Proteinase-K-buffer	add 100 µl of Proteinase K (20 mg/ml)
10.	30 seconds	0.2% Glycine in PBS	
11.	2 x 1 min	PBS	
12.	10 min	4 % PFA/PBS	on ice
13.	2 x 5 min	PBS	
14.	10 min	200 ml of 0,1 M triethanolamine-HCl (pH8) (1x TEA)	add 600 µl acetic anhydride; (for the second rack add anothertime 600 µl acetic anhydrid); rapidly stirring
15.	2 x 5 min	2xSSC	
16.	2h	hybridization buffer	prehybridization at temperature of (tm-21) °C
17.	overnight	For hot ISH: 1.5 million cpm	At (tm-21) °C

			probe in 100 ul hybridization buffer was added on each slides; for cold ISH, 4pmol probe in 200 ul in hybridization buffer (~20nM) was used for each slider	

Table 4.27 ISH DAY II

Step	Time	T°C	Solution	Remarks
1.	4 x 5 min	RT	4xSSC	For hot ISH
2.	15 min	(tm-21)	2xSSC	Add 0.1% triton x100 and 1 mM DTT (50ul 5M DTT into 250ml)
3.	2 x 15 min	(tm-21)	1xSSC	Add 0.1% triton x100 and 1 mM DTT
4.	2 x 15 min	(tm-21)	0.2xSSC	Add 0.1% triton x100 and 1 mM DTT
5.	10 min	RT	0.2xSSC	
For hot ISH, processed to step 6; for cold ISH, processed to step 12.				
6.	1 min	RT	30 % Ethanol in 300 mM NH$_4$OAc	
7.	1 min	RT	50 % Ethanol in 300 mM NH$_4$OAc	
8.	1 min	RT	70 % Ethanol in 300 mM NH$_4$OAc	
9.	1 min	RT	95 % Ethanol	
10.	2 x 1 min	RT	100 % Ethanol	
11.	After air-drying, the slides were dipped into emulsion NTB2, and later developed as described above(4.2.6.6).			
12.	1h	RT	blocking buffer (10% FBS in PBS)	
13.	overnight	4	1:2000 anti-DIG antibody in blocking buffer	
14.	5x5 min	RT	PBS	
15.	2x10 min	RT	Buffer I	
16.	10 min	RT	Buffer II	
17.	24h-48h	4	NBT/BCIP staining solution	stop in TE or H$_2$O
18.	mounted with aqeous mounting medium			

4.2.7 Histology

4.2.7.1 Nissl staining (cresyl violet staining)

Nissl staining of rehydrated sections was performed according to the following protocol:

Step	Time	Solution
1	1-5 min	cresyl violet staining solution
2	1 min	H$_2$O
3	2 x 1 min	70 % ethanol
4	10-60 sec	96 % ethanol + 0.5 % acetic acid

5	2 x 1 min	96 % ethanol
6	2 x 2 min	100 % ethanol
7	2 x 5 min	Xylene

The slides were immediately mounted using DPX, and dried overnight in the hood.

4.2.7.2 Immunohistochemistry

4.2.7.2.1 Pretreatment of paraffin sections

Paraffin sections were dewaxed and rehydrated in a standard alcohol series using the following protocol:

Step	Time	Solution
dewaxing	10 min	Xylene
dewaxing	15 min	Xylene
rehydration	2 x 3 min	100 % ethanol
rehydration	3 min	95 % ethanol
rehydration	3 min	85 % ethanol
rehydration	3 min	70 % ethanol
rehydration	3 min	60 % ethanol
rehydration	3 min	30 % ethanol
rehydration	2 x 5 min	H_2O

Afterwards, rehydrated sections were placed in a rack, put into a beaker filled with 1x Citrate buffer, and boiled in a microwave oven at 630 W for 3x 3 min to unmask the antigen. Between each boiling step, 1x Citrate buffer was refilled up to the top of the beaker. After that, slides were cooled down at RT. The slides were washed 5min in H_2O and 5min in PBS and used for immunostaining afterwards.

4.2.7.2.2 Immunostaining of mounted sections

Pretreated (see above) paraffin sections and cryosections were blocked with 10% FBS in PBS (for cryosections, 0.1% triton X-100 was added for permeabilization of the membranes) for 1 hr at RT, and then incubated with primary antibody diluted in blocking solution at 4° C overnight. On the following day, the sections were washed with PBS 3 x 10 minutes, and further incubated with fluorescence conjugated secondary antibody for 1.5 hrs at RT in dark place. Afterwards, the sections was washed in PBS for 10 minutes, counterstained with DAPI for 10 minutes at RT, and washed in PBS 2 x 10 minutes. Finally the sections were mounted using Aqua-polymount (polyscience, USA) to prevent fading of the fluorescent signal and stored at 4°C. The immunostaining for cleaved Caspase3 on cultured cells and tissue sections

was amplified using the Tyramide Signal Ampification kit (PerkinElmer, USA) according to the manufacturer's instructions.

4.2.7.2.3 Immunostaining of free floating sections

All steps were performed in 6 well plates with cell strainers on a shaker, unless otherwise stated.

Step	Time and temperature	Solution	Remarks
wash	4 x 10 min, RT	1x PBS	removal of cryoprotection solution
blocking	60 min, RT	10 % FBS in 1x PBS with 0.1% triton X-100 (blocking buffer)	
Incubation with 1st antibody	overnight, 4 °C	Primary antibody in blocking buffer	in 24 well plate
wash	3 x 10 min, RT	1x PBS	
Incubation with 2nd antibody	2 hrs	fluorescence conjugated 2nd antibody in blocking buffer	in 24 well plate
wash	10 min, RT	1x PBS	
counterstaining	10 min, RT	DAPI	
wash	2 x 10 min, RT	1x PBS	

Afterwards the sections were transferred into PBS and mounted on slides using Aqua-Polymount (polyscience, USA).

4.2.7.2.4 BrdU staining

Bromodeoxyuridine (5-bromo-2'-deoxyuridine, BrdU) is an analogue of thymidine, and can be incorporated into the newly synthesized DNA by substituting for thymidine during DNA replication (during the S phase of the cell cycle) in proliferating cells. BrdU is commonly used in the detection of proliferating cells in living tissues. Incorporated BrdU can then be detected with an anti-BrdU antibody. Binding of the antibody requires denaturation of the DNA, usually by exposing the cells to acid or heat.

100mg/kg (body weight) BrdU was intraperitoneally injected into pregnant dams 2hrs or 24hrs before sacrifice. Embryos were collected, fixed, dehydrated and embedded in paraffin. Pretreated-paraffin sections (see step 4.2.7.2.1) were incubated in 2N HCl for 30 minutes, followed by 2x15 minutes in 0.1 M Borate buffer. After washes in PBS for 2x5 minutes, sections were blocked and further incubated with primary antibody and secondary antibody as described above.

4.2.7.3 EdU labeling

Like BrdU, EdU (5-Ethynyl-2'-deoxyuridine), a new analogue of thymidine, can be also incorporated into DNA during replication of DNA, thus labeling the proliferating cells. EdU (10µg per gram (mouse body weight)) was intraperitoneally injected into pregnant dams 2hrs or 24hrs before sacrifice. Embryos were collected, fixed, dehydrated and embedded in paraffin. After pretreatment (see step 4.2.7.2.1), paraffin sections were processed for EdU staining with Click-iT^{TM} EdU Imaging Kit (Invitrogen, USA) according to the supplied protocol. Briefly, sections were washed with 3% BSA in PBS, and then incubated in the reaction solution containing $CuSO_4$ and Alexa Fluor 488 azide for 30 minutes at RT to conjugate the dye with EdU. EdU-stained sections were used for immunostaining and DAPI counterstaining as described above.

Fluorescent images were taken with an Axiovert 200M inverted microscope (Zeiss, Germany), Olympus BX51 microscope (Olympus, Japan) or LSM510 confocal microscope (Zeiss, Germany), and processed with Adobe Photoshop 7.0 or CS software.

4.2.7.4 LacZ staining

The *lacZ* gene is commonly used as a reporter in various experiments because it encodes the enzyme β-galactosidase which converts X-Gal into the blue insoluble pigment 5,5'-dibromo-4,4'-dichloro-indigo. For the detection of β-galactosidase activity in mice, the following protocol was used. The embryos were collected and fixed in LacZ fix for 10-30 minutes depending on the stage of the embryos (i.e. 10 min for E10.5 embryos), washed for 15 minutes in the wash buffer, and stained in X-Gal staining solution for 2-12 hrs at RT or 30°C (avoid light). Afterwards, the embryos were washed in wash buffer and post-fixed 4% PFA overnight at 4°C. The stained embryos were photographed using light microscope (Zeiss, Germany). To maintain the activity of β-galactosidase, all solutions used for LacZ staining were supplemented with MgCl2 and EGTA, and the staining was performed as soon as possible after preparation for optimal results.

4.2.8 Intrastriatal injections of GDNF

Adult male rats (n=5) were anaesthetized with chloral hydrate (400 mg/kg, i.p.), and were fixed in the stereotactic apparatus (Stoelting, USA) using ear and tooth bars. Eye ointment was applied to prevent corneal drying during the surgery. The fur on head was shaved, the skin on the skull was disinfected with 70 % ethanol, and then the scalp was opened with a sterile scalpel along the midline. The position of Bregma point was set to coordinate origin and the injection sites (according to Bregma: anterior/posterior: +0.7, medial/lateral: ±3.5)

were marked on the skull. Small holes were carefully drilled at the injection sites with a hand-held drill and then the micropipette was positioned at the correct coordinates (according to Bregma: anterior/posterior: +0.7, medial/lateral: ±3.5, dorsal/ventral: -4.0). With a Hamilton syringe, 20 µl of a 15 ng/µl GDNF solution in 0.9% saline were injected into the right striatum. Vehicle (0.9% saline) was injected into the contralateral striatum. The injection rate was 1 µl/min, and the canula was left in place for another 10 min before it was slowly retracted. Finally, the surgery area was disinfected and was subsequently sutured using an absorbable thread. After 48 hrs, animals were sacrificed by CO_2 asphyxiation. For immunohistochemical analyses, animals were intracardially perfused with PBS followed by 4% PFA and brains were collected, post-fixed in 4% PFA for 24 hrs, cryosectioned and processed as described above. For Western blot analyses, brains were immediately removed and ventral midbrain tissue was dissected and processed as described before.

4.2.9 MiRNA profiling

Tissues comprising the caudal diencephalon, mesencephalon and rostral rhombomere 1 were microdissected from E10.5 and E12.5 control (*En1*$^{+/Cre}$; *Dicer1*$^{+/flox}$) and the *Dicer1 cKO* embryos. Tissues from 3 embryos were pooled according to genotypes. JM8 (C57BL/6N agouti) (Pettitt et al., 2009) mouse embryonic stem cells (mESC) were cultured and differentiated into glutamatergic neurons following the protocol of (Bibel et al., 2007a). Cell samples (cells from a 10 cm Ø dish or from 4 wells of 6-well plate) were collected at day 4 (ESC), day 12 (embryoid bodies), and day 20 (neurons) of the differentiation procedure. Successful differentiation of the mESC into neurons was confirmed in a fraction of the cells by immunostaining for Sox2 and Tubb3. Total RNA was isolated from MH tissues and cell samples using Trizol Reagent (Invitrogen). 10 µg of each total RNA was used to isolate small RNAs (10–40 nt) which was further ligated with adaptors by T4 RNA ligase and then amplified by RT-PCR using the kit (FC-102-1009-KIT, SAMPLE PREP, DGE SMALL RNA, Illumina) according to the supplied manual. The PCR products were purified and used to generate clusters on flowcell using the kit (RS-220-0122-TF, DGE-SMALL RNA CLUSTER GEN KIT V2 – GAII, Illumina) according to the supplied manual. Finally the DNA clusters were sequenced for 36 cycles on the Illumina/GAII sequencer using the kit (FC-104-4002-36 Cycle Sequencing Kit v4, Illumina) according to the manufacturer's instructions. For the mapping of small RNA sequencing reads, 3' adapter sequences were first removed from the sequencing reads using an in-house Perl script (MDC Berlin/Germany). The reads between 17 and 30 nt were retained and mapped to known mouse pre-miRNA sequences deposited in

miRBase (v16.0) (Kozomara and Griffiths-Jones, 2011), without any mismatches using soap.short software (Li et al., 2008). For data analysis, miRNAs with less than 10 read numbers in the heterozygous sample were excluded from further analyses, because these extremely low-abundance miRNAs are unlikely to cause the severe phenotype in the *Dicer1 cKO* mice.

4.2.10 Cell culture

4.2.10.1. Cell lines

COS-7, HEK-293, and SH-SY5Y cells were cultured in DMEM medium (Invitrogen, USA) containing 10% FBS (Invitrogen, USA) at 37 ° C and 5% CO_2. The dish/plate used for SH-SY5Y cells were coated with poly-D-lysine (Sigma, USA). All cell lines were passaged every 4 days and the medium was changed every second day. For medium change, DMEM medium was mixed with FBS in a ratio of 9:1, and warmed in 37° C waterbath. The old medium was sucked off from the dish and 10 ml fresh prewarmed medium was slowly added to dish. For passaging cells, the cells were washed once with 10 ml PBS after the old medium was sucked off and trypsinized with 2 ml of 0.05% trypsin (Invitrogen, USA) at 37° C for 2-4 min depending on the cell line. Trypsinization was stopped by adding 8 ml DMEM medium containing 10% FBS, and the cells were resuspended by pipetting gently. The cell suspension was transferred into 15 ml falcon tubes and centrifuged at 1100 rpm for 4 minutes. The supernatant was removed carefully and the pellet was resuspended in 1 ml of medium and added 1:10 to a new plate with 10 ml fresh medium.

4.2.10.2 Primary neuron cultures and treatments

4.2.10.2.1 Primary ventral midbrain (VM) cultures and treatments.

To culture midbrain dopaminergic neurons, the ventral midbrain (floor plate) was micro-dissected from E14 rat embryos or E11.5 *Pitx3*$^{+/GFP}$ and *Pitx3*$^{GFP/GFP}$ mouse embryos in D'Hanks containing 10 mM D-glucose, 50U/ml penicillin and 50 µg/ml streptomycin, and collected in 1.5 ml sterile tubes. The tissue was washed once with D'Hanks, and then transferred into a 15 ml falcon tube with 3 ml of 0.025% trypsin plus 0.05% DNase (Invitrogen) for trypsinization at room temperate for 5 min. The trypsinization was stopped by adding 300 µl FBS, and the cells were dissociated by gently pipetting up and down several times. The falcon tube was placed in a rack for 2 min to let the cell clumps settle down, and then the cell suspension (avoiding cell clumps) was removed to a new 15 ml tube. The remaining cell clumps were further dissociated in 2 ml DMEM/F12 medium containing 10% FBS and the cell suspension was removed to the tube. The last step was repeated once more.

The cell suspension was centrifuged at 1100 rpm for 4 min and the dissociated cells were resuspended in 3 ml DMEM/F12 medium containing 10% FBS. The number of cells in the suspension was counted, and then the cells were seeded on 20 μg/ml Poly-D-Lysine-coated coverslips in 24-well plates at a density of 1.4 x10^5 viable cells per well, and grown at 37° C and 5% CO_2.

For GDNF treatments, E14 rat primary VM cells were treated after 7 days in vitro (DIV) with 10 ng/ml recombinant rat GDNF (Sigma, USA) in 0.9% saline or with 0.9% saline alone (control) for 3, 24 or 48 hrs. In some cases, 10 μg/ml NF-κB inhibitor (SN50; Calbiochem, USA) were added for 1 hr to the culture medium prior to the GDNF treatment. Cells were harvested for immunostainings and RT-PCR assays after 3 or 24 hrs, and for Western blot analyses after 2 days (d) of GDNF treatment. For BDNF treatments, dissociated E11.5 *Pitx3*$^{+/GFP}$ or *Pitx3*$^{GFP/GFP}$ mouse VM cells were plated at a density of 1.4x10^5 cells/well, and cultured in DMEM/F12 with 2% B27 supplement (Invitrogen, USA) containing 20 ng/ml recombinant human BDNF (R&D Systems, USA) in 0.1% bovine serum albumin (BSA) or 0.1% BSA alone. BDNF or vehicle (0.1% BSA) was added with each medium change every second day. Cells were fixed for immunostainings after 4 d.

For siRNA treatments, three different mouse *Pitx3*-specific short hairpin RNA (shRNA) oligonucleotide pairs were designed and synthesized by Shanghai GeneChem (Shanghai, China). Downregulation of *Pitx3* mRNA by these shRNAs was tested in SH-SY5Y cells stably expressing mouse *Pitx3* (Peng et al., 2007). Under these conditions, one *Pitx3* specific shRNA oligonucleotide (anti-sense: 5'-GCACGCCUCUUUCAGCUAUdTdT-3'; sense: 5'-AUAGCUGAAAGAGGCGUGCdTdT-3'; targeting sequences around position 956 to 974 in *Pitx3* Exon 4, Acc. Nr. NM_008852.4) resulted in ~80% knock-down of *Pitx3* mRNA (data not shown). A non-silencing shRNA oligonucleotide, as indicated by the manufacturer, (anti-sense: 5'-CGUGACACGUUCGGAGAAdTdT-3'; sense: 5'-UUCUCCGAACGUGUC ACGUdTdT-3') was used as control. E14 rat primary VM cells were transfected with *Pitx3* or control shRNA oligonucleotides (40 pmol) after 7 DIV using Lipofectamine 2000 (Invitrogen, USA) right after addition of GDNF to the culture medium. Cells were harvested after 24 hrs (for RT-PCR assays) or 2 d (for Western blot analyses).

For 6-OHDA Treatments, dissociated E11.5 *Pitx3*$^{+/GFP}$ or *Pitx3*$^{GFP/GFP}$ mouse VM cells were plated at a density of 1.4x10^5 cells/well, and cultured in DMEM/F12 with 2% B27 supplement for 3 DIV. Cells were treated after 3 DIV with 20 ng/ml BDNF or 20 ng/ml recombinant human GDNF (R&D Systems, USA), or with vehicle (0.1% BSA) alone, 2 hrs prior to the addition of 10 μM 6-hydroxydopamine (6-OHDA (Cat. Nr. H116); Sigma, USA)

106

or vehicle alone (phosphate buffered saline, PBS) to the culture medium. Cells were fixed 24 hrs after the addition of 6-OHDA for immunostainings.

4.2.10.2.2 Primary ventral mid-/hindbrain (vMH) cultures and transfection.

Primary ventral mid-/hindbrain cultures were prepared from E11.5 C57BL/6 mouse embryos as described above. Briefly, the ventral mid-/hindbrain was micro dissected and trypsinized with 0.025% trypsin plus 0.1% DNase (Invitrogen) for 5 min at room temperate. Dissociated cells were seeded in a 24-well plate at a density of $2x10^5$ cells per well, cultured in DMEM:F12 medium containing 10% FBS (Invitrogen). After 18 hrs the medium was changed to DMEM:F12 medium containing 2% B27 (Invitrogen), and cells were transfected separately with miR-200 sponge vector, miR-200 overexpression vector and the corresponding control vectors, using Lipofectamine™ LTX and Plus Reagent (Invitrogen, USA). The medium was changed 1 day post transfection (dpt). Cells were fixed with 4% PFA for immunostaining or lysed with RIPA buffer for western-blot assay at 3dpt.

4.2.10.2.3 Differentiation of mouse embryonic stem cells

According to Bibel's protocol, JM8 ESCs were thawed and cultured for two or three passages without feeder cells on 0.2% gelatine-coated plates in ES medium at 37° C and 7% CO_2. ESCs were split every 2nd d and plated at a density of about 3×10^6 cells on 10-cm dishes (Corning). Then, 4×10^6 cells were plated in nonadherent bacterial dishes (Greiner) in EB medium and cultured for 4 d without retinoic acid, and 4 d in the presence of 5μM retinoic acid. Medium was changed every second day. Embryoid bodies (EB) were then dissociated in N2 medium and cells were plated on PDL- and laminin-coated 6-well plates at a density of 2.3×10^6 cells per well. The N2 medium was changed after 2 h and again after 1 d. After 2 d, the medium was replaced by B27 medium, and the medium was partially changed after 5 d. after 8 d, the cells were either fixed with 4% PFA for immunostaining or lysed with Trizol for RNA extraction.

4.2.11 Cell cycle exit assay

Pregnant dams were injected i.p. with EdU on E11.5 (t0). After 24 hrs, a fraction of the cells that had incorporated EdU exited the cell cycle (G0 cells, EdU$^+$, Ki67$^-$), and the rest re-entered the cell cycle (EdU+, Ki67$^+$ cells). Embryos were dissected 24 hrs later (t24) at E12.5 and processed for EdU-fluorescent reaction and Ki67 fluorescent immunostaining. The index Tc of cell cycle re-entry after 24 hrs was calculated by dividing the number of Ki-67/EdU double labeled cells by the total number of EdU$^+$ cells.

4.2.12 Cell counting

For the first project, TH$^+$, Pitx3$^+$ and DAPI$^+$ cells in E14 rat VM cultures were counted in 10 random fields/well for 6 wells, and data were collected from 3 independent experiments. Pitx3$^+$ cells were counted on every fourth serial coronal hemisection through the midbrain of E12.5, and on every fourth serial sagittal section through the midbrain of E14.5 *Ret$^{+/+}$* and *Ret$^{-/-}$* embryos. GFP$^+$ and cCasp3$^+$ cells were counted on every fourth serial coronal hemisection through the midbrain of E12.5 *Pitx3$^{+/GFP}$* and *Pitx3$^{GFP/GFP}$* embryos. GFP$^+$, TH$^+$, cCasp3$^+$ and DAPI$^+$ cells in E11.5 *Pitx3$^{+/GFP}$* and *Pitx3$^{GFP/GFP}$* VM cultures were counted in 12 random fields/well, and data were collected from at least 3 independent experiments.

For the second project, Pitx3$^+$ and Pou4f1$^+$ cells were counted on three anterior-posterior (A/P) position-matched coronal midbrain sections, and Ist1$^+$ and 5-HT$^+$ cells were counted on every fifth serial coronal hemisection of the ventral mid- or hindbrain of E12.5 *En1$^{+/Cre}$; Dicer1$^{flox/flox}$* CAG-CAT-*GFP* embryos and *En1$^{+/Cre}$ Dicer1$^{+/flox}$* CAG-CAT-*GFP* embryos. Sox2$^+$, Ki67$^+$, E2F3$^+$ and EdU$^+$ cells were counted on three A/P position-matched coronal hemisections through the ventral mid/hind brain of E11.5 and E12.5 *Dicer1 cKO* embryos and wild type controls. GFP$^+$, Sox2$^+$, Tubb3$^+$ and E2F3$^+$ cells in primary ventral mid/hind brain cultures derived from E11.5 C57/Bl6 mouse embryos were counted in 20 random fields/coverslip (20x), and data were collected from at least three independent experiments.

4.2.13 Photography

Images were taken using bright- and dark-field optics on an Axioplan2 microscope or StemiSV6 stereomicroscope, AxioCam MRc camera and Axiovision 4.6 software (Zeiss, Germany). Fluorescent images were taken on confocal microscopes (BX51, Olympus; LSM510, Zeiss). All pictures were processed with Adobe Photoshop 7.0 or CS software (Adobe Systems Inc., USA).

4.2.14 Luciferase reporter assays

For promoter luciferase assay, SH-SY5Y cells growing in 24-well plates were transfected with 400 ng/well *pGL3-Pitx3* promoter vector and 8 ng/well *pRL-SV40* vector using Lipofectamine 2000 (Invitrogen). 10 µg/ml SN50 was added 30 min before 10 ng/ml or 20 ng/ml GDNF were given to the medium. HEK293 cells were co-transfected with 200 ng/well *pGL3-BDNF* wild-type or mutant promoter vector, 400 ng/well *pcDNA3.1-Pitx3* (Peng et al., 2007) or *pcDNA3.1* alone, and 8 ng/well *pRL-SV40* using Lipofectamine™ LTX and Plus Reagent (Invitrogen, USA). Cells were lysed in 100 µl Passive Lysis Buffer 24 h (*BDNF*

promoter assays) or 36 h (*Pitx3* promoter assays) post-transfection, and 10 µl lysate was used to measure Luciferase luminescence of Firefly and Renilla in a Centro LB 960 Luminometer (Berthold Technologies, Germany) with the Dual-Luciferase® Reporter Assay system (Promega, USA) according to the manufacturers' instructions. Firefly luminescence was normalized against Renilla luminescence for each well, and relative values (fold-induction) were calculated by setting the normalized value of the control transfection as 1.

To test the efficacy of miR-200 overexpression vectors and miR-200 sponge vector, COS-7 cells were co-transfected with 300 ng/well *pGL3*-Sox2 3'UTR vector, 8 ng/well *pRL-SV40,* with or without 600 ng/well miR-200 sponge vector, along with 600 ng/well *pcDNA6.2-EmGFP-miR-200c-141* or *pcDNA6.2-EmGFP-miR-200c or pCAG-GFP-U6-miR-200c-141 or pcDNA6.2-EmGFP* using Lipofectamine™ LTX and Plus Reagent (Invitrogen, USA). The miRNA sensor assays were conducted in COS-7 cells co-transfected with 300 ng/well *pGL3-Sox2-3'UTR* or *pGL3-E2F3-3'UTR* sensor vectors, and 10 or 30 nM precursor miRNA *mmu-miR-200c* (Ambion, PM11714) or negative control (NG[#2], Ambion, AM17111). The corresponding rescue assays were done in COS-7 cells co-transfected with 300 ng/well *pGL3-mut-Sox2-3'UTR* or *pGL3-mut-E2F3-3'UTR* sensor, 600 ng/well *pcDNA6.2-EmGFP-miR-200c-141* OE or empty control (*pcDNA6.2-EmGFP*), and 8 ng/well *pRL-SV40* vectors. Cells were lysed in Passive Lysis Buffer 30 hrs post-transfection, and Firefly and Renilla Luciferase luminescence were measured as describe above.

For *mmu-miR-200c/141* promoter luciferase assay, 300 ng *pGL-miR-200c* promoter vector was cotransfected into HEK-293 cells with 400 ng *pcDNA3.1-E2F3* plasmid or 400 ng *pcDNA3.1-Sox2* plasmid. Cells were lysed in Passive Lysis Buffer 28 hrs post-transfection, and Firefly and Renilla Luciferase luminescence were measured as describe above.

4.2.15 Construction of target vector for generating *Aldh1a1*[+/Cre-ERT2] knock-in mice

The 5' and 3' homologous arms were cloned using C57/BL6 mouse genomic DNA as template and with the primers listed in table 4. 28 (5'armAldh1.1F and 5'armAldh1.2R for 5' homologous arm; 3'armAldh1.1F and 3'armAldh1.2R for 3' homologous arm). The PCR products from 3 independent PCR reactions were gel-electrophoresed separately, afterwards the gel slices containing the correct bands were cut out and the PCR products were purified using gel-purification kit and cloned into TOPO-TA vector. Several colonies from each of three independent PCR-cloning experiments were cultured and used for plasmid preparation. After confirming that the size of inserted DNA is correct, three plasmids from three independent cloning experiments were sequenced. Afterwards, the homologous arms without

mutations and a *Cre-ERT2* cassette were subcloned into target vector JGV NTB5. The final *Aldh1a1*$^{+/Cre-ERT2}$ target vector was fully sequenced using the primers listed below to confirm the sequence and to exclude any mutation. The 5' and 3' external probes were also amplified using primers listed in table 4. 28 and cloned into TOPO-TA vector. The sequences of two probes were confirmed whithout mutations by sequencing.

Table 4.28 primers used for construction of *Aldh1a1*$^{+/Cre-ERT2}$ target vector

Primers for cloning & sequencing	sequence
5'extprobAldh1.1F	GTAACCTATACCCTGTAATTCC
5'extprobAldh1.1R	GACCCTAAAACATGGTCATCAC
5'armAldh1.1F	GTCCTCTACACATTACCTAAATG
5'armAldh1.1R	GCACATATTTCTAGTATCTGATAC
5'armAldh1.2F	GCTTCCAGTGTCTGGAGCAGC
5'armAldh1.2R	GGCTCCTGGAACACAGGTG
3'armAldh1.1F	GTCAACTGAAGCTTATGGAAC
3'armAldh1.1R	CTACATGTCTGTTTCCTTTCAG
3'armAldh1.2F	GAAATCAAGTTGGTGTTTCAGG
3'armAldh1.2R	GGAACAGAACTTCGAAAGGTTTC
3'extprobAldh1.1F	GCACAGGGTCAATCTCCTCTC
3'extprobAldh1.1R	GTGAATTCTACGTCCCTAAGTC
5'arm-Raldh1.7F	GTCATCTTAGTCTTTCTGG
5'arm-Raldh1.8F	GAGCTCTGACACTCTCTG
5'arm-Raldh1.9F	CCAATGGAGGAGCTAGAG
5'arm-Raldh1.10F	CACTCTGTGTTATGTAACAG
5'arm-Raldh1.11F	CGATATCAAGGAAGGTCTAG
3'arm-Raldh1.7F	CTTTCCTCTTAAAGTTAGCTG
3'armAldh1a-3R	CAATCTTCAGGAAACACTGG
3'armAldh1a-4R	GGAGTGGTCACAGGCATAG
CreB	ACCCTGATCCTGGCAATTTCGGC
Cre-R1	GTTGCATCGACCGGTAATGC
Cre-3F	GCCAGGATATACGTAATCTGGC
Cre-4F	CTATATCCGTAACCTGGATAGTG
ERT2-F	CTGTCCAGCACCCTGAAGTC
Neo 13R	GGTGAGATGACAGGAGATC
Neo 14F	GCTCGACGTTGTCACTGAAGC
TK 10F	CGCGACGATATCGTCTACGT
TK 5	CGCACCGTATTGGCAAGC

4.2.16 Statistical analysis

All values shown in this work are mean±SEM. Statistical significance between groups was assessed by paired t-tests, independent-samples t-tests or one-way ANOVA followed by post-hoc S-N-K multiple comparisons using the SPSS 10.0 software (SPSS Inc., USA). A *P*-value < 0.05 was considered significant.

5 References

Adams, M.R., Sears, R., Nuckolls, F., Leone, G., and Nevins, J.R. (2000). Complex transcriptional regulatory mechanisms control expression of the E2F3 locus. Mol Cell Biol *20*, 3633-3639.

Airaksinen, M.S., and Saarma, M. (2002). The GDNF family: signalling, biological functions and therapeutic value. Nat Rev Neurosci *3*, 383-394.

Ambros, V. (2004). The functions of animal microRNAs. Nature *431*, 350-355.

Ameres, S.L., Horwich, M.D., Hung, J.H., Xu, J., Ghildiyal, M., Weng, Z., and Zamore, P.D. (2010). Target RNA-directed trimming and tailing of small silencing RNAs. Science *328*, 1534-1539.

Arnold, K., Sarkar, A., Yram, M.A., Polo, J.M., Bronson, R., Sengupta, S., Seandel, M., Geijsen, N., and Hochedlinger, K. (2011). Sox2(+) adult stem and progenitor cells are important for tissue regeneration and survival of mice. Cell Stem Cell *9*, 317-329.

Avilion, A.A., Nicolis, S.K., Pevny, L.H., Perez, L., Vivian, N., and Lovell-Badge, R. (2003). Multipotent cell lineages in early mouse development depend on SOX2 function. Genes Dev *17*, 126-140.

Baquet, Z.C., Bickford, P.C., and Jones, K.R. (2005). Brain-derived neurotrophic factor is required for the establishment of the proper number of dopaminergic neurons in the substantia nigra pars compacta. J Neurosci *25*, 6251-6259.

Barroso-Chinea, P., Cruz-Muros, I., Aymerich, M.S., Rodriguez-Diaz, M., Afonso-Oramas, D., Lanciego, J.L., and Gonzalez-Hernandez, T. (2005). Striatal expression of GDNF and differential vulnerability of midbrain dopaminergic cells. Eur J Neurosci *21*, 1815-1827.

Bartel, D.P. (2004). MicroRNAs: genomics, biogenesis, mechanism, and function. Cell *116*, 281-297.

Beck, K.D., Irwin, I., Valverde, J., Brennan, T.J., Langston, J.W., and Hefti, F. (1996). GDNF induces a dystonia-like state in neonatal rats and stimulates dopamine and serotonin synthesis. Neuron *16*, 665-673.

Berezikov, E., Chung, W.J., Willis, J., Cuppen, E., and Lai, E.C. (2007). Mammalian mirtron genes. Mol Cell *28*, 328-336.

Bergman, O., Hakansson, A., Westberg, L., Nordenstrom, K., Carmine Belin, A., Sydow, O., Olson, L., Holmberg, B., Eriksson, E., and Nissbrandt, H. (2010). PITX3 polymorphism is associated with early onset Parkinson's disease. Neurobiol Aging *31*, 114-117.

Bibel, M., Richter, J., Lacroix, E., and Barde, Y.A. (2007a). Generation of a defined and uniform population of CNS progenitors and neurons from mouse embryonic stem cells. Nat Protoc *2*, 1034-1043.

Bibel, M., Richter, J., Lacroix, E., and Barde, Y.A. (2007b). Generation of a defined and uniform population of CNS progenitors and neurons from mouse embryonic stem cells. Nat Protoc *2*, 1034-1043.

Bjorklund, A., and Dunnett, S.B. (2007). Dopamine neuron systems in the brain: an update. Trends Neurosci *30*, 194-202.

Black, E.P., Hallstrom, T., Dressman, H.K., West, M., and Nevins, J.R. (2005). Distinctions in the specificity of E2F function revealed by gene expression signatures. Proc Natl Acad Sci U S A *102*, 15948-15953.

Blum, M. (1998). A null mutation in TGF-alpha leads to a reduction in midbrain dopaminergic neurons in the substantia nigra. Nat Neurosci *1*, 374-377.

Borchert, G.M., Lanier, W., and Davidson, B.L. (2006). RNA polymerase III transcribes human microRNAs. Nat Struct Mol Biol *13*, 1097-1101.

Bremer, J., O'Connor, T., Tiberi, C., Rehrauer, H., Weis, J., and Aguzzi, A. (2010). Ablation of Dicer from murine Schwann cells increases their proliferation while blocking myelination. PLoS One *5*, e12450.

Brennecke, J., Stark, A., Russell, R.B., and Cohen, S.M. (2005). Principles of microRNA-target recognition. PLoS Biol *3*, e85.

Brodersen, P., and Voinnet, O. (2009). Revisiting the principles of microRNA target recognition and mode of action. Nat Rev Mol Cell Biol *10*, 141-148.

Brodski, C., Weisenhorn, D.M., Signore, M., Sillaber, I., Oesterheld, M., Broccoli, V., Acampora, D., Simeone, A., and Wurst, W. (2003). Location and size of dopaminergic and serotonergic cell populations are controlled by the position of the midbrain-hindbrain organizer. J Neurosci *23*, 4199-4207.

Cai, J., Wu, Y., Mirua, T., Pierce, J.L., Lucero, M.T., Albertine, K.H., Spangrude, G.J., and Rao, M.S. (2002). Properties of a fetal multipotent neural stem cell (NEP cell). Dev Biol *251*, 221-240.

Cao, J.P., Wang, H.J., Yu, J.K., Liu, H.M., and Gao, D.S. (2008). The involvement of NF-kappaB p65/p52 in the effects of GDNF on DA neurons in early PD rats. Brain Res Bull *76*, 505-511.

Chauhan, N.B., Siegel, G.J., and Lee, J.M. (2001). Depletion of glial cell line-derived neurotrophic factor in substantia nigra neurons of Parkinson's disease brain. J Chem Neuroanat *21*, 277-288.

Chen, C., Ridzon, D.A., Broomer, A.J., Zhou, Z., Lee, D.H., Nguyen, J.T., Barbisin, M., Xu, N.L., Mahuvakar, V.R., Andersen, M.R.*, et al.* (2005). Real-time quantification of microRNAs by stem-loop RT-PCR. Nucleic Acids Res *33*, e179.

Chen, H.Z., Tsai, S.Y., and Leone, G. (2009). Emerging roles of E2Fs in cancer: an exit from cell cycle control. Nat Rev Cancer *9*, 785-797.

Chen, Y., Shi, L., Zhang, L., Li, R., Liang, J., Yu, W., Sun, L., Yang, X., Wang, Y., Zhang, Y.*, et al.* (2008). The molecular mechanism governing the oncogenic potential of SOX2 in breast cancer. J Biol Chem *283*, 17969-17978.

Chi, C.L., Martinez, S., Wurst, W., and Martin, G.R. (2003). The isthmic organizer signal FGF8 is required for cell survival in the prospective midbrain and cerebellum. Development *130*, 2633-2644.

Choi-Lundberg, D.L., and Bohn, M.C. (1995). Ontogeny and distribution of glial cell line-derived neurotrophic factor (GDNF) mRNA in rat. Brain Res Dev Brain Res *85*, 80-88.

Choi, P.S., Zakhary, L., Choi, W.Y., Caron, S., Alvarez-Saavedra, E., Miska, E.A., McManus, M., Harfe, B., Giraldez, A.J., Horvitz, H.R.*, et al.* (2008). Members of the miRNA-200 family regulate olfactory neurogenesis. Neuron *57*, 41-55.

Chun, H.S., Yoo, M.S., DeGiorgio, L.A., Volpe, B.T., Peng, D., Baker, H., Peng, C., and Son, J.H. (2002). Marked dopaminergic cell loss subsequent to developmental, intranigral expression of glial cell line-derived neurotrophic factor. Exp Neurol *173*, 235-244.

Chung, S., Hedlund, E., Hwang, M., Kim, D.W., Shin, B.S., Hwang, D.Y., Jung Kang, U., Isacson, O., and Kim, K.S. (2005). The homeodomain transcription factor Pitx3 facilitates differentiation of mouse embryonic stem cells into AHD2-expressing dopaminergic neurons. Mol Cell Neurosci *28*, 241-252.

Chung, S., Leung, A., Han, B.S., Chang, M.Y., Moon, J.I., Kim, C.H., Hong, S., Pruszak, J., Isacson, O., and Kim, K.S. (2009). Wnt1-lmx1a forms a novel autoregulatory loop and controls midbrain dopaminergic differentiation synergistically with the SHH-FoxA2 pathway. Cell Stem Cell *5*, 646-658.

Cloud, J.E., Rogers, C., Reza, T.L., Ziebold, U., Stone, J.R., Picard, M.H., Caron, A.M., Bronson, R.T., and Lees, J.A. (2002). Mutant mouse models reveal the relative roles of E2F1 and E2F3 in vivo. Mol Cell Biol 22, 2663-2672.

Cobb, B.S., Nesterova, T.B., Thompson, E., Hertweck, A., O'Connor, E., Godwin, J., Wilson, C.B., Brockdorff, N., Fisher, A.G., Smale, S.T.*, et al.* (2005). T cell lineage choice and differentiation in the absence of the RNase III enzyme Dicer. J Exp Med *201*, 1367-1373.

Conaco, C., Otto, S., Han, J.J., and Mandel, G. (2006). Reciprocal actions of REST and a microRNA promote neuronal identity. Proc Natl Acad Sci U S A *103*, 2422-2427.

Coolen, M., and Bally-Cuif, L. (2009). MicroRNAs in brain development and physiology. Curr Opin Neurobiol *19*, 461-470.

Dauer, W., and Przedborski, S. (2003). Parkinson's disease: mechanisms and models. Neuron *39*, 889-909.

Davis, T.H., Cuellar, T.L., Koch, S.M., Barker, A.J., Harfe, B.D., McManus, M.T., and Ullian, E.M. (2008). Conditional loss of Dicer disrupts cellular and tissue morphogenesis in the cortex and hippocampus. J Neurosci *28*, 4322-4330.

De Pietri Tonelli, D., Pulvers, J.N., Haffner, C., Murchison, E.P., Hannon, G.J., and Huttner, W.B. (2008). miRNAs are essential for survival and differentiation of newborn neurons but not for expansion of neural progenitors during early neurogenesis in the mouse embryonic neocortex. Development *135*, 3911-3921.

DeGregori, J. (2002). The genetics of the E2F family of transcription factors: shared functions and unique roles. Biochim Biophys Acta *1602*, 131-150.

Deng, Q., Andersson, E., Hedlund, E., Alekseenko, Z., Coppola, E., Panman, L., Millonig, J.H., Brunet, J.F., Ericson, J., and Perlmann, T. (2011). Specific and integrated roles of Lmx1a, Lmx1b and Phox2a in ventral midbrain development. Development *138*, 3399-3408.

Dyson, N. (1998). The regulation of E2F by pRB-family proteins. Genes Dev *12*, 2245-2262.

Ebelt, H., Hufnagel, N., Neuhaus, P., Neuhaus, H., Gajawada, P., Simm, A., Muller-Werdan, U., Werdan, K., and Braun, T. (2005). Divergent siblings: E2F2 and E2F4 but not E2F1 and E2F3 induce DNA synthesis in cardiomyocytes without activation of apoptosis. Circ Res 96, 509-517.

Ebert, M.S., Neilson, J.R., and Sharp, P.A. (2007). MicroRNA sponges: competitive inhibitors of small RNAs in mammalian cells. Nat Methods 4, 721-726.

Epstein, D.J., McMahon, A.P., and Joyner, A.L. (1999). Regionalization of Sonic hedgehog transcription along the anteroposterior axis of the mouse central nervous system is regulated by Hnf3-dependent and -independent mechanisms. Development 126, 281-292.

Farkas, L.M., Dunker, N., Roussa, E., Unsicker, K., and Krieglstein, K. (2003). Transforming growth factor-beta(s) are essential for the development of midbrain dopaminergic neurons in vitro and in vivo. J Neurosci 23, 5178-5186.

Feldman, B., Poueymirou, W., Papaioannou, V.E., DeChiara, T.M., and Goldfarb, M. (1995). Requirement of FGF-4 for postimplantation mouse development. Science 267, 246-249.

Fischer, T., Faus-Kessler, T., Welzl, G., Simeone, A., Wurst, W., and Prakash, N. (2011). Fgf15-mediated control of neurogenic and proneural gene expression regulates dorsal midbrain neurogenesis. Dev Biol 350, 496-510.

Fuchs, J., Mueller, J.C., Lichtner, P., Schulte, C., Munz, M., Berg, D., Wullner, U., Illig, T., Sharma, M., and Gasser, T. (2009). The transcription factor PITX3 is associated with sporadic Parkinson's disease. Neurobiol Aging 30, 731-738.

Gage, F.H. (2000). Mammalian neural stem cells. Science 287, 1433-1438.

Golden, J.P., DeMaro, J.A., Osborne, P.A., Milbrandt, J., and Johnson, E.M., Jr. (1999). Expression of neurturin, GDNF, and GDNF family-receptor mRNA in the developing and mature mouse. Exp Neurol 158, 504-528.

Goodwin, G.H., and Johns, E.W. (1973). Isolation and characterisation of two calf-thymus chromatin non-histone proteins with high contents of acidic and basic amino acids. Eur J Biochem 40, 215-219.

Goodwin, G.H., Sanders, C., and Johns, E.W. (1973). A new group of chromatin-associated proteins with a high content of acidic and basic amino acids. Eur J Biochem 38, 14-19.

Graham, V., Khudyakov, J., Ellis, P., and Pevny, L. (2003). SOX2 functions to maintain neural progenitor identity. Neuron 39, 749-765.

Grimm, D., Streetz, K.L., Jopling, C.L., Storm, T.A., Pandey, K., Davis, C.R., Marion, P., Salazar, F., and Kay, M.A. (2006). Fatality in mice due to oversaturation of cellular microRNA/short hairpin RNA pathways. Nature 441, 537-541.

Guillemot, F., and Zimmer, C. From cradle to grave: the multiple roles of fibroblast growth factors in neural development. Neuron 71, 574-588.

Guo, C., Qiu, H.Y., Huang, Y., Chen, H., Yang, R.Q., Chen, S.D., Johnson, R.L., Chen, Z.F., and Ding, Y.Q. (2007). Lmx1b is essential for Fgf8 and Wnt1 expression in the isthmic organizer during tectum and cerebellum development in mice. Development 134, 317-325.

Harley, V.R., Lovell-Badge, R., and Goodfellow, P.N. (1994). Definition of a consensus DNA binding site for SRY. Nucleic Acids Res 22, 1500-1501.

Haubenberger, D., Reinthaler, E., Mueller, J.C., Pirker, W., Katzenschlager, R., Froehlich, R., Bruecke, T., Daniel, G., Auff, E., and Zimprich, A. (2009). Association of transcription factor polymorphisms PITX3 and EN1 with Parkinson's disease. Neurobiol Aging 32, 302-307.

He, L., Yang, H., Ma, Y., Pledger, W.J., Cress, W.D., and Cheng, J.Q. (2008). Identification of Aurora-A as a direct target of E2F3 during G2/M cell cycle progression. J Biol Chem 283, 31012-31020.

Hellmich, H.L., Kos, L., Cho, E.S., Mahon, K.A., and Zimmer, A. (1996). Embryonic expression of glial cell-line derived neurotrophic factor (GDNF) suggests multiple developmental roles in neural differentiation and epithelial-mesenchymal interactions. Mech Dev 54, 95-105.

Hirata, H., Tomita, K., Bessho, Y., and Kageyama, R. (2001). Hes1 and Hes3 regulate maintenance of the isthmic organizer and development of the mid/hindbrain. EMBO J 20, 4454-4466.

Howells, D.W., Porritt, M.J., Wong, J.Y., Batchelor, P.E., Kalnins, R., Hughes, A.J., and Donnan, G.A. (2000). Reduced BDNF mRNA expression in the Parkinson's disease substantia nigra. Exp Neurol 166, 127-135.

Huang, T., Liu, Y., Huang, M., Zhao, X., and Cheng, L. (2010). Wnt1-cre-mediated conditional loss of Dicer results in malformation of the midbrain and cerebellum and failure of neural crest and dopaminergic differentiation in mice. J Mol Cell Biol *2*, 152-163.

Humbert, P.O., Verona, R., Trimarchi, J.M., Rogers, C., Dandapani, S., and Lees, J.A. (2000). E2f3 is critical for normal cellular proliferation. Genes Dev *14*, 690-703.

Hwang, D.Y., Ardayfio, P., Kang, U.J., Semina, E.V., and Kim, K.S. (2003). Selective loss of dopaminergic neurons in the substantia nigra of Pitx3-deficient aphakia mice. Brain Res Mol Brain Res *114*, 123-131.

Ishida, S., Huang, E., Zuzan, H., Spang, R., Leone, G., West, M., and Nevins, J.R. (2001). Role for E2F in control of both DNA replication and mitotic functions as revealed from DNA microarray analysis. Mol Cell Biol *21*, 4684-4699.

Jacobs, F.M., Smits, S.M., Noorlander, C.W., von Oerthel, L., van der Linden, A.J., Burbach, J.P., and Smidt, M.P. (2007). Retinoic acid counteracts developmental defects in the substantia nigra caused by Pitx3 deficiency. Development *134*, 2673-2684.

Jacobs, F.M., van Erp, S., van der Linden, A.J., von Oerthel, L., Burbach, J.P., and Smidt, M.P. (2009). Pitx3 potentiates Nurr1 in dopamine neuron terminal differentiation through release of SMRT-mediated repression. Development *136*, 531-540.

Jing, S., Wen, D., Yu, Y., Holst, P.L., Luo, Y., Fang, M., Tamir, R., Antonio, L., Hu, Z., Cupples, R., et al. (1996). GDNF-induced activation of the ret protein tyrosine kinase is mediated by GDNFR-alpha, a novel receptor for GDNF. Cell 85, 1113-1124.

Johnson, D.G., Ohtani, K., and Nevins, J.R. (1994). Autoregulatory control of E2F1 expression in response to positive and negative regulators of cell cycle progression. Genes Dev *8*, 1514-1525.

Katsuki, H., Kurimoto, E., Takemori, S., Kurauchi, Y., Hisatsune, A., Isohama, Y., Izumi, Y., Kume, T., Shudo, K., and Akaike, A. (2009). Retinoic acid receptor stimulation protects midbrain dopaminergic neurons from inflammatory degeneration via BDNF-mediated signaling. J Neurochem *110*, 707-718.

Kholodilov, N., Yarygina, O., Oo, T.F., Zhang, H., Sulzer, D., Dauer, W., and Burke, R.E. (2004). Regulation of the development of mesencephalic dopaminergic systems by the selective expression of glial cell line-derived neurotrophic factor in their targets. J Neurosci *24*, 3136-3146.

Kim, J., Inoue, K., Ishii, J., Vanti, W.B., Voronov, S.V., Murchison, E., Hannon, G., and Abeliovich, A. (2007). A MicroRNA feedback circuit in midbrain dopamine neurons. Science *317*, 1220-1224.

Kimmel, R.A., Turnbull, D.H., Blanquet, V., Wurst, W., Loomis, C.A., and Joyner, A.L. (2000). Two lineage boundaries coordinate vertebrate apical ectodermal ridge formation. Genes Dev *14*, 1377-1389.

Knusel, B., Winslow, J.W., Rosenthal, A., Burton, L.E., Seid, D.P., Nikolics, K., and Hefti, F. (1991). Promotion of central cholinergic and dopaminergic neuron differentiation by brain-derived neurotrophic factor but not neurotrophin 3. Proc Natl Acad Sci U S A *88*, 961-965.

Kokaia, Z., Airaksinen, M.S., Nanobashvili, A., Larsson, E., Kujamaki, E., Lindvall, O., and Saarma, M. (1999). GDNF family ligands and receptors are differentially regulated after brain insults in the rat. Eur J Neurosci *11*, 1202-1216.

Konstantoulas, C.J., Parmar, M., and Li, M. (2010). FoxP1 promotes midbrain identity in embryonic stem cell-derived dopamine neurons by regulating Pitx3. J Neurochem *113*, 836-847.

Kozomara, A., and Griffiths-Jones, S. (2011). miRBase: integrating microRNA annotation and deep-sequencing data. Nucleic Acids Res *39*, D152-157.

Kovesdi, I., Reichel, R., and Nevins, J.R. (1986). Identification of a cellular transcription factor involved in E1A trans-activation. Cell *45*, 219-228.

Kramer, E.R., Aron, L., Ramakers, G.M., Seitz, S., Zhuang, X., Beyer, K., Smidt, M.P., and Klein, R. (2007). Absence of Ret signaling in mice causes progressive and late degeneration of the nigrostriatal system. PLoS Biol *5*, e39.

Krichevsky, A.M., Sonntag, K.C., Isacson, O., and Kosik, K.S. (2006). Specific microRNAs modulate embryonic stem cell-derived neurogenesis. Stem Cells *24*, 857-864.

Lagos-Quintana, M., Rauhut, R., Yalcin, A., Meyer, J., Lendeckel, W., and Tuschl, T. (2002). Identification of tissue-specific microRNAs from mouse. Curr Biol *12*, 735-739.

Lau, P., Verrier, J.D., Nielsen, J.A., Johnson, K.R., Notterpek, L., and Hudson, L.D. (2008). Identification of dynamically regulated microRNA and mRNA networks in developing oligodendrocytes. J Neurosci *28*, 11720-11730.

Le, W., Nguyen, D., Lin, X.W., Rawal, P., Huang, M., Ding, Y., Xie, W., Deng, H., and Jankovic, J. (2009). Transcription factor PITX3 gene in Parkinson's disease. Neurobiol Aging *32*, 750-753.

Lebel, M., Gauthier, Y., Moreau, A., and Drouin, J. (2001). Pitx3 activates mouse tyrosine hydroxylase promoter via a high-affinity binding site. J Neurochem *77*, 558-567.

Lees, J.A., Saito, M., Vidal, M., Valentine, M., Look, T., Harlow, E., Dyson, N., and Helin, K. (1993). The retinoblastoma protein binds to a family of E2F transcription factors. Mol Cell Biol *13*, 7813-7825.

Leone, G., DeGregori, J., Yan, Z., Jakoi, L., Ishida, S., Williams, R.S., and Nevins, J.R. (1998). E2F3 activity is regulated during the cell cycle and is required for the induction of S phase. Genes Dev *12*, 2120-2130.

Leone, G., Nuckolls, F., Ishida, S., Adams, M., Sears, R., Jakoi, L., Miron, A., and Nevins, J.R. (2000). Identification of a novel E2F3 product suggests a mechanism for determining specificity of repression by Rb proteins. Mol Cell Biol *20*, 3626-3632.

Leucht, C., Stigloher, C., Wizenmann, A., Klafke, R., Folchert, A., and Bally-Cuif, L. (2008). MicroRNA-9 directs late organizer activity of the midbrain-hindbrain boundary. Nat Neurosci *11*, 641-648.

Li, Q., Bian, S., Hong, J., Kawase-Koga, Y., Zhu, E., Zheng, Y., Yang, L., and Sun, T. (2011). Timing Specific Requirement of microRNA Function is Essential for Embryonic and Postnatal Hippocampal Development. PLoS One *6*, e26000.

Li, R., Li, Y., Kristiansen, K., and Wang, J. (2008). SOAP: short oligonucleotide alignment program. Bioinformatics 24, 713-714.

Lim, L.P., Lau, N.C., Garrett-Engele, P., Grimson, A., Schelter, J.M., Castle, J., Bartel, D.P., Linsley, P.S., and Johnson, J.M. (2005). Microarray analysis shows that some microRNAs downregulate large numbers of target mRNAs. Nature *433*, 769-773.

Lin, L.F., Doherty, D.H., Lile, J.D., Bektesh, S., and Collins, F. (1993). GDNF: a glial cell line-derived neurotrophic factor for midbrain dopaminergic neurons. Science *260*, 1130-1132.

Lin, Y.Z., Yao, S.Y., Veach, R.A., Torgerson, T.R., and Hawiger, J. (1995). Inhibition of nuclear translocation of transcription factor NF-kappa B by a synthetic peptide containing a cell membrane-permeable motif and nuclear localization sequence. J Biol Chem *270*, 14255-14258.

Liu, C., and Zhao, X. (2009). MicroRNAs in adult and embryonic neurogenesis. Neuromolecular Med *11*, 141-152.

Liu, J., Sato, C., Cerletti, M., and Wagers, A. Notch signaling in the regulation of stem cell self-renewal and differentiation. Curr Top Dev Biol *92*, 367-409.

Liu, N., Okamura, K., Tyler, D.M., Phillips, M.D., Chung, W.J., and Lai, E.C. (2008). The evolution and functional diversification of animal microRNA genes. Cell Res *18*, 985-996.

Livak, K.J., and Schmittgen, T.D. (2001). Analysis of relative gene expression data using real-time quantitative PCR and the 2(-Delta Delta C(T)) Method. Methods *25*, 402-408.

Loya, C.M., Lu, C.S., Van Vactor, D., and Fulga, T.A. (2009). Transgenic microRNA inhibition with spatiotemporal specificity in intact organisms. Nat Methods *6*, 897-903.

Lu, Y., Thomson, J.M., Wong, H.Y., Hammond, S.M., and Hogan, B.L. (2007). Transgenic over-expression of the microRNA miR-17-92 cluster promotes proliferation and inhibits differentiation of lung epithelial progenitor cells. Dev Biol *310*, 442-453.

Lund, E., Guttinger, S., Calado, A., Dahlberg, J.E., and Kutay, U. (2004). Nuclear export of microRNA precursors. Science *303*, 95-98.

Luo, D., Renault, V.M., and Rando, T.A. (2005). The regulation of Notch signaling in muscle stem cell activation and postnatal myogenesis. Semin Cell Dev Biol *16*, 612-622.

Lytle, J.R., Yario, T.A., and Steitz, J.A. (2007). Target mRNAs are repressed as efficiently by microRNA-binding sites in the 5' UTR as in the 3' UTR. Proc Natl Acad Sci U S A *104*, 9667-9672.

Maden, M. (2007). Retinoic acid in the development, regeneration and maintenance of the nervous system. Nat Rev Neurosci 8, 755-765.

Martinez, N.J., and Gregory, R.I. (2010). MicroRNA gene regulatory pathways in the establishment and maintenance of ESC identity. Cell Stem Cell *7*, 31-35.

Martinez, S., Crossley, P.H., Cobos, I., Rubenstein, J.L., and Martin, G.R. (1999). FGF8 induces formation of an ectopic isthmic organizer and isthmocerebellar development via a repressive effect on Otx2 expression. Development *126*, 1189-1200.

Masui, S., Nakatake, Y., Toyooka, Y., Shimosato, D., Yagi, R., Takahashi, K., Okochi, H., Okuda, A., Matoba, R., Sharov, A.A., *et al.* (2007). Pluripotency governed by Sox2 via regulation of Oct3/4 expression in mouse embryonic stem cells. Nat Cell Biol *9*, 625-635.

Maxwell, S.L., Ho, H.Y., Kuehner, E., Zhao, S., and Li, M. (2005). Pitx3 regulates tyrosine hydroxylase expression in the substantia nigra and identifies a subgroup of mesencephalic dopaminergic progenitor neurons during mouse development. Dev Biol *282*, 467-479.

McMahon, A.P., and Bradley, A. (1990). The Wnt-1 (int-1) proto-oncogene is required for development of a large region of the mouse brain. Cell *62*, 1073-1085.

Mertin, S., McDowall, S.G., and Harley, V.R. (1999). The DNA-binding specificity of SOX9 and other SOX proteins. Nucleic Acids Res *27*, 1359-1364.

Metzker, M.L. (2010). Sequencing technologies - the next generation. Nat Rev Genet *11*, 31-46.

Meyer, M., Zimmer, J., Seiler, R.W., and Widmer, H.R. (1999). GDNF increases the density of cells containing calbindin but not of cells containing calretinin in cultured rat and human fetal nigral tissue. Cell Transplant *8*, 25-36.

Mijatovic, J., Airavaara, M., Planken, A., Auvinen, P., Raasmaja, A., Piepponen, T.P., Costantini, F., Ahtee, L., and Saarma, M. (2007). Constitutive Ret activity in knock-in multiple endocrine neoplasia type B mice induces profound elevation of brain dopamine concentration via enhanced synthesis and increases the number of TH-positive cells in the substantia nigra. J Neurosci *27*, 4799-4809.

Millar, A. A., and Waterhouse, P. M. (2005). Plant and animal microRNAs: similarities and differences. Funct Integr Genomics *5*, 129-135.

Miyazaki, H., Okuma, Y., Nomura, J., Nagashima, K., and Nomura, Y. (2003). Age-related alterations in the expression of glial cell line-derived neurotrophic factor in the senescence-accelerated mouse brain. J Pharmacol Sci *92*, 28-34.

Mogi, M., Togari, A., Kondo, T., Mizuno, Y., Komure, O., Kuno, S., Ichinose, H., and Nagatsu, T. (1999). Brain-derived growth factor and nerve growth factor concentrations are decreased in the substantia nigra in Parkinson's disease. Neurosci Lett *270*, 45-48.

Morozova, O., and Marra, M.A. (2008). Applications of next-generation sequencing technologies in functional genomics. Genomics *92*, 255-264.

Mukherji, S., Ebert, M.S., Zheng, G.X., Tsang, J.S., Sharp, P.A., and van Oudenaarden, A. (2011). MicroRNAs can generate thresholds in target gene expression. Nat Genet *43*, 854-859.

Muller, H., Bracken, A.P., Vernell, R., Moroni, M.C., Christians, F., Grassilli, E., Prosperini, E., Vigo, E., Oliner, J.D., and Helin, K. (2001). E2Fs regulate the expression of genes involved in differentiation, development, proliferation, and apoptosis. Genes Dev *15*, 267-285.

Nakamura, T., Colbert, M.C., and Robbins, J. (2006). Neural crest cells retain multipotential characteristics in the developing valves and label the cardiac conduction system. Circ Res *98*, 1547-1554.

Nishimoto, M., Fukushima, A., Okuda, A., and Muramatsu, M. (1999). The gene for the embryonic stem cell coactivator UTF1 carries a regulatory element which selectively interacts with a complex composed of Oct-3/4 and Sox-2. Mol Cell Biol *19*, 5453-5465.

Nornes, H.O., Dressler, G.R., Knapik, E.W., Deutsch, U., and Gruss, P. (1990). Spatially and temporally restricted expression of Pax2 during murine neurogenesis. Development *109*, 797-809.

Nunes, I., Tovmasian, L.T., Silva, R.M., Burke, R.E., and Goff, S.P. (2003). Pitx3 is required for development of substantia nigra dopaminergic neurons. Proc Natl Acad Sci U S A *100*, 4245-4250.

Oo, T.F., Kholodilov, N., and Burke, R.E. (2003). Regulation of natural cell death in dopaminergic neurons of the substantia nigra by striatal glial cell line-derived neurotrophic factor in vivo. J Neurosci *23*, 5141-5148.

Oo, T.F., Marchionini, D.M., Yarygina, O., O'Leary, P.D., Hughes, R.A., Kholodilov, N., and Burke, R.E. (2009). Brain-derived neurotrophic factor regulates early postnatal developmental cell death of dopamine neurons of the substantia nigra in vivo. Mol Cell Neurosci *41*, 440-447.

Oo, T.F., Ries, V., Cho, J., Kholodilov, N., and Burke, R.E. (2005). Anatomical basis of glial cell line-derived neurotrophic factor expression in the striatum and related basal ganglia during postnatal development of the rat. J Comp Neurol *484*, 57-67.

Packer, A.N., Xing, Y., Harper, S.Q., Jones, L., and Davidson, B.L. (2008). The bifunctional microRNA miR-9/miR-9* regulates REST and CoREST and is downregulated in Huntington's disease. J Neurosci *28*, 14341-14346.

Parain, K., Murer, M.G., Yan, Q., Faucheux, B., Agid, Y., Hirsch, E., and Raisman-Vozari, R. (1999). Reduced expression of brain-derived neurotrophic factor protein in Parkinson's disease substantia nigra. Neuroreport *10*, 557-561.

Paratcha, G., and Ledda, F. (2008). GDNF and GFRalpha: a versatile molecular complex for developing neurons. Trends Neurosci *31*, 384-391.

Paratcha, G., Ledda, F., and Ibanez, C.F. (2003). The neural cell adhesion molecule NCAM is an alternative signaling receptor for GDNF family ligands. Cell *113*, 867-879.

Parsian, A., Sinha, R., Racette, B., Zhao, J.H., and Perlmutter, J.S. (2004). Association of a variation in the promoter region of the brain-derived neurotrophic factor gene with familial Parkinson's disease. Parkinsonism Relat Disord *10*, 213-219.

Pascual, A., Hidalgo-Figueroa, M., Piruat, J.I., Pintado, C.O., Gomez-Diaz, R., and Lopez-Barneo, J. (2008). Absolute requirement of GDNF for adult catecholaminergic neuron survival. Nat Neurosci *11*, 755-761.

Peng, C., Fan, S., Li, X., Fan, X., Ming, M., Sun, Z., and Le, W. (2007). Overexpression of pitx3 upregulates expression of BDNF and GDNF in SH-SY5Y cells and primary ventral mesencephalic cultures. FEBS Lett *581*, 1357-1361.

Pereira, J. A., Baumann, R., Norrmen, C., Somandin, C., Miehe, M., Jacob, C., Luhmann, T., Hall-Bozic, H., Mantei, N., Meijer, D., and Suter, U. (2010). Dicer in Schwann cells is required for myelination and axonal integrity. J Neurosci 30, 6763-6775.

Peter, M.E. (2009). Let-7 and miR-200 microRNAs: guardians against pluripotency and cancer progression. Cell Cycle *8*, 843-852.

Pettitt, S.J., Liang, Q., Rairdan, X.Y., Moran, J.L., Prosser, H.M., Beier, D.R., Lloyd, K.C., Bradley, A., and Skarnes, W.C. (2009). Agouti C57BL/6N embryonic stem cells for mouse genetic resources. Nat Methods *6*, 493-495.

Pevny, L.H., and Nicolis, S.K. (2010). Sox2 roles in neural stem cells. Int J Biochem Cell Biol *42*, 421-424.

Polager, S., Kalma, Y., Berkovich, E., and Ginsberg, D. (2002). E2Fs up-regulate expression of genes involved in DNA replication, DNA repair and mitosis. Oncogene *21*, 437-446.

Porritt, M.J., Batchelor, P.E., and Howells, D.W. (2005). Inhibiting BDNF expression by antisense oligonucleotide infusion causes loss of nigral dopaminergic neurons. Exp Neurol *192*, 226-234.

Poteryaev, D., Titievsky, A., Sun, Y.F., Thomas-Crusells, J., Lindahl, M., Billaud, M., Arumae, U., and Saarma, M. (1999). GDNF triggers a novel ret-independent Src kinase family-coupled signaling via a GPI-linked GDNF receptor alpha1. FEBS Lett *463*, 63-66.

Poulsen, K.T., Armanini, M.P., Klein, R.D., Hynes, M.A., Phillips, H.S., and Rosenthal, A. (1994). TGF beta 2 and TGF beta 3 are potent survival factors for midbrain dopaminergic neurons. Neuron *13*, 1245-1252.

Prakash, N., Brodski, C., Naserke, T., Puelles, E., Gogoi, R., Hall, A., Panhuysen, M., Echevarria, D., Sussel, L., Weisenhorn, D.M.*, et al.* (2006). A Wnt1-regulated genetic network controls the identity and fate of midbrain-dopaminergic progenitors in vivo. Development *133*, 89-98.

Prakash, N., and Wurst, W. (2006). Development of dopaminergic neurons in the mammalian brain. Cell Mol Life Sci *63*, 187-206.

Puelles, E., Acampora, D., Lacroix, E., Signore, M., Annino, A., Tuorto, F., Filosa, S., Corte, G., Wurst, W., Ang, S.L.*, et al.* (2003). Otx dose-dependent integrated control of antero-posterior and dorso-ventral patterning of midbrain. Nat Neurosci *6*, 453-460.

Rieger, D.K., Reichenberger, E., McLean, W., Sidow, A., and Olsen, B.R. (2001). A double-deletion mutation in the Pitx3 gene causes arrested lens development in aphakia mice. Genomics *72*, 61-72.

Roussa, E., Wiehle, M., Dunker, N., Becker-Katins, S., Oehlke, O., and Krieglstein, K. (2006). Transforming growth factor beta is required for differentiation of mouse mesencephalic progenitors into dopaminergic neurons in vitro and in vivo: ectopic induction in dorsal mesencephalon. Stem Cells *24*, 2120-2129.

Ruby, J.G., Jan, C.H., and Bartel, D.P. (2007). Intronic microRNA precursors that bypass Drosha processing. Nature *448*, 83-86.

Saito, K., Ishizuka, A., Siomi, H., and Siomi, M.C. (2005). Processing of pre-microRNAs by the Dicer-1-Loquacious complex in Drosophila cells. PLoS Biol *3*, e235.

Sandberg, M., Kallstrom, M., and Muhr, J. (2005). Sox21 promotes the progression of vertebrate neurogenesis. Nat Neurosci *8*, 995-1001.

Sass, S., Dietmann, S., Burk, U.C., Brabletz, S., Lutter, D., Kowarsch, A., Mayer, K.F., Brabletz, T., Ruepp, A., Theis, F.J., *et al.* (2011). MicroRNAs coordinately regulate protein complexes. BMC Syst Biol *5*, 136.

Schepers, G.E., Teasdale, R.D., and Koopman, P. (2002). Twenty pairs of sox: extent, homology, and nomenclature of the mouse and human sox transcription factor gene families. Dev Cell *3*, 167-170.

Schwarz, M., Alvarez-Bolado, G., Urbanek, P., Busslinger, M., and Gruss, P. (1997). Conserved biological function between Pax-2 and Pax-5 in midbrain and cerebellum development: evidence from targeted mutations. Proc Natl Acad Sci U S A *94*, 14518-14523.

Semina, E.V., Murray, J.C., Reiter, R., Hrstka, R.F., and Graw, J. (2000). Deletion in the promoter region and altered expression of Pitx3 homeobox gene in aphakia mice. Hum Mol Genet *9*, 1575-1585.

Semina, E.V., Reiter, R.S., and Murray, J.C. (1997). Isolation of a new homeobox gene belonging to the Pitx/Rieg family: expression during lens development and mapping to the aphakia region on mouse chromosome 19. Hum Mol Genet *6*, 2109-2116.

Seroogy, K.B., Lundgren, K.H., Tran, T.M., Guthrie, K.M., Isackson, P.J., and Gall, C.M. (1994). Dopaminergic neurons in rat ventral midbrain express brain-derived neurotrophic factor and neurotrophin-3 mRNAs. J Comp Neurol *342*, 321-334.

Shan, Z., Lin, Q., Deng, C., Li, X., Huang, W., Tan, H., Fu, Y., Yang, M., and Yu, X.Y. (2009). An efficient method to enhance gene silencing by using precursor microRNA designed small hairpin RNAs. Mol Biol Rep *36*, 1483-1489.

Simon, H.H., Saueressig, H., Wurst, W., Goulding, M.D., and O'Leary, D.D. (2001). Fate of midbrain dopaminergic neurons controlled by the engrailed genes. J Neurosci *21*, 3126-3134.

Smidt, M.P., Asbreuk, C.H., Cox, J.J., Chen, H., Johnson, R.L., and Burbach, J.P. (2000). A second independent pathway for development of mesencephalic dopaminergic neurons requires Lmx1b. Nat Neurosci *3*, 337-341.

Smidt, M.P., and Burbach, J.P. (2007). How to make a mesodiencephalic dopaminergic neuron. Nat Rev Neurosci *8*, 21-32.

Smidt, M.P., Smits, S.M., Bouwmeester, H., Hamers, F.P., van der Linden, A.J., Hellemons, A.J., Graw, J., and Burbach, J.P. (2004). Early developmental failure of substantia nigra dopamine neurons in mice lacking the homeodomain gene Pitx3. Development *131*, 1145-1155.

Smidt, M.P., van Schaick, H.S., Lanctot, C., Tremblay, J.J., Cox, J.J., van der Kleij, A.A., Wolterink, G., Drouin, J., and Burbach, J.P. (1997). A homeodomain gene Ptx3 has highly restricted brain expression in mesencephalic dopaminergic neurons. Proc Natl Acad Sci U S A *94*, 13305-13310.

Smits, S.M., Burbach, J.P., and Smidt, M.P. (2006). Developmental origin and fate of meso-diencephalic dopamine neurons. Prog Neurobiol *78*, 1-16.

Soriano, P. (1999). Generalized lacZ expression with the ROSA26 Cre reporter strain. Nat Genet 21, 70-71.

Stahl, K., Mylonakou, M.N., Skare, O., Amiry-Moghaddam, M., and Torp, R. (2011). Cytoprotective effects of growth factors: BDNF more potent than GDNF in an organotypic culture model of Parkinson's disease. Brain Res *1378*, 105-118.

Suh, H., Consiglio, A., Ray, J., Sawai, T., D'Amour, K.A., and Gage, F.H. (2007). In vivo fate analysis reveals the multipotent and self-renewal capacities of Sox2+ neural stem cells in the adult hippocampus. Cell Stem Cell *1*, 515-528.

Sun, D., Melegari, M., Sridhar, S., Rogler, C.E., and Zhu, L. (2006). Multi-miRNA hairpin method that improves gene knockdown efficiency and provides linked multi-gene knockdown. Biotechniques *41*, 59-63.

Takebayashi, K., Sasai, Y., Sakai, Y., Watanabe, T., Nakanishi, S., and Kageyama, R. (1994). Structure, chromosomal locus, and promoter analysis of the gene encoding the mouse helix-loop-helix factor HES-1. Negative autoregulation through the multiple N box elements. J Biol Chem *269*, 5150-5156.

Tanaka, S., Kamachi, Y., Tanouchi, A., Hamada, H., Jing, N., and Kondoh, H. (2004). Interplay of SOX and POU factors in regulation of the Nestin gene in neural primordial cells. Mol Cell Biol *24*, 8834-8846.

Taranova, O.V., Magness, S.T., Fagan, B.M., Wu, Y., Surzenko, N., Hutton, S.R., and Pevny, L.H. (2006). SOX2 is a dose-dependent regulator of retinal neural progenitor competence. Genes Dev *20*, 1187-1202.

Tay, Y., Zhang, J., Thomson, A.M., Lim, B., and Rigoutsos, I. (2008). MicroRNAs to Nanog, Oct4 and Sox2 coding regions modulate embryonic stem cell differentiation. Nature 455, 1124-1128.

Thai, T.H., Calado, D.P., Casola, S., Ansel, K.M., Xiao, C., Xue, Y., Murphy, A., Frendewey, D., Valenzuela, D., Kutok, J.L., *et al.* (2007). Regulation of the germinal center response by microRNA-155. Science *316*, 604-608.

Tomac, A., Widenfalk, J., Lin, L.F., Kohno, T., Ebendal, T., Hoffer, B.J., and Olson, L. (1995). Retrograde axonal transport of glial cell line-derived neurotrophic factor in the adult nigrostriatal system suggests a trophic role in the adult. Proc Natl Acad Sci U S A *92*, 8274-8278.

Tomioka, M., Nishimoto, M., Miyagi, S., Katayanagi, T., Fukui, N., Niwa, H., Muramatsu, M., and Okuda, A. (2002). Identification of Sox-2 regulatory region which is under the control of Oct-3/4-Sox-2 complex. Nucleic Acids Res *30*, 3202-3213.

Tompkins, D.H., Besnard, V., Lange, A.W., Keiser, A.R., Wert, S.E., Bruno, M.D., and Whitsett, J.A. (2010). Sox2 activates cell proliferation and differentiation in the respiratory epithelium. Am J Respir Cell Mol Biol *45*, 101-110.

Treanor, J.J., Goodman, L., de Sauvage, F., Stone, D.M., Poulsen, K.T., Beck, C.D., Gray, C., Armanini, M.P., Pollock, R.A., Hefti, F., et al. (1996). Characterization of a multicomponent receptor for GDNF. Nature 382, 80-83.

Trupp, M., Belluardo, N., Funakoshi, H., and Ibanez, C.F. (1997). Complementary and overlapping expression of glial cell line-derived neurotrophic factor (GDNF), c-ret proto-oncogene, and GDNF receptor-alpha indicates multiple mechanisms of trophic actions in the adult rat CNS. J Neurosci *17*, 3554-3567.

Trupp, M., Scott, R., Whittemore, S.R., and Ibanez, C.F. (1999). Ret-dependent and -independent mechanisms of glial cell line-derived neurotrophic factor signaling in neuronal cells. J Biol Chem *274*, 20885-20894.

Tsang, J.S., Ebert, M.S., and van Oudenaarden, A. (2010). Genome-wide dissection of microRNA functions and cotargeting networks using gene set signatures. Mol Cell *38*, 140-153.

van de Wetering, M., Oosterwegel, M., van Norren, K., and Clevers, H. (1993). Sox-4, an Sry-like HMG box protein, is a transcriptional activator in lymphocytes. Embo J *12*, 3847-3854.

van den Munckhof, P., Luk, K.C., Ste-Marie, L., Montgomery, J., Blanchet, P.J., Sadikot, A.F., and Drouin, J. (2003). Pitx3 is required for motor activity and for survival of a subset of midbrain dopaminergic neurons. Development *130*, 2535-2542.

Wallen, A., Zetterstrom, R.H., Solomin, L., Arvidsson, M., Olson, L., and Perlmann, T. (1999). Fate of mesencephalic AHD2-expressing dopamine progenitor cells in NURR1 mutant mice. Exp Cell Res 253, 737-746.

Wang, H.J., Cao, J.P., Yu, J.K., Zhang, L.C., Jiang, Z.J., and Gao, D.S. (2008a). Calbindin-D28K expression induced by glial cell line-derived neurotrophic factor in substantia nigra neurons dependent on PI3K/Akt/NF-kappaB signaling pathway. Eur J Pharmacol *595*, 7-12.

Wang, Y., Baskerville, S., Shenoy, A., Babiarz, J.E., Baehner, L., and Blelloch, R. (2008b). Embryonic stem cell-specific microRNAs regulate the G1-S transition and promote rapid proliferation. Nat Genet *40*, 1478-1483.

Weiss, M.A. (2001). Floppy SOX: mutual induced fit in hmg (high-mobility group) box-DNA recognition. Mol Endocrinol *15*, 353-362.

Wurst, W., Auerbach, A.B., and Joyner, A.L. (1994). Multiple developmental defects in Engrailed-1 mutant mice: an early mid-hindbrain deletion and patterning defects in forelimbs and sternum. Development *120*, 2065-2075.

Yan, C.H., Levesque, M., Claxton, S., Johnson, R.L., and Ang, S.L. (2011). Lmx1a and lmx1b function cooperatively to regulate proliferation, specification, and differentiation of midbrain dopaminergic progenitors. J Neurosci *31*, 12413-12425.

Yang, D., Peng, C., Li, X., Fan, X., Li, L., Ming, M., Chen, S., and Le, W. (2008). Pitx3-transfected astrocytes secrete brain-derived neurotrophic factor and glial cell line-derived neurotrophic factor and protect dopamine neurons in mesencephalon cultures. J Neurosci Res *86*, 3393-3400.

Yi, R., Qin, Y., Macara, I.G., and Cullen, B.R. (2003). Exportin-5 mediates the nuclear export of pre-microRNAs and short hairpin RNAs. Genes Dev *17*, 3011-3016.

Yu, J., Vodyanik, M.A., Smuga-Otto, K., Antosiewicz-Bourget, J., Frane, J.L., Tian, S., Nie, J., Jonsdottir, G.A., Ruotti, V., Stewart, R.*, et al.* (2007). Induced pluripotent stem cell lines derived from human somatic cells. Science *318*, 1917-1920.

Yu, X., Zou, J., Ye, Z., Hammond, H., Chen, G., Tokunaga, A., Mali, P., Li, Y.M., Civin, C., Gaiano, N.*, et al.* (2008). Notch signaling activation in human embryonic stem cells is required for embryonic, but not trophoblastic, lineage commitment. Cell Stem Cell *2*, 461-471.

Yuan, H., Corbi, N., Basilico, C., and Dailey, L. (1995). Developmental-specific activity of the FGF-4 enhancer requires the synergistic action of Sox2 and Oct-3. Genes Dev *9*, 2635-2645.

Zeng, Y., Yi, R., and Cullen, B.R. (2005). Recognition and cleavage of primary microRNA precursors by the nuclear processing enzyme Drosha. EMBO J *24*, 138-148.

Zhao, C., Sun, G., Li, S., Lang, M.F., Yang, S., Li, W., and Shi, Y. (2010). MicroRNA let-7b regulates neural stem cell proliferation and differentiation by targeting nuclear receptor TLX signaling. Proc Natl Acad Sci U S A *107*, 1876-1881.

Zhao, C., Sun, G., Li, S., and Shi, Y. (2009). A feedback regulatory loop involving microRNA-9 and nuclear receptor TLX in neural stem cell fate determination. Nat Struct Mol Biol *16*, 365-371.

Zhu, Q., Sun, W., Okano, K., Chen, Y., Zhang, N., Maeda, T., and Palczewski, K. (2011). Sponge transgenic mouse model reveals important roles for the microRNA-183 (miR-183)/96/182 cluster in postmitotic photoreceptors of the retina. J Biol Chem *286*, 31749-31760.

Ziebold, U., Reza, T., Caron, A., and Lees, J.A. (2001). E2F3 contributes both to the inappropriate proliferation and to the apoptosis arising in Rb mutant embryos. Genes Dev *15*, 386-391.
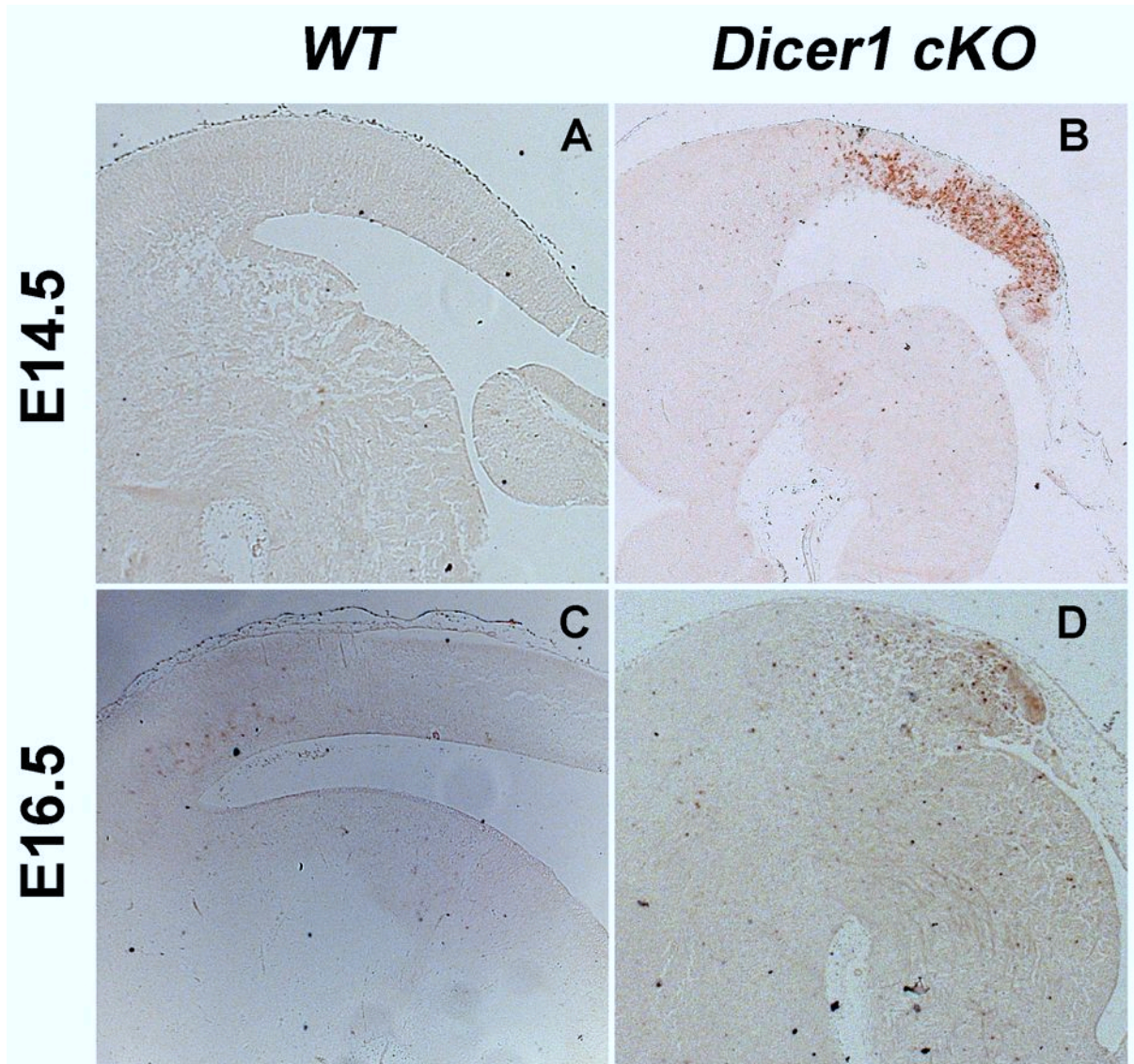
6 Supplementary data
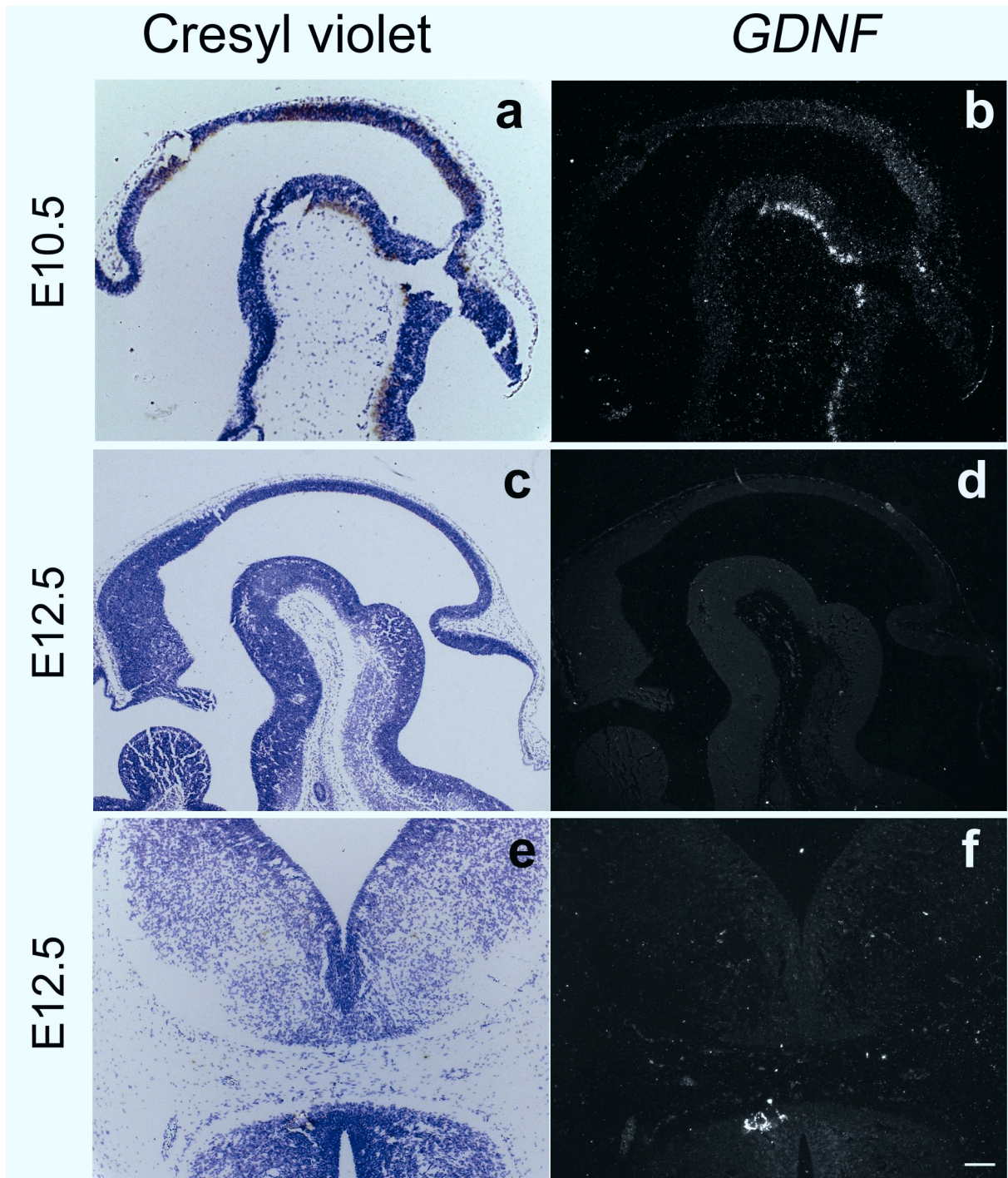
Supplementary Figure S1. *GDNF* **is expressed in the mouse VM at E10.5 but not at E12.5, related to Figure 1.** (**a-f**) Representative sagittal (**a-d**) and coronal midbrain (**e**, **f**) sections of *wild-type* (C57BL/6) mouse embryos at E10.5 (**a**, **b**) and E12.5 (**c-f**), hybridized with a riboprobe for *GDNF*. (**a**, **c**, **e**) are Nissl-stained bright-field views of the dark-field pictures shown in (**b**, **d**, **f**). *GDNF* is expressed in the murine VM at E10.5, but *GDNF* expression is not detectable in the anterior neural tube and VM of the E12.5 mouse embryo. Scale bar: 100 µm.
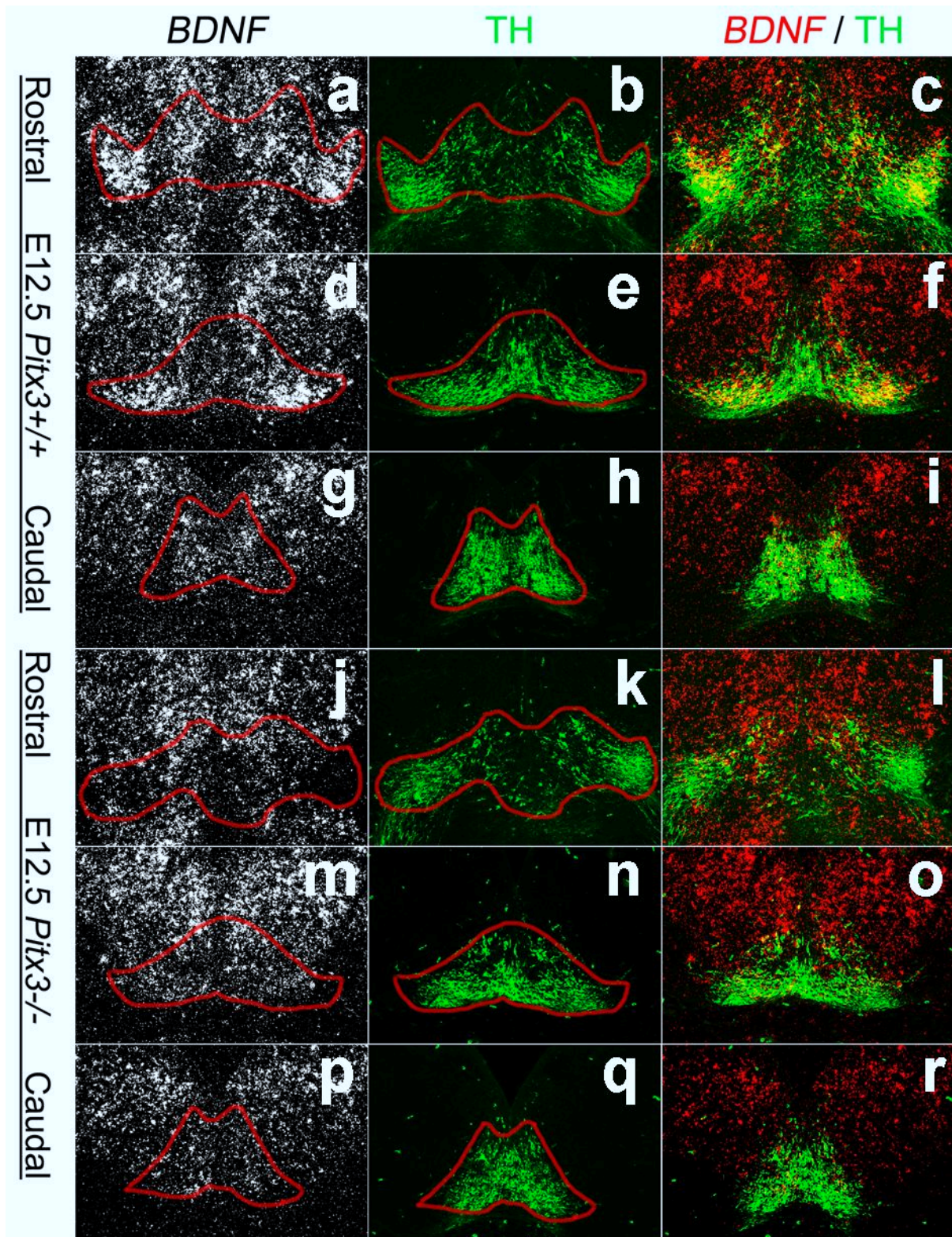
Supplementary Figure S2. *BDNF* **is highly expressed in rostrolateral mdDA neurons of E12.5 wild type but not** *Pitx3* **mutant embryos, related to Figure 4.** (**a-r**) Representative and coronal midbrain sections from E12.5 *wild-type* (*Pitx3*$^{+/+}$) mouse embryos (**a-i**) and *Pitx3*$^{-/-}$ mutant embryos (**j-r**) hybridized with a *BDNF* riboprobe (**a, d, g, j, m, p**) or immunostained for TH (**b, e, h, k, n, q**). Merged images are shown in **c, f, i, l, o and r.** *BDNF* is highly expressed in a rostrolateral TH$^+$ mdDA domain in the wild-type (*Pitx3*$^{+/+}$) embryos (**a-f**), but not in the rostrolateral TH$^+$ mdDA domain of *Pitx3*$^{GFP/GFP}$ embryos (**j-o**).

Supplementary Figure S3. Increased apoptosis in the E14.5 and E16.5 *Dicer1 cKO* embryos, related to Figure 18.

(**A-B**) Immunostaining for cCasp3 showed that apoptosis is increased in the MHR of E14.5 *Dicer1 cKO* embryos.

(**C-D**) Immunostaining for cCasp3 showed that apoptosis is increased in the MHR of E16.5 *Dicer1 cKO* embryos.
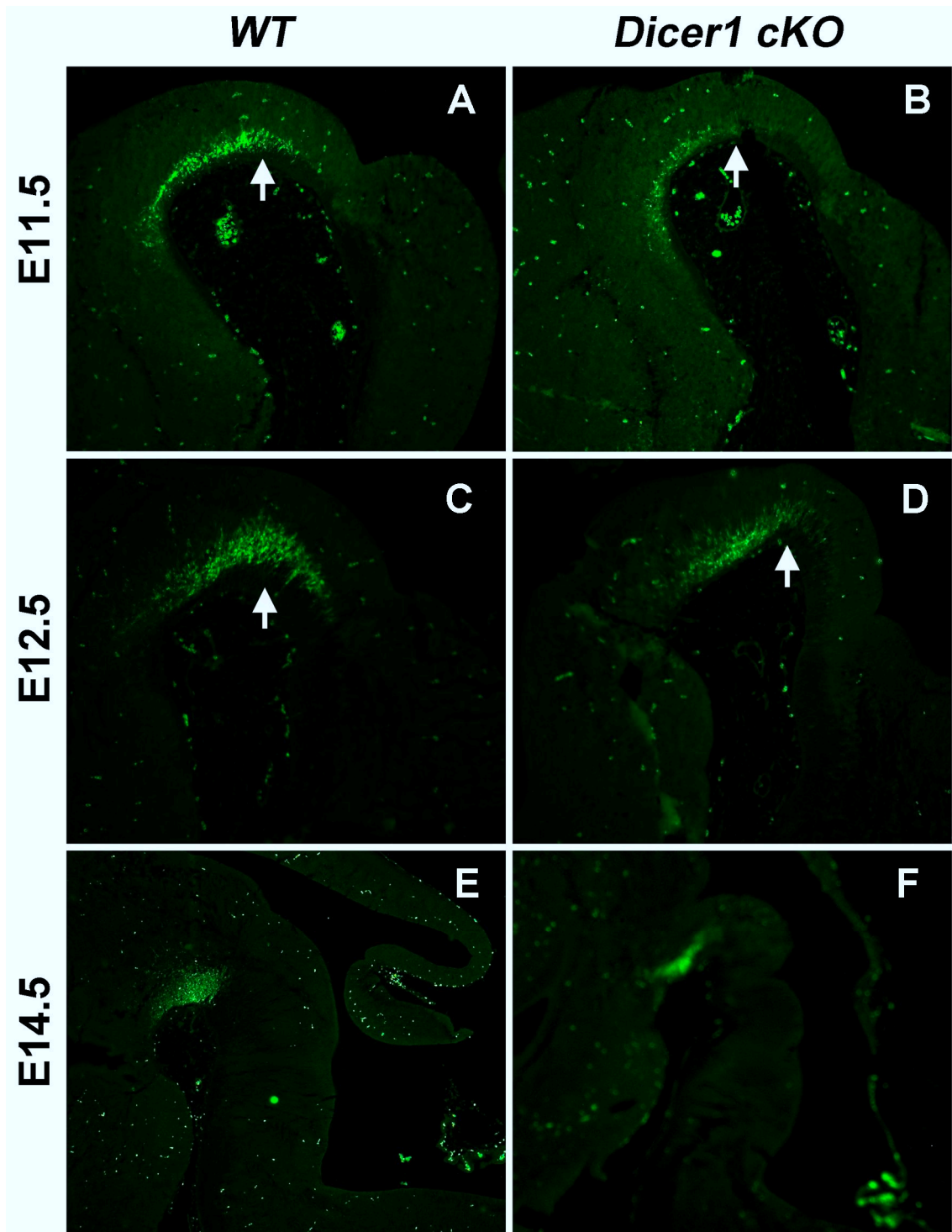
Supplementary Figure S4. TH⁺ mdDA neurons are progressively lost in the *Dicer1 cKO* mice from E11.5 onwards, related to Figure 23.

(**A-B**) Immunostaining for TH on E11.5 sagittal sections from *WT* and the *Dicer1 cKO* embryos.

(**C-D**) Immunostaining for TH on E12.5 sagittal sections from *WT* and the *Dicer1 cKO* embryos.

(**E-F**) Immunostaining for TH on E14.5 sagittal sections from *WT* and the *Dicer1 cKO* embryos.
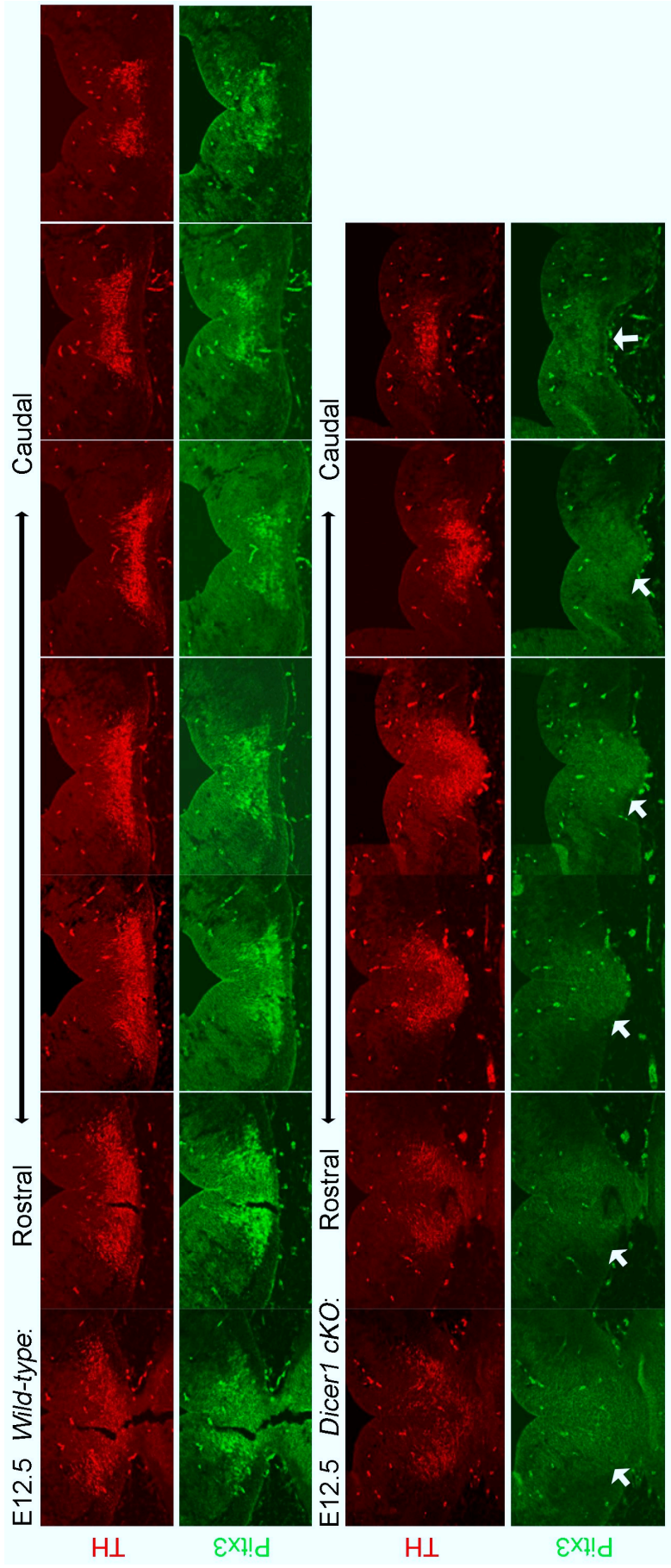
Supplementary Figure S5. TH+ mdDA neurons are not expressing Pitx3 at later E12.5 Dicer1 cKO mice , related to Figure 23.
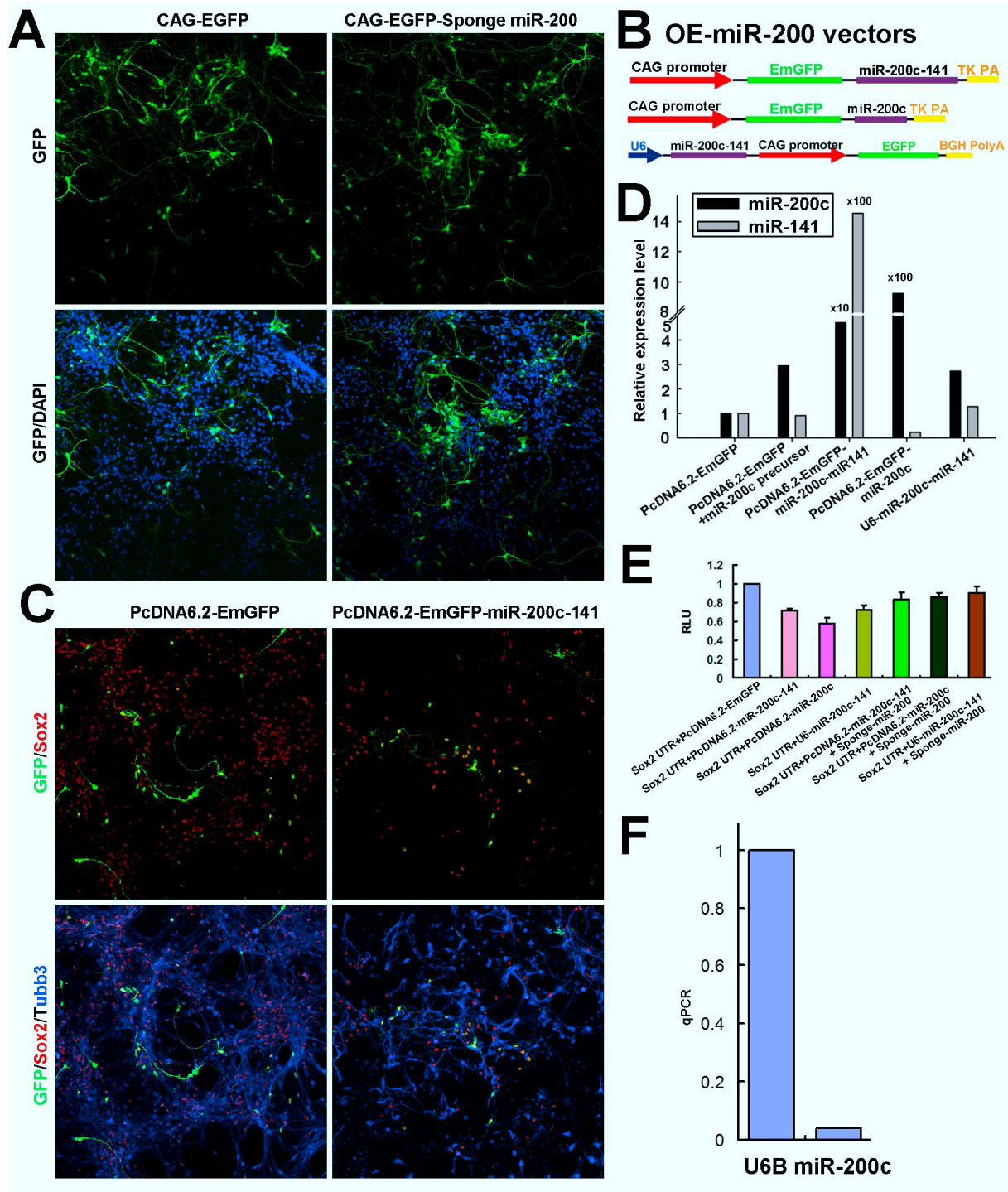
Figure S6 (related to Figure 6). Validation of *miR-200* OE and sponge vectors.

(A) Lipofection of primary vMH cultures with the *miR-200* sponge vector resulted in a transfection efficiency of approximately 5%–10%. GFP expression driven by the *CAG* promoter in this vector was used to identify transfected cells.

(B) Structure of the three *miR-200* OE vectors tested and/or used in this work. Top: The *mmu-miR-200c-141* gene was co-expressed with EmGFP from a *CAG* promoter in the *pcDNA6.2-EmGFP-miR-200c-141* OE vector. Middle: Removal of the *mmu-miR-141* gene from this vector resulted in the *pcDNA6.2-EmGFP-miR-200c* OE vector. Bottom: Expression of the *mmu-miR-200c-141* gene was under the control of an *U6* promoter and was monitored by *CAG* promoter-driven eGFP expression in the *pU6-miR-200c-141-CAG-EGFP* OE vector.

(C) Overexpression of *miR-200c-141* in primary vMH cells using the *pcDNA6.2-EmGFP-miR-200c-141* OE vector caused a severe cell loss in these cultures as compared to the *pcDNA6.2-EmGFP* control vector-transfected group. This vector was therefore not used for further experiments.

(D) Quantification of the *miR-200c* and *miR-141* expression levels by qRT-PCR after transfection of the three different *miR-200* OE vectors into HEK-293 cells. The *pcDNA6.2-EmGFP* ("empty") vector served as control and was set as "1". Co-transfection of *pcDNA6.2-EmGFP* ("empty") vector and the *mmu-miR-200c* precursor miRNA was used to test the specificity of the qRT-PCR assays. In fact, an increase of only *miR-200c* but not of *miR-141* expression was detected after co-transfection of *pcDNA6.2-EmGFP* + *mmu-miR-200c* precursor. A ~50-fold increase of *miR-200c* and a ~1400-fold increase of *miR-141* expression were detected after transfection of the *pcDNA6.2-EmGFP-miR-200c-141* OE vector. Transfection of the *pcDNA6.2-EmGFP-miR-200c* OE vector resulted in a ~1000-fold increase of *miR-200c* expression but barely detectable miR-141 levels. A modest (between 1.3 and 2.7-fold) increase of *miR-200c* and *miR-141* expression levels was detected after transfection of the *pU6-miR-200c-141-CAG-EGFP* OE vector. Thus, *miR-200c* expression levels from these OE vectors were (from highest to lowest): *pcDNA6.2-EmGFP-miR-200c* > *pcDNA6.2-EmGFP-miR-200c-141* > *pU6-miR-200c-141-CAG-EGFP*.

(E) Functional validation of the *miR-200* OE and sponge vectors. Co-transfection of the *pGL3-Sox2-3'UTR* sensor vector and of each of the three *miR-200* OE vectors in COS-7 cells resulted in a dose-dependent (see above) repression of luciferase expression. Luciferase expression was rescued back to normal levels after additional transfection of the *mir-200* sponge vector together with the sensor and OE vectors. Co-transfection of the *pGL3-Sox2-3'UTR* sensor and *pcDNA6.2-EmGFP* ("empty") vector served as control and was set as "1". (*pGL3-Sox2-3'UTR* + *pcDNA6.2-EmGFP-miR-200c-141*: 0.720 ± 0.021; *pGL3-Sox2-3'UTR* + *pcDNA6.2-EmGFP-miR-200c*: 0.580 ± 0.061; *pGL3-Sox2-3'UTR* + *pU6-miR-200c-141-CAG-EGFP*: 0.722 ± 0.054; *pGL3-Sox2-3'UTR* + *pcDNA6.2-EmGFP-miR-200c-141* + *miR-200* sponge: 0.837 ± 0.074; *pGL3-Sox2-3'UTR* + *pcDNA6.2-EmGFP-miR-200c* + *miR-200* sponge: 0.862 ± 0.04; *pGL3-Sox2-3'UTR* + *pU6-miR-200c-141-CAG-EGFP* + *miR-200* sponge: 0.903 ± 0.069; mean ± SEM; N=3).

(F) Quantification of *miR-200c* expression level in primary vMH cultures at 4 days in vitro (DIV) by qRT-PCR. Expression level of *miR-200c* is low in these cultures (1/25 relative to *U6B* snRNA).

7 Abbreviations

6-OHDA	6-Hydroxydopamine
A/P	anterior/posterior
ATP	adenosine triphosphate
BP	basal plate
BCA	bicinchoninic acid
BDNF	brain-derived neurotrophic factor
bp	base pair
BrdU	bromodesoxy uridin
BS	binding site
BSA	bovine serum albumin
°C	degree Celsius
cDNA	complementary DNA
cKO	conditional knockout
CO_2	carbon dioxide
DA	dopamine
Dig	digoxigenin
DIV	day in vitro
dpt	day post transfection
DMSO	dimethylsulfoxide
DNA	deoxyribonucleic acid
dNTP	desoxyribonucleotide triphosphate
DTT	1,4-dithiothreitol
D/V	dorsal/ventral
E	embryonic day
EB	embryoid bodies
E.coli	Escherichia coli
EDTA	ethyldiaminetetraacetate
EdU	5-Ethynyl-2'-deoxyuridine
EGFP	enhanced green fluorescent
EmGFP	emerald GFP
ESCs	embryonic stem cells
FP	floor plate
g	gramme
Gapdh	gyceraldehyde-3-phosphate dehydrogenase

GDNF   glial cell line-derived neurotrophic factor

hrs   hours

HCl   hydrochloric acid

HMG   high-mobility-group

HPRT   hypoxanthine phosphoribosyl transferase

i.p.   intraperitoneal

ISH   in situ hybridization

IZ   intermediate zone

Kb   kilo base

KD   kilo Dalton

l   litre

LacZ   β-Galactosidase gene

LNA   locked nucleic acid

m   metre

m   milli (10^{-3})

M   molar (mol/l)

mdDA   meso-diencephalic dopaminergic

MHB   mid/hind brain doundary

MHR   mid/hind brain region

miRNA   microRNA

μ   micro (10^{-6})

NP-40   nonidet P-40

NSCs   neural stem cells

P   postnatal day

PBS   phosphate buffer saline

PCR   polymerase chain reaction

PD   Parkinson's disease

PFA   paraformaldehyde

RA   retinoic acid

RB   retinoblastoma protein

RIPA   radioimmunoprecipitation assay (buffer)

RNA   ribonucleic acid

rpm   rounds per minute

RT   room temperature

RT   reverse transcription

RT-PCR	reverse transcription PCR
SBE1	Shh brain enhancer 1
SDS	sodiumdodecylsulphate
sec or s	second(s)
SEM	standard error of the mean
SNc	substantia nigra pars compacta
SSC	sodium saline citrate
SVZ	sub ventricular zone
TAE	tris acetate with EDTA
TE	tris-EDTA
U	unit(s)
UTR	untranslated region
V	volt
VM	ventral midbrain
VMHB	ventral mid/hind brain
VTA	ventral tegmental area
VZ	ventricular zone
wt	wild-type

8 Acknowledgements

9 Lebenslauf

Changgeng Peng

Geburtsdatum: 16. Dezember 1979

Staatsangehörigkeit: Chinesisch

Familienstand: Verheiratet

Handy-Nummer: 0049-17627621887

E-mail-adresse: cgpeng3@hotmail.com

Ausbildung

2.2008– 2.2012	Doktor rerum naturalium, Hauptfach: Genetik Institut für Entwicklungsgenetik, Helmholtz Zentrum München, Deutschland. (Eingegangen an der Technischen Universität München, in Bearbeitung.)
9.2003– 7.2006	Master of Science, Hauptfach: Biochemie und Molekulabiologie Shanghai Institute for Biological Sciences, Chinese Academy of Science, Shanghai, China.
9.1999– 7.2003	Bachelor of Science, Hauptfach: Biotechnologie College of Life Science, Shanxi University, Shanxi, China.

Arbeit

7.2006- 12.2007 Wissenschaftlicher Mitarbeiter, Neurogenetisches Labor, Shanghai Institutes for Biological Sciences, Chinese Academy of Science, Shanghai.

Kurse und Tagungen

1. Helmholtz Alliance on Systems Biology "Spring School 2008 on Systems Biology"

2. Helmholtz Zentrum München "Publishing in peer-reviewed journals" 2010

3. Helmholtz Zentrum München "Protection and Commercialization of Intellectual Property" 2010

4. Interact 2009-Munich PhD symposium, Ludwig-Maximilians-Universität, München, Germany.

5. Annual Conference of the German Genetics Society. Sep. 16-19, 2009. Heidberg. Poster: Dicer/miRNA function in mid-/hindbrain development of the mouse. C. PENG, N. LI, W. CHEN, M. MERKENSCHLAGER, W. WURST, N. PRAKASH.

6. 40th Annual meeting of Society for Neuroscience. Nov. 13-17, 2010. San Diego. Poster: Dicer/miRNA function in mid-/hindbrain development of the mouse. C. PENG, N. LI, W. CHEN, M. MERKENSCHLAGER, W. WURST, N. PRAKASH.

Publikationen

Peng C, Li N, Zhang J, Ng Y, Meier F, Chen W, Merkenschlager M, Wurst W and Prakash N. A unilateral negative feedback loop between miR-200 microRNAs and Sox2/E2F3 controls neural progenitor cell cycle exit and differentiation. J Neurosci. 2012 Sep;*19*, 13292-13308.

Peng C, Aron L, Klein R, Li M, Wurst W, Prakash N and Le W. Pitx3 is a critical mediator of GDNF-induced BDNF expression in nigrostriatal dopaminergic neurons. J Neurosci. 2011 Sep;*31*, 12802-12815.

Fukusumi Y, Götz S, Faus-Kessler T, Minina E, **Peng C,** Zhang J, Rauser B, Grosschedl R, Arenas E, Niehrs C, Simeone A, Wurst W and Prakash N. Dkk3 modulation of Wnt/β-catenin signaling promotes the differentiation andsurvival of Substantia nigra dopaminergic neurons. (Submitted)

Yang D, **Peng C**, Li X, Fan X, Li L, Ming M, Chen S, and Le W. Pitx3-transfected astrocytes secrete brain-derived neurotrophic factor and glial cell line-derived neurotrophic factor and protect dopamine neurons in mesencephalon cultures. J Neurosci Res.2008 Nov; 86(15), 3393-3400.

Peng C, Fan S, Li X, Fan X, Ming M, Sun Z, Le W. Overexpression of pitx3 upregulates expression of BDNF and GDNF in SH-SY5Y cells and primary ventral mesencephalic cultures. FEBS Lett. 2007 Apr 3;581(7):1357-61. Epub 2007 Mar 2.

Li X, **Peng C**, Li L, Ming M, Yang D, Le W. Glial cell-derived neurotrophic factor protects against proteasome inhibition-induced dopamine neuron degeneration by suppression of endoplasmic reticulum stress and caspase-3 activation. J Gerontol A Biol Sci Med Sci. 2007 Sep;62(9):943-50.

Li X, Yang D, Li L, **Peng C**, Chen S, Le W. Proteasome inhibitor lactacystin disturbs the intracellular calcium homeostasis of dopamine neurons in ventral mesencephalic cultures. Neurochem Int. 2007 Jun;50(7-8):959-65. Epub 2007 May 3.